On the anticancer activity and mechanism of action of pinostrobin

Thesis submitted to the Jawaharlal Nehru University
for the award of the degree of

DOCTOR OF PHILOSOPHY
IN
BIOTECHNOLOGY

By

ALKA JADAUN

2017

SCHOOL OF BIOTECHNOLOGY
JAWAHARLAL NEHRU UNIVERSITY
NEW DELHI-110067
INDIA

SCHOOL OF BIOTECHNOLOGY
JAWAHARLAL NEHRU UNIVERSITY
NEW DELHI
INDIA

CERTIFICATE

This is to certify that the research work in this thesis entitled ***"On the anticancer activity and mechanism of action of pinostrobin"*** *submitted to the School of Biotechnology, Jawaharlal Nehru University, New Delhi, India in partial fulfillment of the requirement for the award of the degree of Doctor of Philosophy, embodies faithful record of original research work carried out by* ***Alka Jadaun.*** *This work is original and has not been submitted in part or full for any other degree or diploma of any university/Institution elsewhere.*

Alka Jadaun

Alka Jadaun

Candidate

Aparna Dixit 21/07/2017

Prof. Aparna Dixit
Supervisor
School of Biotechnology
Jawaharlal Nehru University
New Delhi-110067

PROF. APARNA DIXIT
School of Biotechnology
Jawaharlal Nehru University
New Delhi-110067, INDIA

Prof. Pawan K. Dhar
Dean
School of Biotechnology
Jawaharlal Nehru University
New Delhi-110067

पवन कुमार धर
PAWAN K. DHAR
डीन/DEAN
जैव प्रौद्योगिकी संस्थान
School of Biotechnology
जवाहरलाल नेहरू विश्वविद्यालय
Jawaharlal Nehru University
नई दिल्ली/New Delhi-110067

Acknowledgements

*To begin with I would like to express my deep gratitude to merciful God for all the countless support that you have given me and thanks to all my family (**Grandmother**, **parents, sister, brother, husband, and in-laws**) for their love and constant support.*

*I am very grateful to Prof. **Aparna Dixit** for her meticulous guidance, congenial discussions, incessant help, constructive criticism, constant encouragement and debonair discussion throughout this investigation. I would like to express my thanks to **Dr. Devapriya Chaudhary** and my doctoral committee members (**Prof. Pawan K Dhar, Dr. Rahul pal and Dr. Maitreyi Rajala**) for their valuable suggestions in advancement of my research work. My sincere thanks to **Dr. Lalit Garg** for the encouragement he offered in carrying out my research work.*

*I would like to express my deepest thank to Dean, **Prof. Pawan K Dhar** for providing the necessary research facility in the department and essential paperwork during this period. I am heartily thankful to **Prof. Rajiv Bhat**, **Prof. K.J. Mukherjee**, **Prof. Rakesh Bhatnagar**, **Dr. Swati Tiwari**, **Dr. Maitreyi Rajala**, **Dr. Ranjana Arya** and other faculty members for their kind cooperation, guidance and constant help throughout the Ph.D. period. I genuinely acknowledge the technical and instrumentation support provided by **Prof. Rakesh Bhatnagar's lab.***

*I am also thankful to technical staff (CIF) and administrative staff of my school (**Vinod sir**, **Tiwari sir**, **Ajay bhaiya**, **Sajjan bhaiya**, **Surjit ji**, **Sahni ji** and **Yadav ji)** for essential paperwork, for always being considerate and helpful during this period. I also would like to thank our **library staff** for providing me enough space to conduct my thesis writing peacefully. I am thankful to all staff of AIRF, I can never forget the help and technical support provided by **Dr. Gajendar, Dr. Prabhat, Ashok ji** and **Sharma ji.** My special thanks to **Pandey ji** and **Naresh bhaiya** for their support during animal experiment.*
*My experiments and paper work would not have been completed without support extended by **Rinku bhaiya, Naresh bhaiya, Amresh ji, Sheenu** and **Geeta**. I am very thankful to all of you for your assistance in technical as well as paperwork.*

*I am blessed to have wonderful seniors and juniors and would like to take this opportunity to thank them especially **Dr.Sunita , Dr.Vibhuti , Dr.Preeti , Dr.Rachna ,***

Dr.Ankita , Dr.Pratibha , Dr.Himani , Dr.Bharti , Dr.Shailesh , Dr.Keshav , Dr.Gagan , Dr.Gaurav , Dr.Zaheer, Noopur, Jasveer , Neetu , Ritu , Ankita , Jeetesh , Rohit , Prashant , Nusrat , Amit , Rimi *for helping me at every stage of my research work. Their immense help and cooperation has been a great support.*

My special thank to ***Dr. Sapna, Dr. Mahima , Radha*** *and* ***Bharti ,*** *for the invaluable support right from the beginning of my research through various stages including thesis writing, without your help my research work would not have been accomplished.*

This section would be incomplete without a word for my friends who encouraged me and supported me through all my ups and down. I owe special thanks to ***Akanksha , Jaya , Meenu , Pratibha , Monisha , Mamta , Saurabh , Utkarsh , Joyline , Charak , Gourav , Sapna, Amruta, Poonam, Usha , Dilip , Ambrish , Shashank , Sudeep , Durga Prasad and Farozan*** *for their love and support.*

Last but not least, I am very grateful to ***JNU, DBT*** *and* ***DST*** *(PURSE and DBT-BUILDER grant) for providing the financial assistance.*

Alka Jadaun

Table of contents

Abbreviation	Full form
Å	Armstrong
AT	Adenine-Thymine
ATP	Adenosine5 triphosphate
BCA	Bicinchoninic acid
bp	Base pairs
BAD	Bcl-2-associated death promoter protein
BAX	Bcl-2-associated X protein
BAK	Bcl-2 homologous antagonist/killer protein
BAG	BAG family molecular chaperone regulator
Bcl-10	B-cell CLL/lymphoma 10
Bcl-2	B-cell lymphoma 2
Bcl-x	Bcl-2-associated X protein
Bcl-XL	B-cell lymphoma-extra large
Bcl-XS	B-cell lymphoma-extra short
BD	Becton Dickinsion
Bid	BH-3 interacting domain death antagonist
BIK	Bcl-2-interacting killer
BID	BH3 interacting-domain death agonist
BIM	Bcl-2 interacting mediator of cell death
b wt.	Body weight
BSA	Bovine serum albumin
°C	Degree celsius
cm	centimeter
CO_2	Carbon dioxide
CT_{50}	50% cytotoxicity
DNA	Deoxyribonucleic acid
dH_20	Deionized water
ddw	Double distilled water
E2F1	Transcription factor E2F1
ELISA	Enzyme linked immunosorbent assay
et al	and others
FACS	Fluorescence-activated cell sorting
GSH	Reduced glutathione
h	Hour(s)
IP	Intraperitonial
IT	Intratumoral
IFN	Interferon
L	Liter(s)
LB	Luria bertani broth
mA	Mili ampere
Mcl-1	Myeloid Cell Leukemia 1
mg	Milligrams
min	Minute(s)

ml	Milliliter(s)
mM	Millimoles
MQ	milliQ water
mV	Millivolts
Mwt	Molecule weight
N	Normal
O/N	Over night
OD	Optical density
P53	protein 53 kilodaltons in size
PS	Phosphatidyle serine
pRb	Retinoblastoma protein
RNA	Ribonucleic acid
RNase	Ribonuclease
rpm	Rounds per minutes
RT	Room temperature
S.D.	Standard deviation
sec	Second(s)
spp	Species
TAE	Tris-acetate-EDTA buffer
TE	Tris-EDTA buffer
Triton x 100	Polyethylene glycol tert-octylphenyl ether
U	Unit(s)
UV	Ultraviolet
V	Volts
v/v	Volume to volume ratio
W	Watt(s)
α	Alpha
β	Beta
× g	Centrifugal force
≤	Less than or equal to
µg	Microgram/s
µl	Microliter/s
µM	Micromolar
ΔΨ	Mitochondrial membrane potential
%	percent
×	Times
2D	Two dimension
3ˈ OH	3ˈ hydroxyl

Chapter 1

Introduction

Cancer has emerged as one of the major cause of morbidity and mortality globally. While in the developed countries, cancer has been a significant cause of mortality trailing the cardiovascular diseases[1], it is the major leading cause of the death in the developing countries[2]. According to the World Health Organization (WHO), 7.6 million people died of cancer worldwide in 2005, accounting for around 13% of the total deaths caused by various diseases[3]. Number of cancer related mortalities has increased upto 84 million from 2005 to 2015, indicating the severity of this fatal disease[3]. The global burden of cancer is expected to increase with new cancer cases arising every year by 1.5 folds by 2030[4].

In the worldwide distribution of cancer, perceptible variations have been observed on the basis of gender as well as the economic status of the country. In developed countries, prostate, lung and colorectal cancer are the most common types of cancer noticed amongst males; whereas breast, colorectal and lung cancer have been frequently observed in females. Likewise in the developing economies, it has been observed that males suffer predominantly from lung, liver, and stomach cancer; while females were diagnosed mainly with breast, cervix uteri, and lung cancer[3].

Cancer growth is brought about by both external agents (e.g. tobacco, infectious organisms, poor diet, chemicals and radiations) as well as internal physiological factors (mutation, hormonal imbalance and inadequate immune response)[5]. Cancer can be described as a group of diseases, characterized by the malignant growth arising from uncontrolled cell proliferation and division. This leads to death, if this proliferation continues uncontrolled and unchecked[5].Cancer development is a multi stage process and metastasis is a hallmark of cancer progression. Metastasis involves a number of factors, and deregulated programmed cell death such as apoptosis, autophagy and necroptosis play an important role in cancer metastasis[6,7].

[1]Fitzmaurice, C., Dicker, D., Pain, A., Hamavid, H., Moradi-Lakeh, M., MacIntyre, M.F., Allen, C., Hansen, G., Woodbrook, R., Wolfe, C. and Hamadeh, R.R., 2015. The global burden of cancer 2013. JAMA Oncology, 1, pp.505-527.

[2]GLOBOCAN 2012: Estimated cancer incidence, mortality and prevalence worldwide in 2012: World Health Organization (WHO) .

[3]Cheng, Y. and Walkom, E., 2008. Proposal for the inclusion of ifosfamide in the WHO model list of essential medicines. WHO, Geneva, Switzerland.

[4]Ferlay, J., Soerjomataram, I., Dikshit, R., Eser, S., Mathers, C., Rebelo, M., Parkin, D.M., Forman, D. and Bray, F., 2015. Cancer incidence and mortality worldwide: sources, methods and major patterns in GLOBOCAN 2012. International Journal of Cancer, 136, pp.E359-E386.

[5]Cancer facts & figures. 2017.American Cancer Society,Inc.,Surveillance Research, Atlanta, pp.1-76.

[6]Staunton, M.J. and Gaffney, E.F., 1998. Apoptosis: basic concepts and potential significance in human cancer. Archives of Pathology & Laboratory Medicine, 122, pp. 310-319.

[7]Su, Z., Yang, Z., Xu, Y., Chen, Y. and Yu, Q., 2015. Apoptosis, autophagy, necroptosis, and cancer metastasis. Molecular Cancer, 14, pp.1-14.

Various strategies have been employed to treat cancer such as surgery, radiation therapy, chemotherapy, immunotherapy, hormone therapy, and targeted or biologic drug delivery therapy, depending on the type of cancer[8]. However, each of these has adverse side effects on the normal tissues causing the patient much discomfort and agony. Considering the severity of the disease and adverse effects of currently available therapies, there is a need to develop new cancer therapeutics in order to prevent unfavourable effects of the currently available therapeutics on normal tissues and overcome drug resistance. A better therapeutic strategy would selectively target the proteins involved in the neoplastic process with less adverse effect to normal cell functionality. Therefore, scientists have been engaged in investigations that would lead to the development of innovative therapeutics/procedure for curing cancer that would induce apoptosis in cancerous cells without affecting the healthy normal cells[9].

Apoptosis is one of the programmed cell death processes that cause cell death in a controlled manner, with minimum disruption in the functioning of neighbouring cells, involved in the basic physiological processes such as immune response reactions, cellular development and tissue homeostasis[10]. Apoptosis starts with a cascade of molecular events involving cellular disintegration, cytoplasm and nuclear condensation resulting apoptotic bodies formation. These apoptotic bodies are engulfed by macrophages, eventually bringing out changes in cell's shape and size that leads to cell death[11]. Apoptosis of a cell is mediated by mainly two pathways; Death receptor pathway (extrinsic)[12] and mitochondrial mediated pathway (intrinsic)[13]. Death receptor (extrinsic) pathway is activated by binding of extracellular ligands on death receptors (DR) like FasR, TNF related apoptosis-inducing ligand receptor (TRAILR) and tumor necrosis factor receptors (TNFR)[14] whereas, intrinsic pathway is activated by different stimuli including DNA damage, chemotherapeutic agents and Reactive oxygen species (ROS)[15].

[8]Saini, R.K., Chouhan, R., Bagri, L.P. and Bajpai, A.K., 2012. Strategies of targeting tumors and cancers. Journal of Cancer Research Updates, 1, pp.129-152.
[9]Targeted cancer therapies fact sheet - National Cancer Institute (NIH). 2017, (www.cancer.gov/about-cancer/treatment/types/targeted-therapies/targeted-therapies-fact-sheet).
[10]Kerr, J.F., Wyllie, A.H. and Currie, A.R., 1972. Apoptosis: a basic biological phenomenon with wide-ranging implications in tissue kinetics. British Journal of Cancer, 26, pp.239-257.
[11]Darzynkiewicz, Z., Juan, G., Li, X., Gorczyca, W., Murakami, T. and Traganos, F., 1997. Cytometry in cell necrobiology: analysis of apoptosis and accidental cell death (necrosis). Cytometry, 27, pp.1-20.
[12]Jo, M., Kim, T.H., Seol, D.W., Esplen, J.E., Dorko, K., Billiar, T.R. and Strom, S.C., 2000. Apoptosis induced in normal human hepatocytes by tumor necrosis factor-related apoptosis-inducing ligand. Nature Medicine, 6, pp. 564-567.
[13]Sangiuliano, B., Pérez, N.M., Moreira, D.F. and Belizário, J.E., 2014. Cell death-associated molecular-pattern molecules: inflammatory signaling and control. Mediators of Inflammation, pp. 1-14.
[14]Lavrik, I., Golks, A. and Krammer, P.H., 2005. Death receptor signaling. Journal of Cell Science, 118, pp. 265-267.
[15]Armstrong, J.S., 2006. Mitochondria: a target for cancer therapy. British Journal of Pharmacology, 147, pp. 239-248.

ROS are mainly generated in mitochondria, therefore mitochondria are considered as novel target of cancer treatment[13,15]. On the other hand, cells and tissues are also protected by intracellular antioxidant enzymes such as glutathione peroxidase (GPx), catalase and superoxide dismutase (SOD), that constitute an innate defence mechanism and against the harmful effects of ROS species[16]. Some of the therapeutics/phytochemicals have been reported to mediate cancer cell death by ROS generation[17,18].

Increase in cell's proliferative activity is paralleled by its ability to efficiently replicate the genetic material. Topoisomerases are an essential component of DNA replication machinery. Thus, while apoptosis inducing agents are potential anti-cancer agents that inhibit topoisomerase activity can reduce the rate of cell proliferation. Indeed, a number of compounds such as quercetin, myricetin, morin, taxol, topotecan and camptothecin that bind to topoisomerase and are its potent inhibitor have been reported to prevent cell proliferation and result in cell death[19].

Keeping the multitudes of the activities that can be targeted in a cell to induce cancer cell death, natural compounds such as flavonoids have emerged as a promising therapeutics agents and have been found to be effective against cancer[20,21,22] and other diseases like neurological degeneration[23], inflammatory disorders[24] and obesity[25,26]. Flavonoids have also been recognized for their effective antioxidant activity against oxidative stress[27,28,29]. Anti-viral activities of flavonoids have been well reported throughout the literature[30].

---

[16]Garaiová, I., Muchová, J., Šustrová, M., Blaž íč ek, P., Sivoň ová, M., Kvasnič ka, P., Pueschel, S. and Ďurač ková, Z., 2004. The relationship between antioxidant systems and some markers of oxidative stress in persons with down syndrome. Biologia, 59, pp.787-794.

[17]Farhan, M., Khan, H.Y., Oves, M., Al-Harrasi, A., Rehmani, N., Arif, H., Hadi, S.M. and Ahmad, A., 2016. Cancer therapy by catechins involves redox cycling of copper ions and generation of reactive oxygen species. Toxins, 8, pp.2-16.

[18] Zubair, H., Azim, S., Khan, H.Y., Ullah, M.F., Wu, D., Singh, A.P., Hadi, S.M. and Ahmad, A., 2016. Mobilization of intracellular copper by gossypol and apogossypolone leads to reactive oxygen species-mediated cell death: Putative Anticancer Mechanism. International Journal of Molecular Sciences, 17, pp.2-12.

[19]Baikar, S. and Malpathak, N., 2010. Secondary metabolites as DNA topoisomerase inhibitors: a new era towards designing of anticancer drugs. Pharmacognosy. Reviews, 4, pp.12-26.

[20]Zhao, X., Pang, L., Li, J., Song, J.L. and Qiu, L.H., 2014. Apoptosis inducing effects of kuding tea polyphenols in human buccal squamous cell carcinoma cell line BcaCD885. Nutrients, 6, pp.3084-3100.

[21]Ding, Y., Yao, H., Yao, Y., Fai, L.Y. and Zhang, Z., 2013. Protection of dietary polyphenols against oral cancer. Nutrients, 5, pp.2173-2191.

[22]Li, F., Li, S., Li, H.B., Deng, G.F., Ling, W.H., Wu, S., Xu, X.R. and Chen, F., 2013. Antiproliferative activity of peels, pulps and seeds of 61 fruits. Journal of Functional Foods, 5, pp.1298-1309.

[23]Essa, M.M., Braidy, N., Bridge, W., Subash, S., Manivasagam, T., Vijayan, R.K., Al-Adawi, S. and Guillemin, G.J., 2014. Review of natural products on parkinson's disease pathology. J Aging Res Clin Pract, 3, pp.1-8.

[24]Larrosa, M., Luceri, C., Vivoli, E., Pagliuca, C., Lodovici, M., Moneti, G. and Dolara, P., 2009. Polyphenol metabolites from colonic microbiota exert anti-inflammatory activity on different inflammation models. Molecular Nutrition & Food Research, 53, pp.1044-1054.

[25] Meydani, M. and Hasan, S.T., 2010. Dietary polyphenols and obesity. Nutrients, 2, pp.737-751.

[26]Chuang, C.C. and McIntosh, M.K., 2011. Potential mechanisms by which polyphenol-rich grapes prevent obesity-mediated inflammation and metabolic diseases. Annual Review of Nutrition, 31, pp.155-176.

[27]Pecorari, M., Villaño, D., Francesca Testa, M., Schmid, M. and Serafini, M., 2010. Biomarkers of antioxidant status following ingestion of green teas at different polyphenol concentrations and antioxidant capacity in human volunteers. Molecular Nutrition & Food Research, 54, pp.S278-S283.

Flavonoids are polyphenolic phytochemicals extracted from various parts of plants such as seeds, fruits, flowers and bark. These are also present in dietary products like fruits, vegetables, tea leaves, soybeans, herbs, pigmented cereals and rice[31]. Some flavonoids extracted from green tea, apple and soya such as Epigallocatechin gallate (EGCG), quercetin and genistein have been extensively evaluated for their anti-proliferative activity both *in-vitro* & *in-vivo*[32]. Intake of adequate amounts of fruits and vegetables that retain high concentrations of flavonoides can protect cells from oxidative stress. Epidemiological studies have suggested an inverse relationship between flavonoid rich food and different types of cancer. In 1992, Block and co-workers showed a positive correlation between high consumption of fruits or vegetables and cancer reduction[33].Earlier studies have identified many anti-cancer drugs such as quercetin, myricetin and morin derived from natural sources[34]. Such natural compounds have been reported to cause cell death by modulating the key factors that are involved in signal transduction pathways essential for cell growth and survival. Quercetin has been shown to inhibit tumor growth by upregulating tumor suppressor p53, activating caspase-6 & caspase-8 activity, and suppressing the activity of NF-κ B, COX-2 and Akt[35,36,37]. Similarly, Naringenin, EGCG and Genistein has been reported to down regulate PI3K and Akt activity[38,39,40].

Earlier report indicates that *Boesenbergia pandurata* Roxb. *(*Zingiberaceae*)*, a culinary herb also known as "temu kunci", contains different types of flavonoids, offering

[28]Wu, Z., Ming, J., Gao, R., Wang, Y., Liang, Q., Yu, H. and Zhao, G., 2011. Characterization and antioxidant activity of the complex of tea polyphenols and oat β -glucan. Journal of Agricultural and Food Chemistry, 59, pp.10737-10746.
[29]Bandyopadhyay, P., Ghosh, A.K. and Ghosh, C., 2012. Recent developments on polyphenol–protein interactions: effects on tea and coffee taste, antioxidant properties and the digestive system. Food & Function, 3, pp.592-605.
[30]Hong-Xi, X.U., Min, W.A.N., Hui, D.O.N.G., BuT, P.P.H. and Foo, L.Y., 2000. Inhibitory activity of flavonoids and tannins against HIV-1 protease. Biological and Pharmaceutical Bulletin, 23, pp.1072-1076.
[31]Deng, G.F., Xu, X.R., Zhang, Y., Li, D., Gan, R.Y. and Li, H.B., 2013. Phenolic compounds and bioactivities of pigmented rice. Critical Reviews in Food Science and Nutrition, 53, pp.296-306.
[32]Fantini, M., Benvenuto, M., Masuelli, L., Frajese, G.V., Tresoldi, I., Modesti, A. and Bei, R., 2015. *In vitro* and *in vivo* antitumoral effects of combinations of polyphenols, or polyphenols and anticancer drugs: perspectives on cancer treatment. International Journal of Molecular Sciences, 16, pp.9236-9282.
[33]Block, G., Patterson, B. and Subar, A., 1992. Fruit, vegetables, and cancer prevention: a review of the epidemiological evidence. Nutrition and Cancer, 18, pp.1-29.
[34]Gordaliza, M., 2007. Natural products as leads to anticancer drugs. Clinical and Translational Oncology, 9, pp.767-776.
[35]Anand, P., Kunnumakara, A.B., Sundaram, C., Harikumar, K.B., Tharakan, S.T., Lai, O.S., Sung, B. and Aggarwal, B.B., 2008. Cancer is a preventable disease that requires major lifestyle changes. Pharmaceutical Research, 25, pp.2097-2116.
[36]Chou, C.C., Yang, J.S., Lu, H.F., Ip, S.W., Lo, C., Wu, C.C., Lin, J.P., Tang, N.Y., Chung, J.G., Chou, M.J. and Teng, Y.H., 2010. Quercetin-mediated cell cycle arrest and apoptosis involving activation of a caspase cascade through the mitochondrial pathway in human breast cancer MCF-7 cells. Archives of Pharmacal Research, 33, pp.1181-1191.
[37]Lee, Y.K., Park, S.Y., Kim, Y.M., Lee, W.S. and Park, O.J., 2009. AMP kinase/cyclooxygenase-2 pathway regulates proliferation and apoptosis of cancer cells treated with quercetin. Experimental & Molecular Medicine, 41, pp.201-207.
[38]Park, J.H., Jin, C.Y., Lee, B.K., Kim, G.Y., Choi, Y.H. and Jeong, Y.K., 2008. Naringenin induces apoptosis through downregulation of Akt and caspase-3 activation in human leukemia THP-1 cells. Food and Chemical Toxicology, 46, pp.3684-3690.
[39]Sen, P., Chakraborty, P.K. and Raha, S., 2006. Tea polyphenol epigallocatechin 3-gallate impedes the anti-apoptotic effects of lowgrade repetitive stress through inhibition of Akt and NFκ B survival pathways. FEBS Letters, 580, pp.278-284.
[40]Gong, L., Li, Y., Nedeljkovic-Kurepa, A. and Sarkar, F.H., 2003. Inactivation of NF-κ B by genistein is mediated via Akt signaling pathway in breast cancer cells. Oncogene, 22, pp.4702-4709.

protection to the cells from oxidative stress as well as treating dry cough and asthma[41]. *B. pandurata* contains an active flavanone pinostrobin (5-hydroxy-7-methoxy flavanone), a type of flavonoid, which has gained considerable interest of researchers due to its anti-dengue[42], anti-venom[43], anti-ulcerogenic[44] and nociceptive activities[45]. Many studies have been carried out to investigate its anti-proliferation property in cancer as well as normal cell lines[46,47].Pinostrobin (extract from *Polygonum lapathifolium ssp. nodosum*) has been demonstrated to exhibit anti-leukemic properties against Jurkat and HL-60 cell lines[48], Pinostrobin has also been shown to inhibit cell growth of HepG2 and MCF-7 cells by down regulating the activity of topoisomerase I and aromatase respectively[49,50]. Antiviral activity of pinostrobin against Herpes simplex virus-1 (HSV-1) has also been reported[51]. Pinostrobin does not only inhibit cell growth but also targets some important cellular enzymes that are involved in detoxification and signalling pathway such as mammalian phase 2 detoxication enzyme[52] and phosphodiesterase type 4 (PDE4) enzyme[53], respectively.

However, to the best of our knowledge, anti-cancerous property of pinostrobin in cancer cells as well as Cancer Stem like Cells (CSCs) and its mechanism of action have not been

[41]Eng-Chong, T., Yean-Kee, L., Chin-Fei, C., Choon-Han, H., Sher-Ming, W., Li-Ping, C.T., Gen-Teck, F., Khalid, N., Abd Rahman, N., Karsani, S.A. and Othman, S., 2012. *Boesenbergia rotunda*: from ethnomedicine to drug discovery. Evidence-Based Complementary and Alternative Medicine, 2012, pp. 1-25.

[42]de Sousa, L.R.F., Wu, H., Nebo, L., Fernandes, J.B., Kiefer, W., Kanitz, M., Bodem, J., Diederich, W.E., Schirmeister, T. and Vieira, P.C., 2015. Flavonoids as noncompetitive inhibitors of dengue virus NS2B-NS3 protease: Inhibition kinetics and docking studies. Bioorganic & Medicinal Chemistry, 23, pp.466-470.

[43]Gómez-Betancur, I., Benjumea, D., Patiño, A., Jiménez, N. and Osorio, E., 2014. Inhibition of the toxic effects of Bothrops asper venom by pinostrobin, a flavanone isolated from *Renealmia alpinia* (Rottb.) MAAS. Journal of Ethnopharmacology, 155, pp.1609-1615.

[44] Abdelwahab, S.I., Mohan, S., Abdulla, M.A., Sukari, M.A., Abdul, A.B., Taha, M.M.E., Syam, S., Ahmad, S. and Lee, K.H., 2011. The methanolic extract of *Boesenbergia rotunda* (L.) Mansf. and its major compound pinostrobin induces anti-ulcerogenic property *in vivo*: possible involvement of indirect antioxidant action. Journal of Ethnopharmacology, 137, pp.963-970.

[45]Gómez-Betancur, I., Cortés, N., Benjumea, D., Osorio, E., León, F. and Cutler, S.J., 2015. Antinociceptive activity of extracts and secondary metabolites from wild growing and micropropagated plants of *Renealmia alpinia*. Journal of Ethnopharmacology, 165, pp.191-197.

[46]Sopanaporn, J., Apirattikul, N. , Palaga, T., Yingyongnarongkul, B-ek. & Yompakdee, C., 2014. Anti-proliferation activity of pinostrobin from *Boesenbergia pandurata* and its efficacy improvement using cationic liposome on human cancer cell lines. TSB, The 26th Annual Meeting of the Thai society for Biotechnology and International Conference.

[47]Siekmann, T.R.L., Burgazli, K.M., Bobrich, M.A., Nöll, G. and Erdogan, A., 2013. The antiproliferative effect of pinostrobin on human umbilical vein endothelial cells (HUVEC). European Review for Medical and Pharmacological Sciences, 17, pp.668-672.

[48]Smolarz, H.D., Mendyk, E., Bogucka-Kocka, A. and Kockic, J., 2006. Pinostrobin–an anti-leukemic flavonoid from *Polygonum lapathifolium* L. ssp. nodosum (Pers.) Dans. Zeitschrift für Naturforschung C, 61, pp.64-68.

[49]Darwanto, A., Tanjung, M. and Darmadi, M.O., 2000. Cytotoxic mechanism of flavonoid from Temu Kunci (*Kaempferia pandurata*) in cell culture of human mammary carcinoma. Clinical Hemorheology and Microcirculation, 23, pp.185-190.

[50]Le Bail, J.C., Aubourg, L. and Habrioux, G., 2000. Effects of pinostrobin on estrogen metabolism and estrogen receptor transactivation. Cancer Letters, 156, pp.37-44.

[51]Wu, N., Kong, Y., Zu, Y., Fu, Y., Liu, Z., Meng, R., Liu, X. and Efferth, T., 2011. Activity investigation of pinostrobin towards herpes simplex virus-1 as determined by atomic force microscopy. Phytomedicine, 18, pp.110-118.

[52]Fahey, J.W. and Stephenson, K.K., 2002. Pinostrobin from honey and Thai ginger (*Boesenbergia pandurata*): a potent flavonoid inducer of mammalian phase 2 chemoprotective and antioxidant enzymes. Journal of Agricultural and Food Chemistry, 50, pp.7472-7476.

[53]Abd El-Hady, F.K., Shaker, K.H., Imhoff, J.F., Zinecker, H., Salah, N.M. and Ibrahim, A.M., 2013. Bioactive metabolites from propolis inhibit superoxide anion radical, acetylcholinesterase and phosphodiesterase (PDE4). International Journal of Pharmaceutical Sciences Review and Research, 21, pp.338-344.

investigated. Therefore, the present study was undertaken to elucidate the probable mechanism of pinostrobin underlying its anti-cancer activity. The main objectives of the study are:

1. To evaluate cytotoxic potential of pinostrobin in different cancer and normal cell lines *in vitro.*
2. To investigate morphological alteration induced by pinostrobin in cancer cells.
3. To examine apoptosis-inducing effect of pinostrobin and investigate possible mechanism of action *in vitro*.
4. To assess the effect of pinostrobin on Cancer Stem like Cells (CSCs) *in vitro*.
5. To investigate anticancer activity of pinostrobin *in vivo* using murine model.
6. To elucidate interaction of pinostrobin with topoisomerase I: *in silico* and *in vitro* studies.

Chapter 2

Review of literature

Cancer has emerged as a global health problem. It is characterized by the uncontrolled proliferation of cells that ultimately leads to imbalance of tissue homeostasis[1]. According to global cancer statistics, almost 12.7 million cancer cases were diagnosed in 2008[2] and approximately 8.2 million people died by cancer in 2012[3]. Deaths caused due to cancer account for approximately 13% of all deaths every year. The most common occurring cancers are lung cancer (1.4 million deaths), stomach cancer (740,000 deaths), liver cancer (700,000 deaths), colorectal cancer (610,000 deaths) and breast cancer (460,000 deaths)[4]. With new cancer cases, global burden of cancer is expected to increase from 12.7 million to 22.2 million by 2030[5]. Human Development Index (HDI) has also mentioned that cancer burden is rapidly increased in low-income and middle-income countries[5].

The increasing burden of cancer may be attributed to the modern day lifestyles such as smoking, lack of physical activity, poor diet, alcohol and tobacco. Besides, unhealthy lifestyle external (viral infection, chemicals and radiation exposure) and internal factors (mutation, hormonal imbalance and inadequate immune response) are also responsible for cancer growth[6]. As per the survey, majority of cancers (~ 90–95%) originate due to environmental exposures and remaining 5–10% cancers arise due to inherent genetics. The most common environmental factors that contribute to cancer death are diet and obesity (30–35%), tobacco (25–30%), infections (15–20%), radiation (both ionizing and non-ionizing, approximately 10%), stress, lack of physical activity, and some environmental pollutants[7].

2.1 Different phases of cancer

Hippocrates coined the Greek word carcinos for tumors that refers to the crab. Thereafter, Roman physician, Celsus coined the term cancer, the Latin word for the crab[8,9].

[1]Lockshin, R.A. and Zakeri, Z., 2007. Cell death in health and disease. Journal of Cellular and Molecular Medicine, 11, pp.1214-1224.
[2]Jemal, A., Bray, F., Center, M.M., Ferlay, J., Ward, E. and Forman, D., 2011. Global cancer statistics. CA: A Cancer Journal for Clinicians, 61, pp.69-90.
[3]Lozano, R., Naghavi, M., Foreman, K., Lim, S., Shibuya, K., Aboyans, V., Abraham, J., Adair, T., Aggarwal, R., Ahn, S.Y. and AlMazroa, M.A., 2013. Global and regional mortality from 235 causes of death for 20 age groups in 1990 and 2010: a systematic analysis for the global burden of disease study 2010. The Lancet, 380, pp.2095-2128.
[4]Cancer fact sheet N°297. 2011.World Health Organization(WHO).
[5]Bray, F., Jemal, A., Grey, N., Ferlay, J. and Forman, D., 2012. Global cancer transitions according to the Human Development Index (2008–2030): a population-based study. The Lancet Oncology, 13, pp.790-801.
[6]Ferlay, J., Soerjomataram, I., Dikshit, R., Eser, S., Mathers, C., Rebelo, M., Parkin, D.M., Forman, D. and Bray, F., 2015. Cancer incidence and mortality worldwide: sources, methods and major patterns in GLOBOCAN 2012. International Journal of Cancer, 136, pp. E359-E386.
[7]Anand, P., Kunnumakara, A.B., Sundaram, C., Harikumar, K.B., Tharakan, S.T., Lai, O.S., Sung, B. and Aggarwal, B.B., 2008. Cancer is a preventable disease that requires major lifestyle changes. Pharmaceutical Research, 25, pp.2097-2116.
[8]Hajdu, S.I., 2011. A note from history: landmarks in history of cancer, part 1. Cancer, 117, pp.1097-1102.

Hippocrates has proposed the earliest scientific theory of cancer according to which "cancer is developed by the loss of blood, phlegm, yellow bile and black bile balance in the body"[9]. Cancer is also defined as a heterogeneous group of diseases that gradually invade any part of the body and spreads throughout the body, ultimately causing death[4].Cancer growth or carcinogenesis is a complex, multi-sequence process and has three basic phases namely initiation, promotion and progression. During initiation phase of cancer, DNA is mutated /altered affecting the gene expression profile, followed by the promotion phase characterized by constant multiplication of cells and progressive focal lesion, whereas in progression phase of cancer, cells grow aggressively and migrate from original site and spread to distant sites.

2.2 Classification of cancer

Cancer is classified on the basis of origin or by the type of cells that formed them. Few major types of cancer namely Leukemia, Lymphomas, Carcinomas and Sarcomas described as below:

2.2.1 Carcinoma

Carcinoma is the most common cancer amongst all ages and generally arises in the cells of breast, prostate, lung, pancreas and colon. These types of cancer are derived from epithelial cells[10], which cover the cavities/surfaces of different vessels and organs. Carcinoma arising from different types of epithelial cells such as adenocarcinoma originates from fluids or mucus forming epithelial cells.

2.2.2 Sarcoma

Sarcoma cancer prevails in soft tissues of the body such as muscle, tendons, cartilage, bone, fat, blood vessels, lymph vessels, nerves and tissue around joints. The progression of sarcoma cancer is initiated from mesenchymal cells that are located outside the bone marrow. Osteosarcoma and Kaposi sarcoma are some of the frequently occurring examples of sarcoma cancer.

[9]Mitrus, I., Bryndza, E., Sochanik, A. and Szala, S., 2012. Evolving models of tumor origin and progression. Tumor Biology, 33, pp.911-917.
[10]Lemoine, K., Nigel & R, Nicholas., 2001. Progress in pathology. Greenwich Medical Media, London, p. 52, ISBN 9781841100500.

2.2.3 Leukemia

Leukemia arises from the hematopoietic (blood-forming) cells of the bone marrow when these cells leave bone marrow for maturation in the lymph nodes and blood. During leukemia, solid tumor is not formed but the white blood cell population increases abnormally. There are four main types of leukemia[11]: Acute lymphoblastic leukemia (ALL), Acute myeloid leukemia (AML), Chronic lymphocytic leukemia (CLL) and Chronic myeloid leukemia (CML). While the frequency of occurrence of acute lymphoblastic leukemia (ALL) is more in children (~ 30 %), adults are diagnosed with Acute myeloid leukemia (AML) and Chronic lymphocytic leukemia (CLL).

2.2.4 Lymphoma

Lymphoma arises from the abnormal growth of T and B lymphocytes (disease-fighting immune cells) in lymph vessels and lymph nodes.

There are two main types of lymphoma[12]:

- **Hodgkin's lymphoma** This cancer usually originates from B cells.
- **Non-Hodgkin's lymphoma** This cancer originates both from B cells and T cells.

2.2.5 Blastoma

This type of cancer is derived from the immature "precursor" cells or embryonic tissue. It is most commonly reported in children. Few examples of these are nephroblastoma, medulloblastoma and retinoblastoma.

2.3 Hallmarks of cancer

As mentioned earlier, cancer growth is a multistep mechanism. It is triggered by both extracellular and intracellular stimulus that affects normal cells functioning. Symptoms of diseases usually appear at later stages of manifestation. The following six characteristic hallmarks of cancer have been proposed by Hanahan and Weinberg[13] (Figure 2.1):

[11]"A Snapshot of leukemia" 2014, National Cancer Institute (NCI), 2014.
[12]The lymphoma guide information for patients and caregivers. 2013. Leukemia and Lymphoma Society, pp. 1-45.
[13]Hanahan, D. and Weinberg, R.A., 2000. The hallmarks of cancer. Cell, 100, pp. 57–70.

2.3.1 Self sufficiency of growth signals

It is well known that normal cells grow in the presence of external growth factors while cancer cells can proliferate on their own and rarely depend on external growth factors[14].

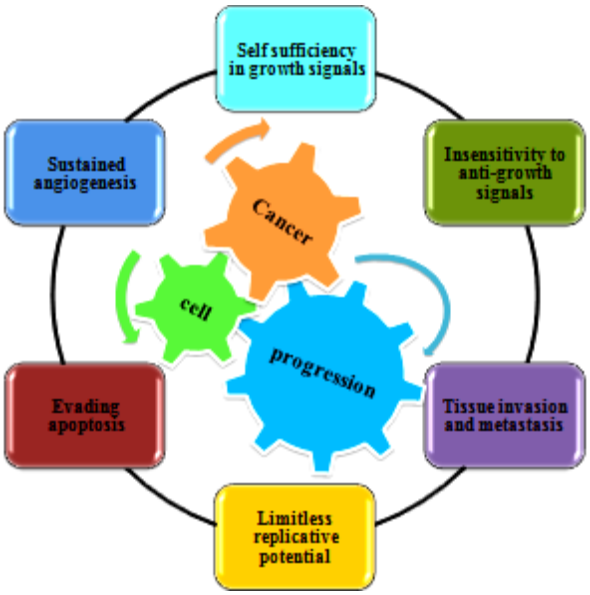

Figure 2.1. Hallmarks of cancer (Adapted form Hanahan and Weinberg , 2000)[13]

2.3.2 Insensitivity to anti-growth signals

Normal cells contain some anti-growth signals that control uncontrolled growth of the cells. However, the cancer cells are able to grow continuously, replicate and invade neighbouring cells even the presence of anti growth signals.

2.3.3 Tissue invasion and metastasis

Metastasis process is a systematic progression of cancer cells. Cancer cells witness reduction in cell-cell adhesion and higher production of extracellular matrix/basal lamina degrading proteases. This leads to higher mobility of the cells and their invasion into the surrounding tissues through the bloodstream.

2.3.4 Limitless replicative potential

Cancer cells are subjected to uncontrolled proliferation of cells that may be attributed to enhanced telomerase activity resulting in limitless DNA replication and cell divisions. As a result cancer cells retain the ability to divide indefinitely and show immortality[15].

[14]Yarden, Y. and Ullrich, A., 1988. Molecular analysis of signal transduction by growth factors. Biochemistry, 27, pp.3113-3119.

2.3.5 Sustained angiogenesis

For continuous growth of cancer, a continuous supply of growth factors is required resulting in the development of an intensive vascular network around a neoplasm. The formation of new blood vessels around the neoplasm is known as angiogenesis. The angiogenesis is not an inherent process of a normal cells, it is a property of cells of small and localized neoplasms and essential for the development of a large, potential metastatic tumor.

2.3.6 Evading apoptosis

The apoptosis occurs almost in all types of healthy cells contributing significantly to the maintainece of cell number, shape and structure of the various tissues and organs[13]. On the other hand, cancer cells are capable of avoiding or escaping the programmed cell death through impairment of p53 pathway mediated apoptosis[16].

Beside the six hallmarks of cancer (described above), Hanahan and Weinberg[13] have added two more highly potential hallmarks of cancer in 2011, which are listed below:

2.3.6.1 Deregulation of cellular energies

Cancer cells generally rely on the aerobic glycolysis for their metabolic energy requirements[17]. Cancer cells prefer glycolytic pathway over the mitochondrial oxidative phosphorylation for oxidation of carbohydrate derivatives. In hypoxic condition, cancer cells preferentially utilize glucose for their survival and growth and release lactate as a waste product. The released lactate can further get utilized by neighboring cells as a fuel material[18].

2.3.6.2 Avoiding immune destruction

Normal cells are equipped with a shield of immune system against any infection. However, cancer cells master themselves in avoiding this defence shield for their invasion and proliferation[19].

---

[15]Bryan, T.M., Englezou, A., Gupta, J.Y.O.T.H.I., Bacchetti, S. and Reddel, R.R., 1995. Telomere elongation in immortal human cells without detectable telomerase activity. The EMBO Journal, 14, pp. 4240–4248.
[16]Zusman, I.G.O.R., 1997. The role of p53 tumor-associated protein in colon cancer detection and prevention. International Journal of Oncology, 10, pp.1241-1250.
[17]Warburg, O., 1956. On respiratory impairment in cancer cells. Science, 124, pp.269-270.
[18]Kennedy, K.M. and Dewhirst, M.W., 2010. Tumor metabolism of lactate: the influence and therapeutic potential for MCT and CD147 regulation. Future Oncology, 6, pp.127-148.
[19]Vajdic, C.M. and van Leeuwen, M.T., 2009. Cancer incidence and risk factors after solid organ transplantation. International Journal of Cancer, 125, pp.1747-1754.

2.4 Mechanisms of cell death

As stated above, all the somatic cells have a definite life span and undergo limited cell division after which these cells enter senescence. When a cell's normal functioning is affected, natural phenomenon leads to its death. The term "cell death" is commonly identified as an irreversible loss of plasma membrane integrity[20]. Cell death is a cascade of molecular events that occur at both morphological and biochemical levels. Disturbance in cell death program may often result in autoimmune diseases, unbalanced immune response and cancer. Cell death is typically classified into two broad categories: as necrosis and apoptosis, that define unregulated and regulated pathways of cell death, respectively[21]. These have been described below in detail.

2.4.1 Necrosis

Necrosis is a passive, catabolic and unregulated cell death process. In other terms it is the "non-specific" form of cell death. Necrotic cell death occurs suddenly by external stimuli such as heat, acidification, osmotic shock, mechanical stress, freeze-thawing of cells[22]. This cell death process is very speedy and unregulated and therefore, it is also termed as accidental cell death. In early stage of necrosis, some alterations in cells are observed which include swelling of organelles, increase in cell volume (oncosis), loss of homeostasis, loss of plasma membrane integrity and loss of intracellular contents[23,24]. The released intracellular content affects surrounding tissue by chemotactic signals resulting in inflammation and cells damage. These infected and damaged cells are not phagocytosed by macrophages, therefore, neighbours tissue are inflammated[25]. In addition, necrosis cell death is not initiated by any initial and execution caspase (cysteine-dependent aspartate-specific proteases)[26]. Thus, necrosis cell death is unplanned and accidental death of cells.

---

[20]Kroemer, G., El-Deiry, W.S., Golstein, P., Peter, M.E., Vaux, D., Vandenabeele, P., Zhivotovsky, B., Blagosklonny, M.V., Malorni, W., Knight, R.A. and Piacentini, M., 2005. Classification of cell death: recommendations of the nomenclature committee on cell death. Cell Death & Differentiation, 12, pp.1463-1467.

[21]Ziegler, U. and Groscurth, P., 2004. Morphological features of cell death. Physiology, 19, pp.124-128.

[22]Duprez, L., Wirawan, E., Berghe, T.V. and Vandenabeele, P., 2009. Major cell death pathways at a glance. Microbes and Infection, 11, pp.1050-1062.

[23]Golstein, P. and Kroemer, G., 2007. Cell death by necrosis: towards a molecular definition. Trends in Biochemical Sciences, 32, pp.37-43.

[24]Edinger, A.L. and Thompson, C.B., 2004. Death by design: apoptosis, necrosis and autophagy. Current Opinion in Cell Biology, 16, pp.663-669.

[25]Kurosaka, K., Takahashi, M., Watanabe, N. and Kobayashi, Y., 2003. Silent cleanup of very early apoptotic cells by macrophages. The Journal of Immunology, 171, pp.4672-4679.

[26]Martin, S.J., Henry, C.M. and Cullen, S.P., 2012. A perspective on mammalian caspases as positive and negative regulators of inflammation. Molecular Cell, 46, pp.387-397.

2.4.2 Apoptosis

Apoptosis is one of the natural weapons to eliminate virus-infected or damaged cells from the body[24,27]. Naturally occurring cell death or programmed cell death i.e apoptosis was discovered by Vogt[28] in 1842 as documented by investigators[29,30]. Apoptosis is a complex energy-dependent cellular process mediated by group of cysteine proteases called "caspases". Apoptosis proceeds via a series of morphological changes including cell shrinkage, reduction of cellular volume (pyknosis), membrane blebbing, chromatin condensation, nuclear fragmentation (karyorrhexis), apoptotic bodies formation, caspase activation, loss of mitochondrial potential ($\Delta\Psi$), permeabilization of the mitochondrial outer membrane[31], exposure of phosphatidylserine (PS) residues[32] and macrophage activation for phagocytosis of the damaged and infected cells. DNA fragmentation and caspases activation are mainly observed during apoptosis[33]. Therefore, these features are helpful in differentiating the apoptotic or necrotic cells death (Table 2.1).

Table 2.1. Difference between apoptosis and necrosis cell death

Apoptosis	**Necrosis**
Cell shrinkage and convolution	Cell swellingg
Pyknosis and karyorrhexis	Karyolysis, pyknosis, and karyorrhexis
Intact cell membrane	Disintegration in cell membrane
Cytoplasm retained in apoptotic bodies	Cytoplasmic content released from cells
DNA fragmentation	No DNA fragmentation
No inflammation	Inflammation usually present
Energy requirement	No energy requirement
Caspases activation	No caspases activation

(Adapted form Duprez *et al.*, 2009)[22]

Apoptosis or programmed cell death triggers some signals for disintegration of cells that are identified as "commited suicide". A large number of physiological and pathological factors promote apoptosis, but it is not essential that apoptosis in all the cells is mediated

[27]Kerr, J.F., Wyllie, A.H. and Currie, A.R., 1972. Apoptosis: a basic biological phenomenon with wide-ranging implications in tissue kinetics. British Journal of Cancer, 26, pp. 239–257.
[28]Vogt, C., 1842. Untersuchungen (ber die Entwicklungs-geschichte der Geburtshelferkroete (Alytes obstetricans) Jent und Gassmann , Solothurn.
[29]Clarke, P.G.H. & Clarke, S., 1995. Historic apoptosis. Nature, 378, pp.230–230.
[30]Clarke, P.G. and Clarke, S., 1996. Nineteenth century research on naturally occurring cell death and related phenomena. Anatomy and Embryology, 193, pp.81-99.
[31]Green, D. and Kroemer, G., 1998. The central executioners of apoptosis: caspases or mitochondria?. Trends in Cell Biology, 8, pp.267-271.
[32]Green, D.R. and Kroemer, G., 2004. The pathophysiology of mitochondrial cell death. Science, 305, pp.626-629.
[33]Cohen, G.M. 1997. Caspases: the executioners of apoptosis. Biochem J. 15, pp.1–16.

by the same factors. Apoptosis is a cascade of molecular events that is essential for development of organism, homeostasis, tissue remodelling, repairing and removal of damaged and infected cells[34]. Apoptosis also plays an important role in defense mechanism such as in immune reactions, fighting against infectious agents and harmful agents. However, excessive apoptosis may become a reason of atrophy and insufficient rate of apoptosis may lead to cancer. Apoptosis is positively and negatively regulated by some proteins that promote or reduce apoptosis process, known as pro-apoptotic and anti-apoptotic proteins (Table 2.2)[35]

Table 2.2. List of pro-apoptotic and anti-apoptotic proteins

Pro-apoptotic proteins	Anti-apoptotic proteins
Bax	Bcl-2
Bak	Bcl-x
Bik	BAG
Bid	Mcl-1
Bad	Bcl-w
Bim	Bcl-XL
Bcl-10	Bcl-XS

(Adapted form Jourdan *et al.*, 2009)[35]

2.4.3 Apoptosis pathways

Apoptosis is a well studied complex and sophisticated process that is mediated by two major pathways: extrinsic and intrinsic pathway[22]. These pathways are described in detail in the following sections:

2.4.3.1 Extrinsic pathway

The extrinsic pathway of apoptosis is initiated from transmembrane receptor-mediated interactions that lead to death-inducing signalling complex (DISC) formation and ultimately causes cell death[36]. These transmembrane receptors are members of the tumor necrosis factor (TNF) receptor gene superfamily[37] that share similar structure of cysteine-

[34]Israels, L.G. & Israels, E.D., 1999. Apoptosis, Oncologist, 4, pp. 332-339.
[35]Jourdan, M., Reme, T., Goldschmidt, H., Fiol, G., Pantesco, V., De Vos, J., Rossi, J.F., Hose, D. and Klein, B., 2009. Gene expression of anti-and pro-apoptotic proteins in malignant and normal plasma cells. British Journal of Haematology, 145, pp.45-58.
[36]Alberts, B., Johnson, A., Lewis, J., Raff, M., Roberts, K. and Walter, P., 2002. Molecular biology of the cell, New York: Garland Science, 4th edn., Ann Bot, 91, 401. doi: 10.1093/aob/mcg023.
[37]Locksley, R.M., Killeen, N. and Lenardo, M.J., 2001. The TNF and TNF receptor superfamilies: integrating mammalian biology. Cell, 104, pp.487-501.

rich extracellular domains and cytoplasmic "death domain"[38].These death receptors are activated by binding of the extracellular ligands and then transmit the death signal from transmembrane to intracellular signalling pathways (Figure 2.2).

Some well identified ligands and their corresponding receptors involved in extrinsic apoptosis pathway are TNF-α/TNFR1, FasL/FasR, Apo3L/DR3, Apo2L/DR4 and Apo2L/DR5[39,40]. In the extrinsic pathway, FasL/FasR and TNF-α/TNFR1 ligands and their receptors have been well investigated in comparison to their counterparts. Both of these ligands and receptors fall under the TNF receptor (TNFR) family. Binding of Fas ligand (FasL) on Fas receptor (also known as Apo-1 or CD95) is a sequence of events that form aggregates and is processed with adapter protein FADD (Fas-Associated protein with Death Domain), caspase 8 and caspase 10, resulting in the formation of death-inducing signalling complex (DISC) that triggers and activates execution caspase for cell death[41,42] (Figure 2.2, Table 2.3).

Similarly binding of TNF ligand on TNF receptor (alpha: TNFR1 and TNFR2) recruits adapter proteins TRADD, FADD and RIP[41,43]. Further adaptor molecules initiate dimerization of death domain in presence of procaspase-8 and form DISC for cell death[44]. After that execution caspases are activated and lead to cell death. Thus, Fas ligand and TNF ligand activate initial and execution caspase that cause cell death. Major extrinsic pathway proteins are listed in table 2.3 along with their common names.

2.4.3.2 Intrinsic pathway

Intrinsic pathway of apoptosis is also known as mitochondrial pathway. Intrinsic pathway is initiated by non-receptor mediated stimuli and directly targets the mitochondria and other cellular organelles. Various stimuli like DNA damage, chemotherapeutic agents and oxidative stress or Reactive oxygen species (ROS)[45] activate intrinsic pathway through

[38]Ashkenazi, A. and Dixit, V.M., 1998. Death receptors: signaling and modulation. Science, 281, pp.1305-58.
[39]Peter, M.E. and Krammer, P.H., 1998. Mechanisms of CD95 (APO-1/Fas)-mediated apoptosis. Current Opinion in Immunology, 10, pp.545-551.
[40]Suliman, A., Lam, A., Datta, R .& Srivastava, R. K., 2001. Intracellular mechanisms of TRAIL: apoptosis through mitochondrial-dependent and -independent pathways. Oncogene. 20, pp.2122–2133.
[41]Wajant, H., 2002. The Fas signaling pathway: more than a paradigm. Science, 296, pp.1635-1636.
[42]Rubio-Moscardo, F., Blesa, D., Mestre, C., Siebert, R., Balasas, T., Benito, A., Rosenwald, A., Climent, J., Martinez, J.I., Schilhabel, M. and Karran, E.L., 2005. Characterization of 8p21. 3 chromosomal deletions in B-cell lymphoma: TRAIL-R1 and TRAIL-R2 as candidate dosage-dependent tumor suppressor genes. Blood, 106, pp.3214-3222.
[43]Kelliher, M.A., Grimm, S., Ishida, Y., Kuo, F., Stanger, B.Z. and Leder, P., 1998. The death domain kinase RIP mediates the TNF-induced NF-κ B signal. Immunity, 8, pp.297-303.
[44]Boatright, K.M. and Salvesen, G.S., 2003. Mechanisms of caspase activation. Current Opinion in Cell Biology, 15, pp.725-731.
[45]Armstrong, J.S., 2006. Mitochondria: a target for cancer therapy. British Journal of Pharmacology, 147, pp.239-248.

mitochondrial dysfunction. Dysfunctioning of mitochondria is a cascade of events which include loss of mitochondrial transmembrane potential, mitochondrial permeability and

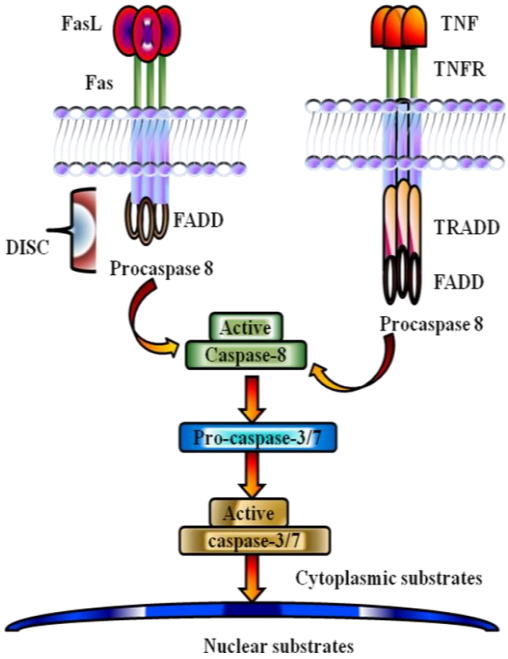

Figure 2.2. Diagrammatic representation of extrinsic pathway of apoptosis (Adapted from Marquez *et al.*, 2013)[46]

Table 2.3. List of major extrinsic pathway proteins with their full name (Modified from Elmore *et al.*, 2007) [47]

Extrinsic pathway proteins	
Abbreviation	**Full Name**
TNF-α	Tumor necrosis factor alpha
TNFR1	Tumor necrosis factor receptor 1
FasL	Fatty acid synthetase ligand
FasR D95	Fatty acid synthetase receptor
Apo3L	Apo3 ligand
DR3	Death receptor 3
Apo2L	Apo2 ligand
DR4	Death receptor 4
DR5	Death receptor 5
FADD	Fas-associated death domain
TRADD	TNF receptor-associated death domain
RIP	Receptor-interacting protein
DED	Death effector domain
caspase-8	Cysteinyl aspartic acid-protease 8
c-FLIP	FLICE-inhibitory protein

[46]Marquez, R.T., Tsao, B.W., Faust, N.F. and Xu, L., 2013. Drug resistance and molecular cancer therapy: apoptosis versus autophagy. Chapter 8, doi.org/10.5772/55415.
[47]Elmore, S., 2007. Apoptosis: a review of programmed cell death. Toxicologic Pathology, 35, pp.495-516.

release pro-apoptotic proteins from inter-membrane space of mitochondria into the cytosol[48].These released pro-apoptotic proteins such as cytochrome c, Smac/DIABLO, and serine protease HtrA2/Omi promote apoptosis through mitochondria[49,50]. Further, cytochrome c binds to Apaf-1 (Apoptotic protease activating factor-1) in the presence of ATP and forms apoptosome complex[51]. Subsequently, apoptosome recruits procaspase-9 and converts it to caspase-9 after proteolytic cleavage. (Figure 2.3). The exact mechanism of cytochrome c release has not been elucidated yet, and needs more clarification.

Other group of pro-apoptotic proteins such as Smac/DIABLO and HtrA2/Omi is involved in initiation of apoptosis by iinhibiting IAP (inhibitors of apoptosis proteins) activity[52] (Figure 2.4).In addition, endonuclease G and CAD are released from mitochondria and translocate into the nucleus to causing DNA fragmentation (upto ~ 50–300 kb) and condensing peripheral nuclear chromatin[53]. Thus, mitochondria are involved in activation of the intrinsic pathway of apoptosis[54]. At the end of apoptosis process, apoptotic cells are rapidly phagocytosed by antigen presenting cells (APCs), monocytes and macrophages without any inflammatory response as the apoptotic cells give the "eat-me" signals (phosphatidylserine, HSP70, HSP90, opsonins, thrombospondin, HMGB1 and other signalling molecules) to the phagocytotic cells[55]. The major intrinsic pathway proteins with their common names are listed in table 2.4.

Also, the ratio of pro-apoptotic and anti-apoptotic proteins govern mitochondrial membrane permeability and activate intrinsic pathway. Pro-apoptosis protein Bad (unphosphorylated) initiates intrinsic pathway by release of cytochrome c from mitochondria[56].

[48]Saelens, X., Festjens, N., Walle, L.V., Van Gurp, M., van Loo, G. and Vandenabeele, P., 2004. Toxic proteins released from mitochondria in cell death. Oncogene, 23, pp.2861-2874.

[49]Du, C., Fang, M., Li, Y., Li, L. and Wang, X., 2000. Smac, a mitochondrial protein that promotes cytochrome c–dependent caspase activation by eliminating IAP inhibition. Cell, 102, pp.33-42.

[50]Garrido, C., Galluzzi, L., Brunet, M., Puig, P. E., Didelot, C. and Kroemer, G., 2006. Mechanisms of cytochrome c release from mitochondria. Cell Death Differ,13, pp.1423–1433.

[51]Hill, M.M., Adrain, C., Duriez, P.J., Creagh, E.M. and Martin, S.J., 2004. Analysis of the composition, assembly kinetics and activity of native Apaf-1 apoptosomes. The EMBO Journal, 23, pp.2134-2145.

[52]Schimmer, A.D., 2004. Inhibitor of apoptosis proteins: translating basic knowledge into clinical practice. Cancer Research, 64, pp.7183-7190.

[53]Joza, N., Susin, S.A., Daugas, E., Stanford, W.L., Cho, S.K., Li, C.Y., Sasaki, T., Elia, A.J., Cheng, H.Y.M., Ravagnan, L. and Ferri, K.F., 2001. Essential role of the mitochondrial apoptosis-inducing factor in programmed cell death. Nature, 410, pp.549-554.

[54]Galluzzi, L., Morselli, E., Kepp, O., Vitale, I., Rigoni, A., Vacchelli, E., Michaud, M., Zischka, H., Castedo, M. and Kroemer, G., 2010. Mitochondrial gateways to cancer. Molecular Aspects of Medicine, 31, pp.1-20.

[55]Krysko, D.V., D'Herde, K. and Vandenabeele, P., 2006. Clearance of apoptotic and necrotic cells and its immunological consequences. Apoptosis, 11, pp.1709-1726.

[56]Zha, J., Harada, H., Yang, E., Jockel, J. and Korsmeyer, S.J., 1996. Serine phosphorylation of death agonist BAD in response to survival factor results in binding to 14-3-3 not BCL-X L. Cell, 87, pp.619-628.

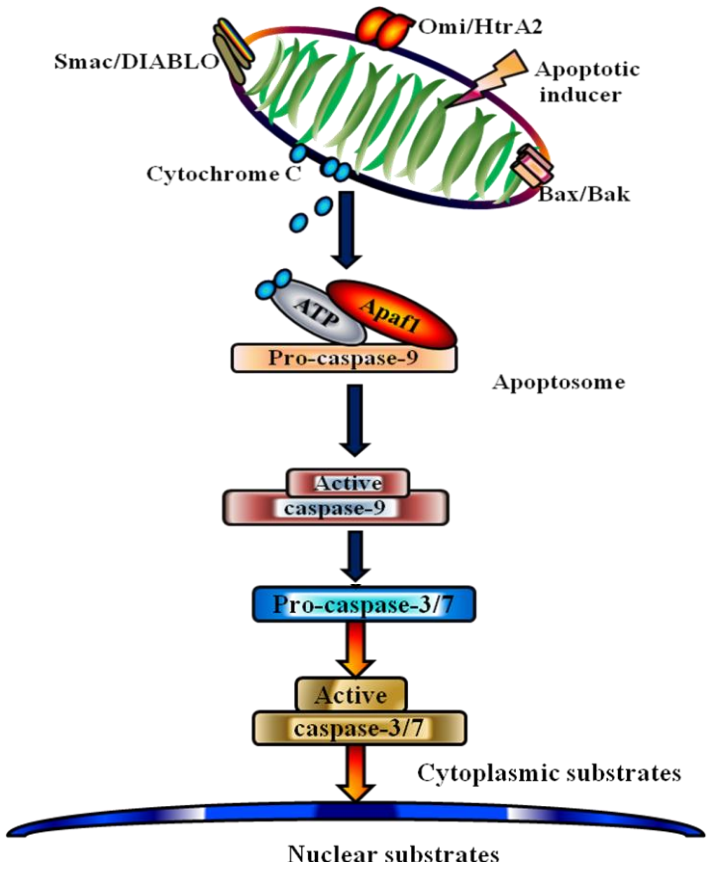

Figure 2.3. Diagrammatic representation of intrinsic pathway of apoptosis (Adapted from Marquez *et al.,* 2013)[45]

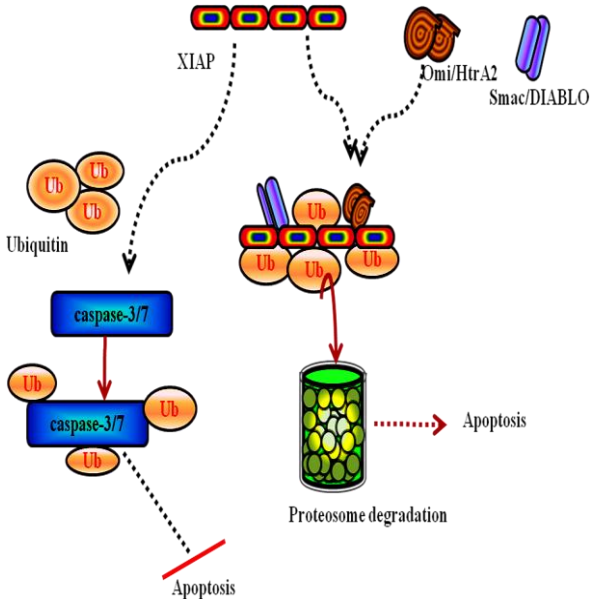

Figure 2.4. Diagrammatic representation of anti-apoptotic protein inhibition (XIAP : inhibitors of apoptosis proteins)(Adapted from Obexer *et al.,* 2014)[57]

[57]Obexer, P. and Ausserlechner, M.J., 2014. X-linked inhibitor of apoptosis protein–a critical death resistance regulator and therapeutic target for personalized cancer therapy. Frontiers in Oncology, 4, pp.1-10

Table 2.4. List of major intrinsic pathway proteins with their full name (Modified from Elmore *et al.*, 2007)[46]

Intrinsic pathway proteins	
Aberration	**Full Name**
Smac/DIABLO	Second mitochondrial activator of caspases/direct IAP binding protein with low PI
HtrA2/Omi	High-temperature requirement
IAP	Inhibitor of Apoptosis Proteins
Apaf-1	Apoptotic protease activating factor
AIF	Apoptosis Inducing Factor
CAD	Caspase-Activated DNAse
Caspase-9	Cysteinyl aspartic acid-protease-9
Bcl-2	B-cell lymphoma protein 2
BID	BH3 interacting domain death agonist
BAX	BCL2 associated X protein
BAK	BCL2 antagonist killer 1
BAD	BCL2 antagonist of cell death
Puma	BCL2 binding component 3

Bad also makes heterodimer with Bcl-Xl or Bcl-2 to neutralize its anti-apoptotic effect and promotes cell death[58]. Other pro-apoptotic proteins Bax and Bak promote apoptosis by increasing permeability of mitochondrial outer membrane (MOMP), facilitating the release of cytochrome c followed by activation of caspase and finally cell death[59]. Over expression of Bax is also involved in activation of p53 upregulated modulator of apoptosis (PUMA) which induces apoptosis through p53 mediated pathway[60].

It has been reported that both apoptosis pathways (extrinsic and intrinsic) are inter linked through an alliance of caspase 8 and cleaved Bid. The C terminal part of Bid (tBid) translocates to mitochondria and releases cytochrome c to activate intrinsic pathway[61]. This inter link is an example of "cross-talk" between the extrinsic (death-receptor) and intrinsic (mitochondrial) pathways[62].

[58]Yang, E., Zha, J., Jockel, J., Boise, L.H., Thompson, C.B. and Korsmeyer, S.J., 1995. Bad, a heterodimeric partner for Bcl-XL and Bcl-2, displaces Bax and promotes cell death. Cell, 80, pp.285-291.
[59]Youle, R.J. and Strasser, A., 2008. The BCL-2 protein family: opposing activities that mediate cell death. Nature Reviews Molecular Cell Biology, 9, pp.47-59.
[60]Liu, F.T., Newland, A.C. and Jia, L., 2003. Bax conformational change is a crucial step for PUMA-mediated apoptosis in human leukemia. Biochemical and Biophysical Research Communications, 310, pp.956-962.
[61]Gewies, A., 2003. Apo Review - Introduction to Apoptosis: pp. 1- 26.
[62]Igney, F.H. and Krammer, P.H., 2002. Death and anti-death: tumour resistance to apoptosis. Nature Reviews Cancer, 2, pp.277-288.

2.4.3.3 Execution pathway

The final destination of extrinsic and intrinsic pathways of apoptosis is execution pathway. Execution pathway is initiated by effectors or execution caspases such as caspase-3, caspase-6 and caspase-7, which further activate endonucleases and proteases to degrade nuclear material and cytoskeletal proteins, respectively. After that, these execution caspases cleave various cellular substrates such as PARP (poly ADP ribose polymerase), cytoskeletal protein alpha fodrin, cytokeratins and Nuclear Mitotic Apparatus protein (NuMA) resulting in cell death[63]. The proteins of major execution pathway with their common names are listed in table 2.5. Caspase 3 is the main execution caspase and is activated by initiator caspase-8, caspase-9 and caspase-10. In proliferating cells, endonuclease CAD makes complex with inhibitor ICAD (inhibitor of caspase-activated DNase) and becomes inactive. The caspace 3 then cleaves ICAD and releases CAD from the inhibitor. After that, free form of CAD degrades chromosomal DNA[64] and disintegrates cytoskeleton and ultimately leads to apoptosis. At the end of the apoptosis, cells are phagocytosed by antigen presenting cells (APCs) monocytes and macrophages and cleared the damage and infected cells from the body.

Table 2.5. List of major execution pathway proteins with their full name (Modified from Elmore *et al.*, 2007)[46].

Execution pathway proteins	
Aberration	**Full Name**
Caspase 3	Cysteinyl aspartic acid - 3
Caspase 6	Cysteinyl aspartic acid - 6
Caspase7	Cysteinyl aspartic acid - 7
Caspase 10	Cysteinyl aspartic acid - 10
PARP	Poly (ADP ribose) polymerase
Alpha fodrin	Spectrin alpha chain
NuMA	Nuclear mitotic apparatus protein
CAD	Caspase activated DNAse
ICAD	Inhibitor of CAD

Thus, execution phase plays a major and important role in maintenance of homeostasis, elimination of virus-infected and damaged cells from the body. Induction of apoptosis has also been proved as an attractive therapy for cancer treatment.

[63]Slee, E.A., Adrain, C. and Martin, S.J., 2001. Executioner caspase-3,-6, and-7 perform distinct, non-redundant roles during the demolition phase of apoptosis. Journal of Biological Chemistry, 276, pp.7320-7326.
[64]Enari, M., Sakahira, H., Yokoyama, H., Okawa, K., Iwamatsu, A. and Nagata, S., 1998. A caspase-activated DNase that degrades DNA during apoptosis, and its inhibitor ICAD. Nature, 391, pp.43-50.

2.5 Characteristics of apoptosis

Apoptosis is a complex cell death process. Nevertheless, it is essential for normal functioning of the body, cells growth and developments. Apoptosis is characterized by a number of features which have been described below:

2.5.1 Externalization of phosphatidylserine

Cell membrane integrity is essential for normal cell shape and survival. Apoptosis is accountable for multiple modifications within the cell such as externalization of phosphatidylserine (PS)[65]. Phosphatidylserine located in the inner side of mitochondria is a major constituent of mitochondrial architecture. During apoptosis, phosphatidylserine is externalized from inner side of mitochondria to the outer side[66]. Mechanism of externalization of phosphatidylserine is not yet fully understood. However, it has been suggested that ATP- dependent amino phospholiphid translocase is down regulated and flippase is up regulated during this event[67]. The externalization of phosphatidyserine gives signal to macrcrophages to recognize and phagocytose apoptotic cells[68]. Thus, externalization of phosphatidyserine is a hallmark of apoptosis cells. The annexinV assay has been used to examine the externalization of phosphatidylserine in apoptosis cells using flow cytometer[69,70].

2.5.2 Calcium influx

Calcium (Ca^{2+}) influx is mainly accountable for membrane fluidity. During apoptosis, activated hydrolytic enzymes degrade cytoskeletan, disturb the energy production balance, enhance membrane fluidity leading to high Ca^{2+} influx and cell death[71]. During apoptosis, increased intracellular Ca^{2+} levels and heightened oxidative stress activate

[65]Wyllie, A.H., Morris, R.G., Smith, A.L. and Dunlop, D., 1984. Chromatin cleavage in apoptosis: association with condensed chromatin morphology and dependence on macromolecular synthesis. The Journal of Pathology, 142, pp.67-77.
[66]Martin, S., Reutelingsperger, C.P., McGahon, A.J., Rader, J.A., Schie, R.C.V., LaFace, D.M. and Green, D.R., 1995. Early redistribution of plasma membrane phosphatidylserine is a general feature of apoptosis regardless of the initiating stimulus: inhibition by overexpression of Bc1-2 and Abl. Journal of Experimental Medicine, 182, pp.1545-1556.
[67]Bratton, D.L., Fadok, V.A., Richter, D.A., Kailey, J.M., Guthrie, L.A. and Henson, P.M., 1997. Appearance of phosphatidylserine on apoptotic cells requires calcium-mediated nonspecific flip-flop and is enhanced by loss of the aminophospholipid translocase. Journal of Biological Chemistry, 272, pp.26159-26165.
[68]Erwig, L.P. and Henson, P.M., 2008. Clearance of apoptotic cells by phagocytes. Cell Death & Differentiation, 15, pp.243-250.
[69]Koopman, G., Reutelingsperger, C.P., Kuijten, G.A., Keehnen, R.M., Pals, S.T. and Van Oers, M.H., 1994. Annexin V for flow cytometric detection of phosphatidylserine expression on B cells undergoing apoptosis. Blood, 84, pp.1415-1420.
[70]Boersma, A.W., Nooter, K., Oostrum, R.G. and Stoter, G., 1996. Quantification of apoptotic cells with fluorescein isothiocyanate-labeled annexin V in chinese hamster ovary cell cultures treated with cisplatin. Cytometry Part A, 24, pp.123-130.
[71]Nicotera, P. and Orrenius, S., 1998. The role of calcium in apoptosis. Cell Calcium, 23, pp.173-180.

calcium-dependent endonucleases and damage DNA[72]. Thus, enhancement of Ca^{2+} is an indicator of apoptosis.

2.5.3 Apoptotic body formation

During apoptosis process, cells exhibit distinctive changes like condensation of chromatin and nuclei, reduction in cell volume and membrane blebbing. Subsequently, cells are detached from surface (*in vitro*) and form apoptotic bodies, which is also one of the major characteristics of apoptosis[73].

2.5.4 Reactive oxygen species (ROS) generation

ROS are generated by endogenous and exogenous agents such as hydroxyl radicals, singlet oxygen, peroxyl redicals, hydrogen peroxide and superoxide anions[74]. During apoptosis, ROS are mainly produced in mitochondria. Further, these ROS enhance oxidative stress and degrade DNA, inducing apoptosis[75]. Increased levels of oxidative stress are prominent indicator of apoptosis and initiate of cell death.

2.5.5 Reduction in antioxidant defense proteins

Under normal circumstances, ROS production is countered by intracellular antioxidant defense systems such as glutathione peroxidase (Gpx)[76,77], superoxide dismutase (SOD)[77], catalase[77]and tripeptide glutathione (GSH)[78]. GSH is a multifunctional, non-enzymatic intracellular antioxidant polypeptide. It is reported in soluble form in cytosol, mitochondria and nucleus. Glutathione shows antioxidant capacity due to sulphur atom which manages single electron loss[79]. GSH is involved in reducing various disulfides and maintains cell viability in oxidative stress condition. Intracellular GSH is able to protect

[72]Wiseman, H., Kaur, H. and Halliwell, B., 1995. DNA damage and cancer: measurement and mechanism. Cancer Letters, 93, pp.113-120.
[73]Srinivas, G., Anto, R.J., Srinivas, P., Vidhyalakshmi, S., Senan, V.P. and Karunagaran, D., 2003. Emodin induces apoptosis of human cervical cancer cells through poly (ADP-ribose) polymerase cleavage and activation of caspase-9. European Journal of Pharmacology, 473, pp.117-125.
[74]Halliwell, B., 1989. Free radicals, reactive oxygen species and human disease: a critical evaluation with special reference to atherosclerosis. British Journal of Experimental Pathology, 70, pp.737–757.
[75]Shokolenko, I., Venediktova, N., Bochkareva, A., Wilson, G.L. and Alexeyev, M.F., 2009. Oxidative stress induces degradation of mitochondrial DNA. Nucleic Acids Research, 37, pp.2539-2548.
[76]Han, D., Antunes, F., Canali, R., Rettori, D. and Cadenas, E., 2003. Voltage-dependent anion channels control the release of the superoxide anion from mitochondria to cytosol. Journal of Biological Chemistry, 278, pp.5557-5563.
[77]Michiels, C., Raes, M., Toussaint, O. and Remacle, J., 1994. Importance of Se-glutathione peroxidase, catalase, and Cu/Zn-SOD for cell survival against oxidative stress. Free radical Biology and Medicine, 17, pp.235-248.
[78]Sies, H., 1999. Glutathione and its role in cellular functions. Free Radical Biology and Medicine, 27, pp.916-921.
[79]Karoui, H., Hogg, N., Fréjaville, C., Tordo, P. and Kalyanaraman, B., 1996. Characterization of sulfur-centered radical intermediates formed during the oxidation of thiols and sulfite by peroxynitrite ESR-spin trapping and oxygen uptake studies. Journal of Biological Chemistry, 271, pp.6000-6009.

cell from damage by antineoplastic agents, free radicals and ROS[80]. It is well known that apoptosis is induced by ROS generation and depletion of intracellular GSH[81.] Thus reduction of antioxidant defence molecules such as GSH can also be considered as a marker of apoptosis.

2.5.6 Depolarization of mitochondrial membrane potential (ΔΨm)

During apoptosis mitochondria become dysfunctional or depolarized and lose their membrane potential (ΔΨm) due to release of cytochrome c[82,83,84]. Sun *et al., (*2007) have demonstrated that depolarization of mitochondria is a sequential process involving loss of ΔΨm, release of cytochrome c and vasiculation in mitochondria[85]. Thus, reduction of mitochondrial membrane potential is also an indicator of apoptosis.

2.5.7 DNA fragmentation and chromatin condensation

DNA fragmentation and chromatin condensation are major hallmarks of apoptosis. Generally DNA fragmentation and chromatin condensation are mediated by some pro-apoptotic proteins such as AIF, endonuclease G and CAD. During apoptosis, these proteins move to nucleus and condense peripheral nuclear chromatin and fragments DNA approximately 50-300 kb size[53]. Similarly, endonuclease G cleaves nuclear chromatin and produces oligonucleosomal DNA fragment[86]. Both of these mechanisms occur in caspase-independent manner, whereas pro-apoptotic protein CAD is activated by caspase 3, condenses chromatin and fragments oligonucleasomal DNA[53].

2.5.8 Activation of caspases

Caspases are a family of cysteine proteases that exist as zymogens. These caspases get activated by proteolytic cleavage and then promote apoptosis[87]. They are present either as

---

[80]Arrick, B.A. and Nathan, C.F., 1984. Glutathione metabolism as a determinant of therapeutic efficacy: a review. Cancer Research, 44, pp.4224-4232.
[81]Fernandes, R.S. and Cotter, T.G., 1994. Apoptosis or necrosis: intracellular levels of glutathione influence mode of cell death. Biochemical Pharmacology, 48, pp.675-681.
[82] Green, D.R. and Reed, J.C., 1998. Mitochondria and apoptosis. Science, 281, pp.1309-12.
[83]Goldstein, J.C., Munoz-Pinedo, C., Ricci, J.E., Adams, S.R., Kelekar, A., Schuler, M., Tsien, R.Y. and Green, D.R., 2005. Cytochrome c is released in a single step during apoptosis. Cell Death & Differentiation, 12, pp.453-462.
[84]Goldstein, J.C., Waterhouse, N.J., Juin, P., Evan, G.I. and Green, D.R., 2000. The coordinate release of cytochrome c during apoptosis is rapid, complete and kinetically invariant. Nature Cell Biology, 2, pp.156-162.
[85]Sun, M.G., Williams, J., Munoz-Pinedo, C., Perkins, G.A., Brown, J.M., Ellisman, M.H., Green, D.R. and Frey, T.G., 2007. Correlated three-dimensional light and electron microscopy reveals transformation of mitochondria during apoptosis. Nature Cell Biology, 9, pp.1057-1065.
[86]Li, L.Y., Luo, X. and Wang, X., 2001. Endonuclease G is an apoptotic DNase when released from mitochondria. Nature, 412, pp.95-99.
[87]Alnemri, E.S., Livingston, D.J., Nicholson, D.W., Salvesen, G., Thornberry, N.A., Wong, W.W. and Yuan, J., 1996. Human ICE/CED-3 protease nomenclature. Cell, 87, p.171.

monomer or dimer and it is the dimeric form that has the catalytic activity through its dimeric domain (α β β'α' symmetry)[88]. As mentioned earlier, apoptosis is mediated by initiator (Caspase-2, -8,-9,-10) and execution (Caspase-3,-6,-7) caspases, of which execution caspase -3 is mainly accountable for cell death. Therefore, caspases activation is also a most important marker of apoptosis.

2.6 Cell cycle

Cell cycle is an ordered series of events, comprising mainly of two phases: interphase and mitotic phase. The interphase is divided into G1 (Gap), S (synthesis) and G2 (Gap) phases. Cells that are metabolically active in G1 phase enter into S phase for DNA synthesis and duplication, whereas cells of the G2 phase are involved in production of the components of mitosis. Cells of M (mitotic) phase produce two daughter cells after cell division. Sometime external stimuli cause metabolic inactivation of cells, and the cells enter into G0 phase or in quiescence state. When cells are exposed to favourable conditions, they re-enter into early G1 phase[89].

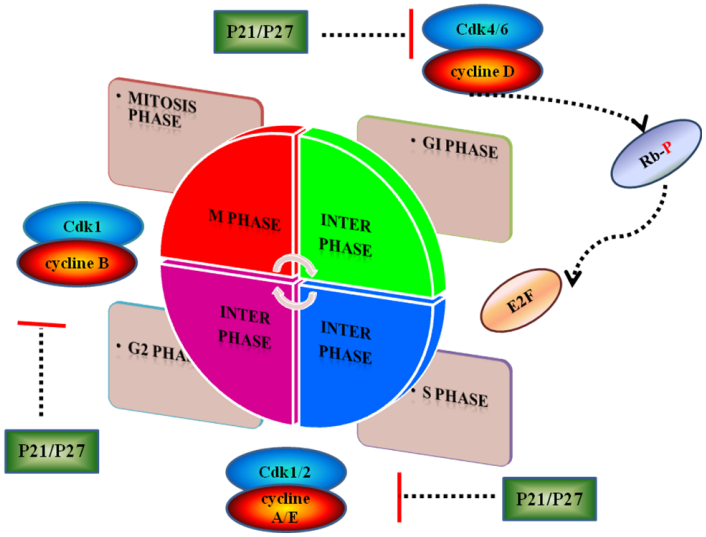

Figure 2.5. Schematic representation of cell cycle regulation (Adapted from Berndt, 1999)[90]

The cell cycle regulation is essential for DNA repairing, cell survival and progression. There are some regulatory proteins (cyclins and cyclin dependent kinases; cdks) that resist the progression of cell growth at specific points which are known as "checkpoint"

[88]Pop, C. and Salvesen, G.S., 2009. Human caspases: activation, specificity, and regulation. Journal of Biological Chemistry, 284, pp.21777-21781.
[89]Israels, E.D. and Israels L.G.,2000, The cell cycle. Oncologist, 5, pp. 510-513.
[90]Berndt, N., 1999. Protein dephosphorylation and the intracellular control of the cell number. Front Biosci, 4, pp.D22-D42.

(Figure 2.5). Two major check points that have been identified in cell cycle are the G1 to S transition and G2 to M transition[91]. The cell cycle regulation is essential for cell growth, development and preventing uncontrolled proliferation of cells.

2.6.1 Role of cyclins and cyclin dependent kinases (cdks) in cell cycle regulation

Cell cycle regulation is mainly coordinated by cyclin and cdks. Cell cycle regulation also relies on cyclin and cdks inhibitors. Cdks are catalytic units that are expressed throughout the cell cycle. Cdks bind to specific cyclins and phosphorylate intracellular targets, allowing the cell to enter into next phase of cell cycle. Expression levels of each cyclin independently increase or decrease at different stages of the cell cycle[92], thus providing a direction to the cell to move from one phase to another. These cyclins differ from one phase to another. For example, cyclin D associates with cdk4/6 in early G1 phase, while cyclin E associates with cdk2 in late G1 phase and makes a complex for phosphorylation, which further allows G1 to S transition of cells. These kinase complexes phosphorylate Retinoblastoma protein (Rb) and release E2F transcription factor. Further, E2F regulates expression of essential replicating enzymes which are required in S phase[93]. Cyclin A binds with cdk2 in S phase and phosphorylates target proteins that allow DNA synthesis and replication. Similarly, cyclin B binds with cdk1 (cdc2) in G2 phase and activates structural components that are associated with mitotic division (Figure 2.5).

Besides cyclin and cdks, cells growth is also regulated by kinases such as ataxia-telangiectasia mutated (ATM) kinase and phosphatidylinositol 3-kinase like protein kinase (PIKKs)[94]. ATM phosphorylates and activates several downstream proteins to arrest the cells in G1/S and G2/M phases. Likewise, ATM phosphorylates p53 to enhance its stability and activity[95]. p53 is negatively regulated by Mouse double minute 2 homolog (MDM2) or E3 ubiquitin-protein ligase Mdm2, also phosphorylated by ATM[96].

---

[91]Ree, A.H., Stokke, T., Bratland, Å., Patzke, S., Nome, R.V., Folkvord, S., Meza-Zepeda, L.A., Flatmark, K., Fodstad, Ø. and Andersson, Y., 2006. DNA damage responses in cell cycle G2 phase and mitosis-tracking and targeting. Anticancer Research, 26, pp.1909-1916.

[92]Dorée, M.A.R.C.E.L. and Galas, S., 1994. The cyclin-dependent protein kinases and the control of cell division. The FASEB Journal, 8, pp.1114-1121.

[93]Weinberg, R.A., 1995. The retinoblastoma protein and cell cycle control. Cell, 81, pp.323-330.

[94]Khanna, K.K. and Jackson, S.P., 2001. DNA double-strand breaks: signaling, repair and the cancer connection. Nature Genetics, 27, pp.247-254.

[95]Saito, S.I., Goodarzi, A.A., Higashimoto, Y., Noda, Y., Lees-Miller, S.P., Appella, E. and Anderson, C.W., 2002. ATM mediates phosphorylation at multiple p53 sites, including Ser46, in response to ionizing radiation. Journal of Biological Chemistry, 277, pp.12491-12494.

[96]Maya, R., Balass, M., Kim, S.T., Shkedy, D., Leal, J.F.M., Shifman, O., Moas, M., Buschmann, T., Ronai, Z.E., Shiloh, Y. and Kastan, M.B., 2001. ATM-dependent phosphorylation of Mdm2 on serine 395: role in p53 activation by DNA damage. Genes & Development, 15, pp.1067-1077.

MDM2 loses its activity post phosphorylation and activates p53 to arrest cell cycle in G1/S phase. In addition, activated p53 inhibits the activity of cyclin B1/cdc2 in G2 phase[97,98].

As stated earlier, the cell cycle is also regulated by cyclin-cdk complex inhibitors such as $p21^{cip1}$ and $p27^{kip1}$. These inhibitors bind to cdk and inhibit their kinase activity. $p27^{Kip1}$ has been shown to bind with cyclin/cdk complex of G1-phase and deactivate this complex, allowing the cells to enter into G0 phase[99]. Another cyclin-cdk regulatory factor $p21^{cip1}$ regulates enzymatic activity of cyclin/cdk complexes in late G1-phase. These checkpoints help in keeping a check on uncontrolled proliferation of cells.

2.7 Treatment of cancer

Various standard methods that have been in use to treat cancer include surgical removal, hormonal therapy, radiation therapy, chemotherapy, immunotherapy and targeted therapy. The suitability of treatment methodology depends on the location, stage and types of the tumor. The earliest Egyptians were aware to the surgical correction of tumour and executed around 2750 BC in Egypt. Later hormone therapy was discovered and came in practice since 1896, while radiation therapy came in application in 1899[100]. Besides these traditional therapies, few novel and advance therapies like chemotherapy, immunotherapy and targeted therapies that developed during 20^{th} century have also been used for cancer treatment. However, all of this therapeutics has severe adverse effects associated with their usage as described below:

2.7.1 Surgical therapy

Surgery is a primary method for the removal of tumor without affecting the neighbouring cells and tissues. Surgical treatment is effective against many localized tumors viz. breast cancer, cervical cancer and colorectal cancer, in their early stage of progression[101]. However, surgical therapy is impractical and failed when cancer cells have already metastasized to other parts of the body. In this situation, single cancer cell proliferate

[97]Park, M., Chae, H.D., Yun, J., Jung, M., Kim, Y.S., Kim, S.H., Han, M.H. and Shin, D.Y., 2000. Constitutive activation of cyclin B1-associated cdc2 kinase overrides p53-mediated G2-M arrest. Cancer Research, 60, pp.542-545.
[98]Alarcon-Vargas, D. and Ronai, Z.E., 2002. p53–Mdm2—the affair that never ends. Carcinogenesis, 23, pp.541-547.
[99]Sherr, C.J. and Roberts, J.M., 1995. Inhibitors of mammalian G1 cyclin-dependent kinases. Genes & Development, 9, pp.1149-1163.
[100]Sudhakar, A., 2009. History of cancer, ancient and modern treatment methods. Journal of Cancer Science & Therapy, 1, pp.1-4.
[101]Subotic, S., Wyler, S. & Bachmann, A., 2012. "Surgical treatment of localised renal cancer". European Urology Supplements. 11, pp. 60–65.

again and again and form a new tumor. This process of re-proliferation is known as recurrence. Thus, surgical therapy is mainly effective against localized tumor in early stages but not for all types of cancer.

2.7.2 Radiation therapy

In radiation therapy (also called radiotherapy, X-ray therapy), high-energy radiations are used to destroy or shrink tumors. Low energy X-ray beam is most commonly used for treatment of skin cancers while higher energy X-ray beam is applied for the treatment of cancers inside the body[102]. These ionizing radiations are capable of killing cancer cells by damaging their DNA (genetic material), leading to cell death. Radiation therapy relies on various factors like stages of cancer, skin sensitivity, irritation and tumor location. This therapy can cure or reduce severity in all types of solid tumors like brain, breast, cervix, larynx, liver, lung, pancreas, prostate, skin, stomach and uterus. Although, cancer cells are more sensitive to radiation and typically die after treatment, it also has a potential to damage the nearby healthy cells. Thus, these adverse effects of radiation on the healthy cells and tissues discourage the use of this therapy.

2.7.3 Hormonal therapy

Hormone therapy is an old method of cancer treatment that started in 1896. It has been reported that specific hormones act as therapeutic drugs and inhibit tumor growth at lower cost. For example, estrogen, progestogen and their analogues inhibit tumor growth in certain cancers[103]. Hormonal treatment of recurrent endometrial cancer majorly relies on expression of these hormone receptors[103]. Tumors that express these receptors are the most sensitive to this therapy, while lower expression of hormone receptors showed less sensitivity, loss of functional property due to methylation[104] and failed to inhibit proliferation of cancerous cells.

2.7.4 Chemotherapy

Chemotherapy utilizes drugs or medicines to eliminate the cancer cells. The term "chemotherapy" refers to the use of cytotoxic drugs and medicines that affect and stop

[102]Hill, R., Healy, B., Holloway, L., Kuncic, Z., Thwaites, D. and Baldock, C., 2014. Advances in kilovoltage x-ray beam dosimetry. Physics in Medicine and Biology, 59, pp.R183-231.
[103]Carlson, M.J., Thiel, K.W. and Leslie, K.K., 2014. Past, present, and future of hormonal therapy in recurrent endometrial cancer. Int J Womens Health, 6, pp.429-435.
[104]Wajed, S.A., Laird, P.W. and DeMeester, T.R., 2001. DNA methylation: an alternative pathway to cancer. Annals of Surgery, 234, pp.10-20.

rapid cells division. Normally chemotherapeutic drugs (taxol, docetaxel and doxorubucin) inhibit the growth of rapidly dividing cells by interfering in the molecular mechanism of the DNA replication. It is reported that if chemotherapy is added to surgical and radiation therapy, it improves effectiveness of therapies. Likewise some drugs perform better if applied in combination form rather than alone at similar time intervals, known as "combination chemotherapy"[105]. Chemotherapy affects the entire body and not a single part of the body. It targets rapidly dividing cancer cells. In addition, the other quickly dividing cells in the body such as hair follicle, cells in the bone marrow and cells that line our stomachs also get affected by chemotherapy. Since the drugs are not able to distinguish the cancer cells and our bodies's rapidly dividing cells, chemotherapy results in adverse side effects like alopecia (hair loss), myelosuppression (decreased production of blood cells), stomach upset and mucositis (inflammation of the lining of the digestive tract) .Chemotherapeutic drugs that specifically target the cancer cells would therefore be more acceptable.

2.7.5 Immunotherapy

Immunotherapy is an immune stimulating therapy that promotes our body's immune system to fight cancer. In this, cancer patient is administered with various anti-cancer immune agents, factors and proteins such as interferons (IFN-α & IFN-β) and interleukins (IL-2, IL-15 & IL-21) to promote the immune system and prevent cancer growth[106]. Allogeneic hematopoietic stem cell transplantation ("bone marrow transplantation" from a genetically non-identical donor) is a part of immunotherapy, also given for cancer treatment. In allogeneic transplantation, donor's immune cells are genetically dissimilar to the recipient's tumor cells. This phenomenon is known as graft-versus-tumor effect. Therefore, its side effects are more severe. Besides, allogeneic treatment, Autologous Immune Enhancement Therapy (AIET- transplantation of cells or tissues obtained from the same individual) is also given to patient according to physiological condition of cancer patient and did not exert any side effects[107]. Many a times, immunotherapy is not successful due to lack of or low levels expression of given interferon and interleukins, For example, active immunotherapy for cancer treatment

[105]Takimoto, C.H. and Calvo, E., 2008. Principles of oncologic pharmacotherapy. Cancer Management: A Multidisciplinary Approach, 11, pp.1-9.
[106]Lee, S. and Margolin, K., 2011. Cytokines in cancer immunotherapy. Cancers, 3, pp.3856-3893.
[107]Damodar, S., Terunuma, H., Sheriff, A.K., Farzana, L., Manjunath, S., Senthilkumar, R., Shastikumar, G. and Abraham, S., 2006. Autologous Immune Enhancement Therapy (AIET) for a case of Acute Myeloid Leukemia (AML)-our experience. Journal of Stem Cells and Regenerative Medicine, 1, pp.40-41.

require appropriate target antigens and good optimization between antigen presenting cells and T cells interaction, while passive immunotherapy used monoclonal antibodies and receptor Fc-fusion protein , therefore passive immunotherapy shows great clinical applications. In addition, eleven monoclonal antibodies have been approved to prevent allogenic transplant rejection and treat cancer[108]. Thus, the efficiency of treatment can be improved with addition of drugs which induce our body's immune system.

2.7.6 Targeted therapy

Targeted therapy is an advanced and new method for cancer treatment first reported in 1990s, showing significant impact in cancer treatment. Presently this therapy is one of the most preferred methods for cancer treatment. This therapy uses drugs and natural substances to target cancer cells only through blocking the biological processes of tumors, cuting off growth factor and blood supply to the tumor that ultimately leads to cancerous cell death. For example, imatinib (BCR–ABL:a fusion gene is created by juxt a positioning the Abl1 gene on chromosome 9 to a part of the BCR & PDGFR:platelet-derived growth factor receptor) and gefitinib (EGFR:epidermal growth factor receptor) able to bind the catalytic cleft of these tyrosine kinases and inhibiting its activity[109,110]. The first targeted therapy was developed to block the estrogen receptor functionality to control breast cancer growth[111]. Similarly chronic myelogenous leukemia (CML) was treated by Bcr-Abl inhibitors[112]. It is thought that targeted therapies may overcome the most concerning issue of drug resistance and differentiate specific molecular targets on cancer cells, thus not affecting the normal cells.

All the therapies available till date except for targeted therapy have shown severe adverse effects in patients post treatment. Therefore, researchers are actively engaging in search of advanced treatment techniques, offering maximum protection from the tumor in question with minimal adverse affects. Recently, scientific findings have highlighted the therapeutic potential of natural products against different types of cancer. These biocompatible plant derivatives are inexpensive in terms of cost of production, safe to inject/intake by the patient and easily available. A large number of natural products have

[108]Waldmann, T.A., 2003. Immunotherapy: past, present and future. Nature Medicine, 9, pp.269-277.
[109]Chen, Y.F. and Fu, L.W., 2011. Mechanisms of acquired resistance to tyrosine kinase inhibitors. Acta Pharmaceutica Sinica B, 1, pp.197-207.
[110]Weinberg, R.A., 2007. The nature of cancer. The Biology of Cancer, pp.25-56.
[111]Joo, W.D., Visintin, I. and Mor, G., 2013. Targeted cancer therapy–are the days of systemic chemotherapy numbered?. Maturitas, 76, pp.308-314.
[112]Fausel, C., 2007. Targeted chronic myeloid leukemia therapy: seeking a cure. Journal of Managed Care Pharmacy, 13, pp.8-12.

already been approved for treatment of many diseases[113,114,115] which will be discussed in detail in the forthcoming section.

2.8 Natural products and cancer

Phytochemicals are chemical constituents of different plants, and have received tremendous attention among nutritionists owing to their antioxidant property and associated health benefits[116]. Epidemiological studies revealed that more than 50% approved anticancer drugs are derived from natural sources[117] for example taxol and vinca alkaloids are extensibly used and prevent rapid proliferation of cancer cells[118]. These phytochemicals vary in their biological functions, having antioxidant, anti-carcinogenic, anti-oestrogenic, anti-inflammatory, immune potentiating activity as well as serving as a source of dietary fiber[119]. Phytochemicals have also been reported to inhibit various metabolic and signalling pathways such as MAPKs, PI3K / AKT or NFkB[120,121] which inhibit cancer cell growth. A number of reports have been put forth depicting their role in prevention of cell growth, proliferation, differentiation, survival and cell death[122,123,124]. Different biological activities of different phytochemicals have been attributed to variation in their structures. Phytochemicals are mainly classified into five groups that are listed along with their subclasses in table 2.6.

Polyphenols is the biggest group of phytochemicals and abundant in plant-derived foods. Polyphenols are secondary metabolites of plants and present as micronutrients in our diet[125],.

---

[113]Pan, M.H., Lai, C.S., Wang, H., Lo, C.Y., Ho, C.T. and Li, S., 2013. Black tea in chemo-prevention of cancer and other human diseases. Food Science and Human Wellness, 2, pp.12-21.

[114]Saxena, M., Saxena, J. and Pradhan, A., 2012. Flavonoids and phenolic acids as antioxidants in plants and human health. Int. J. Pharm. Sci. Rev. Res, 16, pp.130-134.

[115]Zhang, A., Sun, H. and Wang, X., 2013. Recent advances in natural products from plants for treatment of liver diseases. European Journal of Medicinal Chemistry, 63, pp.570-577.

[116]Dai, J. and Mumper, R.J., 2010. Plant phenolics: extraction, analysis and their antioxidant and anticancer properties. Molecules, 15, pp.7313-7352.

[117]Balunas, M.J. and Kinghorn, A.D., 2005. Drug discovery from medicinal plants. Life sciences, 78, pp.431-441.

[118]Prasain, J.K. and Barnes, S., 2007. Metabolism and bioavailability of flavonoids in chemoprevention: current analytical strategies and future prospectus. Molecular Pharmaceutics, 4, pp.846-864.

[119]Das, L., Bhaumik, E., Raychaudhuri, U. and Chakraborty, R., 2012. Role of nutraceuticals in human health. Journal of Food Science and Technology, 49, pp.173-183.

[120]Weng, C.J. and Yen, G.C., 2012. Chemopreventive effects of dietary phytochemicals against cancer invasion and metastasis: phenolic acids, monophenol, polyphenol, and their derivatives. Cancer Treatment Reviews, 38, pp.76-87.

[121]Vauzour, D., Rodriguez-Mateos, A., Corona, G., Oruna-Concha, M.J. and Spencer, J.P., 2010. Polyphenols and human health: prevention of disease and mechanisms of action. Nutrients, 2, pp.1106-1131.

[122]Youns, M. and Hegazy, W.A.H., 2017. The natural flavonoid fisetin inhibits cellular proliferation of hepatic, colorectal, and pancreatic cancer cells through modulation of multiple signaling pathways. PLoS One, 12, pp.1-18.

[123]Zhou, Y., Zheng, J., Li, Y., Xu, D.P., Li, S., Chen, Y.M. and Li, H.B., 2016. Natural polyphenols for prevention and treatment of cancer. Nutrients, 8, pp. 1-35.

[124]Sung, B., Chung, H.Y. and Kim, N.D., 2016. Role of Apigenin in cancer prevention via the induction of apoptosis and autophagy. Journal of Cancer Prevention, 21, pp.216-226.

[125]Manach, C., Scalbert, A., Morand, C., Rémésy, C. and Jiménez, L., 2004. Polyphenols: food sources and bioavailability. The American Journal of Clinical Nutrition, 79, pp.727-747.

Table 2.6. List of class and sub-class of phytochemicals (Modified from Bellik *et al.*, 2012)[126]

Classes	Sub class of phytochemicals
Carotenoids	Lycopene, alfa and beta-Carotenes, Lutein, beta-Cryptoxanthin, Zeaxanthin, Astaxanthin
Polyphenols/Phenolic compounds	Phenolic acids, Flavonoids, Stibenes, Coumarins Tannins
Alkaloids	True alkaloids, Protoalkaloids, Polyamine alkaloids, Pseudoalkaloids, Peptide and cyclopeptide alkaloids
Nitrogenous-compounds	Non-protein amino acid, amines, cyanogenic glyucosides, glucosinolates, alkamides
Organosulphur compounds	Isothiocyanates, Allylic sulphur compounds, Indoles

Polyphenols have also been reported to confer protection against cancer, cardiovascular diseases, diabetes, osteoporosis and neurodegenerative diseases[127]. This therapeutic activity of polyphenols depends on the amount of consumption and bioavailability. The effect of plant-derived foods against cancer may differ due to varying composition of polyphenols in different plants. Cancer growth has been shown to be inhibited by consumption of diets mainly consisting of plant derived fruits, vegetables and whole grains[128]. Presently a large number of polyphenols have been identified capable of exhibiting anti-cancer activity but their biological activity still remains undefined. Therefore, understanding of polyphenols properties is necessary for their therapeutic application in cancer prevention/reduction and improvement in human health.

2.8.1 Polyphenols and flavonoides

In 1930s, scientists Rusznyák and Szent-Györgyi identified a substance in lemon peel that could reduce capillary permeability. On the basis of its function, they named it as "Vitamin P," (P for permeability)[129]. Subsequently, it was confirmed that Vitamin P was a mixture of polyphenols. Polyphenol or phenolic compounds are a group of chemical

[126]Bellik, Y., Boukraâ, L., Alzahrani, H.A., Bakhotmah, B.A., Abdellah, F., Hammoudi, S.M. and Iguer-Ouada, M., 2012. Molecular mechanism underlying anti-inflammatory and anti-allergic activities of phytochemicals: an update. Molecules, 18, pp.322-353.
[127]Pandey, K.B. and Rizvi, S.I., 2009. Plant polyphenols as dietary antioxidants in human health and disease. Oxidative Medicine and Cellular Longevity, 2, pp.270-278.
[128]Kushi, L.H., Byers, T., Doyle, C., Bandera, E.V., McCullough, M., Gansler, T., Andrews, K.S. and Thun, M.J., 2006. American cancer society guidelines on nutrition and physical activity for cancer prevention: reducing the risk of cancer with healthy food choices and physical activity. CA: A Cancer Journal for Clinicians, 56, pp.254-281.
[129]Geleijnse, J.M. and Hollman, P.C., 2008. Flavonoids and cardiovascular health: which compounds, what mechanisms?. The American Journal of Clinical Nutrition, 88, pp.12-13.

substances with hydroxyl groups on aromatic rings. Polyphenols are the key constituents of healthy and balanced diet and are found in dietary products such as fruit, vegetables, cereals, olive oil, dry legumes, beverages, tea, coffee and wine[130,131]. Polyphenols are the most abundant secondary metabolites, derived from primary metabolites of plants. Polyphenols are actively involved in various defence mechanisms of plant such as UV protection, defence against biotic and abiotic stresses, pigmentation, and participate in the growth and development of plant[132]. Many epidemiological studies have suggested that long term consumption of polyphenols rich diets offer protection against cardiovascular diseases[133], cancer[122] and diabetes[134]. Polyphenols are further classified on the basis of their basic chemical structure into phenolic acids, flavonoids, lignans, stilbenes, coumarins and tannins.

Flavonoids are the most abundant and ubiquitously distributed polyphenolic compounds of plant[131].The chemical structure and activity of several flavonoides are similar to naturally occurring estrogens, also known as phytoestrogens[135]. From the different drugs available for cancer treatment, 1073 chemical compounds have been approved between 1981 and 2010, of which 36% were pure synthetic chemicals, and more than the half of these have been derived or inspired from natural sources[136].

Flavonoids can also be modified to form diverse chemical compounds by substitutions of hydroxyl, methoxyl, methyl, isoprenyl and benzyl groups at different positions in the flavonoid structures. Flavonoids are also classified into different groups on the basis of their heterocyclic ring C such as flavonols, flavones, isoflavones, flavanols, flavanones and anthocyanidins[137]. Some common subclasses flavonoids which are important constituents of healthy diet are listed in table 2.7 along with their food sources.

[130] Oliveira, L.D.L.D., Carvalho, M.V.D. and Melo, L., 2014. Health promoting and sensory properties of phenolic compounds in food. Revista Ceres, 61, pp.764-779.
[131]Durazzo, A., 2017. Study approach of antioxidant properties in foods: update and considerations. Foods, 6,pp.1-7
[132]Mierziak, J., Kostyn, K. and Kulma, A., 2014. Flavonoids as important molecules of plant interactions with the environment. Molecules, 19, pp.16240-16265.
[133]Ponzo, V., Goitre, I., Fadda, M., Gambino, R., De Francesco, A., Soldati, L., Gentile, L., Magistroni, P., Cassader, M. and Bo, S., 2015. Dietary flavonoid intake and cardiovascular risk: a population-based cohort study. Journal of Translational Medicine, 13, pp.1-13.
[134]Vinayagam, R. and Xu, B., 2015. Antidiabetic properties of dietary flavonoids: a cellular mechanism review. Nutrition & Metabolism, 12, pp.1-20.
[135]Kummer, V., Maskova, J., Canderle, J., Zraly, Z., Neca, J. and Machala, M., 2001. Estrogenic effects of silymarin in ovariectomized rats.Veterinarni Medicina-Praha, 46, pp.17-23.
[136]Newman, D.J. and Cragg, G.M., 2012. Natural products as sources of new drugs over the 30 years from 1981 to 2010. Journal of Natural Products, 75, pp.311-335.
[137]Hollman, P.H. and Katan, M.B., 1999. Dietary flavonoids: intake, health effects and bioavailability. Food and Chemical Toxicology, 37, pp.937-942.

Table 2.7. Sub-classes and common dietary sources of flavonoids (Modified from Hollman *et al.*, 1999)[138].

Flavonoid sub-class	Major food sources	Examples
Flavonols	Onions, spinach, cherries, apples, broccoli, kale, tomato, berries, almond, tea, red wine	Kaempherol, Myricetin, Quercetin
Flavones	Parsley, thyme, celery, peppers, rosemary	Apigenin, Luteolin, Chrysin
Isoflavones	Soybeans, legumes, peanuts, fava beans, red clover	Daidzein, Genistein
Flavanols	Apples, tea, red wine, chocolate	(+)-Catechin
Flavanones	Oranges, grapes, lemons, psoralea	Naringenin, Methylnaringenin
Anthocyanidins	Berries, grapes, cherries, plums, cashews, hazelnuts, eggplant	Cyanidin

2.8.2 Flavonoides structure and stability

Flavonoides are naturally occurring polyphenols that are structurally characterized by the presence of a di-phenyl-propane moiety (C6-C3-C6)[138]. Chemical structure of flavonoids comprises two benzene rings: ring 'A' and ring 'B', linked by via a 3-carbon chain bridge (Figure 2.6). This 3-carbon chain bridge combines with oxygen and ring 'A' to form a third central ring which has been identified as ring 'C'[139]. Flavonoids are synthesised from aromatic amino acids phenylalanine and acetate through a series of enzymatic reactions[140], in which the ring A is derived from acetate pathway and ring B is derived from shikimate pathway[141]. The central ring C of flavonoids is identified as a chromane ring that shares its structure with tocopherols and different flavonoids. A double bond between C2 and C3 atoms of the ring C provides quinone-like properties to the compound. Most of the flavonoid structure consists of enclosed hydroxyl and methoxyl groups in its basic skeleton. This detailed structural analysis demonstrates that flavonoids possess diverse bio-chemical properties due to variation in their functional group.

[138]Hertog, M.G., Hollman, P.C. and Katan, M.B., 1992. Content of potentially anticarcinogenic flavonoids of 28 vegetables and 9 fruits commonly consumed in the Netherlands. Journal of Agricultural and Food Chemistry, 40, pp.2379-2383.
[139]Beecher, G.R., 2003. Overview of dietary flavonoids: nomenclature, occurrence and intake. The Journal of Nutrition, 133, pp.3248S-3254S.
[140]Winkel-Shirley, B., 2001. Flavonoid biosynthesis. A colorful model for genetics, biochemistry, cell biology, and biotechnology. Plant Physiology, 126, pp.485-493.
[141]Bravo, L., 1998. Polyphenols: chemistry, dietary sources, metabolism, and nutritional significance. Nutrition Reviews, 56, pp.317-333.

Flavonoids are also heat stable because they loss relatively low after cooking and frying[142]

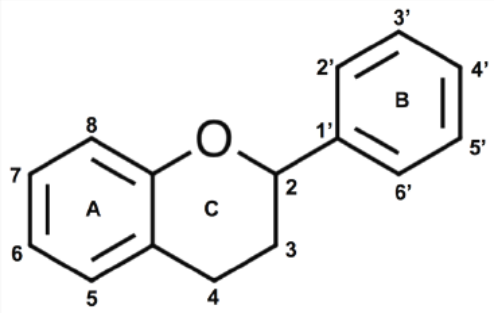

Figure 2.6. Basic stucture of flavonoid (Adapted from Teixeira *et al.*, 2013)[143]

Flavonoids are secondary metabolites that bind to sugar (glycosides) enhancing their water solubility. The most common sugar moiety found associated with flavonoids is glucose and rhamnose followed by galactose, arabinose, xylose and glucuronic acid. Flavonoids also subsist as aglycones in plants. Another study demonstarted superior metabolic stability and slower hepatic metabolism by methylated flavonoids when compared to unmethylated flavonoids[144].

2.8.3 Dietary intake of flavonoids

For flavonoids to be effective as natural therapeutics, their dietary intake for the subject should be standardized. World Health Organization (WHO) has recommended a daily intake of ~400 g/day fruits and vegetables[145]. The consumption of 1 g/day of flavonoid in Western diet was also reported to be beneficial for maintenance of good health[146]. The relation between the dietary intake of flavonoids and risk of cancer was studied in various countries; the daily intake of flavonoids in United States, Netherland, Denmark, Finland and Japan have been estimated as 1.1 g/day, 23 mg/day, 28 mg/day, 2.6 mg/day and 68.2 mg/day[147,141,148,149,150,151], respectively. Therefore dietary intakes of flavonoids are

[142]Hertog, M.G., Hollman, P.C., Katan, M.B. and Kromhout, D., 1993. Intake of potentially anticarcinogenic flavonoids and their determinants in adults in The Netherlands. Nutrition and Cancer, 20, pp.21-29.
[143]Teixeira, A., Eiras-Dias, J., Castellarin, S.D. and Gerós, H., 2013. Berry phenolics of grapevine under challenging environments. International Journal of Molecular Sciences, 14, pp.18711-18739.
[144]Wen, X. and Walle, T., 2006. Methylation protects dietary flavonoids from rapid hepatic metabolism. Xenobiotica, 36, pp.387-397.
[145]Fruit and vegetable promotion initiative–report of the meeting, World Health Organization(WHO) 2003, Geneva, 25–27.
[146]Morris, M.E. and Zhang, S., 2006. Flavonoid–drug interactions: effects of flavonoids on ABC transporters. Life Sciences, 78, pp.2116-2130.
[147]Kühnau, J., 1976. The flavonoids. a class of semi-essential food components: their role in human nutrition. In World Review of Nutrition and Dietetics, pp. 117-191.
[148]Leth, T. and Justesen, U., 1998. Analysis of flavonoids in fruits, vegetables and beverages by HPCL-UV and LC-MS and estimation of the total daily flavonoid intake in Denmark. Polyphenols in Food, pp.39-40.
[149]Hertog, M.G., Kromhout, D., Aravanis, C., Blackburn, H., Buzina, R., Fidanza, F., Giampaoli, S., Jansen, A., Menotti, A., Nedeljkovic, S. and Pekkarinen, M., 1995. Flavonoid intake and long-term risk of coronary heart disease and cancer in the seven countries study. Archives of Internal Medicine, 155, pp.381-386.

appeared varied as per regions[142]. This reported variability in flaovonoid consumption can be attributed to the huge diversity of flavonoids sub-classes and the fact that the entire flavonoids are not accessible as dietary food**.** Another study carried out with Japanese population reported significant (~31%) reduction of stomach cancer upon intake of ≥ 7 cups of green tea per day[152]. Likewise, high consumption rate of green tea and black tea has been associated with reduced risks of precancerous chronic atrophic gastritis[153] and stomach cancer[154] respectively. Similar studies with other flavonoides have shown the importance of correct intake dosage. Epigallocatechin Gallate has been shown to be non-toxic ~ 50-500 mg/kg/day post intravenous bolus administration upto a period of 3 months but is toxic at higher concentrations ~2 gm/kg/day[155]. The information on flavonoides as dietary food is very limited making the evaluation of their dietary intake difficult.

Other factors that affect dietary intake amount of flavonoids include diversity of flavonoids (functional groups involved), climate, sunlight, and food preparation[156]. Therefore, this issue has been shortly resolved by the U.S. Department of Agriculture (USDA) has maintained an updated database of the most commonly occurring flavonoids (~26) in over 500 foods items[157].

2.8.4 Metabolism and bioavailability of flavonoides

Assessment of flavonoids metabolism is a complex process due to the variability in flavonoid structures. It can be analyzed by studying different parameters, mainly absorption, distribution, and excretion. Bioavailability of flavonoids can be easily determined by measuring the amount of flavonoids found in blood or targeted tissue after ingestion. Not all flavonoides are inactivated after metabolism; some of the metabolized

---

[150]Friesenecker, B. and Tsai, A.G., 1995. Cellular basis of inflammation, edema and the activity of Daflon 500 mg. International Journal of Microcirculation, 15, pp.17-21.

[151]Knekt, P., Järvinen, R., Seppänen, R., Heliövaara, M., Teppo, L., Pukkala, E. and Aromaa, A., 1997. Dietary flavonoids and the risk of lung cancer and other malignant neoplasms. American Journal of Epidemiology, 146, pp.223-230.

[152]Inoue, M., Tajima, K., Hirose, K., Hamajima, N., Takezaki, T., Kuroishi, T. and Tominaga, S., 1998. Tea and coffee consumption and the risk of digestive tract cancers: data from a comparative case-referent study in Japan. Cancer Causes and Control, 9, pp.209-216.

[153]Shibata, K., Moriyama, M., Fukushima, T., Kaetsu, A., Miyazaki, M. and Une, H., 2000. Green tea consumption and chronic atrophic gastritis: a cross-sectional study in a green tea production village. Journal of Epidemiology, 10, pp.310-316.

[154]Chow, W.H., Swanson, C.A., Lissowska, J., Groves, F.D., Sobin, L.H., Nasierowska-Guttmejer, A., Radziszewski, J., Regula, J., Hsing, A.W., Jagannatha, S. and Zatonski, W., 1999. Risk of stomach cancer in relation to consumption of cigarettes, alcohol, tea and coffee in Warsaw, Poland. International Journal of Cancer, 81, pp.871-876.

[155]Isbrucker, R.A., Edwards, J.A., Wolz, E., Davidovich, A. and Bausch, J., 2006. Safety studies on epigallocatechin gallate (EGCG) preparations. Part 2: dermal, acute and short-term toxicity studies. Food and Chemical Toxicology, 44, pp.636-650.

[156]Neuhouser, M.L., 2004. Review: Dietary flavonoids and cancer risk: Evidence from human population studies. Nutrition and Cancer, 50, pp.1-7.

[157]Bhagwat, S., Haytowitz, D.B. and Holden, J.M., 2014. USDA database for the flavonoid content of selected foods, Release 3.1. US Department of Agriculture: Beltsville, MD, USA.

products are far more active than the parent compound. For example morphine metabolite product is more potent than the parent compound[158]. Flavonoids are predominantly absorbed by passive diffusion in small intestine and only small fractions of flavonoids are absorbed via the gastric mucosa[159]. Most of the flavonoids occur as glycosylated compounds, influencing their absorption due to increased water solubility[160,161]. After absorption, glycosylated flavonoids are hydrolyzed in the gut and converted into aglycone flavonoid[162]. These aglycones flavonoids then behave as lipophilic compounds and show enhanced absorption via passive diffusion in the gut. Majority of the flavonoides are metabolized in the colon and liver. Initially flavonoids particpate in transformation and conjugation reaction such as glucuronidation, sulfation or methylation in liver, and are degraded by the colon microflora into phenolic acids[144,163]. These transformation and conjugation reactions are necessary for the regulation of phase II detoxification reactions rendering solubility to the flavonoids and enhancing their excretion in bile and urine[164]. The hydrolysis process of flavonoids has been deciphered the role of β -glucosidase and lactase phloridzin hydrolase enzymes in hydrolysis of β-glycoside linkages of glycosylated flavonoids present in enterocytes and small intestine brush border respectively[165]. Another finding shows quercetin 4'-glucoside or genistein 7-glucoside were incubated with human saliva and subcultured oral bacterial colonies, hydrolyzed into quercetin and genistein, respectively. Thus the dietary flavonoid glucosides can hydrolyzed by both bacteria and shedded epithelial cells in the oral cavity and deliver the biologically active aglycones on surface of the epithelial cells, Theses aglycones quercetin and genistein has been reported to inhibit proliferation of oral cancer cells[166].

Various factors affect flavonoid absorption in the gut namely, gut microflora, sugar moiety, and the sub-classes of flavonoid. The absorption of different flavonoids varies

[158]Wittwer, E. and Kern, S.E., 2008. Role of morphine's metabolites in analgesia: concepts and controversies. In Drug Addiction, pp. 609-616.

[159] Piskula, M.K., Yamakoshi, J. and Iwai, Y., 1999. Daidzein and genistein but not their glucosides are absorbed from the rat stomach. FEBS Letters, 447, pp.287-291.

[160] Segi, M., 1965. Formal Discussion of: Epidemiology of Cancer: Spatial-Temporal Aggregation. Cancer Research, 25, pp.1375-1379.

[161] Kolonel, L.N., Nomura, A.M. and Cooney, R.V., 1999. Dietary fat and prostate cancer: current status. Journal of the National Cancer Institute, 91, pp.414-428.

[162]Spencer, J.P., Chowrimootoo, G., Choudhury, R., Debnam, E.S., Srai, S.K. and Rice-Evans, C., 1999. The small intestine can both absorb and glucuronidate luminal flavonoids. FEBS Letters, 458, pp.224-230.

[163]Hollman, P.C.H. and Katan, M.B., 1997. Absorption, metabolism and health effects of dietary flavonoids in man. Biomedicine & Pharmacotherapy, 51, pp.305-310.

[164] Williamson, G., Day, A.J., Plumb, G.W. and Couteau, D., 2000. Human metabolic pathways of dietary flavonoids and cinnamates. Biochemical Society Transactions, 28, pp.16-20.

[165]Day, A.J., Gee, J.M., DuPont, M.S., Johnson, I.T. and Williamson, G., 2003. Absorption of quercetin-3-glucoside and quercetin-4′-glucoside in the rat small intestine: the role of lactase phlorizin hydrolase and the sodium-dependent glucose transporter. Biochemical Pharmacology, 65, pp.1199-1206.

[166]Walle, T., Browning, A.M., Steed, L.L., Reed, S.G. and Walle, U.K., 2005. Flavonoid glucosides are hydrolyzed and thus activated in the oral cavity in humans. The Journal of Nutrition, 135, pp.48-52.

such as quercetin shows good absorption after conjugation of glucose[167]. Free form of tea polyphenols generated using β glucuronidase and sulfatase such as (-)-Epigallocatechin-3-gablate (EGCG), (-)-epigalbocatechin (EGC), (-)-epicatechin-3-gablate (ECG), and (-)-epicatechin (EC) were found from 0.5 to 1.5 ng/ml in plasma or urine sample[168]. Methylated flavonoids have also been shown to exhibit better oral bioavailability, stability, higher accumulation in the cell and high permeability for intestinal than their parent form[169,170]. When flavonoids are consumed with protein, their absorption is reduced[171]. It has been reported that most of the polyphenols cross the plasma baseline levels within 24 h of their consumption[172]. While kinetics of quercetin absorption and metabolism has been well studied[173,174], information on the metabolism of all the available flavonoids is not yet fully defined. This necessitates detailed research into their metabolic distribution and absorption profiles, which are very important for their use as safe non-toxic drugs.

2.8.5 Biological functions of flavonoids

Flavonoids are a subtype of potentially active polyphenols, widely distributed amongst the plants. As mentioned earlier, flavonoids have been shown to exhibit a variety of chemo-preventative activities. Flavanoids have been reported to enhance vitamin C activity leading to increased anti-inflammatory[176], anti-oxidant[175], anti-allergic[176], anti-viral[177], cardiovascular [178] and anti-carcinogenic properties[179](Table 2.8)[180]. A large

[167]Hollman, P.C., de Vries, J.H., van Leeuwen, S.D., Mengelers, M.J. and Katan, M.B., 1995. Absorption of dietary quercetin glycosides and quercetin in healthy ileostomy volunteers. The American Journal of Clinical Nutrition, 62, pp.1276-1282.
[168]Lee, M.J., Wang, Z.Y., Li, H., Chen, L., Sun, Y., Gobbo, S., Balentine, D.A. and Yang, C.S., 1995. Analysis of plasma and urinary tea polyphenols in human subjects. Cancer Epidemiology and Prevention Biomarkers, 4, pp.393-399.
[169]Walle, T., Ta, N., Kawamori, T., Wen, X., Tsuji, P.A. and Walle, U.K., 2007. Cancer chemopreventive properties of orally bioavailable flavonoids—methylated versus unmethylated flavones. Biochemical Pharmacology, 73, pp.1288-1296.
[170]Tsuji, P.A., Winn, R.N. and Walle, T., 2006. Accumulation and metabolism of the anticancer flavonoid 5, 7-dimethoxyflavone compared to its unmethylated analog chrysin in the Atlantic killifish. Chemico-Biological Interactions, 164, pp.85-92.
[171]Hollman, P.C., Van Het Hof, K.H., Tijburg, L.B. and Katan, M.B., 2001. Addition of milk does not affect the absorption of flavonols from tea in man. Free Radical Research, 34, pp.297-300.
[172]Linseisen, J. and Rohrmann, S., 2008. Biomarkers of dietary intake of flavonoids and phenolic acids for studying diet–cancer relationship in humans. European Journal of Nutrition, 47, pp. 60-68
[173]Hollman, P.C., Gaag, M.V., Mengelers, M.J., Van Trijp, J.M., De Vries, J.H. and Katan, M.B., 1996. Absorption and disposition kinetics of the dietary antioxidant quercetin in man. Free Radical Biology and Medicine, 21, pp.703-707.
[174]Manach, C. and Donovan, J.L., 2004. Pharmacokinetics and metabolism of dietary flavonoids in humans. Free Radical Research, 38, pp.771-785.
[175]Chen, X.M., Tait, A.R. and Kitts, D.D., 2017. Flavonoid composition of orange peel and its association with antioxidant and anti-inflammatory activities. Food Chemistry, 218, pp.15-21.
[176]Liang, Q., Chen, H., Zhou, X., Deng, Q., Hu, E., Zhao, C. and Gong, X., 2017. Optimized microwave-assistant extraction combined ultrasonic pretreatment of flavonoids from *Periploca forrestii Schltr*. and evaluation of its anti-allergic activity. Electrophoresis, 38,pp. 1113–1121.
[177]Yang, S., Zhou, J., Li, D., Shang, C., Peng, L. and Pan, S., 2017. The structure-antifungal activity relationship of 5, 7-dihydroxyflavonoids against *Penicillium italicum.* Food Chemistry, 224, pp.26-31.
[178]Wallace, T.C., 2011. Anthocyanins in cardiovascular disease. Advances in Nutrition: An International Review Journal, 2, pp.1-7.
[179]Woo, H.D. and Kim, J., 2013. Dietary flavonoid intake and smoking-related cancer risk: a meta-analysis. PLoS One, 8, pp.1-13.
[180]Liu, R.H., 2013. Health-promoting components of fruits and vegetables in the diet. Advances in Nutrition: An International Review Journal, 4, pp.384S-392S.

number of flavonoids (quercetin, apigenin, tea catechins) have also been shown to display anti-inflammatory activity by inhibiting cycloxygenase-2 (COX2) activity[181,182]. Flavonoids function by both induction (quercetin)[183] as well as inhibition (chrysin, flavone, and genistein 4'-methyl ether-Biochanin A)[184] of key enzymes, involved in important pathways like cell division and proliferation, platelet aggregation, detoxification, inflammatory and immune response[185]. Flavonoids (Resveratrol, kaempferol & kaempferol-3-O-glucuronide) also act as competent inhibitors of molecular targets such as protein kinase C (PKC), tyrosine kinase and PI 3-kinase[186,187].

Table 2.8. Biological function of different plant derived flavonoides (Modified from Liu *et al.*, 2013)[181]

Biological function
Antioxidant activity to reduce free radicals
Inhibition of cell proliferation, oncogene expression, cell adhesion and invasion, nitrosation and nitration , inflammation, signal transduction pathways,
Reduction of Phase I enzyme (blocking activation of carcinogens) , Cyclooxygenase-2,nitric oxide synthase, Xanthine oxidase
Induction of cell differentiation, cell-cycle arrest, apoptosis, tumor suppress gene expression
Enhancement of detoxification and Induction Phase II enzymes, Glutathione peroxidise, Catalase, Superoxide dismutase
Enhancement of life span and immune response
Antiangiogenesis
Prevention of DNA adduct formation or DNA intercalation
Regulation of steroid hormone metabolism and estrogen metabolism
Antiallergic, hepatoprotective, Antithrombotic, Antiviral

Different functional groups of flavoniods are specific for different biological activities. For example, flavonoids like apigenin, luteolin, quercetin, and kaempherol containing a

[181]Raso, G.M., Meli, R., Di Carlo, G., Pacilio, M. and Di Carlo, R., 2001. Inhibition of inducible nitric oxide synthase and cyclooxygenase-2 expression by flavonoids in macrophage J774A.1 Life Sciences, 68, pp.921-931.
[182] Mutoh, M., Takahashi, M., Fukuda, K., Komatsu, H., Enya, T., Matsushima-Hibiya, Y., Mutoh, H., Sugimura, T. and Wakabayashi, K., 2000. Suppression by flavonoids of cyclooxygenase-2 promoter-dependent transcriptional activity in colon cancer cells: structure-activity relationship. Cancer Science, 91, pp.686-691.
[183]Çelik, N., Vurmaz, A. and Kahraman, A., 2017. Protective effect of quercetin on homocysteine-induced oxidative stress. Nutrition, 33, pp.291-296.
[184]Campbell, D.R. and Kurzer, M.S., 1993. Flavonoid inhibition of aromatase enzyme activity in human preadipocytes. The Journal of Steroid Biochemistry and Molecular Biology, 46, pp.381-388.
[185]Gökmen, V., Artı k, N., Acar, J., Kahraman, N. and Poyrazoğ lu, E., 2001. Effects of various clarification treatments on patulin, phenolic compound and organic acid compositions of apple juice. European Food Research and Technology, 213, pp.194-199.
[186]Beekmann, K., De Haan, L.H., Actis-Goretta, L., Van Bladeren, P.J. and Rietjens, I.M., 2016. Effect of glucuronidation on the potential of kaempferol to inhibit serine/threonine protein kinases. Journal of Agricultural and Food Chemistry, 64, pp.1256-1263.
[187]Varoni, E.M., Faro, A.F.L., Sharifi-Rad, J. and Iriti, M., 2016. Anticancer molecular mechanisms of resveratrol. Frontiers in Nutrition, pp.3-8.

5'- and 7'-OH group in A-ring exhibit inhibitory activity against lipogenesis[188]. Flavonoids substituted with hydroxyl groups on the A and B-rings and unsaturated covalent bonds at 2 and 3 position on C-ring show anti-cancer and anti-oxidant activity[189,190]. Similar findings have shown role of adjacent hydroxyl groups on A or B-ring (e.g., myricetin with 3', 4', 5'-OH groups) in strong anti-proliferative effect by the concerned flavonoids[191]. Other findings have suggested a direct correlation between the number of hydroxyl groups in flavonoid structure and related ROS scavenging and anti-inflammatory activity[192]. It can be concluded that diversity amongst different functional groups present in flavonoid structure attribute to enhanced biological activities.

2.8.6 Mechanism of anti-cancer activity of flavonoides

Carcinogenesis is a multifaceted process involving three main phases namely: tumor initiation, promotion, and progression, mediated by both internal and external exposure of carcinogens[7]. Flavonoids act as chemo-preventive agents acting and interfering at different stages of cancer development. Flavonoid [7,12-dimethylbenz[*a*]anthracene and 4-(methylnitrosamino)-1-(3-pyridyl)-1-butanone] have been reported to inactivate carcinogens that cause mutation in genes by activating detoxifying enzymes[193]. Many flavonoids and natural products such as quercetin, dihydroartemisinin & cinnamon extract and *withania somnifera* extract, have been shown to function as anti-cancer agents by suppressing pro-oxidant enzyme activity involved in cancer development, targeting COX-2 enzyme activity, reducing vascular endothelial growth factor(VEGF) action, activating JNK1/2 and p38 MAPK signalling pathways and targeting interleukin-8 and cyclooxygenase-2 activity, inducing cell death[194,195,196,197,198]. One another flavonoid,

[188]Brusselmans, K., Vrolix, R., Verhoeven, G. and Swinnen, J.V., 2005. Induction of cancer cell apoptosis by flavonoids is associated with their ability to inhibit fatty acid synthase activity. Journal of Biological Chemistry, 280, pp.5636-5645.
[189] Benavente-Garcia, O. and Castillo, J., 2008. Update on uses and properties of citrus flavonoids: new findings in anticancer, cardiovascular, and anti-inflammatory activity. Journal of Agricultural and Food Chemistry, 56, pp.6185-6205.
[190]Williams, R.J., Spencer, J.P. and Rice-Evans, C., 2004. Flavonoids: antioxidants or signalling molecules?. Free Radical Biology and Medicine, 36, pp.838-849.
[191] Ortuno, A., Benavente-Garcia, O., Castillo, J., Alcaraz, M., Vicente, V. and Del Rio, J.A., 2007. Beneficial action of citrus flavonoids on multiple cancer-related biological pathways. Current Cancer Drug Targets, 7, pp.795-809.
[192]Chang, H., Mi, M., Ling, W., Zhu, J., Zhang, Q., Wei, N., Zhou, Y., Tang, Y., Yu, X., Zhang, T. and Wang, J., 2010. Structurally related anticancer activity of flavonoids: involvement of reactive oxygen species generation. Journal of Food Biochemistry, 34, pp.1-14.
[193]Shimada, T., 2017. Inhibition of carcinogen-activating cytochrome P450 enzymes by xenobiotic chemicals in relation to antimutagenicity and anticarcinogenicity. Toxicological Research, 33, pp.79-96.
[194]Meydani, M. and Azzi, A., 2017. 6 Dietary antioxidants and bioflavonoids in atherosclerosis and angiogenesis. Nutrigenomics and Proteomics in Health and Disease: Towards a Systems-Level Understanding of Gene–Diet Interactions, pp.125-142.
[195]Raja, S.B., Rajendiran, V., Kasinathan, N.K., Amrithalakshmi, P., Venkabalasubramanian, S., Murali, M.R., Devaraj, H. and Devaraj, S.N., 2017. Differential cytotoxic activity of Quercetin on colonic cancer cells depends on ROS generation through COX-2 expression. Food and Chemical Toxicology, 106, pp.92–106.
[196]Zhang, K., Han, E.S., Dellinger, T.H., Lu, J., Nam, S., Anderson, R.A., Yim, J.H. and Wen, W., 2017. Cinnamon extract reduces VEGF expression via suppressing HIF-1α gene expression and inhibits tumor growth in mice. Molecular Carcinogenesis, 56, pp.436-446.

anthocyanins have been shown to induce apoptosis through MAPK- and PI3K/Akt-mediated mitochondrial pathways[199,200]. Caffeic acid and hydroxycinnamic acid, found in fruit and coffee[201] respectively induce apoptosis by activating Fas, Bax, caspase in human breast cancer cells[202]. Resveratrol, found in grape plays an important role in delay and preventing the onset of cancer (prostate cancer) by inducing cell cycle arrest and apoptosis via activation of p53/p21WAF1/CIP1 and p27KIP1 pathway[203]. These anti-proliferative activities of the mentioned flavonoides make them appropriate candidates for treatment of cancer.

For cancer prevention several well accepted mechanisms of flavonoides have been proposed. Flavonoids play important roles in modulation of mitogenic signalling, cell survival, apoptotic signalling, cell-cycle regulation, preventing angiogenesis and metastatic processes involved in growth and development of cancer[204]. Flavonoids also modulate various key molecules of signal transduction pathways, leading to cell death. Inhibition of DNA topoisomerase I/II activity[205], down-regulation of Bcl-2 and Bcl-xl expression, up-regulation of Bax and Bak expression, release of cytochrome c from mitochondria and activation of caspases-3, 8 and 9[206,207] lead to cell death. Flavonoids also interfere with many signalling enzyme activities such as β glucuronidase, lipoxygenase, cyclooxygenase (COX), nitric oxide synthase (NOSs), monooxygenase, thyroid peroxidase (TPO), xanthine oxidase (XOs), mitochondrial succinoxidase, NADH-oxidase, phosphodiesterase (PDE), phospholipase A2 (PLA2), and protein kinase[192,208].

---

[197]Zhang, S., Shi, L., Ma, H., Li, H., Li, Y., Lu, Y., Wang, Q. and Li, W., 2017. Dihydroartemisinin induces apoptosis in human gastric cancer cell line BGC-823 through activation of JNK1/2 and p38 MAPK signaling pathways. Journal of Receptors and Signal Transduction, 37, pp.174-180.

[198] Balakrishnan, A.S., Nathan, A.A., Kumar, M., Ramamoorthy, S. and Mothilal, S.K.R., 2017. *Withania somnifera* targets interleukin-8 and cyclooxygenase-2 in human prostate cancer progression. Prostate International, 5, pp.75-83.

[199]Lin, B.W., Gong, C.C., Song, H.F. and Cui, Y.Y., 2016. Effects of anthocyanins on the prevention and treatment of cancer. British Journal of Pharmacology, 174, pp. 1226–1243.

[200]Liu, B. and Li, Z., 2016. Black Currant (*Ribes nigrum L.*) extract induces apoptosis of MKN-45 and TE-1 cells through MAPK-and PI3K/Akt-mediated mitochondrial pathways. Journal of Medicinal Food, 19, pp.365-373.

[201]Tyszka-Czochara, M., Konieczny, P. and Majka, M., 2017. Caffeic acid expands anti-tumor effect of metformin in human metastatic cervical carcinoma HTB-34 Cells: Implications of AMPK activation and impairment of fatty acids de novo biosynthesis. International Journal of Molecular Sciences, 18, p.462, EISSN 1422-0067.

[202]Taofiq, O., González-Paramás, A.M., Barreiro, M.F. and Ferreira, I.C., 2017. Hydroxycinnamic acids and their derivatives: cosmeceutical significance, challenges and future perspectives, a review. Molecules, 22, p.281, doi:10.3390/molecules22020281.

[203]Singh, S.K., Banerjee, S., Acosta, E.P., Lillard, J.W. and Singh, R., 2017. Resveratrol induces cell cycle arrest and apoptosis with docetaxel in prostate cancer cells via a p53/p21WAF1/CIP1 and p27KIP1 pathway. Oncotarget, 8, pp.17216–17228.

[204]Singh, R.P.,& Agarwal, R. 2006. Mechanisms of action of novel agents for prostate cancer chemoprevention. Endocr Relat Cancer, 13, pp.751-778.

[205]Snyder, R.D. and Gillies, P.J., 2003. Reduction of genistein clastogenicity in Chinese hamster V79 cells by daidzein and other flavonoids. Food and Chemical Toxicology, 41, pp.1291-1298.

[206]Michels, G., Watjen, W., Niering, P., Steffan, B., Thi, Q.H., Chovolou, Y., Kampkotter, A, Bast, A., Proksch, P.& Kahl, R.2005.Pro-apoptotic effects of the flavonoid luteolin in rat H4IIE cells. Toxicology, 206, pp.337-348.

[207]Wang, I.K, Lin-Shiau, S.Y.,& Lin ,J.K,1999.Induction of apoptosis by apigenin and related flavonoids through cytochrome c release and activation of caspase-9 and caspase-3 in leukaemia HL-60 cells. Eur J Cancer, 35, pp.1517-1525.

[208]Moon, Y.J., Wang, X., Morris, M.E.,2006.Dietary flavonoids: effects on xenobiotic and carcinogen metabolism. Toxicol *in vitro*, 20, pp.187-210.

Different studies describing the anti-cancer role of flavonoides and their molecular targets have been listed in table 2.9.

Table 2.9. Molecular targets of flavonoids (Modified from Aggarwal *et al.*,2006) [209]

Active compound	**Targeted signalling proteins**
Emodin,Curcumin,Quercetin	↑ Caspases 3, 7, 8, 9 , ↑ PARP, ↑ Bax, BID
Capsaicin, Catechins, Resveratrol	↓ CyclinD1, E, ↑ p21/WAF, ↑ p27Kip/Cip,↓ CDK1,2,4,6,7
Yakuchinone, Curcuminoids, Resveratrol	↓ TNF, ↓ EGF, ↓ IFN-γ , ↓ IL-1, 2, 6, 8, ↓ Erythropoietin
Catechins, Anethole, Silybinin	↓ NF-κ B, ↓ AP-1, ↓ STAT1, 3, 5, ↓ β -catenin, ↑ p53
Linalool,Curcuminoids,Caffeoylquinic acids	↓ IKK, ↓ EGFR, ↓ HER2, ↓ Akt, ↓ MAPK
Capsaicin, Boswellic acids, Zerumbone	↓ Bcl-2, ↓ Bcl-XL, ↓ Survivin ,↓ TRAF1, ↓ cFLIP

Note ↓ : Down regulation, ↑ : Up regulation

2.9 Pinostrobin

Pinostrobin, a naturally occurring dietary flavonoid, discovered more than 6 decades ago in the heart-wood of pine (*Pinus strobus*). It is recognized by the name pinostrobin because of its presence in *Pinus strobus*[210]. The dextro-rotatory and levorotatory forms of pinostrobin (2,3- dihydrotecto chrysin) were isolated from *Salvia texana* (Torr.)[211] and *Carya tonkinensis* (lecomte)[212] , respectively. Various source of pinostrobin have been reported in literature namely: *Artemisia campestris*(field wormwood)[213], *Boesenbergia pandurata* (temu kunci/ fingerroot)[214], *Boesenbergia rotunda* (chinese keys/fingerroot)[215],

[209]Aggarwal, B.B. and Shishodia, S., 2006. Molecular targets of dietary agents for prevention and therapy of cancer. Biochemical Pharmacology, 71, pp.1397-1421.
[210]De Carvalho, M.G., Cranchi, D.C. and De Carvalho, A.G., 1996. Chemical constituents from *Pinus strobus var*. chiapensis. J Braz Chem Soc, 7, pp.187-191.
[211]González, A.G., Aguiar, Z.E., Luis, J.G., Ravelo, A.G., Vázquez, J.T. and Dominguez, X.A., 1989. Flavonoids from *Salvia texana*. Phytochemistry, 28, pp.2871-2872.
[212] Cuong, N.M., Sung, T.V., Kamperdick, C. and Adam, G., 1996. Flavanoids from *Carya tonkinensis.* Pharmazie, 51, n°2, p. 128, ISSN0031-7144.
[213]Hurabielle, M., Eberle, J., Paris, M.,., 1982.Flavonoids of *Artemisia campestris, ssp.* glutinosa. Planta Med. ,46, pp.124-125.
[214]Wangkangwan, W., Boonkerd, S., Chavasiri, W., Sukapirom, K., Pattanapanyasat, K., Kongkathip, N., Miyakawa, T. and Yompakdee, C., 2009. Pinostrobin from *Boesenbergia pandurata* is an inhibitor of Ca2+-signal-mediated cell-cycle regulation in the yeast *Saccharomyces cerevisiae*. Bioscience, Biotechnology, and Biochemistry, 73, pp.1679-1682.
[215]Abdelwahab, S.I., Mohan, S., Abdulla, M.A., Sukari, M.A., Abdul, A.B., Taha, M.M.E., Syam, S., Ahmad, S. and Lee, K.H., 2011. The methanolic extract of *Boesenbergia rotunda* (L.) Mansf. and its major compound pinostrobin induces anti-ulcerogenic property *in vivo:* possible involvement of indirect antioxidant action. Journal of Ethnopharmacology, 137, pp.963-970.

Sarcandra glabra (herba sarcandrae/glabrous sarcandra herb)[216], dried leafs of *Polygonum ferrugineum(*knotweed/knotgrass)[217], *Cajanus cajan*(arhar/pigeon pea)[218] *Polygonum lapathifolium* (martweed/knotweed)[219] and honey[220]. Of these, the leaves of *Cajanus cajan* (l.)Millsp and rhizomes of *Boesenbergia pandurata* (Roxb.) are the major sources of pinostrobin. Zhao *et al.,* (2014) extracted pinostrobin from pigeon pea leaf by using standard extraction protocol[221]. Pinostrobin, also derived from *Boesenbergia pandurata* (Roxb.) is also known as *Boesenbergia rotunda*[222], *Kaempferia pandurata* (Roxb) and Thai ginger (Zingiberaceae). *B. pandurata* is recognized as Krachai in Thailand and is distributed in South Eastern Asian countries such as Indonesia and Malaysia. *B. rotunda* is a perennial herb of ginger family (*Zingiberaceae*) used for treatment of colic, oral diseases, urinary disorders, dysentery and inflammation[223]. Rhizomes of *B. rotunda* have also been reported to exhibit several biological activities including anti-mutagenic[224], anticancer[225], anti-*helicobacter pylori*[226], anti-dengue and chikungunya viruses[227], antioxidant[228] and antimicrobial[229] .

Currently, pinostrobin is used as an active ingredient in many marketed botanical nutraceuticals such as falcate crazy weed, Reflexa Hemsl, Weitengning tablets

[216]Yuan, K., Zhu, J.X., Si, J.P., Cai, H.K., Ding, X.D. and Pan, Y.J., 2008. Studies on chemical constituents and antibacterial activity from n-butanol extract of *Sarcandra glabra*. Zhongguo Zhong yao za zhi= Zhongguo zhongyao zazhi= China Journal of Chinese Materia Medica, 33, pp.1843-1846.

[217]López, S.N., Sierra, M.G., Gattuso, S.J., Furlán, R.L. and Zacchino, S.A., 2006. An unusual homoisoflavanone and a structurally-related dihydrochalcone from *Polygonum ferrugineum* (Polygonaceae). Phytochemistry, 67, pp.2152-2158.

[218]Xian, Y.F., Ip, S.P., Lin, Z.X., Mao, Q.Q., Su, Z.R. and Lai, X.P., 2012. Protective effects of pinostrobin on β-amyloid-induced neurotoxicity in PC12 Cells. Cellular and Molecular Neurobiology, 32, pp.1223-1230.

[219]Smolarz, H.D., Mendyk, E., Bogucka-Kocka, A. and Kockic, J., 2006. Pinostrobin–an anti-leukemic flavonoid from *Polygonum lapathifolium L.* ssp. nodosum (Pers.) Dans. Zeitschrift für Naturforschung C, 61, pp.64-68.

[220]Fahey, J.W. and Stephenson, K.K., 2002. Pinostrobin from honey and Thai ginger (*Boesenbergia pandurata*): a potent flavonoid inducer of mammalian phase 2 chemoprotective and antioxidant enzymes. Journal of Agricultural and Food Chemistry, 50, pp.7472-7476.

[221]Zhao, C., Liu, D., Li, C., Fu, Y., Yang, L. and Zu, Y., 2014. Separation of pinostrobin from pigeon pea [*Cajanus cajan* (L) Millsp.] leaf extract using a cation exchange resin for catalytic transformation combined with a polyamide resin. Separation and Purification Technology, 133, pp.168-175.

[222]Larsen, K., 1996. A preliminary checklist of the zingiberaceae of Thailand. Thai Forest Bulletin (Botany) , pp.35-49.

[223]Saralamp P, Chuakul W, Temsiririrkkul R, Clayton T. Medicinal plants in Thailand. Volume 1. Bangkok: Faculty of Pharmacy, Mahidol University. 1996, p 218,ISBN 974836437.

[224]Trakoontivakorn, G., Nakahara, K., Shinmoto, H. and Tsushida, T., 1999. Identification of antimutagenic substances (Ames Test) from *Boesenbergia pandurata Schl.* (fingerroot) and *Languasgalanga* (galanga). JIRCAS J, 7, pp.105-16.

[225]Jing, L.J., Mohamed, M., Rahmat, A. and Bakar, M.F.A., 2010. Phytochemicals, antioxidant properties and anticancer investigations of the different parts of several gingers species (*Boesenbergia rotunda*, *Boesenbergia pulchella var attenuata* and *Boesenbergia armeniaca*). Journal of Medicinal Plants Research, 4, pp.027-032.

[226]Bhamarapravati, S., Mahady, G.B. and Pendland, S.L., 2003. *In vitro* susceptibility of *Helicobacter pylori* to extracts from the Thai medicinal plant *Boesenbergia rotunda* and pinostrobin. In Proceedings of the 3rd world congress on medicinal and aromatic plants for human welfare, Chiang Mai Thailand (p. 521).

[227]Oliveira, A.F.C.D.S., Teixeira, R.R., Oliveira, A.S.D., Souza, A.P.M.D., Silva, M.L.D. and Paula, S.O.D., 2017. Potential antivirals: natural products targeting replication enzymes of dengue and chikungunya viruses. Molecules, 22, pp. 1-20.

[228]Shindo, K., Kato, M., Kinoshita, A., Kobayashi, A. and Koike, Y., 2006. Analysis of antioxidant activities contained in the *Boesenbergia pandurata Schult*. rhizome. Bioscience, Biotechnology, and Biochemistry, 70, pp.2281-2284

[229]Voravuthikunchai, S.P., 2007. Family zingiberaceae compounds as functional antimicrobials, antioxidants, and antiradicals. Food, 1, pp.227-240.

and[230,231,232] Pinostrobin is also a major constituent of some Canadian natural herbal products and United States marketed dietary supplements that are listed in table 2.10[233].

Table 2.10. List of pinostrobin derived natural herbal and dietary supplements

Company	Marketed products
Organika	Bee Propolis liquid
QuantumNutrition labs	Propolis Complex capsules
T.C. unicorn ltd.	Bee Propolis
Himalaya	SoligaForestHoney
Comvita	Manuka Honey
Amazon Herbs	Boesenbergia pandurata tincture
AmazonHerbs	Alpinia galangal tincture
Wedderspoon	Wild dandelion Honey
BeeHealthyFarmsllC	Propolis capsules

(Adapted from Sayre and Davies' 2013)[234]

2.9.1 Structure and chemical synthesis of pinostrobin

The structure of pinostrobin was elucidated from the extract of *Polygonum lapathifolium ssp.nodosum* in 2006[225]. Commercially, pinostrobin (Mw 270.285) is identified as (S)-(-)-2,3-dihydro-5-hydroxy-7-methoxy-2-phenyl-4H-1-benzopyran-4-one, pinocembrin-7-methyl ether and 5-hydroxy-7-methoxy flavanone[234]. Photochemically stable structure of pinostrobin was discovered by Matsuura *et al.*, in 1973[235].

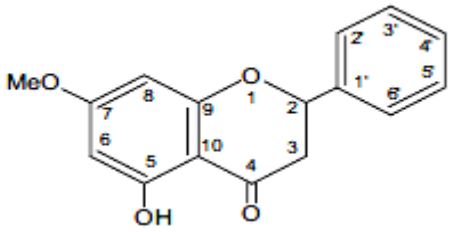

Figure 2.7. Stucture of pinostrobin (Adapted from Smolarz *et al.*, 2006)[220]

[230]Hou, F.H., Yang, H., Hui, H.Q. and Cai, B.C., 2008. An analysis on content of pinostrobin in falcate crazyweed with reversed phase high-performance liquid chromatography. Journal of Nanjing University of Traditional Chinese Medicine, 24, pp.171-172.
[231]Pan, Y.F., Lu, Y.B., Zhang, J.M., Xiao, W.B. and Wu, F.R., 2004. Determination of pinostrobin in *Reflexa Hemsl* by HPLC. Chinese Traditional Herbal Drugs, 39, pp.1059-1060.
[232]Pan, Y.F., Lu, Y.B., Zhang, J.M., Xiao, W.B. and Wu, F.R., 2005. Determination of pinostrobin in Weitengning Tablets by HPLC. Chinese Traditional Patent Medicine, 27, pp.662-663.
[233]Sayre, C. and Davies, N., 2013. Quantification of three chiral flavonoids with reported bioactivity in selected licensed Canadian natural health products and US marketed dietary supplements. Journal of Pharmacy & Pharmaceutical Sciences, 16, pp.272-278.
[234]http://www.chemblink. com/products/480-37-5..
[235]Matsuura, T., Takemoto, T. and Nakashima, R., 1973. Photoinduced reactions—LXXI: Photorearrangement of 3-hydroxyflavones to 3-aryl-3-hydroxy-1, 2-indandiones. Tetrahedron, 29, pp.3337-3340.

Prenylated and optically pure (S)(-) pinostrobin (~99.6%) were also synthesized using the intramolecular Mitsunobu reaction by Poerwono *et al.*, (2010)[236] and Korenaga *et al.*, (2011)[237]. Pinostrobin derivatives have also been synthesized with additional functional groups like hydroxylamine and hydrazine, without disturbing the γ-pyrone ring[238]. Recently, pinostrobin has also been used for the synthesis of coumarin–chalcone hybrids containing a triazole linker[239].

2.9.2 Pharmacokinetics and bioavailability studies of pinostrobin

For good therapeutic drugs, essential to know its distribution, total time of entry and clearance from the system. Hence researchers have elaborated the pharmacokinetics of pinostrobin for its use as therapeutic agent. Pharmacokinetics of pinostrobin was first analyzed by Hua *et al.*, in 2011. The finding of pharmacokinetics study of pinostrobin revealed that 0.5 mg/kg of pinostrobin oral dose corresponds to a good enough score of maximum concentration (C_{max} -615.35±32.89 ng/ml), time taken to reach the maximum drug concentration (T_{max}- 4±0.18 h) and half life (t ½- 4.34±0.24 min)[240], theses finding support its therapeutic potential. Different studies have provided information details on chiral separation of pinostrobin revealing existence of two enantiomers of pinostrobin with serum half-life of ~7 h[241,242,243]. Pharmacokinetic study of both the enantiomers of pinostrobin exhibited similar parameters viz volume of distribution (Vd S-pinostrobin, 8.2 L/kg; Vd R-pinostrobin, 8.9 L/kg), total clearance (S-pinostrobin CL_{total}, 0.959 L/h/kg; R pinostrobin CL_{total}, 1.055 L//h/kg), and area under the curve (S-pinostrobin AUC_{inf}, 23.16µgh/mL; R-pinostrobin AUC_{inf}, 21.296µg h/mL). These studies revealed extensive distribution of pinostrobin into the tissues[244]. These quantitative measurements are good as required for therapeutic agent. Smolarz *et al.*, (2006) have demonstrated quick

[236]Poerwono, H., Sasaki, S., Hattori, Y. and Higashiyama, K., 2010. Efficient microwave-assisted prenylation of pinostrobin and biological evaluation of its derivatives as antitumor agents. Bioorganic & Medicinal Chemistry Letters, 20, pp.2086-2089.
[237]Korenaga, T., Hayashi, K., Akaki, Y., Maenishi, R. and Sakai, T., 2011. Highly enantioselective and efficient synthesis of flavanones including pinostrobin through the rhodium-catalyzed asymmetric 1, 4-addition. Organic Letters, 13, pp.2022-2025.
[238]Patel, N.K., Jaiswal, G. and Bhutani, K.K., 2016. A review on biological sources, chemistry and pharmacological activities of pinostrobin. Natural Product Research, 30, pp.2017-2027.
[239]Mukusheva, G.K., Lipeeva, A.V., Zhanymkhanova, P.Z., Shults, E.E., Gatilov, Y.V., Shakirov, M.M. and Adekenov, S.M., 2015. The flavanone pinostrobin in the synthesis of coumarin-chalcone hybrids with a triazole linker. Chemistry of Heterocyclic Compounds, 51, pp.146-152.
[240]Hua, X., Fu, Y.J., Zu, Y.G., Zhang, L., Wang, W. and Luo, M., 2011. Determination of pinostrobin in rat plasma by LC–MS/MS: application to pharmacokinetics. Journal of Pharmaceutical and Biomedical Analysis, 56, pp.841-845.
[241]Krause, M. and Galensa, R., 1990. Optical resolution of flavanones by high-performance liquid chromatography on various chiral stationary phases. Journal of Chromatography A, 514, pp.147-159.
[242]Asztemborska, M., Miś kiewicz, M. and Sybilska, D., 2003. Separation of some chiral flavanones by micellar electrokinetic chromatography. Electrophoresis, 24, pp.2527-2531.
[243]Wistuba, D., Trapp, O., Gel-Moreto, N., Galensa, R. and Schurig, V., 2006. Stereoisomeric separation of flavanones and flavanone-7-O-glycosides by capillary electrophoresis and determination of interconversion barriers. Analytical chemistry, 78, pp.3424-3433.
[244]Sayre, C.L., Zhang, Y., Martinez, S.E., Takemoto, J.K. and Davies, N.M., 2013. Stereospecific analytical method development and preliminary *in vivo* pharmacokinetic characterization of pinostrobin in the rat. Biomedical Chromatography, 27, pp.548-550.

penetration of pinostrobin from the cytoplasm into nucleus of the cultured cells and further induction of apoptosis[220]. Knowledge of such parameters is very crucial in characterizing pinostrobin as an attractive therapeutic agent for cancer treatment.

2.9.3 Biological and pharmacological activities of pinostrobin

Like other naturally occurring flavonoides, pinostrobin is also known to display a wide variety of pharmacological activities[245,246] which have been discussed in detail in the forthcoming sections:

2.9.3.1 Anti-microbial activity

Pinostrobin has been shown to have anti-microbial effect against a variety of micro-organisms including bacteria as well as fungi. It exhibited significant anti-bacterial activity against *Staphylococcus aureus* with minimum inhibitory concentration (MIC) of 6.94 µg/ml[247,248]. Pinostrobin was also found to inhibit progression of cell cycle in G2/M phase by targeting Ca^{2+} signalling of *Saccharomyces cerevisiae*[220]. Besides having a bacteriostatic effect, pinostrobin was seen to have a growth inhibitory effect on the mycelia of fungus *Cytospora persoonii*[249]. Brunskole *et al.,(*2009) reported pinostrobin as an inhibitor of the recombinant trihydroxynaphthalene reductase of the fungal pathogen *Curvularia lunata* which infects both animals and humans[250].

2.9.3.2 Anti-oxidant activity

Various findings have reported antioxidant behaviour of pinostrobin, justifying its use as a therapeutic agent. Pinostrobin showed significant anti-oxidant activity with IC_{50} value >500 µg/ml using 2,2-diphenyl-1-picrylhydrazyl (dPPH) scavenging assay[251]. Similarly, anti-free radical activity of Propolis (bee glue) has been demonstrated and chemical

[245]Hooper, L., Kroon, P.A., Rimm, E.B., Cohn, J.S., Harvey, I., Le Cornu, K.A., Ryder, J.J., Hall, W.L. and Cassidy, A., 2008. Flavonoids, flavonoid-rich foods, and cardiovascular risk: a meta-analysis of randomized controlled trials. The American Journal of Clinical Nutrition, 88, pp.38-50.

[246]Wu, N., Kong, Y., Zu, Y., Fu, Y., Liu, Z., Meng, R., Liu, X. and Efferth, T., 2011. Activity investigation of pinostrobin towards herpes simplex virus-1 as determined by atomic force microscopy. Phytomedicine, 18, pp.110-118.

[247]Kong, Y., Fu, Y.J., Zu, Y.G., Chang, F.R., Chen, Y.H., Liu, X.L., Stelten, J. and Schiebel, H.M., 2010. Cajanuslactone, a new coumarin with anti-bacterial activity from pigeon pea [*Cajanus cajan* (L.) Millsp.] leaves. Food Chemistry, 121, pp.1150-1155.

[248]Massaro, C.F., Katouli, M., Grkovic, T., Vu, H., Quinn, R.J., Heard, T.A., Carvalho, C., Manley-Harris, M., Wallace, H.M. and Brooks, P., 2014. Anti-staphylococcal activity of C-methyl flavanones from propolis of Australian stingless bees (*Tetragonula carbonaria*) and fruit resins of *Corymbia torelliana* (Myrtaceae). Fitoterapia, 95, pp.247-257.

[249]Geibel, M., 1995. Sensitivity of the fungus *Cytospora persoonii* to the flavonoids of *Prunus cerasus*. Phytochemistry, 38, pp.599-601.

[250]Brunskole, M., Zorko, K., Kerbler, V., Martens, S., Stojan, J., Gobec, S. and Rižner, T.L., 2009. Trihydroxynaphthalene reductase of *Curvularia lunata*—A target for flavonoid action?. Chemico-Biological Interactions, 178, pp.259-267.

[251]Wu, N., Fu, K., Fu, Y.J., Znu, Y.G., Chang, F.R., Chen, Y.H., Liu, X.L., Kong, Y., Liu, W. and Gu, C.B., 2009. Antioxidant activities of extracts and main components of pigeonpea [*Cajanus cajan (L.)* Millsp.] leaves. Molecules, 14, pp.1032-1043.

composition analysis showed pinostrobin to be its major constituent[252]. Abdelwahab *et al.,(*2011) illustrated the comparative ferric reducing/anti-oxidant power (FRAP) values of pinostrobin (116.11 ± 0.004) and ascorbic acid (915 ± 0.01562)[221] Another study reported low circular dichroism [Cd] value<0.56 mM for pinostrobin, exhibiting potent Quinone reductase induction activity comparable to sulphoraphane (Cd value = 0.43 mM), a well known anti-cancer compound. In addition, the chemoprevention index (CI) of pinostrobin (>132) was found to be significantly higher than that of sulphoraphane (25.0)[253]. Pinostrobin was also shown to induce phase II enzyme quinine reductase activity that protects against toxic and reactive chemical species with no cytotoxicity at Cd value ~ 0.9μg/ml[254]. Bail *et al.,(*2000) have demonstrated anti-aromatase activity of pinostrobin (IC_{50}10 μM) independently without affecting dHEAS and oestrogen receptor binding[255]. Additional, pinostrobin showed inhibition of 17β-estradiol formation in JEG-3 cells[256]. Further, pinostrobin resulted in significant induce mammalian phase 2 detoxication enzymes (quinone reductase)[221].

2.9.3.3 Anti-inflammatory, anti-ulcer and anti-viral studies

Anti inflammatory activity of pinostrobin (300 mg/kg) was evaluated using oedema inhibition assay[257]. Pinostrobin (20 mg/kg b.w) significantly reduced the rate of ethanol induced ulcers 83.40% in Sprague dawley rats, higher than omeprazole (76.77%, dose 20 mg/kg)[216] which also utilizes the anti-inflammatory activity to treat acid reflux related stomach disorders. Jain (2016) demonstrated the anti-ulcer potential of pinostrobin against peptic ulcer, it increased thiobarbituric acid reactive substances levels in Ethanol-acid induced ulcer (EIU) animal model and control peptic ulcer by discontinuity of acid secretion[258]. Pinostrobin also inhibited action of TNF-α (IC50<22μM) and IL-1β (IC50<40μM) in RAW264.7 and J774A.1 cells, administration of pinostrobin (20 mg/kg) were found to reduce lipopolysaccharide (LPS) induced TNF and IL-1β levels by 48.6%

[252]Christov, R., Trusheva, B., Popova, M., Bankova, V. and Bertrand, M., 2006. Chemical composition of propolis from Canada, its antiradical activity and plant origin. Natural Product Research, 20, pp.531-536.
[253]Su, B.N., Park, E.J., Vigo, J.S., Graham, J.G., Cabieses, F., Fong, H.H., Pezzuto, J.M. and Kinghorn, A.D., 2003. Activity-guided isolation of the chemical constituents of *Muntingia calabura* using a quinone reductase induction assay. Phytochemistry, 63, pp.335-341.
[254]Gu, J.Q., Park, E.J., Vigo, J.S., Graham, J.G., Fong, H.H., Pezzuto, J.M. and Kinghorn, A.D., 2002. Activity-guided isolation of constituents of *Renealmia nicolaioides* with the potential to induce the phase II enzyme quinone reductase. Journal of Natural Products, 65, pp.1616-1620.
[255]Le Bail, J.C., Aubourg, L. and Habrioux, G., 2000. Effects of pinostrobin on estrogen metabolism and estrogen receptor transactivation. Cancer Letters, 156, pp.37-44.
[256]Saarinen, N., Joshi, S.C., Ahotupa, M., Li, X., Ämmälä, J., Mäkelä, S. and Santti, R., 2001. No evidence for the *in vivo* activity of aromatase-inhibiting flavonoids. The Journal of Steroid Biochemistry and Molecular Biology, 78, pp.231-239.
[257]Panthong A., Kanjanapothi D., Tuntiwachwuttikul, P., Pancharoen, O., Reutrakul, V., 1994. Anti inflammatory activity of flavonoids. Phytomedicine.1, pp.141–144.
[258]Jain, P., 2016. Secondary metabolites for antiulcer activity. Natural Product Research, 30, pp.640-656.

and 53.1%, respectively in Sprague Dawley (SD) rats[259]. Pinostrobin was reported to inhibit the production of nitric oxide[260,261] and regulate the action of COX I and II enzymes[262]. The anti viral activity of pinostrobin was reported against herpes simplex virus-1 (HSV-1) with an EC_{50} of 22.71±1.72 μg/ml[247]. Pinostrobin was also found to non-competitively (K_i ~345 μM) inhibit the action of dengue-2 virus NS3 protease (~88.7%)[263].

2.9.3.4 Anti-parasitic activity

Pinostrobin exhibited anti-malarial activity but its mechanism of action has not yet been elucidated in detail[264]. Duker-Eshun *et al.,* (2004) reported weak anti-plasmodial activity by pinostrobin as constituents of *Cajanus cajan* [265]. An anti-diarrhoeal action of pinostrobin has been also determined by mediated the depolarisation of potassium[266].

2.9.3.5 Anti-protozoal, anti-venom activity and trypanocidal activity

Pinostrobin was found to inhibit the growth of *Entamoeba histolytica* and *Giardia lamblia* with IC_{50} values of 184.0 and 80.8 μg/ml, respectively[267]. Pinostrobin was isolated from *Lychnophora markgravii* aerial parts and reduce of the viability of amastigote stages of *Leishmania amazonensis* at dose 1 mg/ml[268]. It could also neutralize the coagulating effect of the deadly *Bothrops asper*(viper species), venom (venom:pinostrobin/ratio of 1:20), Further examination revealed around 66.7% reduction

[259]Patel, N.K. and Bhutani, K.K., 2014. Pinostrobin and Cajanus lactone isolated from *Cajanus cajan (L.)* leaves inhibits TNF-α and IL-1β production: *In vitro* and *in vivo* experimentation. Phytomedicine, 21, pp.946-953.
[260]Lee, C., Lee, J.W., Jin, Q., Jang, D.S., Lee, S.J., Lee, D., Hong, J.T., Kim, Y., Lee, M.K. and Hwang, B.Y., 2013. Inhibitory constituents of the heartwood of *Dalbergia odorifera* on nitric oxide production in RAW 264.7 macrophages. Bioorganic & Medicinal Chemistry Letters, 23, pp.4263-4266.
[261] Sudsai, T., Prabpai, S., Kongsaeree, P., Wattanapiromsakul, C. and Tewtrakul, S., 2014. Anti-inflammatory activity of compounds from *Boesenbergia longiflora* rhizomes. Journal of Ethnopharmacology, 154, pp.453-461.
[262]Wu, D., Nair, M.G. and Dewitt, D.L., 2002. Novel compounds from *Piper methysticum* Forst (Kava Kava) roots and their effect on cyclooxygenase enzyme. Journal of Agricultural and Food Chemistry, 50, pp.701-705.
[263]Kiat, T.S., Pippen, R., Yusof, R., Ibrahim, H., Khalid, N. and Rahman, N.A., 2006. Inhibitory activity of cyclohexenyl chalcone derivatives and flavonoids of fingerroot, *Boesenbergia rotunda* (L.), towards dengue-2 virus NS3 protease. Bioorganic & Medicinal Chemistry Letters, 16, pp.3337-3340.
[264]Kaur, K., Jain, M., Kaur, T. and Jain, R., 2009. Antimalarials from nature. Bioorganic & Medicinal Chemistry, 17, pp.3229-3256.
[265]Duker-Eshun, G., Jaroszewski, J.W., Asomaning, W.A., Oppong-Boachie, F. and Brøgger Christensen, S., 2004. Antiplasmodial constituents of *Cajanus cajan*. Phytotherapy Research, 18, pp.128-130.
[266]Meckes, M., Paz, D., Acosta, J. and Mata, R., 1998. The effects of chrysin and pinostrobin, two flavonoids isolated from *Teloxys graveolens* leaves, on isolated guinea-pig ileum. Phytomedicine, 5, pp.459-463.
[267]Calzada, F., Velázquez, C., Cedillo-Rivera, R. and Esquivel, B., 2003. Antiprotozoal activity of the constituents of *Teloxys graveolens*. Phytotherapy Research, 17, pp.731-732.
[268]Salvador, M.J., Sartori, F.T., Sacilotto, A.C.B., Pral, E.M., Alfieri, S.C. and Vichnewski, W., 2009. Bioactivity of flavonoids isolated from *Lychnophora markgravii* against *Leishmania amazonensis* amastigotes. Zeitschrift für Naturforschung C, 64, pp.509-512.

in local haemorrhage post pinostrobin treatment[269]. Pinostrobin exhibited trypanocidal activity and prevented transmission of Chagas'disease (American trypanosomiasis). It spreads via infected blood transfusion and becoming the major mechanism of transmission. Only trypanocidal substances prevent infection in blood banks, due to its undesirable effects, new compounds are required to control this transmission. Of the different dosages, pinostrobin exhibited maximum trypanocidal activity at 500 µg/ml ~ 14.7 ± 5.2 and control *Trypanosoma cruzi* infection[270].

2.9.3.6 Anti-cancer activity and toxicology

Many studies have revealed the cytotoxic behaviour of pinostrobin in different cell lines, inhibiting cancer cell growth in a dose-dependent manner as described in the forthcoming section. A direct correlation was observed between the number of cells undergoing apoptosis and the concentration of pinostrobin[220]. Pinostrobin has been reported to inhibit the growth of MCF-7 (Breast cancer) cells, HepG2 (liver cancer) cells and human mammary carcinoma by targeting aromatase[264], phosphodiesterase type 4 (PDE4)[271] and topoisomerse I activity[272]. It also inhibits the growth of prostate cancer cells by arresting the cell cycle in G2/M phase post treatment[273]. Anti-tumour activity against HepG2 and HeLa cell lines has also been reported[274]. Drug resistance against cancer is a main cause of treatment failure, hence Kuete *et al.*, (2014) explore the effect of natural compounds including pinostrobin, (S)-(-)-pinostrobin showed the antiproliferative activity (IC50 >116.41 µM) against drug-sensitive and multidrug -resistant cancer cell lines as a model system[275]. Pinostrobin exhibited good antiproliferative activity against acute T-lymphoblastic leukaemia cell line (CCRF-CEM) in dose-dependent manner, which was

[269]Gómez-Betancur, I., Benjumea, D., Patiño, A., Jiménez, N. and Osorio, E., 2014. Inhibition of the toxic effects of Bothrops asper venom by pinostrobin, a flavanone isolated from *Renealmia alpinia* (Rottb.) MAAS. Journal of Ethnopharmacology, 155, pp.1609-1615.

[270]Takeara, R., Albuquerque, S., Lopes, N.P. and Lopes, J.L.C., 2003. Trypanocidal activity of *Lychnophora staavioides* Mart.(Vernonieae, Asteraceae). Phytomedicine, 10, pp.490-493.

[271]Abd El-Hady, F.K., Shaker, K.H., Imhoff, J.F., Zinecker, H., Salah, N.M. and Ibrahim, A.M., 2013. Bioactive Metabolites from Propolis Inhibit Superoxide Anion Radical, Acetylcholinesterase and Phosphodiesterase (PDE4). International Journal of Pharmaceutical Sciences Review and Research, 21, pp.338-344.

[272]Darwanto, A., Tanjung, M. and Darmadi, M.O., 2000. Cytotoxic mechanism of flavonoid from Temu Kunci (*Kaempferia pandurata*) in cell culture of human mammary carcinoma. Clinical Hemorheology and Microcirculation, 23, pp.185-190.

[273]Haddad, A.Q., Venkateswaran, V., Viswanathan, L., Teahan, S.J., Fleshner, N.E. and Klotz, L.H., 2006. Novel antiproliferative flavonoids induce cell cycle arrest in human prostate cancer cell lines. Prostate Cancer and Prostatic Diseases, 9, pp.68-76.

[274]Cao, X.D., Ding 1, Z.S., Jiang, F.S., Ding, X.H., Chen, J.Z., Chen, S.H. and Lv, G.Y., 2012. Antitumor constituents from the leaves of *Carya cathayensis.* Natural Product Research, 26, pp.2089-2094.

[275]Kuete, V., Nkuete, A.H., Mbaveng, A.T., Wiench, B., Wabo, H.K., Tane, P. and Efferth, T., 2014. Cytotoxicity and modes of action of 4′-hydroxy-2′, 6′-dimethoxychalcone and other flavonoids toward drug-sensitive and multidrug-resistant cancer cell lines. Phytomedicine, 21, pp.1651-1657.

resistant to the doxorubicin resistant sub-line CEM/ADR5000[276]. Pinostrobin showed anti-mutagenic activities at doses of 30 mg/kg (56.5%) and 60 mg/kg (96.5%) body weight, respectively in micronucleated polychromatic cell erythrocytes (MNPCE) from male Balb-c mice (8–12 week) induced by cyclophosphamide [277]. Anti-mutagenic activity of pinostrobin was also observed in *Salmonella typhimurium* TA98 at ID50 ~ 25 n moles[278]. Antimutagenecity is reduced as increased polarity of hydroxyl functions and carbonyl group also be important in planar structure of pinostrobin for its activity. Significant reduction in the mutagenicity of 3-amino-1- methyl-5H-pyrido [4, 3-b]indole (Trp-P-2) and 2-amino-1-methyl-6-phenylimidazo[4,5-b]pyridine (PhIP) (~95%) was observed by addition of pinostrobin at 0.1 μ mol/test in *S. typhimurium* TA98 [279]. Non-toxic and non-genotoxic nature of pinostrobin further support its candidature as an effective and safe anti-cancer therapeutic agent. Pinostrobin exhibited non-toxic and non-genotoxic effects to male Wistar rats at substantive dosage~500 mg/kg, indicating its safe application. Analysis of different biochemical parameters (albumin, albumin–globulin ratio (A/G), alkaline phosphatase, aspartate aminotransferase, alanine aminotransferase and total protein, and urea concentration) and organ weights post pinostrobin treatment further support its use as a therapeutic drug, and suggested that pinostrobin did not cause clastogenicity in rat liver[280]. Pinostrobin has been also reported to inhibit different kinds of metabolic enzymes like aromatase to decrease the growth of MCF-7[256] and changes membrane potential of human umbilical vein endothelial cells (HUVEC) growth[281].

On the basis of different biological aspects of pinostrobin (anti-microbial, anti-oxidant, anti-inflammatory, anti-venom and anti-cancer), its inclusion in the daily dietary products, safe and non-toxic intake, flexibility in adding extra functional groups, pinostrobin can prove to be effective as a chemotherapeutic agent. However, most of the studies conducted thus far are preliminary and do not describe exact mechanism of its

[276]Ashidi, J.S., Houghton, P.J., Hylands, P.J. and Efferth, T., 2010. Ethnobotanical survey and cytotoxicity testing of plants of South-western Nigeria used to treat cancer, with isolation of cytotoxic constituents from *Cajanus cajan Millsp*. leaves. Journal of Ethnopharmacology, 128, pp.501-512.

[277]Atun, S., Arianingrum, R., Sulistyowati, E. and Aznam, N., 2013. Isolation and antimutagenic activity of some flavanone compounds from *Kaempferia rotunda*. International Journal of Chemical and Analytical Science, 4, pp.3-8.

[278]Edenharder, R.V., Von Petersdorff, I. and Rauscher, R., 1993. Antimutagenic effects of flavoniods, chalcones and structurally related compounds on the activity of 2-amino-3-methylinidazo [4, 5-*f*] quinoline (IQ) and other heterocyclic amine mutagens from cooked food. Mutation Research/Fundamental and Molecular Mechanisms of Mutagenesis, 287, pp.261-274.

[279]Trakoontivakorn, G., Nakahara, K., Shinmoto, H., Takenaka, M., Onishi-Kameyama, M., Ono, H., Yoshida, M., Nagata, T. and Tsushida, T., 2001. Structural analysis of a novel antimutagenic compound, 4-hydroxypanduratin A, and the antimutagenic activity of flavonoids in a Thai spice, fingerroot (*Boesenbergia pandurata Schult.)* against mutagenic heterocyclic amines. Journal of Agricultural and Food Chemistry, 49, pp.3046-3050.

[280]Charoensin, S., Punvittayagul, C., Pompimon, W., Mevatee, U. and Wongpoomchai, R., 2010. Toxicological and clastogenic evaluation of pinocembrin and pinostrobin isolated from *Boesenbergia pandurata* in Wistar rats. Thai Journal of Toxicology, 25, pp.29-40.

[281]Siekmann, T.R.L., Burgazli, K.M., Bobrich, M.A., Nöll, G. and Erdogan, A., 2013. The antiproliferative effect of pinostrobin on human umbilical vein endothelial cells (HUVEC). European Review for Medical and Pharmacological Sciences, 17, pp.668-672.

different actions. Though, it has been reported to inhibit cancer cell growth *in vitro*, neither its *in vivo* anti-tumor activity is established nor its cytotoxicity to cancer stem like cells (CSCs) has been demonstrated. Further, the potential molecular target for its anti-proliferative activity has also not been identified. Thus, rational of taking the present study is address these issues and the results from this study will possibly help in answering these questions.

Chapter 3

Materials & Methods

3.1.1 Cell lines

Different cell lines used for the present study namely HeLa (human adeno cervical carcinoma cells, CCL-2™), Ca Ski (Human epidermoidcervical carcinoma cells, CRL-1550™), SiHa (Grade Ii, Squamouscervical carcinoma cells, HTB-35™), A549 (Human epithelial lung carcinoma cells, CRM-CCL-185™), HL-60 (Acute promyelocytic leukemia cells, CCL-240™) and HEK 293 (Embryonic kidney cells, CRL-1573™) were procured from American Type Culture Collection (ATCC, Manassas, VA 20108 USA).

3.1.2 Animals

Swiss albino mice (female 6–8 weeks old, weighing approximately 20–22 gm) were obtained from Animal Facility of Jawaharlal Nehru University (JNU), New Delhi, India. The animals were maintained in an air-conditioned room at ~25-28 ºC with humidity ~ 40-70% and 12 h light/dark cycle in the animal facility of the university. Three to five animals were kept in each cage and provided standard animal diet pellets (Agro Corporation Pvt. Ltd., India) and water ad libitum. Use of the mice was approved by the Institutional Animal Ethics Committee (IAEC) of the university and the animals were handled according the guidelines laid down by the IAEC of the university. The experimental animals (5 mice/group) were either administered with the test chemicals or the vehicle solvent through intraperitoneal (i.p.) or intratumoral (i.t.) route.

3.1.3 Chemicals and Reagents

Chemical, reagents and kits used in the study are listed in table 3.1 with their respective companies details:

Table 3.1.1. List of chemicals, reagents and specialized plasticware

Name of the Company/ Source	Chemicals, reagents and kits
Sigma-Aldrich Chemical Co., USA	Pinostrobin (Cat no. 38790), Doxorubicin (Cat no. D1515), Verapamil (Cat no. 1711202), Dimethyl sulfoxide (DMSO) (Cat no. D8418), Paraformaldehyde (PFA) (Cat no. P6148), Ethylene Diamine tetrachloro acetic acid (EDTA) (Cat no. E 9884), 4-(2-Hydroxyethyl)-1-piperazineethanesulfonic acid (HEPES) (Cat no. H3375), Propidium Iodide (PI) (Cat no. P4170), AnnexinV-FITC (Cat no. A9210), 5,5,6,6-Tetrachloro-1,1,3,3-tetraethyl benzimidazolylcarbocyanineiodide (JC-1) (Cat no. T4069), 6-Carboxy-2,7-Diclorodihydrohydrofluorescin-diacetate (DCFH-DA) (Cat no. D6883), Hydroethidine (HE) (Cat no. D7008), 10-N-nonyl acridine orange (NAO) (Cat no. A7847), Acridine orange (AO) (Cat no. A9231), Ethidium bromide (EtBr) (Cat no. E1510), Trypsin-EDTA (Cat no. T4049), Glucose (Cat no. G0350500), RNaseA (Cat no. R4875), Phenylmethylsulfonyl fluoride (PMSF) (Cat no. P7626), Protease inhibitor cocktail (Cat no. I3786), Sodium nitrite ($NaNO_2$) (Cat no. 237213),

	Glutathione (GSH) (Cat no. 70188), 5,5'-Dithiobis-{2-nitrobenzoic acid} (DTNB) (Cat no. 8130), Xylene cyanol (Cat no. 4126), 2'-[4-Ethoxyphenyl]-5-[4-methyl-1-piperazinyl]-2,5'-bi-1H-benzimidazoletrihydrocloridetri hydrate (Hoechst 33342) (Cat no. B2216), Topoisomerase I (Cat no. T9069), Griess reagent (Cat no. G4410), Wright-Giemsa stain (Cat no. WS1650), Trichloroacetic acid (TCA)(Cat no.T6399), Dulbecco's Modified Eagle's Media (DMEM) (Cat no. D6429), Roswell Park Memorial Institute (RPMI-1640) (Cat no. R4130) and Hydrochloric acid (HCl) (Cat no.H1758)
Biological Industries, Israel	Trypan blue dye (Cat no. 03-102-1B), Fetal Bovine Serum (FBS) (Cat no. 04-001-1A-US), Penicillin (Cat no. 03-031-1B), Streptomycin (Cat no.03-031-1C), Enhanced Chemi Luminescence (ECL) (Cat no. 20-500-120) and Hanks' Balanced Salt Solution (HBSS) (Cat no. 01-017-1A)
Sisco Reasearch Laboratory (SRL), India	3-(4,5-Dimethylthiazol-2-yl)-2,5-diphenyl tetrazoliumbromide (MTT) (Cat no. 2128), Potassium phosphate dibasic (K_2HPO_4) (Cat no. 2128), Monopotassium phosphate (KH_2PO_4) (Cat no.78279), Sodium phosphate dibasic (Na_2HPO_4) (Cat no. 45392), Monobasic sodium phosphate (NaH_2PO_4-) (Cat no.59392), Sodium chloride (NaCl) (Cat no. 33205), Bovine Serum Albumin (BSA) (Cat no. 97350) and Isopropanol (Cat no. 67-63-0)
Merck , India	Methanol (Cat no. 822283), Dimethyl formamide (DMF) (Cat no. 843944), Acetonitrile (CH3CN) (Cat no. 1132122), Sodium Dodecyl Sulfate (SDS) (Cat no. 843944), Triton×-100(Cat no. 9002-93-1), Sodium bicarbonate (NaHCO3) (Cat no.172577), Calcium chloride ($CaCl_2$) (Cat no. 102391), Magnesium chloride ($MgCl_2$) (Cat no.8147330), Ethylene glycol tetraacetic acid (EGTA) (Cat no. 4100-50GM), Dithiothreitol (DTT) (Cat no. 20-265), Glycerol (Cat no. 818709), Agarose (Cat no. 116801), Tween-20 (Cat no. 822184), Chloroform (Cat no. 107024), Ethanol(Cat no. 818760) and Isoamylalcohol (Cat no. 818969)
Qiagen, USA	Mini plasmid DNA extraction kit (Cat no. 12125)
Thermo Fisher Scientific, USA	Pre-stained protein molecular weight ladder (Cat. no. 26620) and unstained protein molecular weight ladder (Cat no. 26610)
Invitrogen, USA	Epidermal Growth Factor (EGF) (Cat no. 9644) and basic Fibroblast Growth Factor (bFGF) (Cat no. F9021)
BD Biosciences, USA	AnnexinV binding buffer (Cat no. 556454), Benzyloxycarbonyl-Val-AlaAsp-(O-methyl)-fluoromethylketone (Z-DEVD-FMK-Caspase-3 Inhibitor) (Cat no. 550378) and FACS sheath fluid (Cat no. 342003)
G-Biosciences, USA	Bicinchoninic Acid assay (BCA) protein estimation kit (Cat no. 786-570) and protease arrest ^{TM} (Cat no. 786-108)
Thermo Scientific, USA	RIPA lysis buffer (Cat no. 89901)
Hi-Media Laboratories, India	LB Agar (Cat no. M1151), LB Broth (Cat no. M1245), Bacto tryptone (Cat no. R014), Bacto agar (Cat no. R001) and Bacto yeast (Cat no. R027)
R& D Systems, USA	Human apoptosis protein profiler array kit (Cat no.ARY009)
Trevigen, Inc., USA	HT TiterTACS^{TM} assay kit (TACS -Trevigen Apoptotic Cell System) (Cat no. 4822-96-K)

3.1.4 Antibodies

Anti-human CD44 antibodies conjugated with fluorescein isothiocyanate and anti-human CD24 antibodies conjugated with R-phycoerythrin were procured from Invitrogen,USA. Dilution and sources of different antibodies that were used in present study is enlisted in the given table:

Table 3.1.2. Details of primary antibodies with their catalogue numbers, hosts and sources

Antibody	Dilution	Host	Catalogue no.	Company
Anti-CD44	1:100	Mouse	#MHCD4401	Invitrogen, USA
Anti-CD24	1:100	Mouse	#MHCD2404	Invitrogen, USA

3.1.5 Plasticware and glassware

Plasticware and glassware used were of analytical and culture grades. Plasticware for mammalian cell culture work; cell culture flasks (T-25 and T-75 cm^2), 35 mm culture glass dish, 60 mm culture dish tissue culture plates (96 well, 24 well, 12 well and 6 well flat bottom), cover slips, glass slides, microcentrifuge tubes (1.5 ml and 2 ml), pipette tips (10/20/200/1000 µl), and cryovials were procured from Greiner (Germany), Corning (USA), Tarsons (India) and Abdos (India). Disposable pipettes, conical bottom culture tubes (15 ml and 50 ml) and FACS sample tubes were purchased from Falcon (USA), Greiner; (Germany) and BD Biosciences (USA) , respectively. Syringe filters (0.2 µm and 0.45 µm pore size) were obtained from Advanced micro devices Pvt.Ltd. (MDI), India. Different glasswares used in the present study were purchased from Borosil (India).

3.2 Methods

3.2.1 Experimental protocols used in *in-vitro* studies

3.2.1.1 Cell culture maintenance

Mammalian cell lines HeLa, SiHa, A549 and HEK293 cells were maintained in DMEM, whereas Ca Ski and HL-60 cells were maintained in RPMI-1640 medium. The media (DMEM and RPMI-1640) powder packets were separately constituted with sodium bicarbonate (3.7 gm/L), 10 % heat inactivated Foetal Bovine Serum (FBS), and 1 % Penicillin -Streptomycin antibiotics in final volume of 1 L with Milli Q water. The media pH was maintained at 7.4. Afterwards, the constituted media were filter sterilized using 0.22 µm pore sized membrane filter and stored at 4ºC. Cells were grown in constituted media in humidified environment at 37 ºC in 5 % CO_2 incubator[1] (HERA Cell -150-Thermo Fisher Scientific, USA**)** and passaged after attaining 70-80% confluency.

3.2.1.2 Sub-culturing of cells

Cell culture was regularly examined to assess the degree of confluency (70-80%), then passaged or sub-cultured for prevention of cell death due to lack of space, continuous growth and lack of nutrient supply. Sub-culturing was carried out as essentially as described earlier by Masters and Stacey (2007)[2]. The spent culture medium was discarded from the confluent T-25 cm^2 culture flasks and the cells were washed with 2 ml of phosphate buffer saline (1×PBS: 137 mM NaCl, 2.7 mM KCl, 10 mM Na_2HPO_4, 1.8 mM KH_2PO_4, pH 7.4). The cells were then trypsinized with 1.5 ml of 1× trypsin-EDTA with gentle shaking so as to cover the adhered monolayer of cells for 5 min. The culture flasks were then examined under microscope to ensure proper detachment of the cells, indicated by their roundness and flatency. Excessive trypsin activity was neutralized by the addition of 1-2 ml of the constituted medium in the culture flasks. The cell suspension was then transferred into 15 ml centrifuge tube, centrifuged at 1000 rpm for 5 min (REMI R-4C, Remi Elektrotechnik Ltd, India). After discarding the supernatant, cells pellet was washed with 1×PBS and resuspended in appropriate volume of the constituted medium (5-10 ml). These cells were again cultured in T-25cm^2 culture flasks as mentioned above.

[1]Freshney, R. I., 2005. Culture of Animal Cells: A Manual of Basic Technique. Edition: 5, Wiley, Science, page 696.
[2]Masters, J.R. and Stacey, G.N., 2007. Changing medium and passaging cell lines. Nature Protocols, 2, pp.2276-2284.

3.2.1.3 Cell counting

For counting the viable cells, trypan blue dye exclusion assay was performed as described by Sandal and Sekai (2011), with minor modifications using hemocytometer[3] (Improved-Neubauer hemocytometer-Chamlab, UK). Trypan blue staining dye is excluded from the viable cells but retained within the damaged plasma membrane of dead cells. For viability counting, appropriate volume (16 µl) of the cell culture obtained after trypsinization (~ 1×10^4 cells/ ml) was mixed with trypan blue solution (4 µl, 1.25 dilution factor) at room temperature (RT) for 2 min. Half of the volume (10 µl) of this cell suspension was added in each chamber of the hemocytometer, and covered with cover slip, filling the chamber by capillary action. The hemocytometer was viewed under light microscope (Leica, DMIL,Germany) at 10× magnifications, focusing on the grid line of each chamber. Viable cells were counted in all the four large squares, without including non-viable (stained blue cells) cells. Total numbers of cells per ml were calculated using the following formula:

Total number of cells/ml = Average count of cells per square × dilution factor × $10^4/4$

3.2.1.4 Cryopreservation of cells

Cryopreservation of the cells was carried out by following method of Grout *et al.*, (1990)[4]. Cells were trypsinized as mentioned above, and centrifuged at 1000 rpm for 5 min at RT. Subsequently, the cells (1×10^6) were washed with 1-2 ml of 1×PBS and resuspended in 1-2 ml of freezing medium (90 % FBS and 10% DMSO). The cells in freezing medium (1-2 ml) were then transferred into sterile cryovials, stored at -20 ºC for 4-5 h, at -80 ºC for 24 h and finally transferred to Liquid Nitrogen container (Cryogenic Dewar flask, MVE Lab, USA) for long time storage.

3.2.1.5 Reviving of cells

Cells were revived according to the protocol standardized by Freshney (2005)[1]. Cryovials stored in liquid nitrogen were retrieved and thawed at 37 ºC (NEOLAB water bath, India) with slow shaking. After thawing, cryovials were wiped with 70 % ethanol and the cells were transferred into 15 ml culture tubes, containing constituted medium followed by centrifugation at 1000 rpm for 5 min at RT. Supernatant was discarded; the pellet

[3]Sandell, L. and Sakai, D., 2011. Mammalian cell culture. Current Protocols Essential Laboratory Techniques, Unit 4.3, doi: 10.1002/9780470089941.
[4]Grout, B., Morris, J. and McLellan, M., 1990. Cryopreservation and the maintenance of cell lines. Trends in Biotechnology, 8, pp.293-297.

obtained was resuspended in 1×PBS, pH 7.4, and centrifuged at 1000 rpm for 5 min at RT. The resultant cell pellet was resuspended in 5 ml of fresh constituted medium and cultured in T-25 cm^2 cell culture flasks under 5 % CO_2 humidified conditions at 37°C. Next day, the exhausted medium was replaced with fresh medium (5 ml) for removing any remaining traces of DMSO. Cells cultures were maintained for three passages prior to their use for further experiments.

3.2.1.6 Cell viability assay

MTT assay for assessing cell viability was carried out essentially as described by Scudiero *et al.,* (1988)[5]. Basic principle of the MTT assay is described as follows:

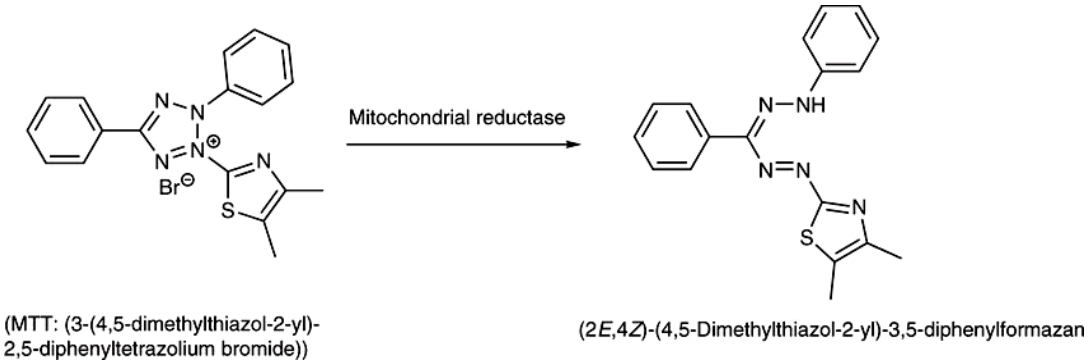

Figure 3.2.1. Chemical reaction showing conversion of MTT to formazan crystal in the presence of mitochondrial reductase (Adapted from Ebada *et al.,* 2008)[6]

MTT is reduced by mitochondrial dehydrogenase enzyme into purple coloured water insoluble formazan crystal. This reaction is executed only in metabolically active cells, correlating the presence of formazan crystal formation directly to cell viability[7].

Different mammalian cells (HeLa, Ca Ski, SiHa, A549, HL-60 and HEK 293; 5×10^3 cells/well) were seeded in flat bottom 96 well plates in 100 µl of constituted media for 24 h at 37 ºC in 5 % CO_2 incubator. After 24 h, used media was replaced with the same amount of fresh media and treated with different concentrations of test chemicals, pinostobin (10, 30, 50, 100 and 200 µM) and doxorubicin (10 µM) in triplicates. Pinostrobin solution was prepared in [Triple solvent (TS-Vehicle); Dimethyl

[5]Scudiero, D.A., Shoemaker, R.H., Paull, K.D., Monks, A., Tierney, S., Nofziger, T.H., Currens, M.J., Seniff, D. and Boyd, M.R., 1988. Evaluation of a soluble tetrazolium/formazan assay for cell growth and drug sensitivity in culture using human and other tumor cell lines. Cancer Research, 48, pp.4827-4833.

[6]Ebada, S.S., Edrada, R.A., Lin, W. and Proksch, P., 2008. Methods for isolation, purification and structural elucidation of bioactive secondary metabolites from marine invertebrates. Nature protocols, 3, pp.1820-1831.

[7]Liu, Y. and Schubert, D., 1997. Cytotoxic amyloid peptides inhibit cellular 3-(4, 5-Dimethylthiazol-2-yl)-2, 5-Diphenyltetrazolium Bromide (MTT) reduction by enhancing MTT formazan exocytosis. Journal of Neurochemistry, 69, pp.2285-2293.

sulfoxide:Dimethyl formamide:Acetonitrile,1:1:1)[8]. Untreated cell cultures and vehicle (corresponding volume of TS used for pinostrobin) treated cell cultures maintained under similar culture conditions were included as controls. After incubation, 10 µl of MTT solution (5 mg/ml stock in 1×PBS, pH 7.4) was added in each well to a final concentration of 0.5 mg/ml and incubated at 37 ºC in 5 % CO_2 incubator for 3-4 h in dark. The medium was then removed, formazan crystals were dissolved in 100 µl DMSO. The plates were incubated for additional 15-20 min at 37 ºC in dark. Absorbance was measured using microplate ELISA reader (TECAN, USA) at 570 nm (with reference wavelength of 630 nm). The absorbance of sample was directly correlated with cell viability. Cytotoxicity was calculated using the following formula:

Cytotoxicity (%) = (Absorption of control- Absorption of test)/ Absorption of control × 100%

The CT_{50} value (the concentration of the drug at which the cell viability is reduced to 50 %) was calculated using dose-response curve (percentage of cell toxicity vs concentration of pinostrobin (µM)) for each cell line.

3.2.1.7 Apoptosis studies

Induction of apoptosis by the treatment was measured by morphological, cell based assay and molecular methods:

- **Inverted and Transmission Electron Microscope (TEM)**

Morphological study was carried out as described by Ariffin *et al.,* (2009)[9]. The cells (5×10^4 cells/well) were grown on 24 mm cover slip in 6-well plates in constituted medium (2 ml) and incubated for 24 h at 37 ºC in 5 % CO_2 humidified incubator. The cells were treated either with doxorubicin (10 µM), pinostrobin (CT_{50} & $2\times CT_{50}$ concentrations) or the vehicle (corresponding volume of TS used for pinostrobin) for 24 and 48 h. Untreated cells were included as the negative control. After 48 h, the cells were washed twice with 1×PBS, pH 7.4 and fixed using of 4 % paraformaldehyde (PFA) for 20 min at RT. The cells were again washed twice with 2 ml of 1×PBS. Morphological changes in the treated and untreated cells were examined under inverted microscope (Nikon eclipse -80i, UK).

[8]Fahey, J.W. and Stephenson, K.K., 2002. Pinostrobin from honey and Thai ginger (*Boesenbergia pandurata*): a potent flavonoid inducer of mammalian phase 2 chemoprotective and antioxidant enzymes. Journal of Agricultural and Food Chemistry, 50, pp.7472-7476.

[9]Ariffin, S.H.Z., Omar, W.H.H.W., Ariffin, Z.Z., Safian, M.F., Senafi, S. and Wahab, R.M.A., 2009. Intrinsic anticarcinogenic effects of *Piper sarmentosum* ethanolic extract on a human hepatoma cell line. Cancer Cell International, 9, pp.1-9.

Transmission Electron Microscope (TEM) was utilized for morphological study of mitochondria, nucleus and cells by following the method of Altinoz *et al.*, (2007)[10]. The cells (5×10^4 cells/well) were fixed with 2 % glutaraldehyde in 0.1 M sodium cacodylate for 1 h at 4 ºC. The cells were then washed twice with 2 ml of 0.1 M sodium cacodylate (pH 7.4), fixed with 1 ml of 2 % osmium tetroxide in 0.1M sodium cacodylate for 1 h at RT, followed by a final wash with 1×PBS (pH 7.4). Following this, the cells were treated with 1 ml of 1% uranil acetate for 1 h and washed twice with 2 ml of 1×PBS. After fixing and sectioning, the cells were dehydrated with 1 ml of absolute ethanol and stained with 1 ml of 5 % uranyl acetate for 30 min. Stained cells were examined at under JEOL 2100F Transmission Electron Microscope at the Advanced Instrument Research Facility (AIRF), JNU, New Delhi, India.

- **Wright-Giemsa and Acridine Orange/ Ethidium Bromide staining (AO/EB staining)**

Giemsa staining was used to detect distinct changes in the apoptotic cells like condensation of chromatin and nuclei, reduction in cell volume, membrane blebbing and formation of apoptotic bodies due to cytoplasmic and nuclear fragmentation[11]. Acridine orange (AO) is a cationic dye which emits red fluorescence when bound to ssDNA or RNA and green fluorescence when bound to dsDNA[12]. On the other hand, ethidium bromide enters through the damaged nuclear membrane and when bound to dsDNA emits red-orange fluorescence, which indicates early and late stages of apoptosis[13].

For Giemsa staining[9], the cells (5×10^4 cells/well) were grown on 24 mm cover slips in 6-well plates in constituted medium (2 ml) and incubated overnight at 37 °C in 5% CO_2 incubator. The cells were subjected to different treatments as mentioned earlier for 24 and 48 h. Vehicle treated and untreated cells were included as controls. After the treatment period, the cells were washed twice with 2 ml of 1× PBS, pH 7.4, fixed with 1 ml of absolute methanol for 10 min at RT, and then stained with 100 µl (1:10 dilution in deionized water) of Wright's Giemsa stain solution for 15 min at RT. Cover slips were rinsed by 1-2 ml of 1× PBS, air dry and mounted on frosted glass slide with anti-fade

[10]Altinoz, M.A., Bilir, A., Gedikoglu, G., Ozcan, E., Oktem, G. and Muslumanoglu, M., 2007. Medroxyprogesterone and tamoxifen augment anti-proliferative efficacy and reduce mitochondria-toxicity of epirubicin in FM3A tumor cells *in vitro*. Cell Biology International, 31, pp.473-481.
[11]Elmore, S., 2007. Apoptosis: a review of programmed cell death. Toxicologic Pathology, 35, pp.495-516.
[12]Ichimura, S., 1975. Differences in the red fluorescence of acridine orange bound to single-stranded RNA and DNA. Biopolymers, 14, pp.1033-1047.
[13]Houssier, C., Hardy, B. and Fredericq, E., 1974. Interaction of ethidium bromide with DNA. optical and electrooptical study. Biopolymers, 13, pp.1141-1160.

reagent. Finally morphological changes were observed under light microscope (HERA Cell -150-Thermo Fisher Scientific, USA **)**.

Similarly, acridine orange/ethidium bromide staining of the cells was performed [9,14]. After treatment, the cells were washed and fixed with 1 ml of absolute methanol. The cells were then stained with 1 µl of acridine orange-ethidium bromide solution (1:1; 10 mg/ml each in Milli Q ultrapure water) in dark for 15 min at RT, and washed twice with 1-2 ml of 1× PBS. The stained cells were visualized and imaged under Olympus Fluoview FV1000 Confocal Laser-Scanning microscope using 1.4NA oil objective at the AIRF, JNU, New Delhi, India.

- **TUNEL assay**

DNA fragmentation has been established as a hallmark of apoptosis. During apoptosis DNA is fragmented or nicked by endonuclease and exposed at the 3'-OH ends. Transferase Biotin-dUTP Nick End Labeling (TUNEL) assay was used to assess the degree of DNA fragmentation[15,16]. The cells were grown in 12-well cell culture plates (1×10^5cells/ml/well) at 37 ºC in 5% CO_2 incubator for 24 h. The cells were subjected to different treatments (in the presence and absence of apoptosis inhibitor z-VAD-FMK ,caspases 3 inhibitor, 50µM) for 48 h. The cells were washed with 0.5 ml of 1×PBS and harvested by centrifugation. For pre-fixation, cells were incubated in 100 µl of 3.7 % buffered formaldehyde solution for 7 min at RT, followed by centrifugation at 1000 ×g (Eppendorf centrifuge 5415R, UK).) for 3 min at RT. The fixative was discarded and the treated cells were washed twice with 0.1ml of 1×PBS. Methanol (1 ml, 100 %) was then added to the cells and allowed to incubate for 20 min followed by washing with 0.1 ml of 1×PBS. Proteinase K solution(50 µl) was added to the cells, incubated for 15 min at RT, centrifuged at 1000×g for 3 min. The cell pellet was then washed with 200 µl of dH_2O. Subsequently, hydrogen peroxide solution (50 µl from 30% stock solution) was added to each sample, followed by incubation for 5 min at RT. These cells were then again washed with dH_2O as described above. After that, 150 µl of 1× TdT labeling buffer was added to each sample followed by incubation and washing to discard the remaining buffer. Labeling reaction mix was added to the resultant pellet and incubated for 1 h at 37 °C in humidified chamber. The reaction was stopped by the addition of 1×TdT stop buffer

[14]Ravikumar, Y.S., Mahadevan, K.M., Manjunatha, H. and Satyanarayana, N.D., 2010. Antiproliferative, apoptotic and antimutagenic activity of isolated compounds from *Polyalthia cerasoides* seeds. Phytomedicine, 17, pp.513-518.

[15]Transferase Biotin-dUTP Nick End Labeling (TUNEL) assay kit: Cat. no. 4822-96-K ,TACS -Trevigen Apoptotic Cell System Trevigen, Inc., USA.

[16]Li, Y., Chopp, M., Jiang, N., Zhang, Z.G. and Zaloga, C., 1995. Induction of DNA fragmentation after 10 to 120 minutes of focal cerebral ischemia in rats. Stroke, 26, pp.1252-1258.

followed by centrifugation. The supernatant containing the stop buffer was discarded. Traces of stop buffer were removed by washing with 1×PBS. Strep-HRP Solution (50 µl) was then added to each sample tubes and incubated for 10 min at RT followed by centrifugation. The used Strep-HRP solution was discarded and the cells were washed four times with 200 µl of 1×PBS containing 0.1 % Tween-20 solution. TACS–Sapphire (100 µl) was added into each microcentrifuge tubes and incubated for 30 min at RT in the dark. For termination of reaction, 100 µl of 5% phosphoric acid or 0.2 N HCl was added into each microcentrifuge tubes and the reaction mix was transferred to 96 well plates to measure optical density at 450 nm using microplate ELISA reader (Tecan, USA).

3.2.1.8 Biochemical studies

Various biochemical studies for analyzing cellular response against pinostrobin were performed with human cancer cells namely HeLa, Ca Ski, SiHa, A549, HL-60 cells. HEK 293 treated with the test chemicals was included as normal cells.

For this purpose, different cancer cells (5×10^4 cells/well) were seeded in constituted medium in a 24-well cell culture plate and incubated for 24 h. The cells were then treated with pinostrobin (CT_{50} and $2\times CT_{50}$ concentrations) in triplicates for 48 h. Cells treated with corresponding volume of TS (vehicle) and doxorubicin (10 µM) were included as negative and positive controls. After the treatment, the cells were subjected to trypsinization as described earlier. The culture supernatant was harvested and the cell lysate was prepared by incubating the washed cell pellet with RIPA (25 mM Tris-HCl (pH 7.6), 150 mM NaCl, 1 % sodium deoxycholate, 1% NP-40, 0.1% SDS, added 1% protease inhibitor) buffer. The cell lysate thus prepared or the harvested culture supernatant was subjected to analyses detailed below:

- **Protein concentration estimation**

Protein concentration in the cell lysate, (prepared using RIPA buffer) was estimated using BCA protein estimation kit as per the manufacturer's instructions[17]. Serial dilutions of the standard solution of Bovine serum albumin (BSA) was prepared (from 2000 µg/ml to 7.81 µg/ml) in Milli Q in a 96-well plate (in triplicates). Test protein sample was also diluted in Milli Q or any buffer that was used as blank for calculation. BCA reagent was prepared by mixing BCA solution and $CuSO_4$ cocktail (50:1) and added to each well so as to maintain total volume of 200 µl/well. The plate was incubated for 30 min at 37 ºC and

[17]Bicinchoninic Acid Assay (BCA) protein estimation kit (Cat no. 786-570), G-Biosciences, St-Louis MO, USA.

absorbance was measured at 562 nm using microplate ELISA reader. Protein concentration of the cell lysate was calculated using the standard curve of known concentrations of BSA.

- **Determination of intracellular nitrite level**

Nitric oxide (NO), an important physiological messenger and effector molecule of many biological processes, is also considered as a biological marker for tumor progression and angiogenesis. Nitric oxide formation is measured by measuring nitrite production (NO_2^-), a breakdown product of NO using Griess reagent that reacts with nitrite[18]. Chemical basis for Griess's method for nitrite determination is shown in figure 3.2.2.

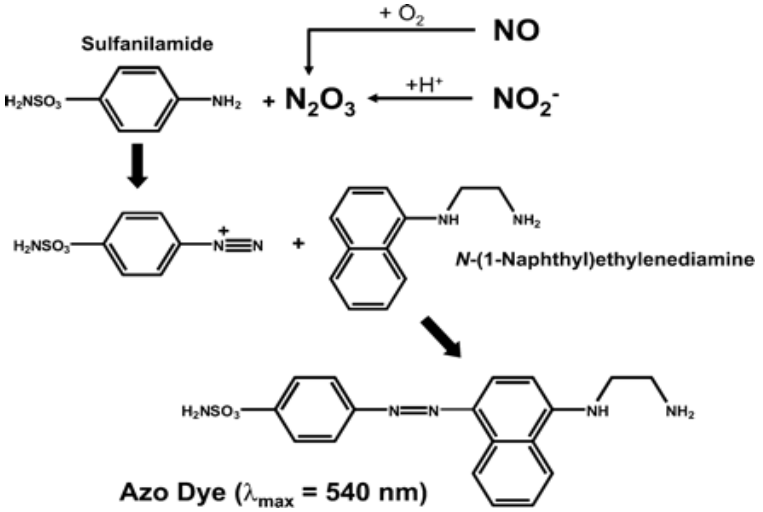

Figure 3.2.2. Chemical reactions involved in the measurement of nitrite using the Griess reagent (Adapted from Tarpey *et al.,* 2004)[19]

Nitrite levels were measured in the culture supernatant of the experimental cells and untreated cells. After the treatment period, 100 µl of culture supernatant was taken out, mixed with 100 µl of Griess reagent [1 % sulfanilamide in 5 % phosphoric acid and 0.1 % N-1-(naphthyl) ethylenediamine dihydro chloride (NED)] and incubated for 10 min at RT. Absorbance was measured at 540 nm using microplate ELISA reader. Standard was prepared using serial dilutions of sodium nitrite (125 µg/ml) and used for calculating the amount of nitrite levels was expressed in µg/mg protein in the experimental samples.

[18]Green, L.C., Wagner, D.A., Glogowski, J., Skipper, P.L., Wishnok, J.S. and Tannenbaum, S.R., 1982. Analysis of nitrate, nitrite, and [15N] nitrate in biological fluids. Analytical Biochemistry, 126, pp.131-138.
[19]Tarpey, M.M., Wink, D.A. and Grisham, M.B., 2004. Methods for detection of reactive metabolites of oxygen and nitrogen: *in vitro* and *in vivo* considerations. American Journal of Physiology-Regulatory, Integrative and Comparative Physiology, 286, pp.R431-R444.

- **Measurement of reduced glutathione (GSH) level**

Glutathione (GSH) is a multifunctional, non-enzymatic intracellular antioxidant that protects the cancer cells from damage generated from antineoplastic agents, free radicals and ROS[20,21]. Reduced glutathione (GSH) level is decreased with an increase in the free radicals level in cells and depletion in the levels of intracellular GSH has been correlated with cell death[22]. GSH levels can be measured using DTNB (Ellman's reagent)[23,24].

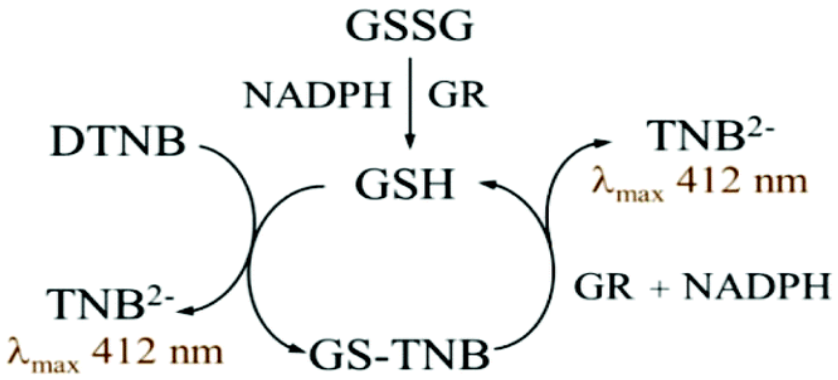

Figure 3.2.3. Principle of glutathione assay (Adapted from Ngamchuea *et al.*, 2016)[25]

Cell lysate of the treated cells was subjected to TCA precipitation by addition of equal volume of 5 % TCA followed by centrifugation at 8000 rpm for 10 min at 4°C. Clear supernatant (100 µl) thus obtained was mixed with phosphate buffer (0.2 M, pH 8) containing DTNB (0.6 mM)[23,24]. An aliquot from the mix was used for measurement of absorbance at 412 nm in a microplate ELISA reader. GSH concentration was determined from the standard curve prepared from standard GSH solution (187.5 µg/ml) and was expressed in µg/mg protein in all experimental groups.

[20]Arrick, B.A. and Nathan, C.F., 1984. Glutathione metabolism as a determinant of therapeutic efficacy: a review. Cancer Research, 44, pp.4224-4232.
[21]Sies, H., 1999. Glutathione and its role in cellular functions. Free Radical Biology and Medicine, 27, pp.916-921.
[22]Fernandes, R.S. and Cotter, T.G., 1994. Apoptosis or necrosis: intracellular levels of glutathione influence mode of cell death. Biochemical Pharmacology, 48, pp.675-681.
[23]Eyer, P. and Podhradský, D., 1986. Evaluation of the micromethod for determination of glutathione using enzymatic cycling and Ellman's reagent. Analytical Biochemistry, 153, pp.57-66.
[24]Moron, M.S., Depierre, J.W. and Mannervik, B., 1979. Levels of glutathione, glutathione reductase and glutathione S-transferase activities in rat lung and liver. Biochimica et Biophysica Acta (BBA)-General Subjects, 582, pp.67-78.
[25]Ngamchuea, K., Batchelor-McAuley, C., Cowen, P.J., Williams, C., Gonçalves, L.M. and Compton, R.G., 2016. Can saliva testing replace blood measurements for health monitoring? Insights from a correlation study of salivary and whole blood glutathione in humans. Analyst, 141, pp.4707-4712.

3.2.1.9 Flow cytometric assay

For flow cytometric analysis, trypsinized cells were pelleted down at 12000 rpm for 5 min at RT, washed with 1 ml of 1×PBS and pooled in FACS tubes. Cells were treated with different cellular probes listed in the Table 3.2.1 to evaluate different cellular parameters indicative of apoptosis:

Table 3.2.1. Measurement of cellular parameters using different dyes with their excitation and emission wavelength

Cellular parameters	Dye/fluorescence probes	Excitation wavelength (nm)	Emission wavelength (nm)
Membrane integrity	Annexin V-FITC	~485 nm	~535 nm
Mitochondrial membrane potential	JC-1	488 nm	530-590 nm
ROS production	DCFH-DA	~485 nm	~530 nm
	NAO	485 nm	560 nm
	HE	~510 nm	~620 nm
DNA fragmentation	PI	535 nm	620 nm

For cell membrane integrity analysis, cells were resuspended in 500 µl of 1×Annexin binding buffer [10×buffer composition: 0.1 M HEPES/NaOH (pH 7.4), 1.4 M NaCl, 25mM $CaCl_2$]. Annexin V-FITC reagent (5 µl; 0.019 mg/ml) was added into sample for staining and mixed using vortex (BioVortexV1, BIOSCAN, USA). Sample was incubated for 10-20 min at 37 ºC in dark for further analysis[26].

Mitochondrial membrane potential of cells was analysed using JC-1 probe. After the treatment, the cells were stained with JC-1 probe (1 µg/ml) using Hank's buffered salt solution (HBSS) for 10-20 min at 37 ºC in dark[27,28]. Samples were centrifuged at 12000 rpm and again cell pellet was resuspended in HBSS for analysis.

ROS production was analysed using 1 ml of cell suspension in HBSS containing different fluorescence probes HE (2.5 µM)[29,30], DCFDA (5.0 µM)[31,32] and NAO (1 µM)[33] . Cells

[26]Fard, S.S., Jeddi-Tehrani, M., Akhondi, M.M., Hashemi, M. and Ardekani, A.M., 2010. Flow cytometric analysis of 4-HPR-induced apoptosis and cell cycle arrest in acute myelocytic leukemia cell line (NB-4). Avicenna Journal of Medical Biotechnology, 2, pp.53-61.
[27]Yong, W.K. and Abd Malek, S.N., 2015. Xanthohumol induces growth inhibition and apoptosis in ca ski human cervical cancer cells. Evidence-Based Complementary and Alternative Medicine, Article ID 921306, pp. 1-10.
[28]Malugin, A., Kopecˇ kovaP. and Kopecˇek, J., 2006. HPMA copolymer-bound doxorubicin induces apoptosis in ovarian carcinoma cells by the disruption of mitochondrial function. Molecular Pharmaceutics, 3, pp.351-361.
[29]Bucana, C., Saiki, I. and Nayar, R., 1986. Uptake and accumulation of the vital dye hydroethidine in neoplastic cells. Journal of Histochemistry & Cytochemistry, 34, pp.1109-1115.
[30]Seleznev, K., Zhao, C., Zhang, X.H., Song, K. and Ma, Z.A., 2006. Calcium-independent phospholipase A2 localizes in and protects mitochondria during apoptotic induction by staurosporine. Journal of Biological Chemistry, 281, pp.22275-22288.
[31]Ling, L.U., Tan, K.B., Lin, H. and Chiu, G.N.C., 2011. The role of reactive oxygen species and autophagy in safingol-induced cell death. Cell death & Disease, 2, pp.1-12.

were incubated for 20-30 min at 37 °C in dark, centrifuged at 12000 rpm for 5 min at RT, and resuspended in 1 ml of HBSS.

For PI staining, cells were fixed with 1 ml of 4% ice cold paraformaldehyde for 20 min and vortexed to remove clumping. Cells treated in this way were incubated on ice for 1 h. Cells were centrifuged at 5000×g for 5 min at 4°C and the pellet was resuspended in 500 µl of PI master mix [prepared in 1×PBS buffer, DNase- free RNAse (100 µ g/ml), PI (40 µ g/ml) and 0.1% Triton×100]. Cells were then incubated for 30 min to 1 h at 37 ºC in dark[26].

Fluorescence of all dyes was measured using FACS Calibur™ (Beckon Dickinson Immuno cytometry system, San Jose, USA) at the specific excitation and emission wavelengths mentioned in Table 3.2.1. The green fluorescence and red fluorescence intensities were acquired by FL1 and FL2 channels with 10,000 events and analysed by FCS Express 5 Flow Cytometry analysis software.

3.2.1.10 Live cell imaging studies

The internalisation of pinostrobin, a fluorescent compound, into the cells and its localization were examined using live cell confocal microscopy[34]. HeLa cells (5×10^4) were grown on 35 mm glass culture dish in 1-2 ml of constituted medium. After 24 h, the cells were washed with 1-2 ml of 1×PBS, pH 7.4 and the exhausted medium was replaced with fresh medium containing 100 µM of pinostrobin. Before the commencement of experiment, the culture environment was maintained at 5 % CO_2 at 37°C in the enclosed microscope chamber. This allowed adequate environment for the cells to grow. The dish thus prepared was kept in the enclosed chamber of live cell confocal microscopy (Nikon, A1R eclipse-Ti at AIRF, JNU, New Delhi). The focus was set onto desirable field via eyepiece. Green and blue fluorescence recorded after excitation (280 nm) was used to visualize pinostrobin internalisation and its retention in nucleus and cytoplasm.

Effect of pinostrobin on deformation of nucleus structure was analysed using Hoechst 33342, a DNA binding dye that preferentiality binds to the adenine-thymine (A-T) region

[32]Li, X., Zhao, H., Wang, Q., Liang, H. and Jiang, X., 2015. Fucoidan protects ARPE-19 cells from oxidative stress via normalization of reactive oxygen species generation through the Ca2+-dependent ERK signaling pathway. Molecular Medicine Reports, 11, pp.3746-3752.

[33]Dietze, E.C., Caldwell, L.E., Grupin, S.L., Mancini, M. and Seewaldt, V.L., 2001. Tamoxifen but not 4-hydroxytamoxifen initiates apoptosis in p53 (−) normal human mammary epithelial cells by inducing mitochondrial depolarization. Journal of Biological Chemistry, 276, pp.5384-5394.

[34]Chua, A.J.S., Netto, P.A. and Ng, M.L., 2012. Molecular characterisation of cell-penetrating peptides through live cell microscopy− the past, the present and the future. Current Microscopy Contributions to Advances in Science and Technology, (A. Méndez-Vilas, Ed.), 1, pp.763-774.

of DNA and emits blue fluorescence[35]. Thus apoptotic cells will show bright blue strain with condensed nuclei and chromatin, fragmented DNA, while normal cells will exhibit dim nuclei with organised structure and dark blue in colour.

The cells were fixed with 4 % PFA for 20 min at RT, washed twice with 1-2 ml of 1×PBS and treated with Hoechst 33342 dye (5 µg/ml) for 30 min at RT followed by two washes with 1× PBS[36]. Deformation of nucleus structure was visualised and imaged under live cell confocal microscope at the AIRF, JNU, New Delhi INDIA. Similarly mitochondrial membrane disturbance was examined using JC-1 probe (1 µg/ml), and analyzed by visualizing JC-1 monomers formation under live cell confocal microscope[27].

3.2.1.11 Protein profiling of pinostrobin-treated cells

For analysing the extrinsic and intrinsic pathways of apoptosis, human apoptosis protein profiler array (R&D, system, USA) kit was used according to manufacturer's protocols[37]. HeLa, Ca Ski, A549 and HL-60 (1×10^6) cells were grown in T-75cm^2 culture flasks with 10 ml of constituted medium, treated with CT_{50} concentration of pinostrobin for 48 h. Post-incubation, these cells were washed with 1-2 ml of 1×PBS and cell lysates were prepared in 1×RIPA buffer and kept on ice for 5 min. The cells were pelleted down by centrifugation at ~12,000×g (Eppendorf centrifuge 5415R, UK) for 15 min at 4 ºC, and protein concentration in cell lysate was estimated by BCA protein assay kit. The nitrocellulose membrane coated in duplicates with 35 different apoptosis related antibodies was placed with 2.0 ml of array buffer 1 in a 4-well multi plate dish. The membrane was incubated for 1 h at RT on a rocking platform shaker in array buffer 1 (blocking buffer). After washing away the array buffer 1, the cell lysate (200 µg prepared in array buffer 1 in a final volume of 1.5 ml) was spread evenly onto each array membrane and incubated overnight at 2-8 °C. Next day, membranes were washed twice with 1×wash buffer on rocking platform shaker for 10 min. Diluted detection antibody cocktail (1.5 ml: dilution 1:1000 in 1×array buffer # 2/3 supplied with the kit) was added into each well of the 4-well multi-dish and incubated for 1 h on a rocking platform shaker at RT. Subsequently, membranes were washed twice with 1×wash buffer and 2 ml of diluted streptavidin-HRP was added (1:1000 in 1×array buffer # 2/3, supplied with the

[35]Yasui, L.S., Chen, K., Wang, K., Jones, T.P., Caldwell, J., Guse, D. and Kassis, A.I., 2007. Using Hoechst 33342 to target radioactivity to the cell nucleus. Radiation Research, 167, pp.167-175.
[36]López, J., Poitevin, A., Mendoza-Martínez, V., Pérez-Plasencia, C. and García-Carrancá, A., 2012. Cancer-initiating cells derived from established cervical cell lines exhibit stem-cell markers and increased radioresistance. BMC Cancer, 12, pp.1-14 .
[37]Human apoptosis protein profiler array, Cat no. ARY009, R & D, System, USA.

kit) into 4-well multi-dish to incubate for 30 min at RT with shaking on a rocking platform shaker. Again membranes were washed twice with 1×wash buffer. Following this, 1 ml of Chemi reagent mix (Chemi Reagent1:Chemi Reagent2, 1:1); provided with kit was spread evenly onto each array membrane. The developed protein profiles were visualized and imaged using Chemidoc, Biospectrum-500, and UVP, USA. Further densitometry analysis of immunoreactive spots on captured image was determined by ImageJ software (http://imagej.net).

3.2.2 Experimental protocols related to Cancer Stem like Cells (CSCs) studies

3.2.2.1 Culture of Sphere Forming Cells (SFCs)

Sphere forming cells (SFCs), also recognised as Cancer Stem like Cells (CSCs) were prepared from HeLa cells by the method of López *et al.,* (2012)[36]. HeLa cells (1×10^5cells/well) were cultured in 2 ml of serum-free media [SFM; epidermal growth factor (EGF) and basic Fibroblast Growth Factor (bFGF), each 20 ng/ml and 0.4% Bovine Serum Albumin (BSA)] in 35 mm culture dish at 37 ºC in 5 % CO_2 incubator. The sphere culture medium was changed every 48 h for making spheres of 100-400 µm in diameter (approximately 6-8 days). After 70-80 % of spheres formation, SFCs were collected by gentle centrifugation at 2,500 rpm for 5 min at RT. Each sphere was separated using 500 µl of 1.0 mM EDTA, and disrupted by Pasteur pipette. Cells suspension (100 µl) was shaken gently to achieve a single-cell suspension and passaged in serum-free medium and constituted fresh DMEM medium.

For morphological examinations of CSCs, HeLa cells ($1x10^4$cells/well) were seeded in 6-well plates with 1 ml of complete serum-free medium and grow at 37 ºC in 5 % CO_2 incubator and sphere formation was promoted by addition of serum-free medium (100 µl) every 48 h. After some time, when the spheres detached from the surface and floated in suspension as clump or aggregates, these were visualized under bright field microscope (Leica, DMIL, Germany) as described by Gu *et al.*, (2011)[38].

3.2.2.2 Characterization of Side Population (SP)

HeLa cells and its CSCs (1×10^5 cells/well) were seeded in 24 well plates with constituted DMEM and serum-free medium and incubated for 24 h. The cells were treated with the

[38]Gu, W., Yeo, E., McMillan, N. and Yu, C., 2011. Silencing oncogene expression in cervical cancer stem-like cells inhibits their cell growth and self-renewal ability. Cancer Gene Therapy, 18, pp. 897-905.

test chemicals i.e. pinostrobin at CT_{50} concentration, or 10 µM doxorubicin. Cells treated with TS were included as vehicle control. After incubation, the cells were washed with 1 ml of 1×PBS and thoroughly dissociated using 1×EDTA(1.0 mM) and resuspended in 1 ml of pre-warmed DMEM (containing 2 % FBS, 1 mM HEPES, and 5 µg/ ml Hoechst 33342) and incubated at 37 °C on rocking platform shaker with slow agitation for 90 min. The cells were stained in the presence or absence of 50 µM verapamil to block Hoechst efflux[39,36]. Subsequently, the cells were washed with HBSS and kept on ice until further analysis. Immediately prior to analysis, PI (2 mg/ml) was added to each sample. Acquisition was performed using FACS Calibur™ (Beckon Dickinson Immuno cytometry system, San Jose, USA) by measuring the fluorescence emission of Hoechst 33342 dye and PI at ~460 nm and ~580 nm respectively. Results were analyzed by FCS Express 5 Flow Cytometry analysis software. A small number of cells that were capable to efflux Hoechst dye with low fluorescing were termed as side population (SP)[38].

3.2.2.3 Sphere-forming efficiency assay

Sphere forming efficiency (SFE) of HeLa cells was determined by the method of López *et al.*,(2012)[36]. Sub-confluent sphere forming HeLa ($1x10^5$cells/well) cells were carefully dissociated with 1×EDTA to make a single cell suspension. The separated cells ($1×10^2$) were seeded in 1ml of sphere forming medium in 6-well culture dish and supplemented with 25 µl of sphere forming medium per well every 48 h. The number of spheres formation in each well was evaluated before and after different treatments (pinostrobin at 50 µM and 100 µM; doxorubicin at 10 µM).

3.2.2.4 Regeneration of HeLa cells from CSCs

Regeneration of HeLa cells from CSCs was carried out as described by Gu *et al.,* (2011) with modifications[38] CSCs ($1×10^4$ cells/well) were grown in 2 ml of constituted DMEM in 35 mm culture dish at 37º C in a humidified incubator with 5 % CO_2 incubator. The CSCs were incubated till they adapted a parental HeLa cells morphology for upto 12 days.

3.2.2.5 CD24/CD44 surface marker analysis (FACS and confocal microscopy)

For analysis of CD24/CD44 surface marker on the HeLa cells and CSCs, method of Gu *et al.,* (2011) was followed[38]. HeLa and CSCs ($1x10^5$cells/well) cells were seeded (grown

[39]Goodell, M.A., Brose, K., Paradis, G., Conner, A.S. and Mulligan, R.C., 1996. Isolation and functional properties of murine hematopoietic stem cells that are replicating *in vivo*. Journal of Experimental Medicine, 183, pp.1797-1806.

on a cover slip for imaging study) in 24-well plate with constituted DMEM and SFM, respectively and incubated for 24 h. The cells were then subjected to different treatments Vehicle (TS), pinostrobin (50 and 100µM) and doxorubicin (10µM)) Cells were washed with 1×PBS and trypsinized with 1×EDTA (1mM), centrifuged at 4000 rpm at RT. HeLa and CSCs were fixed with 2% paraformaldehyde and stained with FITC (fluorescein isothiocyanate)-conjugated anti-CD44 antibodies and R-phycoerythrin (PE)-conjugated anti-CD24 antibodies (1:100) for 30 min at RT. The cells were washed with 1 ml of 1×PBS and expression level of CD24/CD44 was quantified by FACS Calibur™ (Beckon Dickinson Immuno cytometry system, San Jose, USA) at excitation wavelength of 488 nm with 10,000 cell events. The green fluorescence and red fluorescence intensities were visualized in FL1 and FL2 channel using FCS Express 5 Flow Cytometry analysis software. Similarly, morphology of the stained cells was visualized and imaged under Olympus Fluoview FV1000 Confocal Laser-Scanning microscope using 1.4 NA oil objective at the AIRF, JNU, New Delhi.

3.2.2.6 Characterization of CSCs derived from HeLa cells

The HeLa cells/CSCs were subjected to cell viability assay, ROS production, membrane integrity by AnnexinV-FITC, PI staining, mitochondrial membrane potential etc. as described earlier in the methods section (ref. section 3.2.1.9).

3.2.3 Experimental protocols related to *in vivo* animal studies

3.2.3.1. Ehrlich Ascitis Carcinoma (EAC) tumor development and maintenance

Enrich Ascitis Carcinoma (EAC) cells obtained from the National Centre for Cell Sciences, Pune were kindly provided by Prof. Harpal Singh, Centre of Biomedical Engineering, Indian Institute of Technology, New Delhi, India. Female swiss albino mice were injected with EAC cell lines (2×10^6 cells) intraperitoneally for the development of ascites tumor[40]. Ascitis fluid was drawn from EAC tumor bearing mouse at the log phase of the tumor cells (i.e. day 7-8 after ascitis fluid inoculation). EAC cells were maintained *in vivo* by i.p. transplantation of 2×10^6 cells per mouse after every 8 days. After achieving the log phase, the cells were harvested and viable cell count was determined using trypan blue assay (ref. section 3.2.1.3) under microscope using hemocytometer.

[40]Dolai, N., Karmakar, I., Kumar, R.B., Bala, A., Mazumder, U.K. and Haldar, P.K., 2012. Antitumor potential of *Castanopsis indica* (Roxb. ex Lindl.) A. DC. leaf extract against Ehrlich's ascites carcinoma cell. Indian J Exp Biol.,50, pp. 359-65.

3.2.3.2 *In vivo* EAC viability

EAC tumor cell viability (trypan blue assay) was assessed as described earlier section[3] (section 3.2.1.3). Different groups of Swiss albino mice (n=5/group), subjected to different regimen of treatments are given in Table 3.2.3.1. The mice inoculated with EAC cells (2×10^6 EAC cells/0.1 ml) and treated with different concentrations of pinostrobin (i) at 4 days prior (pre-treatment), (ii) 4 days after (post-treatment) (iii) multiple doses at every 4 days after EAC inoculation. Tumor cells were collected from intraperitonial cavity of the different groups of mice to determine the number of viable cells ($\times10^4$) by trypan blue dye exclusion assay.

Table 3.2.3.1. Effect of pinostrobin on cell viability by pre-treatment (GpI), post-treatment (GpII) and multiple treatment (GpIII). Swiss albino mice were divided into three groups (n=5) and administered with pinostrobin (2.5 ,5, 10 and 20 mg/kg b wt.).

Experiment I Pre-treatment	Control group (UT)	No treatment
	Vehicle control group (VC)	TS (vehicle volume corresponding to Pn solution)
	Mice administered with Pn, 4 dpi	Pn doses: 2.5, 5, 10 and 20 mg/kg b wt.
Experiment II Post-treatment	Control group (UT)	No treatment
	Vehicle control group (VC)	TS (vehicle volume corresponding to Pn solution)
	Mice administered with Pn, single dose at day 4 after EAC inoculation	Pn doses: 2.5, 5, 10 and 20 mg/kg b wt.
Experiment III Multiple-dose treatment	Control group (UT)	No treatment
	Vehicle control group (VC)	TS (vehicle volume corresponding to Pn solution)
	Mice administered with multiple Pn doses at every day 4 till 12 days after EAC inoculation	Pn doses: 2.5, 5, 10 and 20 mg/kg b wt.

Note: UT: Untreated, VC: Vehicle control, Pn; Pinostrobin, dpi; days prior to tumor inoculation

3.2.3.3 Determination of tumor volume

To study anti-tumor efficacy of pinostrobin, we determined the tumor growth prior and after pinostrobin administration using two different routes i.e. intraperitoneally and intratumoral. For this set of experiment, all animal groups were first injected with EAC

cells (2×10^6, 0.1 ml) subcutaneously in left thigh of mice for tumor formation[41]. Thereafter, the animal groups were treated with pinostrobin and doxorubicin as described in table 3.2.3.2. Tumor volume was measured using Mitutoyo Vernier Caliper (Mitutoyo 500-196 Digimatic Vernier Caliper). Tumor volume (T) was calculated using the following formula till 16 days after EAC inoculation[42].

$$T = (L\times W^2)/2$$

where, T is tumor volume, W is tumor width, L is tumor length

3.2.3.4 Survival study of tumor bearing mice

The animal life span was assessed by observation of spontaneous death according to established criteria. Treatment-dose specific survival curves were calculated by the Kaplan–Meier method[43] Untreated and vehicle treated mice were included as control groups. The other four groups of mice were administered with pinostrobin (2.5, 5, 10 and 20 mg/kg b wt.) through i.t. route at every 4 days intervals after EAC inoculation. The mean survival time (MST) of different groups was determined as per standard methods[44,45]. The MST and percentage increase in life span (% ILS) was calculated using the following equation:

$$MST = (\text{Day of first death} + \text{Day of last death})/ 2$$

$$ILS\ (\%) = [(\text{Mean survival time of treated group}/ \text{mean survival time of control group}) - 1] \times 100$$

3.2.3.5 Statistical analysis

Statistical analysis was carried out using GraphPad software (Chicago, USA). All experimental results are expressed as mean±SD from at least three independent experiments, performed in triplicates. Statistical significance was calculated using two-way ANOVA (Dunnett's multiple comparison test) and student t-test in comparison with vehicle control group (VC).

[41]Mohamed, E.A., Hashim, I.I.A., Yusif, R.M., Suddek, G.M., Shaaban, A.A.A. and Badria, F.A.E., 2017. Enhanced *in vitro* cytotoxicity and anti-tumor activity of vorinostat-loaded pluronic micelles with prolonged release and reduced hepatic and renal toxicities. European Journal of Pharmaceutical Sciences, 96, pp.232-242.

[42]Zhang, H., Zheng, D., Ding, J., Xu, H., Li, X. and Sun, W., 2015. Efficient delivery of ursolic acid by poly (N-vinylpyrrolidone)-block-poly (ε -caprolactone) nanoparticles for inhibiting the growth of hepatocellular carcinoma *in vitro* and *in vivo*. International Journal of Nanomedicine, 10, pp.1909–1920.

[43] Kaplan, E.L. and Meier, P., 1958. Nonparametric estimation from incomplete observations. Journal of the American Statistical Association, 53, pp.457-481.

[44]Dolai, N., Karmakar, I., Kumar, R.S., Kar, B., Bala, A. and Haldar, P.K., 2012. Evaluation of antitumor activity and *in vivo* antioxidant status of *Anthocephalus cadamba* on Ehrlich ascites carcinoma treated mice. Journal of Ethnopharmacology, 142, pp.865-870.

[45]Osman, M.A., Rashid, M.M., Aziz, M.A. and Habib, M.R., 2011. Inhibition of Ehrlich ascites carcinoma by *Manilkara zapota* L. stem bark in Swiss albino mice. Asian Pacific Journal of Tropical Biomedicine, 1, pp.448-451.

Table 3.2.3.2. Experiment design for studying the effect of pinostrobin (pre- and post-treatment) on tumor volume by different routes of administration (i.t. and i.p.).

Experiment IV				
Routes of Pn administration (i.t. and i.p.)	**Group I**	**Group II**	**Group III**	**Group IV**
	Untreated (UT)	Vehicle Control (VC)	Mice administered with single dose Pn (10 mg/kg b wt.) at 4 dpi	Mice administered with single dose D_X (2.5 mg/kg b wt.) at 4 dpi
Experiment V				
Routes of Pn administration (i.t. and i.p.)	**Group I**	**Group II**	**Group III**	**Group IV**
	Untreated (UT)	Vehicle Control (VC)	Mice administered with single dose Pn (10 mg/kg b wt) at 4 day after EAC inoculation	Mice administered with single dose Dx (2.5 mg/kg b wt.) at 4 day after EAC inoculation
Experiment VI				
Routes of Pn administration (i.t. and i.p.)	**Group I**	**Group II**	**Group III**	**Group IV**
	Untreated (UT)	Vehicle Control (VC)	Mice administered with multiple dose Pn (10 mg/kg b wt) at every 4 day after EAC inoculation	Mice administered with multiple dose Dx (2.5 mg/kg b wt.) at 4 every day after EAC inoculation

Note: UT: Untreated, VC: Vehicle control, Pn: Pinostrobin, dpi: days prior to tumor inoculation, Dx: Doxorubicin

3.2.4 Experimental protocols related to pinostrobin-topoisomeraseI interaction studies

3.2.4.1 Molecular docking of pinostrobin with topoisomerase I-DNA complex

Three dimensional structure of the target human topoisomerase I-DNA complex was obtained from protein data bank[46] (1T8I, Resolution: 3.0 Å, R-Value Free: 0.292). Subsequently, already bound ligands (heteroatoms) and water molecules were removed from the structure prior to docking analysis[47]. The three dimensional (3D) molecular structures of ligand pinostrobin and doxorubicin (included as positive control) were

[46]http:// www.rcsb.org/pdb

[47]Jorgensen, W.L. and Tirado-Rives, J., 2005. Potential energy functions for atomic-level simulations of water and organic and biomolecular systems. Proceedings of the National Academy of Sciences of the United States of America, 102, pp. 6665-6670.

obtained in sdf format from PubChem database[48]. The structure of target topoisomerase I-DNA complex and ligands were saved as in ".pdb" format for docking study.

3.2.4.2 Automated rigid and flexible docking

For understanding of interaction between pinostrobin and topoisomease I-DNA complex, automated rigid docking and flexible docking were performed using AutoDock v 4.2 program[49].Automated docking was started from opening of topoisomease I-DNA complex with grid parameters and added polar hydrogen atoms, and merged nonpolar hydrogen atoms. Kollman united atom partial charges and salvation parameters were assigned on topoisomease I-DNA complex by default setting then saved in "pdbqt" format. The modification in the structure of receptor (topoisomease I-DNA complex) was almost similar in both rigid and flexible docking; while in flexible docking receptor was represented in flexible mode for perfect binding of ligands[50]. Ligands pinostrobin and doxorubicin were opened in ".pdb" form and modified by adding hydrogen atoms and Gasteiger charges, and the best root in the atoms of ligand was fixed by torsion degree of freedom, then ligand structures were also saved in "pdbqt" format. During rigid docking, all bonds of ligands were made nonrotatable and protein was kept rigid, but in case of flexible docking the torsional bonds of the ligands's structure was kept free, thus allowing rotatable bonds to remain flexible for perfect binding on the receptor. The binding sites of ligands on the receptor were defined by grid parameter. Grid box was fixed and area of interest was mapped on the receptor. The mapping was also defined by the types of atoms in the ligand and receptor, grid spacing ~ 0.375A° and dimension of 60×60×60×along with x, y, and z axes at centre of receptor. In case of flexible docking grid-box was generated that covered entire protein binding site; reducing the grid box size and centering on the ligands. The output of grid file was saved in ".gpf" extension. Modified receptor file and ligand file were uploaded and accepeted in "pdbqt" format. Each binding site of ligand on the receptor was evaluated by Lamarckian Genetic Algorithm (LGA)[51] with 100 local search engine and file was saved in ".dpf" format. In each run, docking population of 150 individuals with 27,000 generations and 2,50,000 energy evaluations were used, while in the case of flexible docking, docking population of individuals,

[48]https://pubchem.ncbi.nlm.nih.gov
[49]Hetényi, C. and van der Spoel, D., 2002. Efficient docking of peptides to proteins without prior knowledge of the binding site. Protein Science, 11, pp. 1729-1737.
[50]Cavasotto, C.N., Kovacs, J.A. and Abagyan, R.A., 2005. Representing receptor flexibility in ligand docking through relevant normal modes. Journal of the American Chemical Society, 127, pp.9632-9640.
[51]Morris, G.M., Goodsell, D.S., Halliday, R.S., Huey, R., Hart, W.E., Belew, R.K. and Olson, A.J., 1998. Automated docking using a Lamarckian genetic algorithm and an empirical binding free energy function. Journal of Computational Chemistry, 19, pp.1639-1662.

generations and energy evaluations were enhanced up to 1500, 27, 0000 and 250, 0000, respectively.

During local search in docking process, operator weights for crossover, mutation, elitism, Cauchy alpha, Cauchy beta and Solis-Wets iterations were set at 0.02, 0.8, 1, 0, 1 and 300, respectively. As per the criterion, 2.0˚A of root-mean square-deviation (RMSD) was used for cluster analysis in docking results. Further, automated docking was proceeded with defaults parameter and run using cygwin autodock grid followed by cygwin autodock program, respectively. The result file was automatically saved in ".dlg" format which was used to analyze the energy of different docked complexes. Final calculation of automated docking was done by AutoDock 4.2 tool based on Lamarckian Genetic Algorithm (LGA). During the course, various conformation of docked complex were generated and ranked according to their (receptor-ligand) binding affinity. The docking energy was calculated by the addition of Van der Waals force, bond energy, dissolve energy, electrostatic energy and internal energy. The docked complexes having lowest docking energy were selected for further analysis and visualized by PyMOL v 1.7 1 viewer[52].

3.2.4.3 Validation of docking by rescoring

The results of automated rigid and flexible docking were validated and improved using variety of rescoring functions (FlexX, GOLD, ChemScore, Glide and PMF). Therefore, one of the score functions was tested for validation or re-evaluation of the best docked complex by Glide[53]. During Glide docking, both ligands (pinostrobin and doxorubicin) were prepared using LigPrep module of v2.3 from Schrödinger Suite 2013. This LigPrep module further follows Optimized Potential Liquid Simulations for All Atoms force fields (OPLS-AA) for energy minimization[54]. Receptor structure file (PDB: 1T8I) was retrieved from PDB database, and optimized using protein preparation wizard of Glide program. Energy minimization of the receptor file was also carried out using OPLS-AA force fields. A fixed value of dielectric constant (4.0) and conjugate gradient steps (1000) were applied during energy minimization process. The binding site of topoisomerase I was defined using well known amino acid residues and docking grid was fixed. The program was then run with fixed value of root mean square deviation (RMSD <0.5Å), maximum

[52]Lill, M.A. and Danielson, M.L., 2011. Computer-aided drug design platform using PyMOL. Journal of Computer-Aided Molecular Design, 25, pp.13-19.

[53]Murugesan, A. Rani, S. 2016. *In silico* molecular docking studies on the phytoconstituents of *cadaba fruticosa* (l.) druce for its fertility activity. Asian Journal of Pharmaceutical and Clinical Research, 9, pp. 48-50.

[54]Halgren, T.A., 2009. Identifying and characterizing binding sites and assessing druggability. Journal of Chemical Information and Modeling, 49, pp.377-389.

atomic displacement (<1.2 Å) and default setting of van der Waals radii to reduce the large number of ligand poses. The best docked structure was selected, a maximum of 100 poses per ligand were generated and analyzed based on extra precision (XP) docking score or Glide scores (G-score) function of Glide program.

3.2.4.4. Evaluation of stability of docked complexes

The stability of docked complexes was evaluated by molecular dynamics simulations using the GROningen Machine for Chemical Simulations V4.5.4 (GROMACS)[55,56]. Docked complexes were placed in the centre of the solvated cubic box and assigned GROMOS96 43a1 force field. Topology files for ligands (pinostrobin and doxorubicin) were generated using PRODRG2 server[57]. Simulation cell dimensions were set approximately at 90× 90×90 Å for all simulations, total negative charges on the docked structures were balanced and neutralized using genion program of GROMACS. Energy was minimized for the entire system using steepest descent algorithm for 1000 steps to remove the steric clashes. The stability of docked complexes was determined using potential energy plot derived by GROMACS. For thermodynamic stability study, free energy of docked complex was also calculated by Helmholtz free energy formula. Helmholtz energy, also known as Helmholtz function, Helmholtz free energy and free energy[58] was calculated by following formula:

$$A = U - TS$$

Where A is the Helmholtz free energy, U is the internal energy of the system, T is the absolute temperature (kelvins) and S is the entropy of the system.

3.2.4.5 Determination of free energy of binding by Prime MM/GBSA

The binding free energy of complex was analyzed by Generalized Born Model and Solvent Accessibility (GBSA) method, using Prime MM/GBSA (Prime version 2.1, 2009)[59]. Free energy of binding of pinostrobin-topoisomeraseI-DNA complex and doxorubicin-topoisomeraseI-DNA complex was calculated using following equation:

$$\Delta G_{binding} = E_{R:L} - (E_R + E_L) + G_{SA} + G_{SOLV}$$

[55]Van Der Spoel, D., Lindahl, E., Hess, B., Groenhof, G., Mark, A.E. and Berendsen, H.J., 2005. GROMACS: fast, flexible, and free. Journal of Computational Chemistry, 26, pp.1701-1718.
[56]Berendsen, H.J., van der Spoel, D. and van Drunen, R., 1995. GROMACS: a message-passing parallel molecular dynamics implementation. Computer Physics Communications, 91, pp.43-56.
[57]SchuÈttelkopf, A.W. and Van Aalten, D.M., 2004. PRODRG: a tool for high-throughput crystallography of protein–ligand complexes. Acta Crystallographica Section D: Biological Crystallography, 60, pp.1355-1363.
[58]Souza, A.T., Cardozo-Filho, L., Wolff, F. and Guirardello, R., 2006. Application of interval analysis for Gibbs and Helmholtz free energy global minimization in phase stability analysis. Brazilian Journal of Chemical Engineering, 23, pp.117-124.
[59]Lyne, P.D., Lamb, M.L. and Saeh, J.C., 2006. Accurate prediction of the relative potencies of members of a series of kinase inhibitors using molecular docking and MM-GBSA scoring. Journal of Medicinal Chemistry, 49, pp.4805-4808.

Where $\Delta G_{binding}$ represents binding free energy, $E_R + E_L$ is the total of energy of unbounded receptor and ligand while E_R:E_L is the energy of the docked complex. ΔGSA represents difference of surface area energy of the receptor-ligand complex and the sum of surface area energy for the unbound receptor and ligand individually. ΔGSOLV represents difference in the GBSA solvation energy of the receptor –ligand complex and total solvation energy of unbound receptor and the ligand. Further, all binding pose of ligand was minimized using the local optimization by Prime. Finally, the energies of the docked complexes were calculated using different programs including Optimized Potentials for Liquid Simulations (OPLS) all-atom and force field 2005 and Generalized-Born/Surface area continuum solvent model (GB/SA)[60,61].

3.2.4.6 LIGPLOT

LIGPLOT v.4.5.3 is a HBPLUS based program, used for elucidation of hydrogen bonds, hydrophobic interactions and Van Der Waals contacts among ligands-protein[62]. LIGPLOT algorithm was used to examine interaction between three-dimensional (3D) structure of the ligands and protein from the PDB files and represented as its 2D structure. The output of ligplot was generated in PostScript format and saved in MS format, which converted into color pdf for interaction study.

3.2.4.7 ADMET studies

Evaluation of absorption, distribution, metabolism, excretion and toxicity (ADMET) of the test chemicals i.e. pinostrobin and doxorubicin was performed using MedChem Designer v.3[63]. This generated the score values of different parameters such as permeability (S+logp), distribution (S+logD), topological polar surface area (TPSA), Moriguchi octanol-water partition coefficient (MLogP), molecular weight (Mwt) and total number of nitrogen and oxygen atoms for pinostrobin and doxorubicin. These score values also provided information and validation of "Lipinski rule of 5", revealing the accuracy and efficacy of the ligands. During ADMET analysis, Ligand' file (pinostrobin

[60]Shaikh, F. and Siu, S.W., 2016. Identification of novel natural compound inhibitors for human complement component 5a receptor by homology modeling and virtual screening. Medicinal Chemistry Research, 25, pp.1564-1573.
[61]Jorgensen, W.L., Maxwell, D.S. and Tirado-Rives, J., 1996. Development and testing of the OPLS all-atom force field on conformational energetics and properties of organic liquids. Journal of the American Chemical Society, 118, pp.11225-11236.
[62] Wallace, A.C., Laskowski, R.A. and Thornton, J.M., 1995. LIGPLOT: a program to generate schematic diagrams of protein-ligand interactions. Protein Engineering, 8, pp.127-134.
[63] Suenderhauf, C., Tuffin, G., Lorentsen, H., Grimm, H.P., Flament, C. and Parrott, N., 2014. Pharmacokinetics of paracetamol in Göttingen minipigs: *In vivo* studies and modeling to elucidate physiological determinants of absorption. Pharmaceutical Research, 31, pp.2696-2707(http://www.simulations-plus.com/).

and doxorubucin) in ".sdf" format was uploaded on the server and the program "ADMET calculate properties" was run.

3.2.4.8 Topoisomearse I activity assay

TopoisomearseI activity was carried out using nuclear extract as the source of topoisomeases and plasmids pBSK+ DNA prepared from the E. *coli* cells.

3.2.4.8.1 Plasmid DNA preparation (miniprep)

Plasmid DNA was prepared from *E. coli* cells as described by Sambrook *et al*.,(1989)[64]. *E. coli* DH5α cells harbouring the plasmid pBSK+ were grown in Luria Bertani culture medium in the presence of chloramphenical (30 µg/ml) at 37 °C with shaking (150 rpm) overnight. One ml of overnight culture was aliquoted in 1.5 ml microcentrifuge tube and the bacterial cells were pelleted down at 6,000 rpm for 10 min at RT. The cells were resuspended in 100 µl of solution I (25 mM Tris-HCl, 10 mM EDTA, pH 8.0, 50 mM glucose). Freshly prepared lysozyme (10 mg/ml) was added to the cell suspension and allowed to incubate at RT for 10 min. Solution II (0.2 N NaOH and 1 % SDS, freshly prepared; 200 µl) was then added and the tubes were gently inverted for proper mixing of the solution. Following this, 150 µl of solution III (3 M potassium and 5M acetate, pH adjusted to 5.2 with glacial acetic acid) was added and incubated at 4 ºC for 15 min followed by centrifugation at 13,000 rpm for 15 min at 4 ºC. After centrifugation the supernatant was carefully transferred into new microcentrifuge tube and mixed with equal volume of PCI [Tris-HCl saturated phenol (pH 8.0)-chloroform-isoamylalcohol mixture: 25:24:1)]. The aqueous layer was aspirated out and extracted with equal volume of CI (24:1) followed by centrifugation at 13,000 rpm for 15 min at RT. Aqueous layer was transferred to a fresh centrifuge tube, the plasmid DNA was precipitated with 2.5 volumes of chilled 95 % ethanol and collected by centrifugation at 13,000 rpm for 20 min at 4 ºC. Then DNA pellet was washed with 70 % ethanol, air dried or vaccum dried using Speed Vac (SAVANT ISS110 speed vac concentrator, Thermo scientific, USA) and finally dissolved in 1×TE (10 mM Tris-HCl, 1 mM EDTA, pH 8.0) containing RNase A (20 µg/ml). Plasmid DNA was stored in small aliquots at 4 ºC for short term storage and at -20 ºC for long term storage. For preparation of supercoiled DNA used in the topoisomerase I activity assay, Qiagen plasmid extraction kit was used as per the manufacturer's instructions.

[64]Sambrook, J., Fritsch, E.F. and Maniatis, T., 1989. Molecular cloning: a laboratory manual (No. Ed. 2). Cold spring harbor laboratory press.

3.2.4.8.2 Agarose gel electrophoresis

Agarose gel electrophoresis was performed for analysis of quality and quantity of plasmid DNA[64]. For this 1% of agarose gel was prepared by dissolving adequate amounts of agarose powder in appropriate volume of 1× TAE buffer (40 mM Tris, 20 mM acetic acid, 1 mM EDTA, pH 8.3, adjusted with glacial acetic acid) by boiling.The agarose solution was cooled for 10 min, ethidium bromide (0.5 µg/ml) was then added to it and mixed properly. The gel was then poured into the gel casting tray and the comb was inserted into the gel for well formation and allowed to solidify. After solidification, comb was removed and the gel was placed in a gel tank containing 1 × TAE buffer, pH 8.3. DNA sample was prepared with adequate amounts (1×) of loading dye (6×; 0.25 % bromophenol blue, 0.25 % xylene cyanol, 30 % glycerol/40% sucrose in distilled water), loaded in the well and then electrophoresed at constant voltage (5 V/cm) till the dye front was 1 cm from the bottom. Finally DNA bands were visualized under UV transilluminator (Bio-Rad Laboratories, Inc., USA).

3.2.4.8.3 DNA concentration quantification

DNA concentration was also estimated by spectrophotometer (Perkin-Elmer Lambda 25 Norwalk, CT, USA) and analyzed using UV WinLab software besides agarose gel electrophoresis. For this, DNA samples were prepared in 1×TE (10 mM Tris-HCl, 1 mM EDTA, pH 8.0) at 1:1000 dilution and the optical density of DNA was measured using a quartz cuvette at 260 nm (slit width=1nm, path length=1cm). The buffer used for DNA dilution constituted the blank and its OD was subtracted from the test sample reading. Absorbance of 1 unit at 260 nm for a double stranded DNA solution amounts to a DNA concentration of 50 µg/ml.

3.2.4.8.4 Nuclear extract preparation

Nuclear extract was prepared from cultured Ca Ski cells as described by Chen *et al.,* (2003)[65] with minor modifications. The cells were seeded at a density of 1×10^6/ml and cultured in constituted RPMI-1640 medium in T-75 cm^2 culture flask at 37 °C in humidified CO_2 (5 %) incubator. Once the cell culture attained ~70-80% confluency, the cells were harvested by trypsinization and washed with 1-2 ml of ice-cold 1×PBS, pH 7.4. The cells were then washed with 1 ml of nuclear buffer I [1mM EGTA, 0.1 mM PMSF,

[65]Chen, B.M., Chen, J.Y., Kao, M., Lin, J.B., Yu, M.H. and Roffler, S.R., 2000. Elevated topoisomerase I activity in cervical cancer as a target for chemoradiation therapy. Gynecologic Oncology, 79, pp.272-280.

0.2 mM Dithiothreitol, 150 mM NaCl, 1 mM KH_2PO4, 5 mM $MgCl_2$, 10% glycerol (v/v), pH 6.4] and resuspended in nuclear buffer II (nuclear buffer I containing 0.3% Triton x-100) and homogenized using a dounce homogenizer. The homogenate was centrifuged at 1000×g for 10 min and the nuclear pellet was washed with 1 ml of nuclear buffer I. The nuclei were then gently resuspended in 1 ml of nuclear buffer I containing 0.25 M NaCl, followed by centrifugation at 16,000×g for 30 min. Supernatant (nuclear extract) thus collected and flash frozen in liquid nitrogen and stored in small aliquots in liquid nitrogen. The nuclear extract thus prepared was used as a source of topoisomerases. Protein content of the nuclear extract was estimated using BCA protein estimation kit (G-Biosciences, USA).

3.2.4.8.5 Topoisomerase I relaxation assay

Effect of the test chemical on topoisomerase I activity was evaluated by topoisomerase I relaxation assay[65] with minor modifications. Nuclear extract prepared from Ca Ski cells and plasmid pBSK+ DNA were used as the source of topoisomerase I and the template, respectively in an *in vitro* assay. Plasmid pBSK+ (3 µg) was preheated at 37 °C in 20 µl of reaction buffer (10 mM Tris-HCl pH 7.4, 200 mM KCl, 10 mM $MgCl_2$, 1 mM EDTA, 1 mM DTT, and 1mg/ml BSA) for 15 min. The enzyme reaction was initiated by the addition of nuclear extract (1.5µg) used as a source of topoisomerase I and the reaction mix incubated at 37 °C for 30 min. In order to study the effect of pinostrobin and doxorubicin on topoisomerase I activity, similar reaction was carried out in the presence of different concentrations of pinostrobin (50-,400 µM) and doxorubicin (50-300µM). After incubation for 30 min, the reaction was terminated by adding 4 µl of 10% SDS. Finally, 4µl of 6× loading dye (40 % sucrose, 0.025 % bromophenol blue, 50 mM EDTA) was added to the samples and the samples were analyzed on 1% agarose gel in 1×TAE buffer (40 mM Tris, 20 mM acetic acid, 1 mM EDTA, pH 8.3) at constant voltage (3 V/cm). The gel was then stained with ethidium bromide (0.5 µg/ml) and different forms of DNA generated during the enzyme reaction were visualized under UV transilluminator (Bio-Rad Labortories, Inc., USA).

3.2.4.8.6 Ethidium bromide displacement assay

In order to investigate binding of pinostrobin to plasmid pBSK+, ethidium bromide (EtBr) displacement assay was carried out by the method of Strothkamp *et al.,(*1994) with

minor modifications[66]. Ethidium bromide (0.5µg/ml) was added to plasmid DNA (6 nM) in 50 mM Tris-HCl (pH 7.4) in a final volume of 500 µl and incubated at 25°C for 30 min.Fluorescence emission spectra of ethidium bromide (excitation at 300 nm, emission at 620 nm) were recorded using quartz cuvette (path length 1cm, slit width 5 nm and scan speed of 100 nm/min) in a spectrofluorometer (Cary Eclipse, Varian Optical Spectroscopy Instruments, USA). Binding of pinostrobin or doxorubicin to plasmid DNA and thus displacement of EtBr, was investigated by decrease in ethidium bromide fluorescence intensity at its emission maximum i.e. 620 nm. For this, different concentrations of pinostrobin (50, 100, 200 µM) were added to the reaction mix and incubated at 25°C for 30 min followed by fluorescence measurement. The control samples were prepared by adding corresponding volume of TS (used as vehicle).

3.2.4.6.7 Pinostrobin interaction with topoisomerase I and DNA

Interaction of pinostrobin with purified topoisomerase I (Sigma-Aldrich Chemical Co., USA) and DNA was investigated using fluorescence spectroscopy as described earlier[67]. Florescence emission spectra of pinostrobin and doxorubicin were measured in the presence and absence of topoiomerase I and DNA. For this, pinostrobin (50 & 100 µM), and doxorubicin (50µM) was incubated individually with 1 unit of topoisomerase I in 1×PBS (pH 7.4) at 25°C for 30 min. Fluorescence emission spectra were recorded between 350 nm to 750 nm (slit width 5 nm, path length 1cm) in a quartz cuvette in a spectrofluorimeter fitted with a Peltier temperature controller. The excitation wavelength was set at 250 nm. Fluorescence spectra were plotted after background buffer spectra corrections.

Similarly, pinostrobin-DNA interaction was examined by incubating pinostrobin (50 & 100 µM) and doxorubicin (50 µM) with plasmid pBSK+ DNA (6 nM in 1× TE buffer (10 mM Tris-HCl, 1 mM EDTA, pH 7.4) at 25°C for 30 min followed by fluorescence emission spectra measurement as described above.

[66] Strothkamp, K.G. and Stothkamp, R.E., 1994. Fluorescence measurements of ethidium binding to DNA. J. Chem. Educ, 71, p.77. DOI: 10.1021/ed071p77

[67]Chowdhury, A.R., Sharma, S., Mandal, S., Goswami, A., Mukhopadhyay, S. and Majumder, H.K., 2002. Luteolin, an emerging anti-cancer flavonoid, poisons eukaryotic DNA topoisomerase I. Biochemical Journal, 366, pp.653-661.

Chapter 4

Results

Chapter4.1

Pinostrobin inhibits human cancer cell proliferation and promotes apoptosis in *in-vitro* model system

4.1.1 Cytotoxic effect of pinostrobin

Evaluation of cell viability of several cancer cell lines namely HeLa, Ca Ski, SiHa, A549 and HL-60 as well as in normal HEK 293 (non-cancerous control cells) in the presence of different concentrations of pinostrobin for different time periods was used to measure cytotoxicity. As evident from Figure 4.1.1, pinostrobin significantly reduced the cell viability in dose- and time-dependent manner in all the cancer cells. At these concentrations, pinostrobin showed minimal toxicity in HEK 293 cells, included as non-cancerous normal cells in the study. The CT_{50} values of pinostrobin determined from the dose response curve [percentage cytotoxicity vs pinostrobin concentration (µM)] for different cancer cell lines are given in table 4.1.1. At 48 h, the CT_{50} value from the table it is evident that among the different cancer cell lines used for the study, order of toxicity of pinostrobin in terms of CT_{50} was found to be HL-60>HeLa>Ca Ski>SiHa=A549 with CT_{50} values at 10±1.72 µM, 50±5.16 µM, 75±6.01µM, 100±3.34µM and 100±0.42 µM, respectively (Figure 4.1.1 A,B,C,D,E,F). On the other hand doxorubicin (included as positive control) at 10 µM showed variable cytotoxicity in different cancer cells [62.4% (*p≤0.001*), 33.86% (*p≤0.001*), 34.23% (*ns*), 49.68% (*p≤0.001*) and 59.73% (*p≤0.001*) in HeLa, Ca Ski, SiHa, A549 and HL-60 cells, respectively at 48 h post-treatment], also was toxic to the normal cells (36.14%, *p≤0.001*)(Figure 4.1.1F). Triple solvent (TS-vehicle control) used to dissolve pinostrobin was found to be significantly less cytotoxic as even longer exposure to TS did not result in increase in cytotoxicity.

4.1.2 Morphological assessment of apoptosis:

- **Wright-Giemsa staining**

Wright-Giemsa staining revealed that pinostrobin treatment of different cancer (HeLa, Ca Ski, SiHa, A549 and HL-60) cells resulted in remarkable changes in cell and nucleus morphology with characteristic changes that are hallmark of apoptosis. These included cell shrinkage, condensed nuclei, membrane blebbing and apoptotic bodies' formation at 24 h (Panel A) and 48 h (Panel B) as evident from Figure 4.1.2. A large number of cells were detached from the surface and formed apoptotic bodies after 48 h treatment. Doxorubicin treated cells (included as positive control) also exhibited modified nuclear and cell structure. No change in the morphology was observed in vehicle treated cells in comparison to untreated cells.

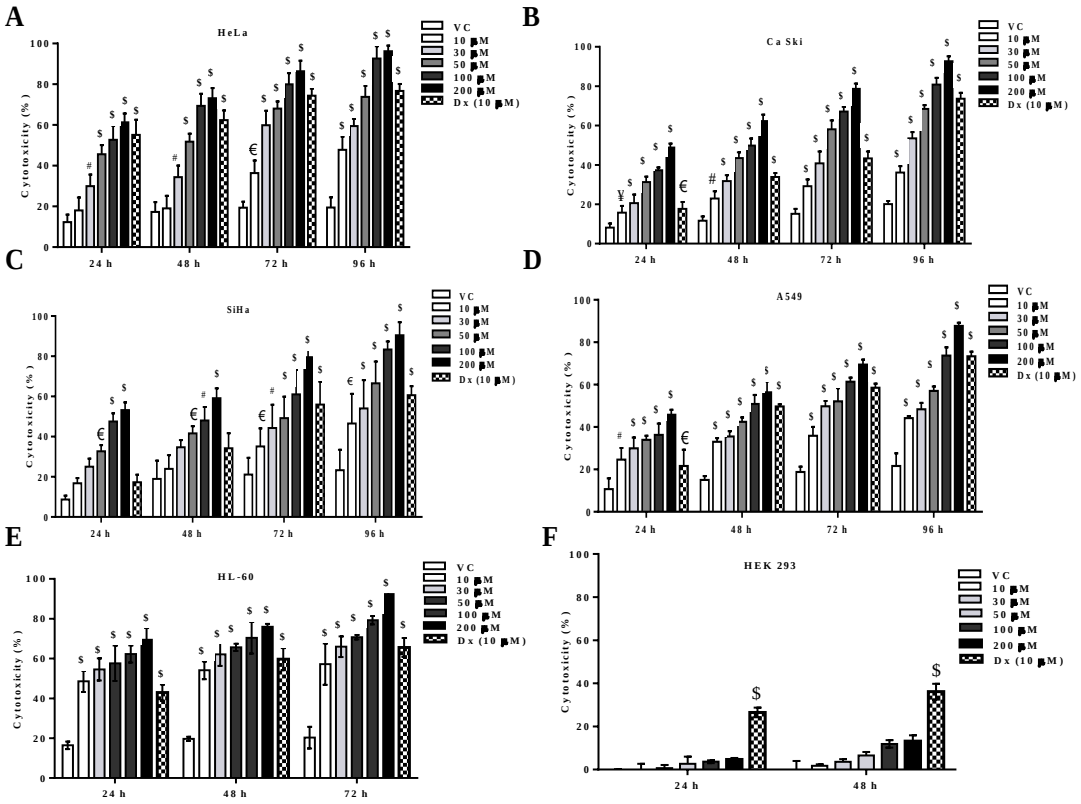

Figure 4.1.1. Cytotoxic effect of different concentrations of pinostrobin on the growth of (A) HeLa, (B) Ca Ski, (C) SiHa, (D) A549, (E) HL-60 and (F) HEK 293 cells at different incubation period during post-treatment. Cytotoxicity of pinostrobin was quantified by MTT assay and expressed as percent (%) of cell death. Doxorubicin (Dx) at 10µM was used as positive control, whereas corresponding volume of triple solvent (TS) used to dissolve pinostrobin was included as a vehicle control (VC). The data represent mean±SD of three independent experiments conducted in triplicates. Significance (*p value*) is calculated with respect to vehicle control cells using ordinary two-way ANOVA (Dunette's multiple comparison test) ¥, $p \leq 0.05$; €, $p \leq 0.01$; #, $p \leq 0.005$; $, $p \leq 0.001$.

Table 4.1.1 CT_{50} value of pinostrobin determined in different cancer cell lines using MTT assay

Cell Lines	CT_{50} (µM)
HeLa	50±5.16
Ca Ski	75±6.01
SiHa	100±3.34
A549	100±0.42
HL-60 (24h)	10 ±1.72

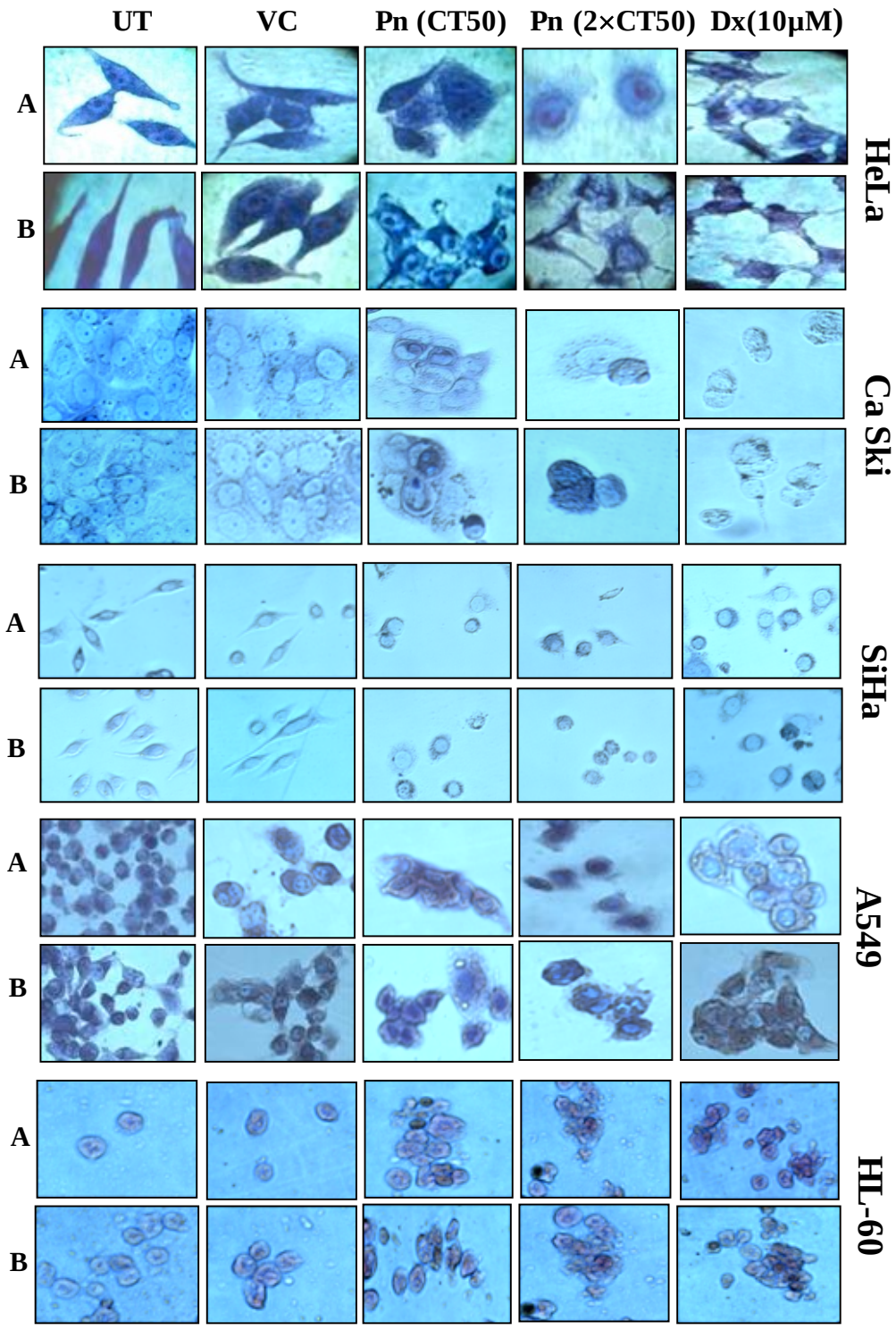

Figure 4.1.2. Wright-Giemsa staining to assess morphological alterations in different cells treated with the test chemicals: HeLa, Ca Ski, SiHa, A549 and HL-60 cells were treated with vehicle control (VC, Triple solvent is used to dissolve pinostrobin), doxorubicin (10 µM) and pinostrobin at CT_{50} and $2xCT_{50}$ concentration for respective cells lines for 24 (panel A) and 48 h (panel B) and visualized at 40× magnifications under bright field microscopy. CT_{50} concentrations for different cell lines, are summarized in table 4.1.1 The characteristic features of apoptosis are observed as reduction of cell size, cytoplasmic shrinkage, nuclear condensation, aggregation of nuclear chromatin and nuclear fragmentation in pinostrobin and doxorubicin treated cells is evident when compared to untreated and vehicle treated cells. UT, Untreated; VC, Vehicle control; Pn, Pinostrobin; Dx, Doxorubicin.

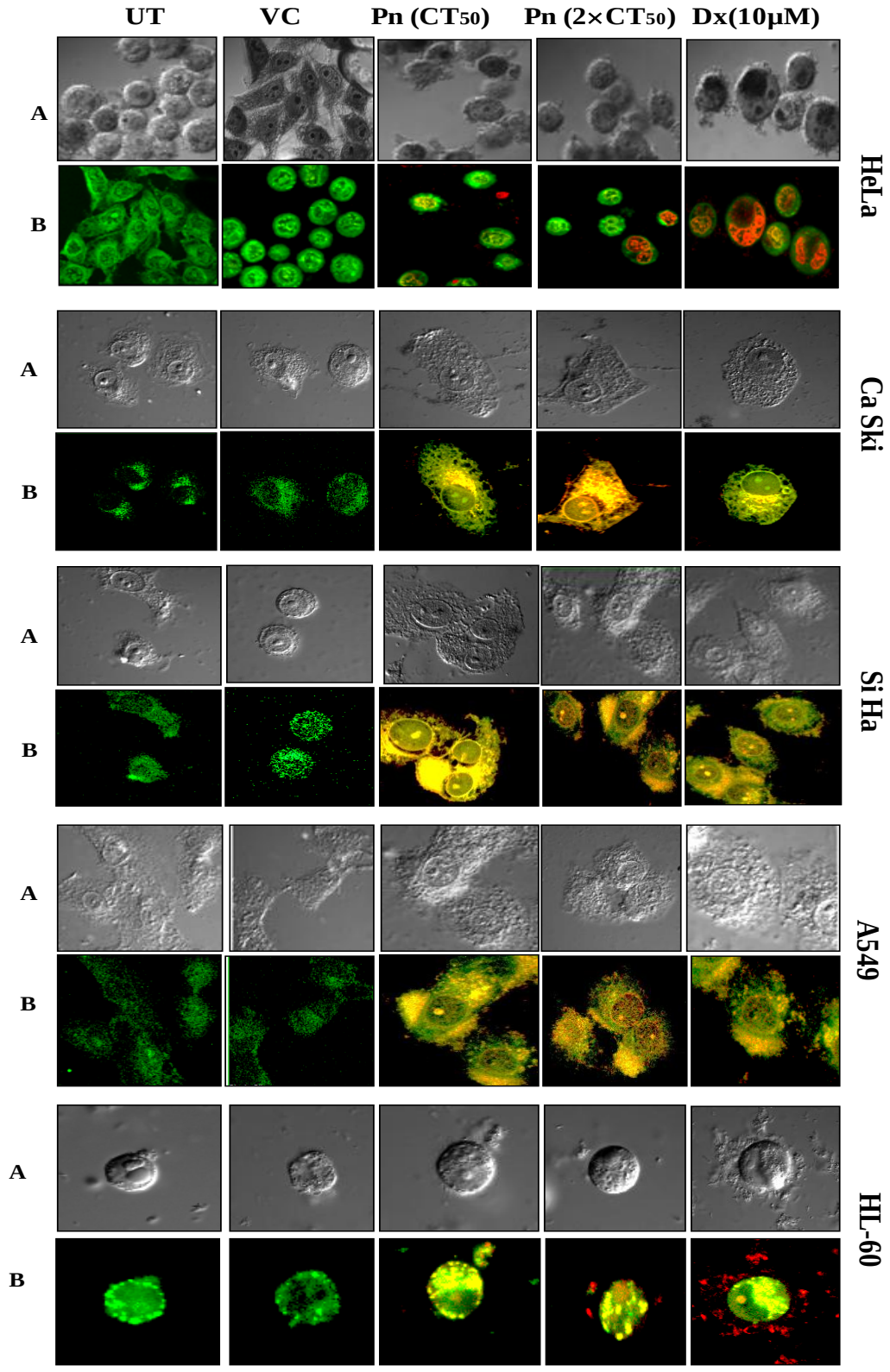

Figure 4.1.3. Assessment of changes in nucleus morphology by AO/EB staining after pinostrobin treatment. Different cells were treated with vehicle control (VC), doxorubicin (10 µM) and pinostrobin at CT_{50} and $2\times CT_{50}$ concentration for respective cells lines for 48 h and visualized at 40× magnifications by confocal microscopy. For CT_{50} concentrations for different cell lines, please refer to table 4.1.1. Treated cells showed condensed nucleus and fragmented chromatin in orange to red colour, whereas untreated and vehicle treated cells did not show these characteristics. UT, Untreated; VC, Vehicle control; Pn, Pinostrobin; Dx, Doxorubicin

- **Acridine Orange/ Ethidium Bromide staining (AO/EB staining)**

In order to examine the changes in the nuclear structure, AO/EB staining was also performed. AO is a cationic dye that stains both live and dead cells and emits green fluorescence upon intercalation into double stranded DNA. On the other hand, ethidium bromide intercalates and stains the DNA of apoptotic cells that have lost their nuclear membrane integrity at early and late stages of apoptosis and emits red-orange fluorescence. As evident from Figure 4.1.3, pinostrobin treated cells showed orange to red colour with condensed nuclei or fragmented chromatin that indicates induction of early and late phase of apoptosis at 48 h, whereas such kind of colour distribution was not observed in untreated and vehicle treated cells that showed only green nuclei with intact cell structure. These data indicated that pinostrobin affected morphology of the nucleus and cell architecture.

- **Transmission electron microscopic examination of mitochondrial, nuclear and cellular architecture**

Morphological changes of mitochondria, nucleus and cells structure were also examined by transmission electron microscopy (TEM). As evident from Figure 4.1.4 Panel A, pinostrobin and doxorubicin treatment resulted in remodelling of inner mitochondrial membrane, vesiculation and swelling of the mitochondrial matrix, evidenced by reduced cristae and expanded matrix space. Swelling of the mitochondria led to disintegration of the mitochondrial membrane. The untreated and vehicle treated cells showed normal matrix compartments with uniform cristae junctions and no vasiculation in mitochondria. Nuclear and cells' morphology was also altered after pinostrobin and doxorubicin treatment as evident from condensed nucleus or fragmented chromatin (Figure 4.1.4 B). Thus, pinostrobin treatment affected both the mitochondria and nucleus structure.

4.1.3 Induction of DNA damage by pinostrobin

Since formation of apoptotic bodies were detected in the cells treated with pinostrobin, TUNEL assay was performed both in the presence and absence of an apoptosis inhibitor to confirm apoptosis-inducing potential of pinostrobin. In the absence of an apoptosis inhibitor (z-VAD-FMK, caspases 3 inhibitor), significantly increase in cell apoptosis unit (HeLa, 24.15±1.9%; Ca Ski, 25.19±4.9%; SiHa, 29.46±1.0%; A549, 20.39±2.5%; HL-60, 25.36±0.42%).

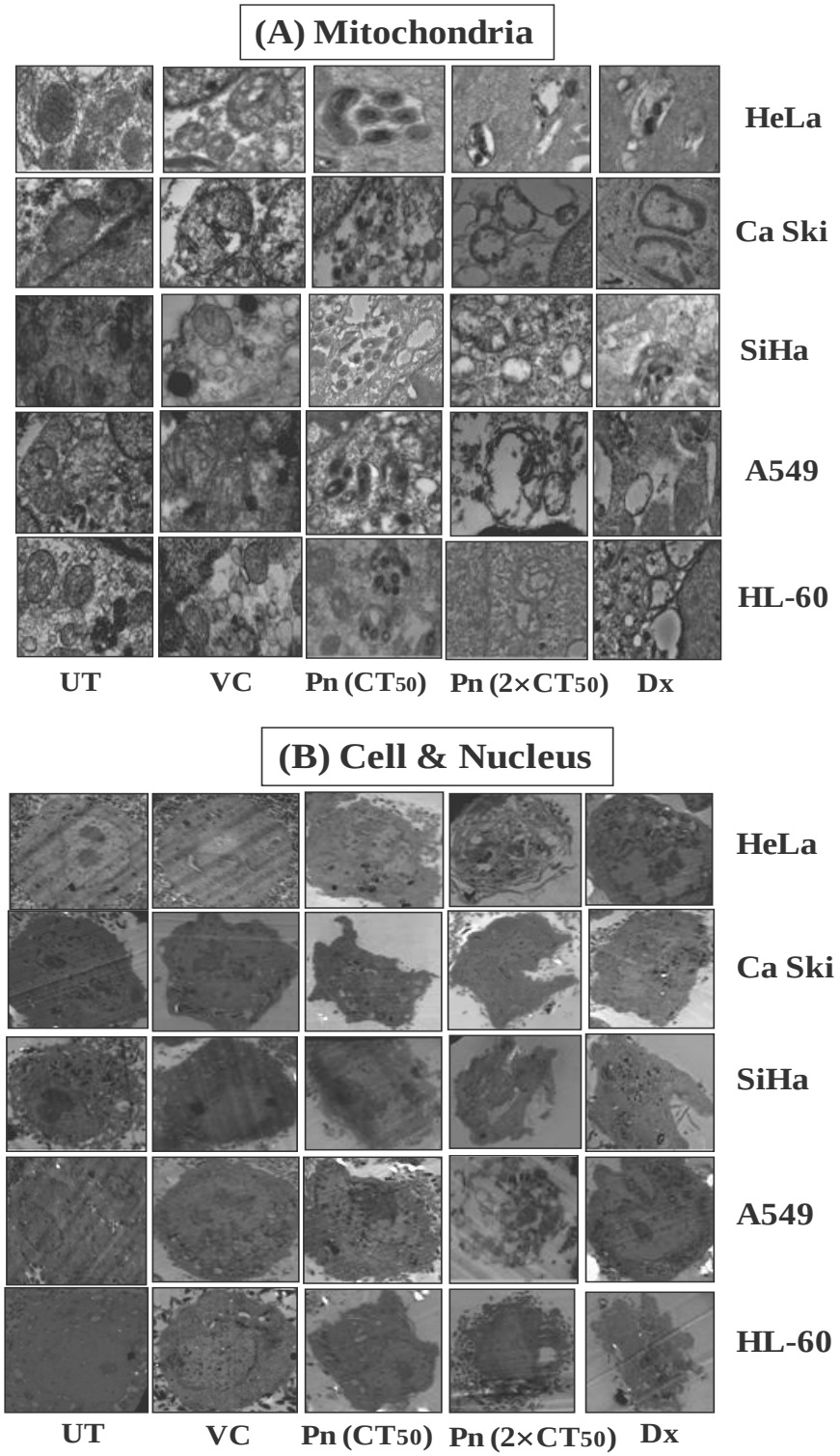

Figure 4.1.4. Transmission electron micrographs of mitochondria and nucleus of different cancer cells treated with pinostrobin at CT_{50} and $2\times CT_{50}$ concentrations for respective cell lines. Images were acquired at 48 h post-pinostrobin treatment. Cells treated with corresponding volume of vehicle and doxorubicin (10µM) was included as negative and positive controls, respectively. For CT_{50} concentrations for different cell lines, please refer to table 4.1.1 Pinostrobin and doxorubicin treated cells showed vasiculation in mitochondria (panel A, magnification 15,000×), and condensed nucleus and disintegrated outer membrane of cells (panel B, magnification 2,000×) when compared to untreated and vehicle treated cells**.** UT, Untreated; VC, Vehicle control; Pn, Pinostrobin; Dx, Doxorubicin.

Ca Ski, 25.19±4.9%; SiHa, 29.46±1.0%; A549, 20.39±2.5%; HL-60, 25.36±0.42%) (Figure 4.1.5 A,B,C,D,E,F). Normal HEK 293 cells showed an increase in DNA fragmentation (5.5±2.1%), which was relatively lower that observed in the cancer cells. An increase in DNA fragmentation was also observed in doxorubicin-treated cells at 48 h. Presence of apoptosis inhibitor in pinostrobin treated cells caused a reduction in cell apoptotic units (6.88±2.4%, 15.11±0.44%, 19.64±1.0%, 7.86±2.5%, 16.54±0.42% and 3.0±1.0% in HeLa, Ca Ski, SiHa, A549, HL-60 and HEK 293 cells) than that determined in the absence of the inhibitor (Figure 4.1.5 A,B,C,D,E,F). Ca Ski, SiHa and HL-60 cell exhibited high apoptotic unit in term of DNA fragmentation *($p \leq 0.001$)*. These findings confirmed that pinostrobin has the potential to fragment DNA and hence induce apoptosis. A decrease in the apoptotic units in pinostroin-treated cells in the presence of the inhibitor further confirmed that pinostrobin induced apoptosis-mediated cell death.

4.1.4 Changes in nitrite and GSH levels

Glutathione (GSH) is importance to alleviate the oxidative stress, which arises though anticancer agents. GSH is master detoxifier and antioxidant, also involves in immune function and control inflammation of the cells. Therefore, GSH level was analysed in presence or absence of anticancer agent pinostrobin in HeLa cell. A notable reduction in GSH level was observed in pinostrobin treated cells compared to vehicle treated cells. Pinostrobin (CT_{50} & $2\times CT_{50}$) treated cells showed reduction in GSH levels i.e. 3.65±0.29 & 2.84±0.47µg/mg protein (*$p \leq 0.05$* & *$p \leq 0.01$*) respectively, whereas vehicle treated control showed 4.11±0.08 µg/mg protein of GSH at 48 h (Figure 4.1.6 A). GSH level was also reduced in doxorubicin treated (3.76±0.11) cells. Our findings indicates pinostrobin is capable to reduced GSH levels that indicates imbalance among antioxidant and free radicle generation levels which further leads to oxidative stress in cancer cells.

In addition, nitrite oxide is also accountable for progression of angiogenesis and metastasis. Its level was examined after pinostrobin exposure to HeLa cell line. The level of nitrite (nitrite a breakdown product of nitrite oxide) was reduced in pinostrobin treated cells as compared to vehicle treated cells at 48 h. Pinostrobin treated HeLa cells showed nitrite 5.83±0.29 & 4.85±0.64 µg/mg protein (*$p \leq 0.005$* & *$p \leq 0.005$*) respectively, whereas vehicle treated cells showed nitrite levels at 7.98±0.51 µg/mg protein (Figure 4.1.6 B).

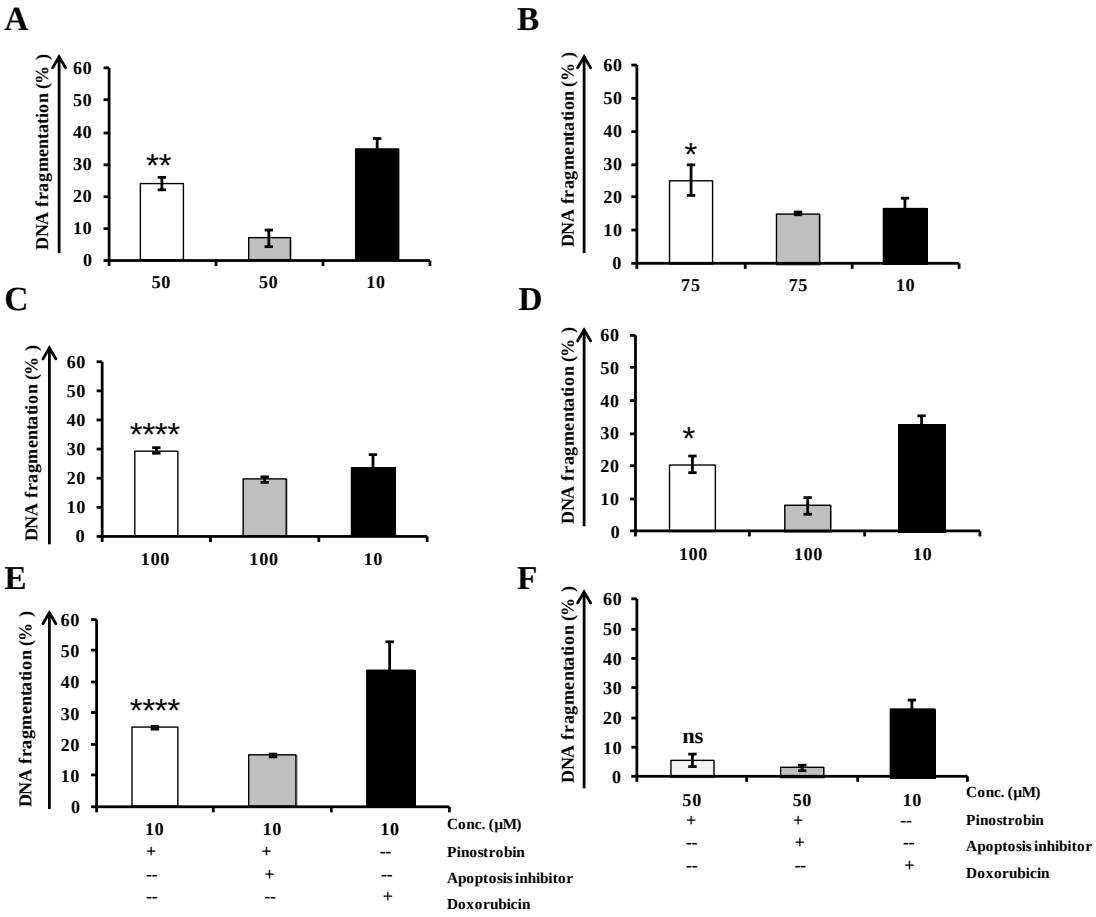

Figure 4.1.5. DNA fragmentation is quantified by TUNEL assay. Different cells HeLa(A), Ca Ski (B), SiHa (C), A549 (D), HL-60 (E) and HEK 293 (F) treated with pinostrobin at CT_{50} concentrations for the respective cells in the presence or absence of apoptosis inhibitor (Z-DEVD-FMK-Caspase-3 Inhibitor: 50µM) for 48 h were subjected to TUNEL staining. Doxorubicin (10 µM) treated cells were included as positive controls respectively. Significance difference *(p value*) is calculated in presence and absence of apoptosis inhibitor in pinostrobin treated cells using student t test. *, $p \leq 0.05$; **, $p \leq 0.01$; ****, $p \leq 0.001$; ns, no significance.

These findings showed reduced GSH and nitrite levels in dose dependent manner. Doxorubicin (10µM) was included as positive control also reduced nitrite level (5.81±0.24, $p \leq 0.005$).

4.1.5 Pinostrobin promotes externalization of phosphatidyl serine

During apoptosis phosphatidylserine is externalized from inner side to outer side of cells and bind to Annexin V-FITC. Annexin V-FITC staining was performed to assess the effect of pinostrobin on apoptotic population by measuring externalization of phosphatidylserine on the cell surface. As shown in Figure 4.1.7 A, B & Figure 4.1.8 A, B pinostrobin treatment resulted in significantly higher percent of Annexin V-FITC labelled population.

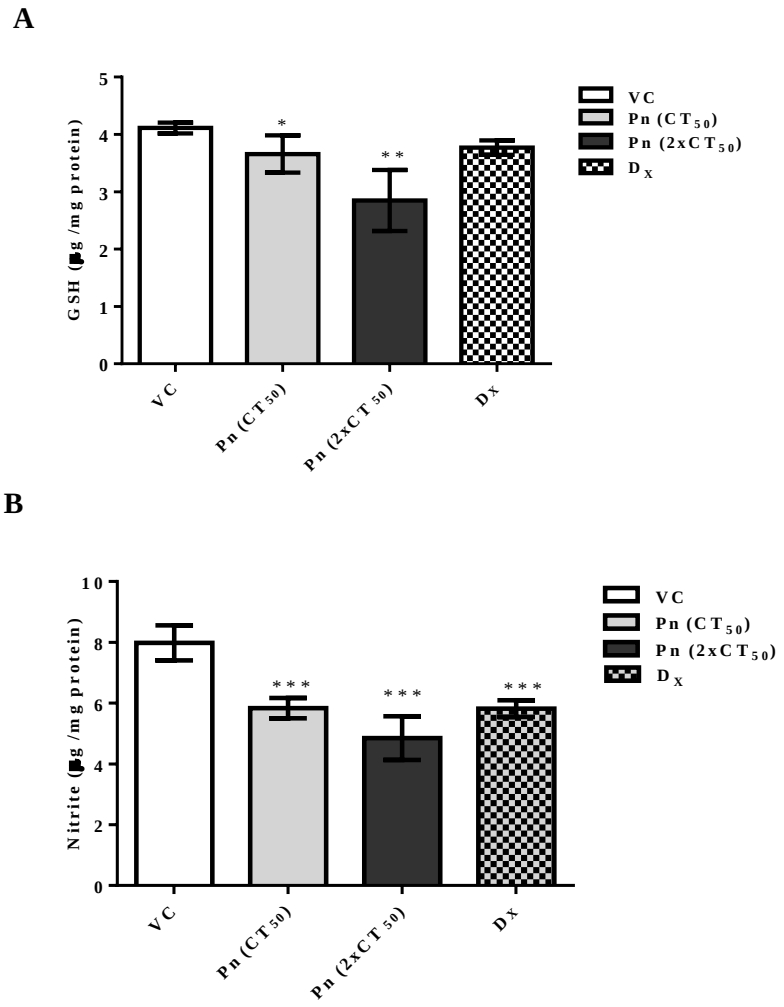

Figure 4.1.6. Effect of pinostrobin (CT_{50} & $2\times CT_{50}$ concentration) on GSH (A) and nitrite (B) level in HeLa cells. The bar diagrams represent the GSH and nitrite level at 48 h. Vehicle treated and doxorubicin (10 µM) treated cells were included as negative and positive controls, respectively. Significance differences (*p value*) of all treated groups are calculated with respect to vehicle control cells using ordinary two-way ANOVA (Dunette's multiple comparison tests). *, $p \leq 0.05$; **, $p \leq 0.01$; ***, $p \leq 0.005$.

The mean of Annexin V positive cells (FL1 channel, %) was determined to be 67.62±10.94%, 49.09±10.17%, 49.68±15.14%, 29.78±2.4% and 31.91±3.21% for HeLa, Ca Ski, SiHa, A549 and HL-60 cells, respectively at 48 h post-pinostrobin ($2\times CT_{50}$) treatment (Figure 4.1.7 C & Figure 4.1.8 C). Vehicle treated (HeLa; 31.73±6.3%, Ca Ski; 22.89±7.3%, SiHa;11.17±2.3%, A549; 10.28±1.0%, and HL-60;11.63±0.61%) cells showed no significant change in Annexin V-FITC fluorescence events, whereas doxorubicin (10µM, included as positive control) treated cells showed significant Annexin V-FITC fluorescence events in FL-1 channel (Figure 4.1.7-8 A,B & C). Pinostrobin-treatment did not appear to affect the non-cancerous HEK 293 cells as almost

negligible AnnexinV-FITC labelled population (4.28±0.85%) (Figure 4.1.8 C). Mean fluorescence of Annexin V positive cells in corresponding cell types are subjected to treatment with the test chemical is shown in Figure 4.1.7 (C) and Figure 4.1.8 (C). As evident from the results obtained, pinostrobin-treatment increase externalization of phosphatidylserine in time and dose dependent manner in treated cells when compared to vehicle treated or non-cancerous cell lines. These results revealed that pinostrobin have ability to externalize phosphatidylserine and induced apoptosis.

4.1.6 Effect on pinostrobin on mitochondrial membrane integrity

After establishing the damaging effect of pinostrobin on cell membrane, mitochondria membrane potential, a marker of mitochondrial membrane integrity and one of the early events in apoptosis, was analyzed using cationic carbocyanine JC-1 dye. JC-1 dye accumulates as aggregates in mitochondrial matrix and emits red fluorescence in normal cells. However, when mitochondrial membrane disintegrates with a decrease in mitochondrial membrane potential ($\Delta\Psi m$), JC-1 forms monomer and emits green fluorescence. Thus, the ratio of green and red fluorescence is an indicator of population of apoptotic cells with reduced $\Delta\Psi m$. As shown in Figure 4.1.9 & Figure 4.1.10, different cancer cells treated with pinostrobin recorded higher green fluorescence of JC-1 monomers in comparison to vehicle treated cells. Vehicle treated cells did not show any significant increase in green fluorescence, whereas doxorubicin treatment caused an increase in JC-1 monomer formation. On the other hand, no significant increase in green fluorescence events of JC-1 monomer was recorded in pinostrobin treated-HEK 293 cells with fluorescence events at 6.75±0.43%, suggesting that Pinostrobin ($2\times CT_{50}$) did not cause mitochondrial membrane damage in non-cancerous cells (Figure 4.1.10 A,B,C). Mean of JC-1 fluorescence events in different cells derived from flow cytometer analysis of the cells is shown in Figure 4.1.9 C & 4.1.10 C. Mean of JC-1 fluorescence events at 48 h post-pinostrobin ($2\times CT_{50}$) treatment were recorded to be 39.96±2.5%, 31.94±1.78%, 49.92±7.47%, 52.40±5.12% and 13±2.63% in HeLa, Ca Ski, SiHa, A549 and HL-60, respectively. Significantly lower JC-1 events of green fluorescence were noted in the respective vehicle treated cells (HeLa; 19.34±3.1%, Ca Ski; 12.74±1.8%, SiHa; 4.76±1.65%, A549; 7.96±0.84% and HL-60; 5.31±0.85 (Figure 4.1.9 C & Figure 4.1.10 C).

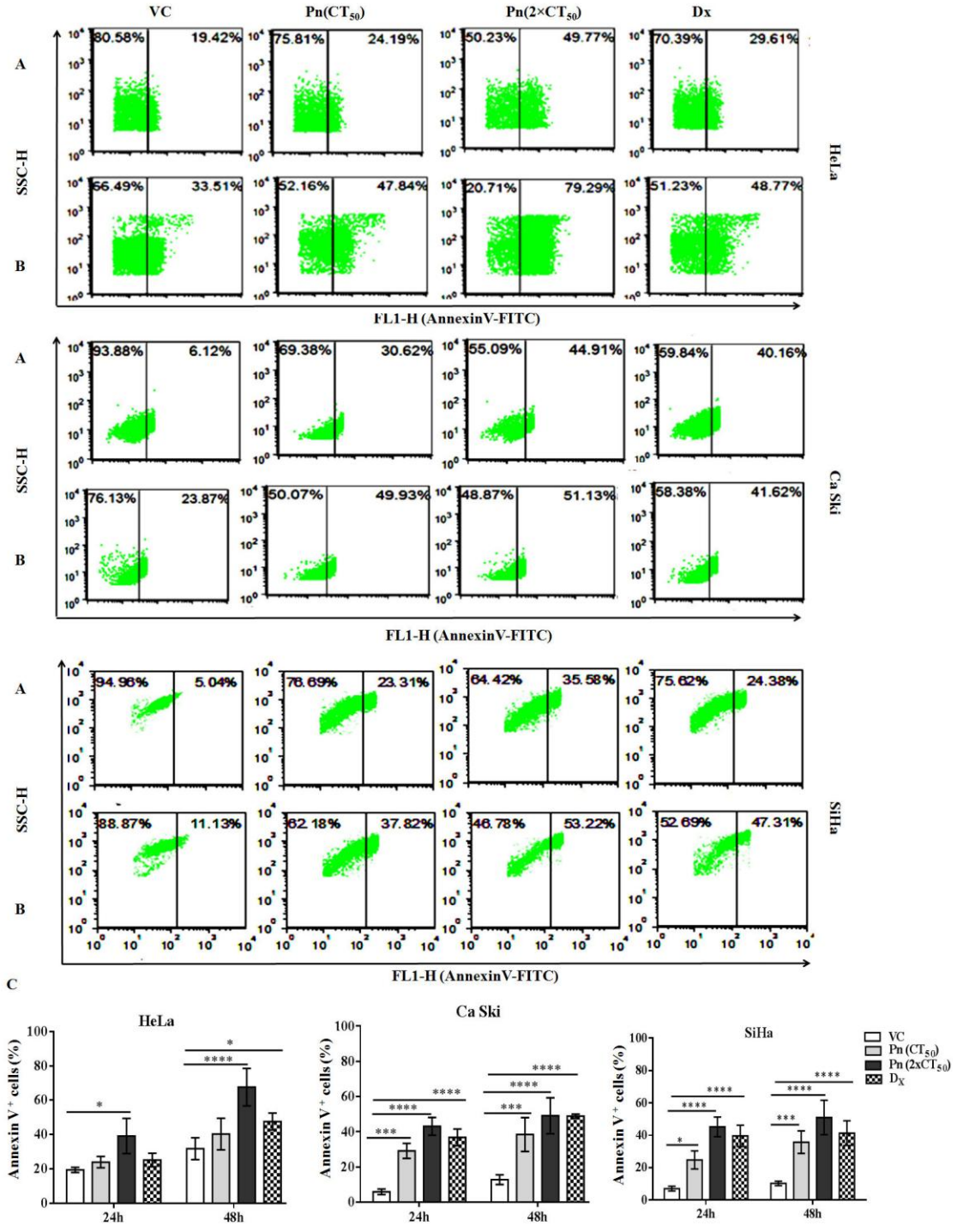

Figure 4.1.7. Representative flow-cytometric analysis of pinostrobin treated cancer cells (HeLa, Ca Ski, SiHa) labelled with AnnexinV-FITC, analyzed by FCS Express v5 software at 24 h (Panel A) and 48 h (Panel B) post treatment. The cells were treated with CT_{50} and $2\times CT_{50}$ (For CT_{50} concentrations for different cell lines, please refer to table 4.1.1) concentrations of pinostrobin for respective cells. (C) Graphical mean representation of changes in AnnexinV-FITC positive population after pinostrobin treatment in different cells at 24 and 48 h post-treatment. The data represent mean±S.D. of three independent experiments performed in triplicates. Vehicle treated and doxorubicin treated cells were included as negative and positive controls, respectively. Significance of difference *(p value*) of all treated groups is calculated using ordinary two-way ANOVA (Dunette's multiple comparison tests) with respect to vehicle control (VC) cells. *, *p≤ 0.05;* ***, *p≤ 0.005;* ****, *p≤0.001*. VC, Vehicle control; Pn, Pinostrobin; Dx, Doxorubicin.

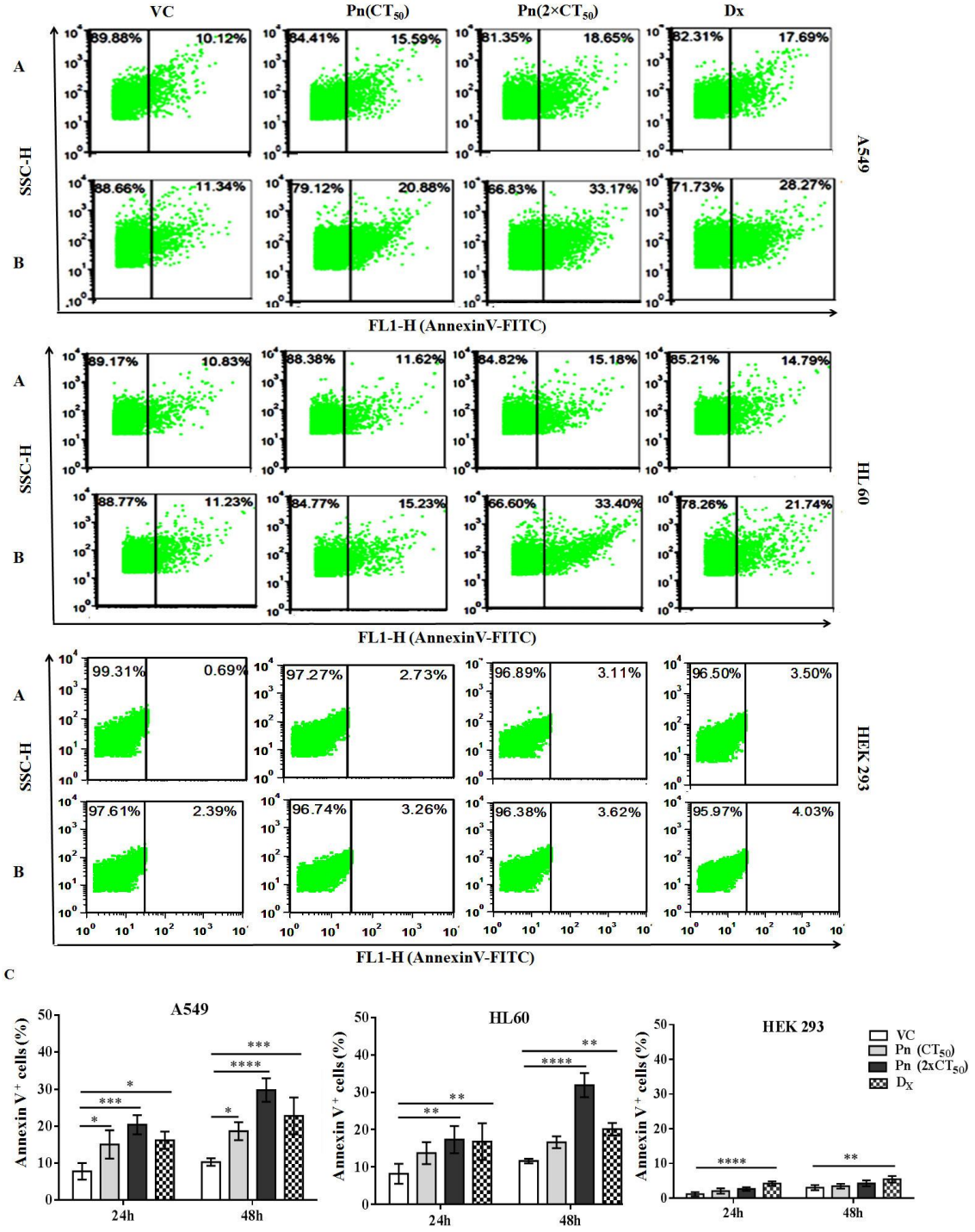

Figure 4.1.8. Representative flow-cytometric analysis of pinostrobin treated cells (A549, HL60, HEK 293) labelled with AnnexinV-FITC, analyzed by FCS Express v5 software at 24 h(Panel A) and 48 h (Panel B) post treatment. The cells were treated with CT_{50} and $2\times CT_{50}$ (For CT_{50} concentrations for different cell lines, please refer to table 4.1.1) concentrations for respective cells. (C) Graphical mean representation of changes in AnnexinV-FITC positive population after pinostrobin treatment in different cells at 24 and 48 h post-treatment. The data represent mean±S.D. of three independent experiments performed in triplicates. Vehicle treated and doxorubicin treated cells were included as negative and positive controls respectively. Significance difference *(p value*) of all treated groups are calculated using ordinary two-way ANOVA (Dunette's multiple comparison test) with respect to vehicle control (VC) cells.*, *p≤0.05*; **, *p≤0.01;* ***, *p≤0.005;* ****, *p≤0.001*. VC, Vehicle control; Pn, Pinostrobin; Dx, Doxorubicin.

These data clearly indicate that both pinostrobin and doxorubicin-treated cells showed lower $\Delta\psi$m or depolarized $\Delta\psi$m with more JC-1 monomers and emitted green fluorescence, while vehicle treated cells showed higher $\Delta\psi$m with intense red fluorescence and less JC-1 monomers forming population in right quadrant.

4.1.7 Effect of pinostrobin on reactive oxygen species (ROS) production

It is a well established fact that increased ROS production and depletion of intracellular antioxidants leads to cell death. Since pinostrobin induced apoptosis, it was imperative to investigate if it upregulated ROS generation using Dihydrochlorofluorescin-diacetate (DCFH-DA) staining. DCFH-DA slowly enters into the cells and gets deacetylated by cellular esterases into non polar derivative i.e. DCFH which then gets oxidised to highly fluorescent Dichlorofluorescin (DCF) in the presence of ROS. Figure 4.1.11 showed representative dot-plot of flow cytometric analysis of DCFH-DA stained cells subjected to different treatments. Different cancer cells treated with pinostrobin exhibited an increase in DCF fluorescence in comparison to vehicle treated cells (Figure 4.1.11 & 4.1.12). No significant increase in DCF-stained cells was noted in HEK 293 cells treated with pinostrobin, suggesting that the flavonoid did not have an adverse effect on normal cells (Figure 4.1.12). Mean DCF fluorescence events of three independent set of stained cells is shown in Figure 4.1.11 C & 4.1.12 C. It is clearly demonstrated that at 48 h post-pinostrobin ($2\times CT_{50}$) treatment, the pinostrobin-treated cells exhibited higher DCF fluorescence events (HeLa; 54.20$\pm$6.7%, Ca Ski; 37.73$\pm$1.20%, SiHa; 14.64$\pm$5.71%, A549; 19.29$\pm$3.64% and HL-60; 80.02$\pm$6.45%) in comparison to respective vehicle treated cells (12.14$\pm$1.4%, 16.26$\pm$2.7%, 6.36$\pm$3.2%, 7.96$\pm$0.84% and 6.36$\pm$0.67% respectively). On the other hand, pinostrobin-treated HEK 293 did not show a significant change in DCF fluorescence with 4.83%$\pm$1.02% events in treated cells. These data suggest that the higher DCF fluorescence in treated cells may be due to oxidation of non polar DCFH-DA into DCF by pinostrobin-induced production of ROS and other peroxides.

4.1.8 Determination of reactive oxygen species (ROS) production site

To determine if ROS are produced in mitochondria, 10 nonyl acridine orange (NAO) staining was employed. NAO specifically binds to cardiolipin in mitochondria and forms a complex. However, in the presence of ROS, cardiolipin is oxidized and loses its binding affinity with NAO. Thus, reduction in the fluorescence events of NAO reflects the

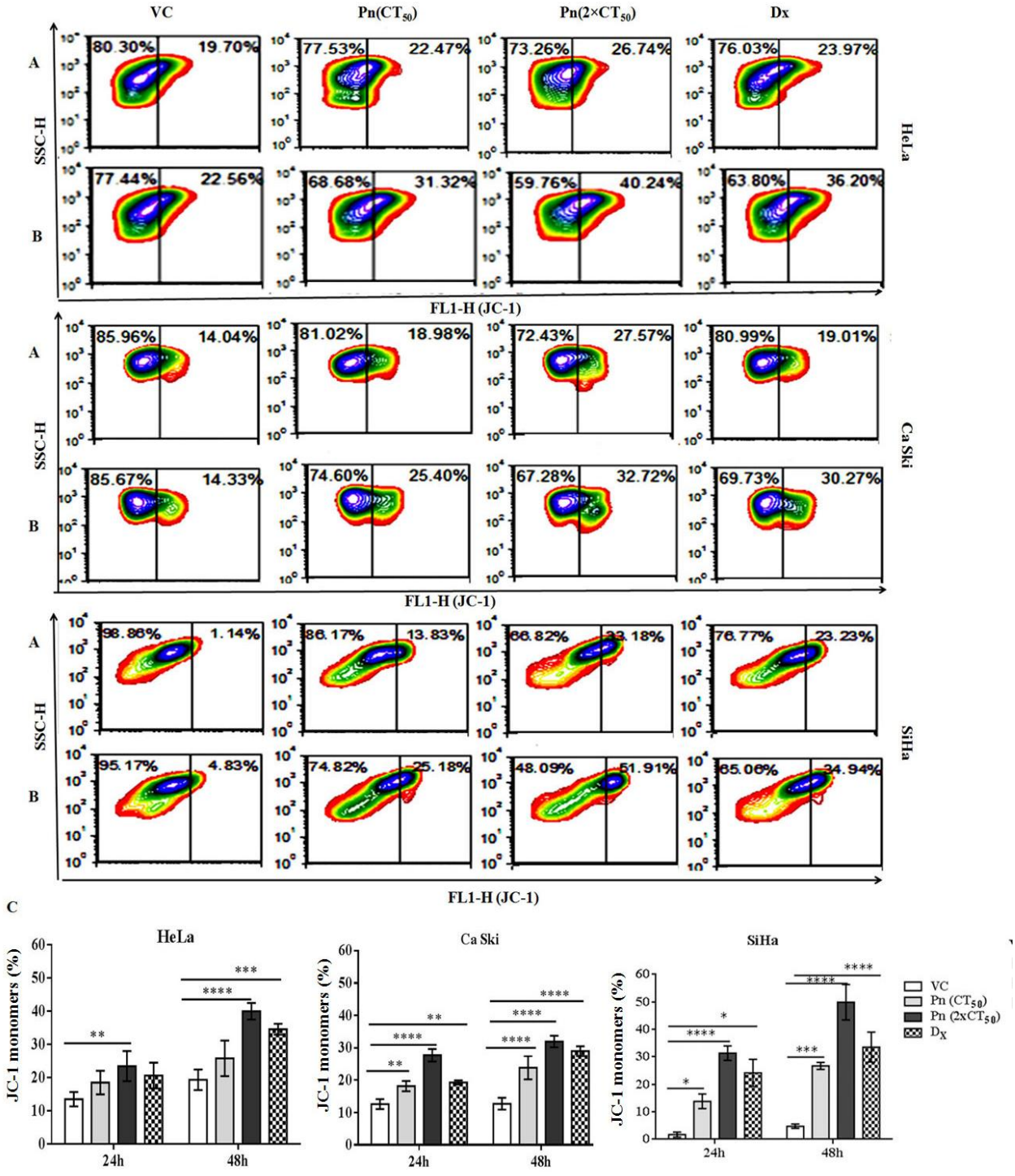

Figure 4.1.9. Assessment of mitochondrial membrane potential (ΔΨM) in pinostrobin treated cells (HeLa, Ca Ski, SiHa) using JC-1 probes. The cells were treated with vehicle, doxorubicin (10µM) and pinostrobin CT_{50} and $2\times CT_{50}$ (For CT_{50} concentrations for different cell lines, please refer to table 4.1.1) concentrations for respective cells. Mitochondrial membrane depolarization analyzed by FCS Express v5 software at 24 h (Panel A) and 48 h (Panel B) post treatment. (C) Mean green fluorescence events of JC-1 monomers were increased in pinostrobin and doxorubicin treated cells compared to vehicle treated cells as evidence of loss of membrane potential. The data represent mean±S.D. of three independent experiments performed in triplicates. Significance differences *(p value)* of all treated groups are calculated using ordinary two-way ANOVA (Dunette's multiple comparison tests) with respect to vehicle control (VC) cells. *, *p≤0.05*; **, *p≤0.01;* ***, *p≤0.005;* ****, *p≤0.001.* VC, Vehicle control; Pn, Pinostrobin; Dx, Doxorubicin.

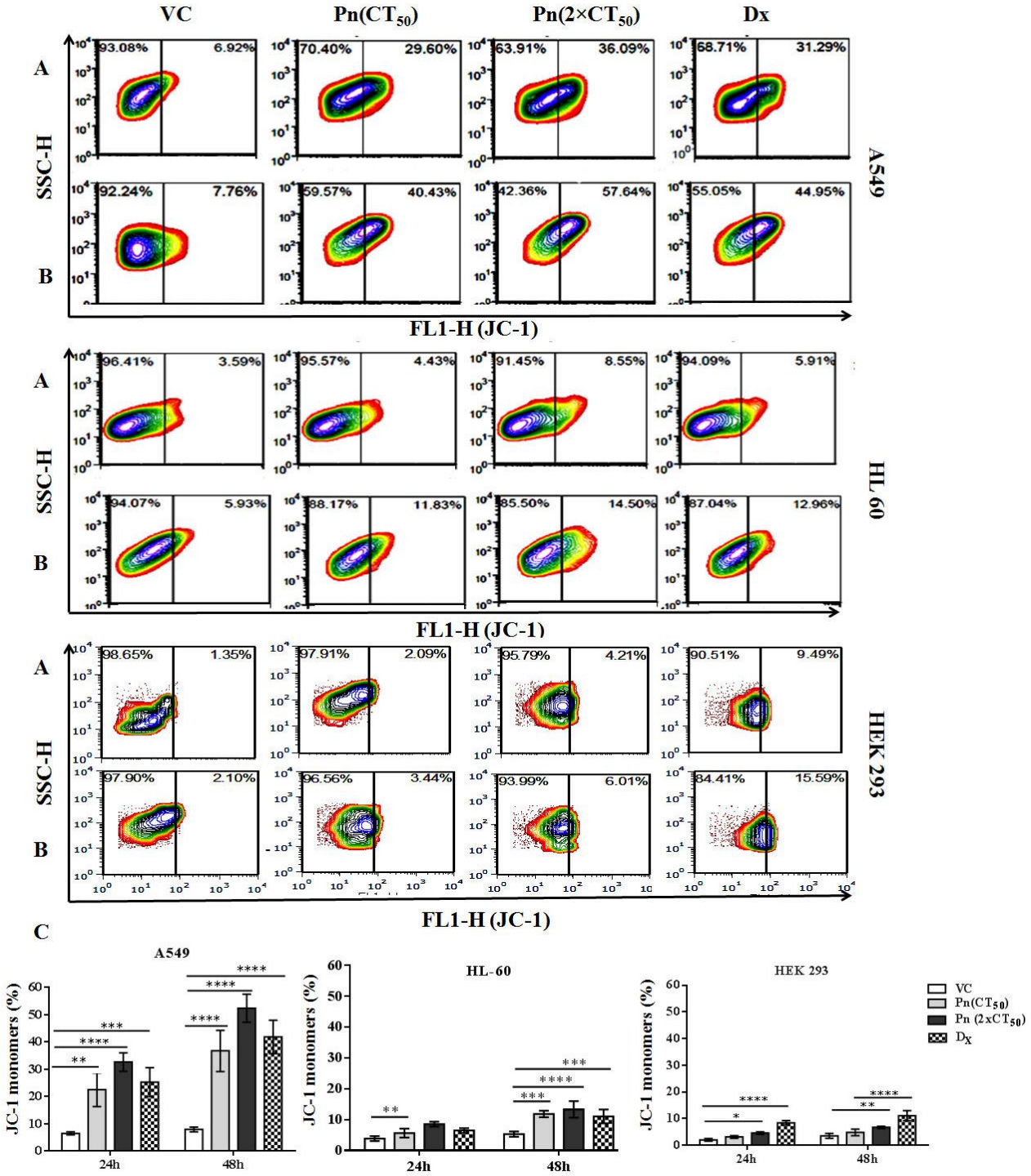

Figure 4.1.10. Representative flow cytometric analysis of assessment of mitochondrial membrane potential (ΔΨM) in pinostrobin treated cells (A549, HL60, HEK 293) using JC-1 probes. The cells were treated with vehicle, doxorubicin(10µM) and pinostrobin CT_{50} and $2\times CT_{50}$ (For CT_{50} concentrations for different cell lines, please refer to table 4.1.1) concentrations for respective cells and mitochondrial membrane depolarization analyzed by FCS Express v5 software at 24 h (Panel A) and 48 h (Panel B) post treatment. (C) Mean green fluorescence events of JC-1 monomers were increased in pinostrobin and doxorubicin treated cells compared to vehicle treated cells as evidence of loss of membrane potential. The data represent mean±S.D. of three independent experiments performed in triplicates. Significance differences (*p value*) of all treated groups are calculated using ordinary two-way ANOVA (Dunette's multiple comparison test) with respect to vehicle control (VC) cells. *, *p≤0.05*; **, *p≤0.01;* ***, *p≤0.005;* ****, *p≤0.001*. VC, Vehicle control; Pn, Pinostrobin; Dx, Doxorubicin.

oxidation of intracellular cardiolipin. Figure 4.1.13 A, B & Figure 4.1.14 A, B shows flow cytometric analysis of NAO-stained cancer cells subjected to different treatments. It can be seen that highest decrease in NAO fluorescence upon pinostrobin treatment was observed in HeLa, Ca Ski, SiHa, A549 and HL-60 cells, when compared to vehicle treated cells. Treatment with vehicle did not cause any significant decrease in NAO fluorescence events in comparison to any of the cancer cells, whereas positive control doxorubicin did cause reduction in NAO fluorescence at 48 h. Unlike cancer cells, normal HEK 293 cells did not exhibit any decrease in NAO fluorescence events upon pinostrobin ($2\times CT_{50}$) treatment (Figure 4.1.14 A, B & C). The mean NAO fluorescence events in different treated cells are shown in Figure 4.1.13 C & Figure 4.1.14 C. NAO fluorescent events in vehicle treated HeLa, Ca Ski, SiHa, A549 and HL-60 cells were determined to be 59.75$\pm$4.6%, 42.81$\pm$5.02%, 90.28$\pm$7.3%, 50.74$\pm$10.47 and 41.32$\pm$4.8 at 48 h, respectively, whereas these cells upon treatment with pinostrobin ($2\times CT_{50}$) had lower NAO fluorescence (34.51$\pm$6.43%, 16.36$\pm$6.16%, 65.95$\pm$8.17%, 32.31$\pm$5.39 and 24.83$\pm$7.89, respectively). HEK 293 cells showed comparable high fluorescence in both vehicles treated (97.15$\pm$0.99%) and pinostrobin-treated cells (95.50$\pm$0.72%) (Figure 4.1.14 A, B & C). Thus, reduction in NAO fluorescence upon pinostrobin treatment further confirms ROS generation which possibly led to cardiolipin oxidation and hence failed to bind to NAO.

4.1.9 Evaluation of ROS consequences

After validating the site of ROS production in mitochondria, investigations were carried out to check the effect of pinostrobin on the cellular components using Hydroethidine (HE) staining. HE is oxidized into ethidium bromide in the presence of superoxide anions, which upon intercalation into DNA produces red fluorescence. Thus, the red fluorescence directly related with oxidation of hydroethidine. Flow cytometric analysis showed an increase in oxidized HE red fluorescence in pinostrobin-treated cancer cells when compared to vehicle treated cells in dose and time-dependent manner (Figure 4.1.15 A,B & Figure 4.1.16 A,B). However, no increase in fluorescence was observed in HEK

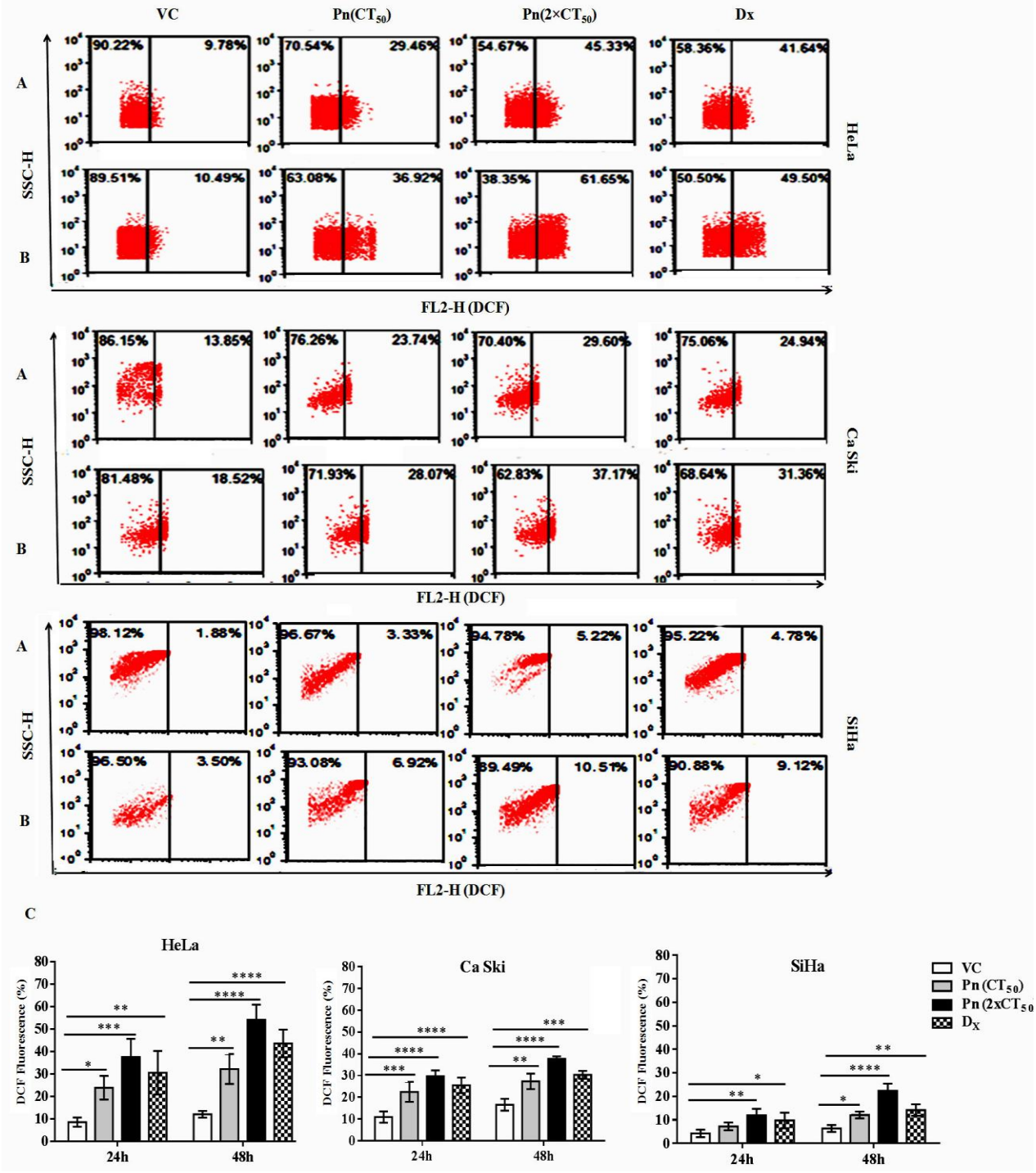

Figure 4.1.11. Analysis of ROS production in pinostrobin treated cells by DCF fluorescence measurements. Different cancer (HeLa, Ca Ski, SiHa) cells were treated with pinostrobin at CT_{50} and $2\times CT_{50}$ concentrations for 24 h (Panel A) and 48 h (Panel B). Panels show representative flow cytometric analysis. Fluorescence events of DCF were analyzed by FCS Express v5 software. Vehicle treated and doxorubicin (10 µM) treated cells were included as negative and positive controls. Representative dot-plot of flow cytometric analysis showed high DCF fluorescence events in pinostrobin and doxorubicin treated cells compared to vehicle treated and non-cancerous cells, reveal oxidative stress induce by pinostrobin in cancer cells. (C) Mean fluorescence events of DCF fluorescence represent in bar diagram is shown in panels A and B. The data represent mean±S.D. of three independent experiments performed in triplicates. Significance differences (*p value*) of all treated groups are calculated using ordinary two-way ANOVA (Dunette's multiple comparison test) with respect to vehicle control (VC) cells. *, *p≤0.05*; **, *p≤0.01;* ***, *p≤0.005;* ****, *p≤0.001*. VC, Vehicle control; Pn, Pinostrobin; Dx, Doxorubicin.

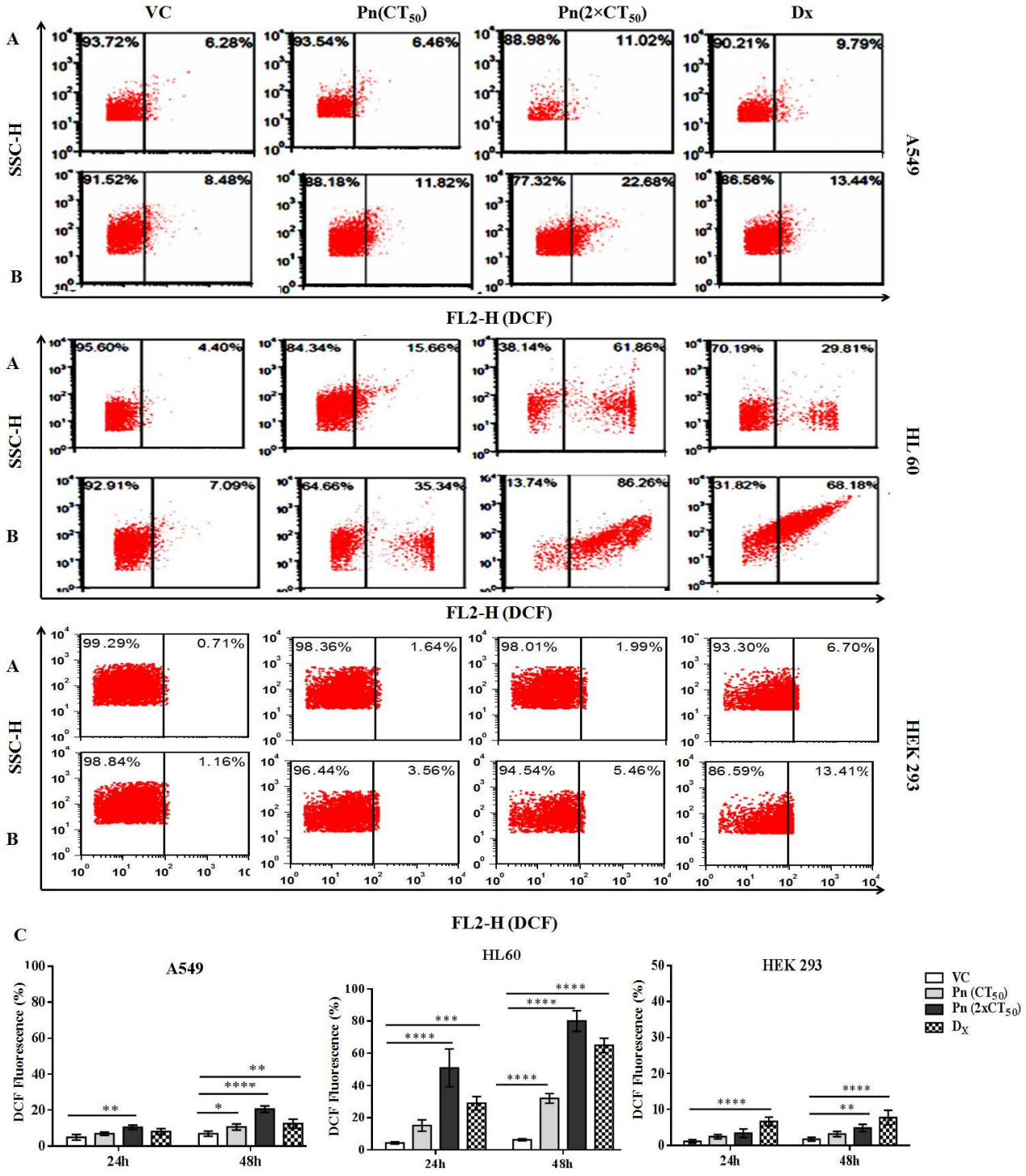

Figure 4.1.12. Analysis of ROS production in pinostrobin treated cells by DCF fluorescence measurements. Different cancer (A549, HL60, HEK 293) cells were treated with pinostrobin at CT_{50} and $2\times CT_{50}$ concentrations for 24 h (Panel A) and 48 h (Panel B). Fluorescence events of DCF were analyzed by FCS Express v5 software. Vehicle treated and doxorubicin (10 µM) treated cells were included as negative and positive controls. Representative dot-plot of flow cytometric analysis showed high DCF fluorescence events in pinostrobin and doxorubicin treated cells compared to vehicle treated and non-cancerous cells, reveal oxidative stress induce by pinostrobin in cancer cells.(C) Quantitative graphical representation of flow cytometric data shown in panels A and B. The data represent mean±S.D. of three independent experiments performed in triplicates. Significance difference *(p value*) of all treated groups is calculated using ordinary two-way ANOVA (Dunette's multiple comparison test) with respect to vehicle treated cells. *, *p≤0.05*; **, *p≤0.01;* ***, *p≤0.005;* ****, *p≤0.001.* VC, Vehicle control; Pn, Pinostrobin; Dx, Doxorubicin.

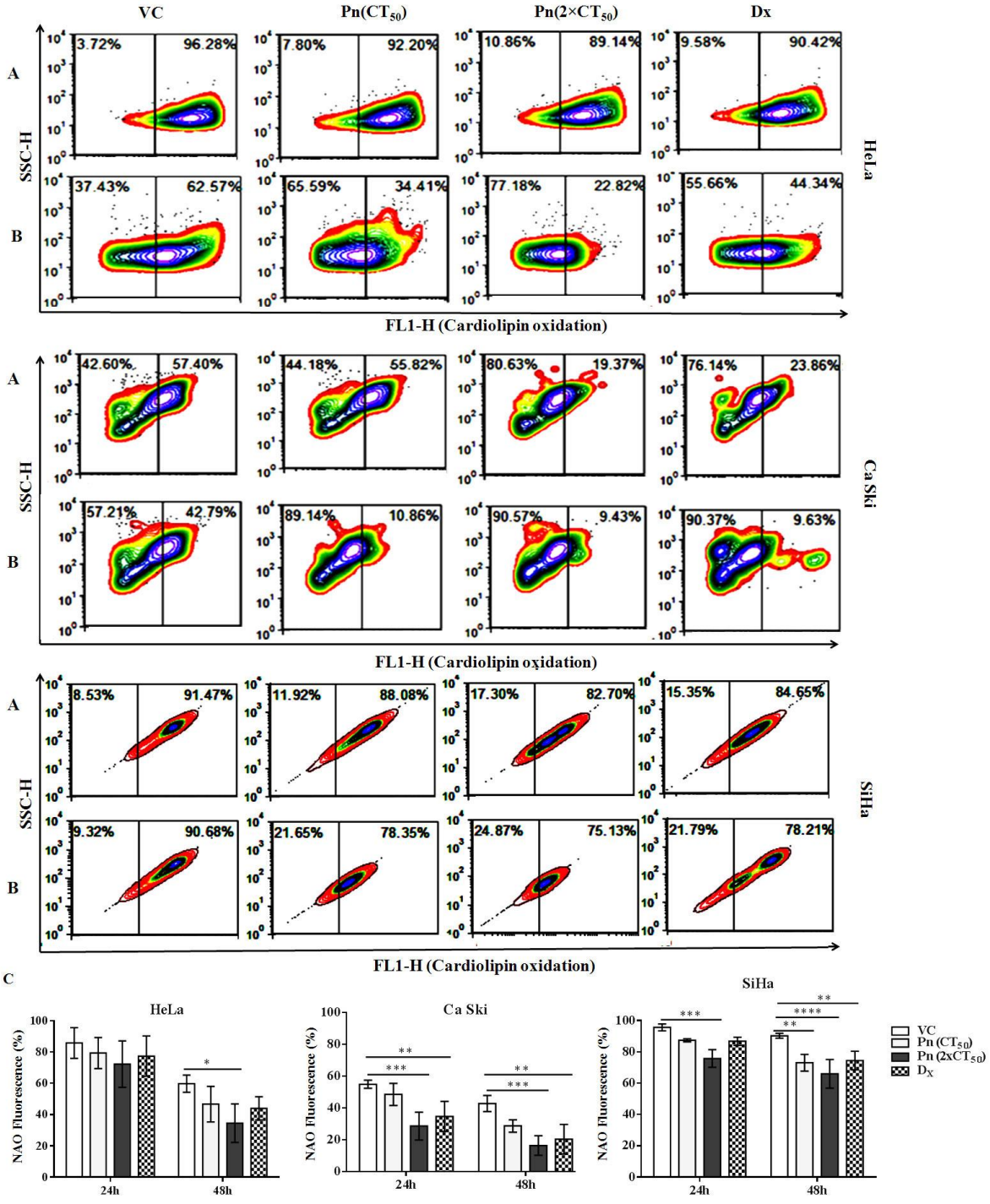

Figure 4.1.13. Representative flow-cytometric analysis of 10- nonyl acridine orange (NAO) stained different cancer (HeLa, Ca Ski, SiHa) cells at 24 h (A) and 48 h (B) post- pinostrobin treatment. Cells were treated with pinostrobin at CT_{50} and $2\times CT_{50}$ concentrations, vehicle (negative control) and doxorubicin (positive control) to analyze the site of ROS production by FCS Express 5 Flow cytometry analysis software. (C) Graphical representation of mean fluorescence of NAO. Data represent mean±S.D. of three independent experiments performed in triplicates. Flow-cytrometric analysis showed high oxidative stress in pinostrobin treated and doxorubicin treated cells that lead to low binding affinity of NAO (low fluorescence) with cardiolipin in mitochondria compared to vehicle control. Significance difference *(p value*) is calculated with respect to observed fluorescence in vehicle treated cells using ordinary two-way ANOVA (Dunette's multiple comparison test). *, *p≤0.05*; **, *p≤0.01;* ***, *p≤0.005;* ****, *p≤0.001*. VC, Vehicle control; Pn, Pinostrobin; Dx, Doxorubicin.

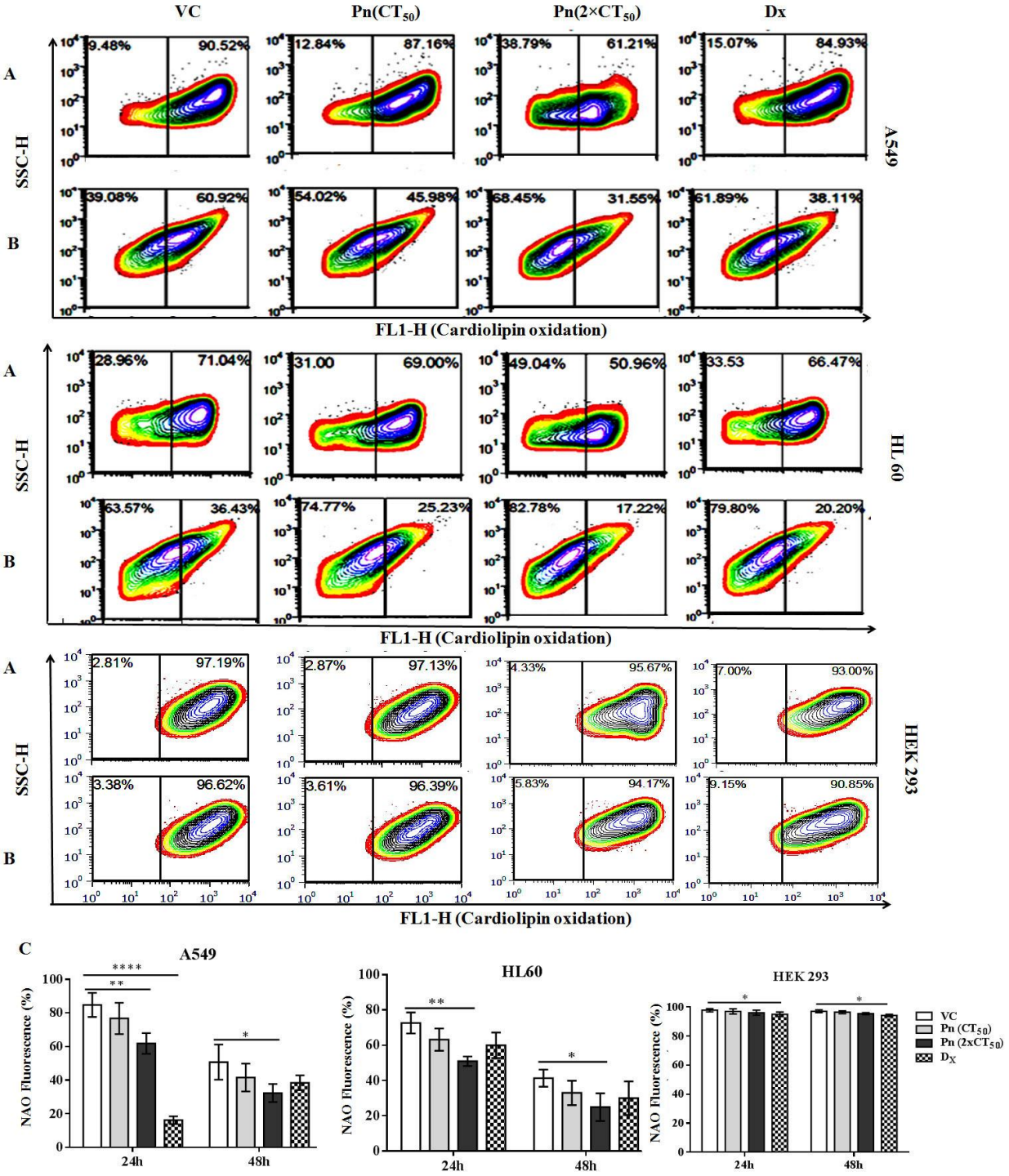

Figure 4.1.14. Representative flow-cytometric analysis of 10-nonyl acridine orange (NAO) stained different cancer (A549, HL-60, HEK 293) cells at 24 h (A) and 48 h (B) post- pinostrobin treatment. Cells were treated with pinostrobin at CT_{50} and $2\times CT_{50}$ concentrations, vehicle (negative control) and doxorubicin (positive control) to analyze the site of ROS production by FCS Express 5 Flow cytometry analysis software. (C) Graphical representation of mean fluorescence of NAO in cells subjected to different treatments. Data represent mean ±S.D. of three independent experiments performed in triplicates. Flow-cytometric analysis showed high oxidative stress in pinostrobin treated and doxorubicin treated cells that lead to low binding affinity of NAO (low fluorescence) with cardiolipin in mitochondria compared to vehicle control. Significance difference (*p value*) is calculated with respect to observed fluorescence in vehicle treated cells using ordinary two-way ANOVA (Dunette's multiple comparison test). *, *p≤0.05*; **, *p≤0.01;* ****, *p≤0.001*. VC, Vehicle control; Pn, Pinostrobin; Dx, Doxorubicin.

293 cells upon pinostrobin treatment (Figure 4.1.16 A, B &C). As expected treatment with vehicle also did not cause any increase in fluorescence in any of the cells, whereas treatment with doxorubicin resulted in increased red fluorescence. Upon pinostrobin ($2\times CT_{50}$) treatment, HeLa, Ca Ski, SiHa, A549 HL-60 and HEK 293 cells showed DNA fragmentation in red fluorescence events of 18.01±1.42%, 21.39±4.05%, 20.1±4.20%, 17.86±2.12%, 14.92±2.08% and 3.07±1.147%, respectively, whereas vehicle treated HeLa, Ca Ski, SiHa, A549, HL-60 and HEK 293 cells had only 5.12±1.9, 6.91±1.8, 7.21±1.7, 8.13±1.8, 2.71±0.41 and 1.8±0.6 events (Figure 4.1.15 C & Figure 4.1.16 C). These results further suggested that pinostrobin was a cause of ROS production and oxidative stress that further lead to DNA fragmentation resulting in an increase in ethidium bromide fluorescence.

4.1.10 Pinostrobin internalization, retention and cell morphology examination by live cell confocal microscopy:

Pinostrobin internalization leads to cells structural deformity

Live cell imaging was performed to examine the progression of cell death following pinostrobin treatment upto 30 h. As shown in the Figure 4.1.17 A, pinostrobin treatment affect the cells soon after treatment as evident from time dependent deformation of cellular architecture and cell morphology that ultimately resulted in cell death. The alterations in morphology in pinostrobin treated cells were prominently were appearance of membrane blebs and loss of adhesion under live cell confocal microscope at various time intervals, clearly indicating initiation of apoptosis (Figure 4.1.17 A). Whether and when this effect was triggered by pinostrobin, internalization and retention of pinostrobin in HeLa cells was investigated by live cell confocal microscopy using its fluorescence properties (emitting green and blue fluorescence at excitation 280 nm) after pinostrobin treatment (Figure 4.1.17 B). Subsequent Z sectioning of the cells indicated that pinostrobin entered into cells within 1h. In comparison to pinostrobin fluorescence at 1 h, significant decrease in its fluorescence was observed at 24 h post-treatment, indicating fast clearance from the cells (Figure. 4.1.17 B).

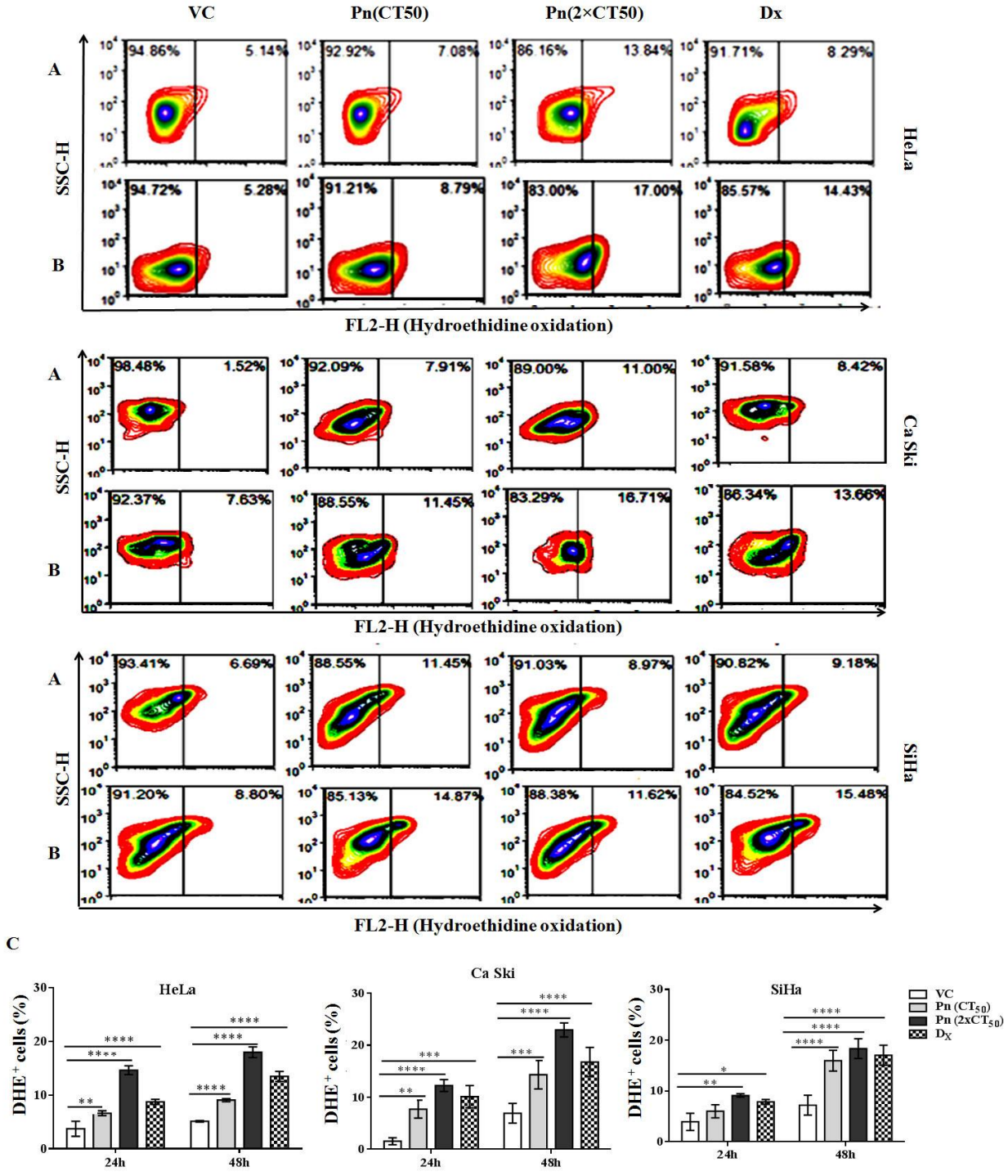

Figure 4.1.15. Representative contour plot for oxidation of hydroethidine (HE) by ROS in pinostrobin treated HeLa, Ca Ski, SiHa cells at 24 h(A) an 48h(B). In presence of ROS hydroethidine is oxidized into ethidium bromide and binds to DNA, produces red fluorescence post pinostrobin treatment. The red fluorescence events were visualized high in pinostrobin (CT_{50} & $2\times CT_{50}$) and doxorubicin (10µM) treated cells compared to vehicle treated and normal cells. Doxorubicin treatment also showed significance red fluorescence in treated cells. (C) Quantitative graphical representation of data shown in panels A and B. The results are mean ±SD of three independent experiments performed in triplicates. Significance difference (*p value*) of all treated group is calculated with respect to observed fluorescence in vehicle treated cells using ordinary two-way ANOVA (Dunette's multiple comparison test. *, *p≤0.05*; **, *p≤0.01;* ***, *p≤0.005;* ****, *p≤0.001*. VC, Vehicle control; Pn, Pinostrobin; Dx, Doxorubicin.

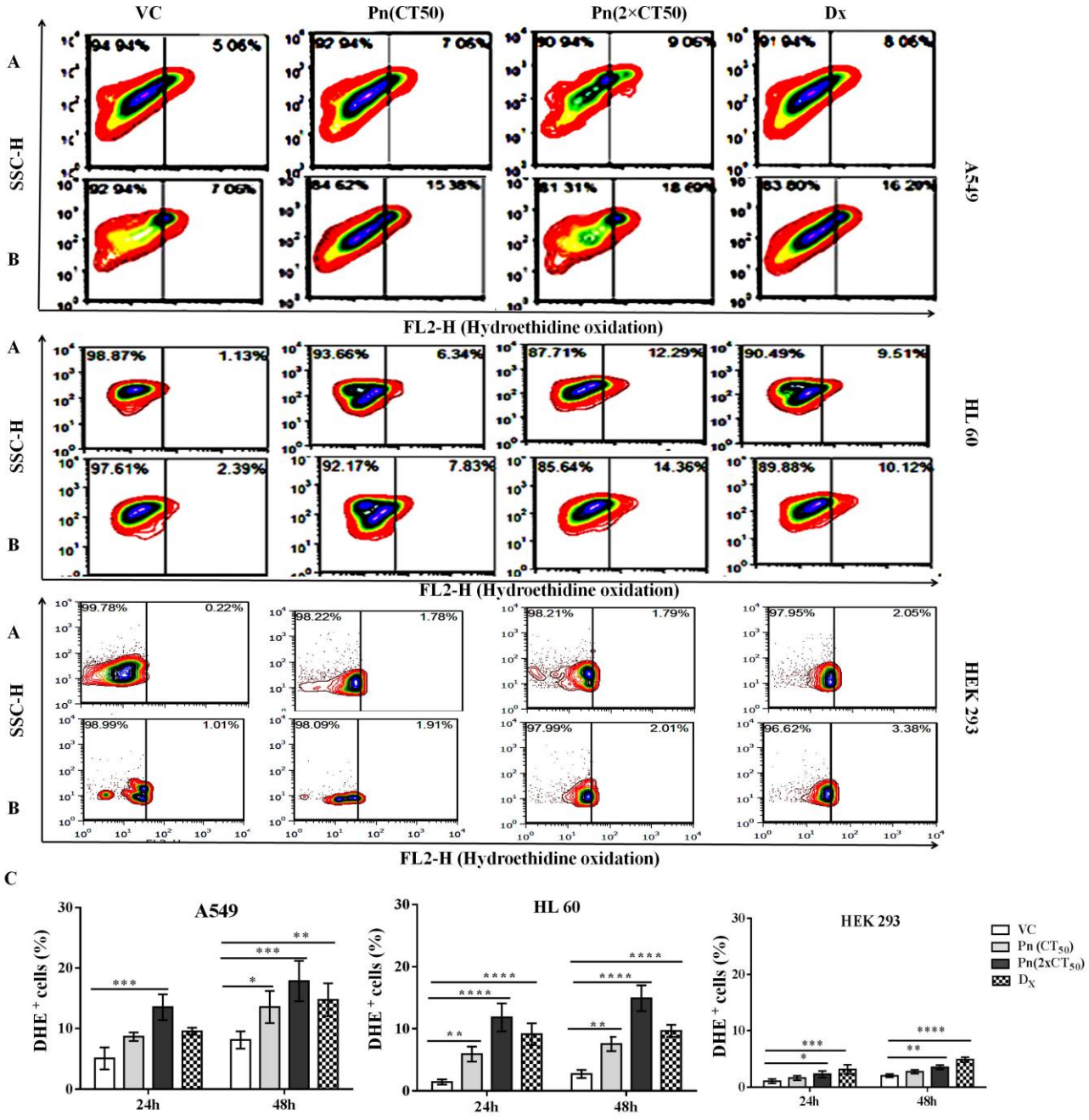

Figure 4.1.16. Representative contour plot for oxidation of hydroethidine (HE) by ROS in pinostrobin treated A549, HL-60 and HEK 293 cells at 24 h(A) an 48h(B). In presence of ROS hydroethidine is oxidized into ethidium bromide and binds to DNA, produces red fluorescence post pinostrobin treatment. The red fluorescence events were visualized high in pinostrobin (CT_{50} & $2\times CT_{50}$) and doxorubicin (10 µM) treated cells compared to vehicle treated and normal cells. Doxorubicin treatment also showed significance red fluorescence in treated cells. (C) Graphical representation of flow cytometric data shown in panels A and B. The results are mean±SD of three independent experiment performed in triplicates. Significance difference *(p value)* of all treated group is calculated with respect to observed fluorescence in vehicle treated cells using ordinary two-way ANOVA (Dunette's multiple comparison test). *, *p≤0.05*; **, *p≤0.01;* ***, *p≤0.005;* ****, *p≤0.001*. VC, Vehicle control; Pn, Pinostrobin; Dx, Doxorubicin.

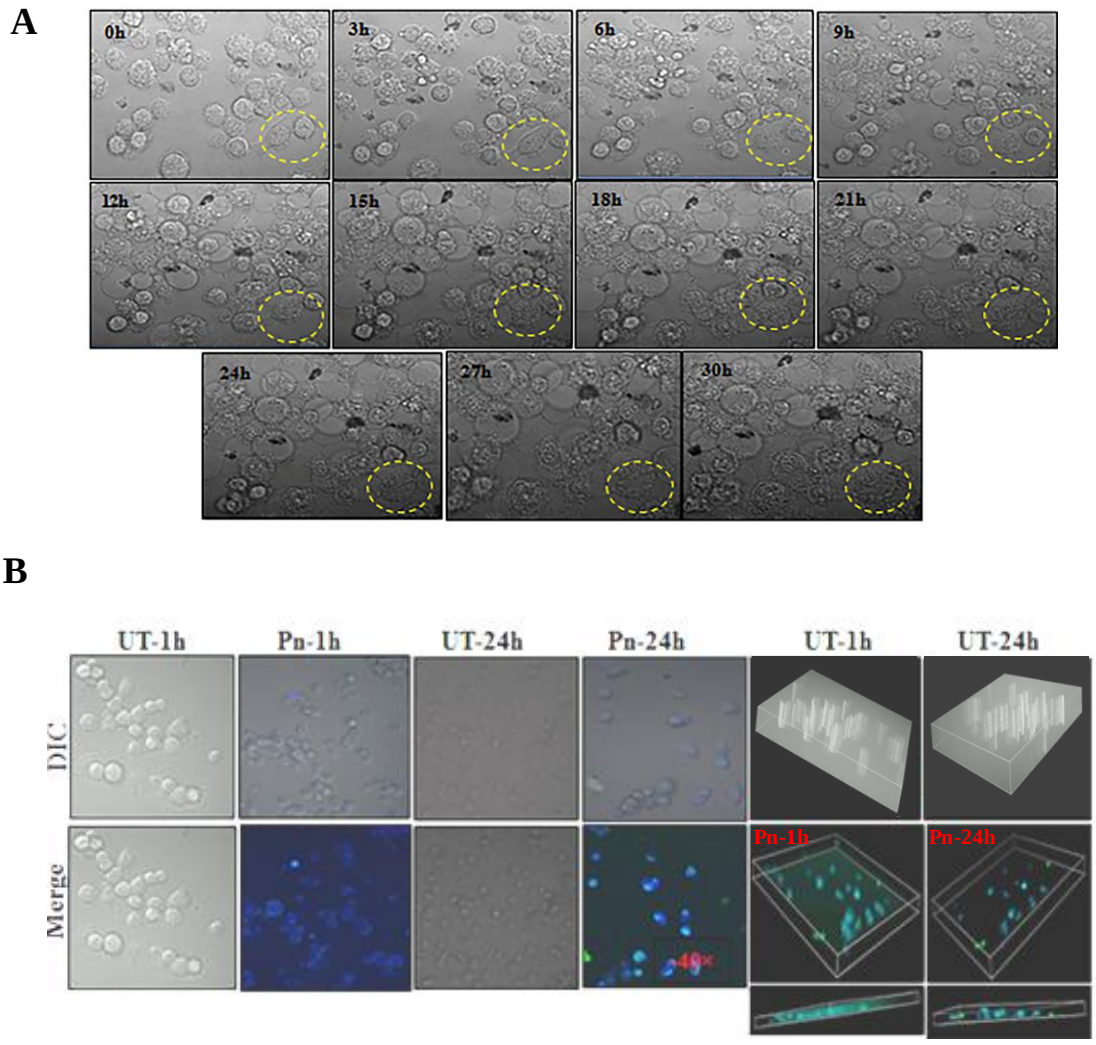

Figure 4.1.17. (A) The morphology of HeLa cells appeared to be modified by pinostrobin treatment such as increase cytoplasmic volume and blebing in cell membrane that indicates initiation of apoptosis. **(B)** Pinostrobin internalization and retention into HeLa cell was examined under live cell confocal microscopy at 40× magnification. Pinostrobin (100µM) easily internalized into HeLa cells within 1 h as detected by the presence of its blue–green fluorescence after excitation at 280 nm. This fluorescence acts as an indicator of penetration and analyzed by Z sectioning of cells**.** UT, Untreated; Pn, Pinostrobin.

4.1.11 Assessment of effect of pinostrobin on redox state of mitochondria and nuclear architecture by live cell confocal microscopy

Reduction in mitochondrial potential was confirmed by live cell confocal microscopy of the HeLa cells, probed with fluorescent cationic carbocyanine JC-1 dye at 24 h (Figure 4.1.18 A) and 48 h (Figure 4.1.18 B) post treatment. As shown in the Figure, pinostrobin-treated cells showed intense green fluorescence of JC-1 monomers, whereas red fluorescence of JC-1 aggregates was seen in vehicle treated control cells. These data suggest reduction in mitochondrial membrane potential ($\Delta\psi$m) in pinostrobin-treated

cells. Positive control doxorubicin also resulted in a decrease in mitochondrial membrane potential as evident by the presence of green fluorescence in doxorubicin treated cells. An increase in the rate of JC-1 monomer formation increased with time dependent manner.

Deformation of nucleus structure was analyzed by Hoechst 33342 staining of treated HeLa cells. Pinostrobin and doxorubicin-treated HeLa cells at 24 h and 48 h post-treatment showed remarkable changes in the nuclei as bright condensed and fragmented nuclei could be seen under live confocal microscope (Figure 4.1.18 A, B). An increase in Hoechst stain was observer with time as the nuclei at 48 h post-treatment showed brighter fluorescence. The untreated and vehicle treated cells showed dim and dark blue color of nucleus and retained intact nuclear membrane. These data suggest that pinostrobin has potential to target both the mitochondria and nucleus simultaneously, and may inhibit their regulatory functions mediating cell death by activation of intrinsic apoptosis pathway.

4.1.12 Alteration in expression profile of apoptosis associated proteins

Apoptosis is mediated by two pathways such as intrinsic and extrinsic. As a change in the mitochondrial potential and nuclear architecture was noted in pinostrobin treated cells, we analysed the expression profile of proteins of these pathways in HeLa, Ca Ski, A549 and HL-60 cells treated with pinostrobin with CT_{50} concentrations for the respective cells using human apoptosis protein profile assay at 48 h. As shown in Figure 4.1.19 (AB,C,D), expression levels of Smac/DIABLO and HtrA2/Omi, that promote release of cytochrome c from mitochondria and initiate apoptosis, were found to be increased in all the four cancer cells treated with pinostrobin when compared to vehicle treated control. An increase in the expression of Bad and Bax, early inducer proteins of apoptosis was also detected in pinostrobin treated cells when compared to vehicle control cells. Pinostrobin treatment brought about an increase in the expression of proteins of extrinsic pathway as well in some of the cells. . Extrinsic apoptosis pathway is mediated and activated by TRAIL R1/D4, TRAIL R2/D5, TNFα, Fas and FADD proteins. The expression level of these proteins was also enhanced in different cancer cells treated with pinostrobin when compared to vehicle treated controls. Figure 4.1.19 shows that pinostrobin treatment resulted in significant increase in TNFα level at 48 h post-treatment in HeLa cells

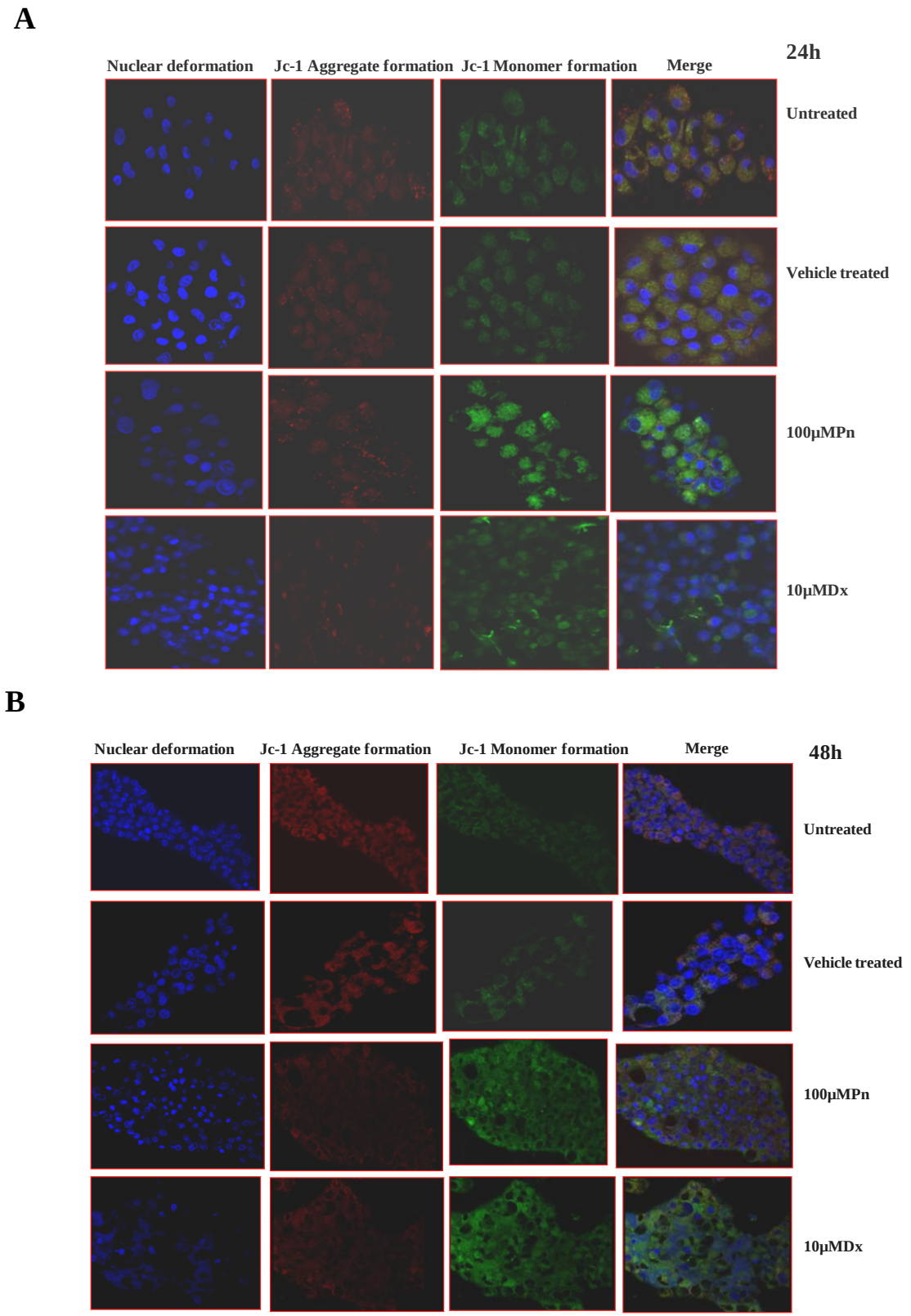

Figure 4.1.18. Redox status of mitochondria and nuclear architecture of HeLa cells post-pinostrobin treatment**.** HeLa cells were treated with the test chemicals for 24 (A) and 48 h (B) and stained with JC-1 probe and Hoechst 33258 stain and visualized under live confocal microscope at 40× magnification**.** Red fluorescence of JC-1 aggregates in the untreated cells and intense green fluorescence of JC-1 monomers in pinostrobin-treated cells is evident, indicating depolarization of mitochondrial membrane potential by pinostrobin treatment (Pn: Pinostrobin, Dx: Doxorubicin).

(*p≤0.001*, Figure 4.1.19 A). No significant change in TNFα was observed in HL-60, Ca Ski and A549 cells (Figure 4.1.19 B,C,D). Expression of DR4 and DR5 was most significantly enhanced in HeLa cells (*p≤0.001*, Figure 4.1.19A) at 48 h treatment, though their expression was also higher in all cancer cells after pinostrobin treatment. Expression levels of FADD and Fas proteins which are required for TNFα and DR interaction, were also increased in pinostrobin treated HeLa (FADD ; *p≤0.001 & Fas; p≤0.001*, Figure 4.1.19A), Ca Ski (FADD; *p≤0.01*, Figure 4.1.19 B), A549 (Fas*; p≤0.05*, Figure 4.1.19 C) and HL60 (FADD*; p≤0.01*, Figure 4.1.19 D), cells in comparison to vehicle treated cells at 48 h post-treatment. Thus, the expression levels of all basic extrinsic apoptosis proteins was observed to be higher, though different proteins showing increase to different extent in different cell types, suggesting that pinostrobin is also capable to induce cell death through extrinsic apoptosis pathway.

The expression level of pro-caspase and cleaved caspase, involved in early apoptosis, was also examined after pinostrobin treatment and significant enhancement in caspase expression was detected in all cell types with HeLa and Ca Ski cells showing maximum increase at 48 h (*p≤0.001* & *p≤0.001*, respectively). HL-60 cells also showed significance increase in pro-caspase-3 expression (*p≤0.005*) at 48 h, while A549 cells showed an increase to the of caspase (*p≤0.05*) level. Thus, in general, expression of caspase-3, key executioner caspase that cleaves numerous cellular substrates and leads to apoptosis, was found to be higher in all the tested cancer cells post-pinostrobin treatment. Likewise, expression of Bad and Bax proteins, involved in early apoptosis, was also found to be increased in all the cells, though to a different degrees (HeLa; both Bad and Bax at *p≤0.001;* Ca Ski, only Bad; *p≤ 0.01,* A549, only Bax *p≤0.05* and in HL-60, no significant change in either of the proteins*)* in comparison to vehicle treated control cells.

Expression of p53, tumor suppressor protein that mediates apoptosis after activation by phosphorylation was also analyzed. While only slight increase in phosphorylated p53 (S392) was noted in A549 and HL-60 cells (Figure 4.1.19 C & D), the HeLa and Ca Ski cells showed significant augmentation in p53 (S392) expression (*p≤0.005* & *p≤0.005*) (Figure 4.1.19 A & B). Since p53 is known to stimulate transcription of cyclin dependent kinase (Cdk) inhibitory protein p21 and p27 that arrest cell cycle in G1 phase, we also analyzed the expression of these downstream proteins. While p21 were significantly increased in HeLa and Ca Ski pinostrobin treated cells (Figure 4.1.19 A, B, *p≤0.005* &

p≤0.001, respectively), p27 was also noted increased in comparison to vehicle treated control cells. A549 and HL-60 cells did not show any significance increase in their expression (p21 and p27) (Figure 4.1.19 C, D).Thus, these data suggest involvement and induction of both intrinsic and extrinsic pathways in pinostrobin-induced apoptosis.

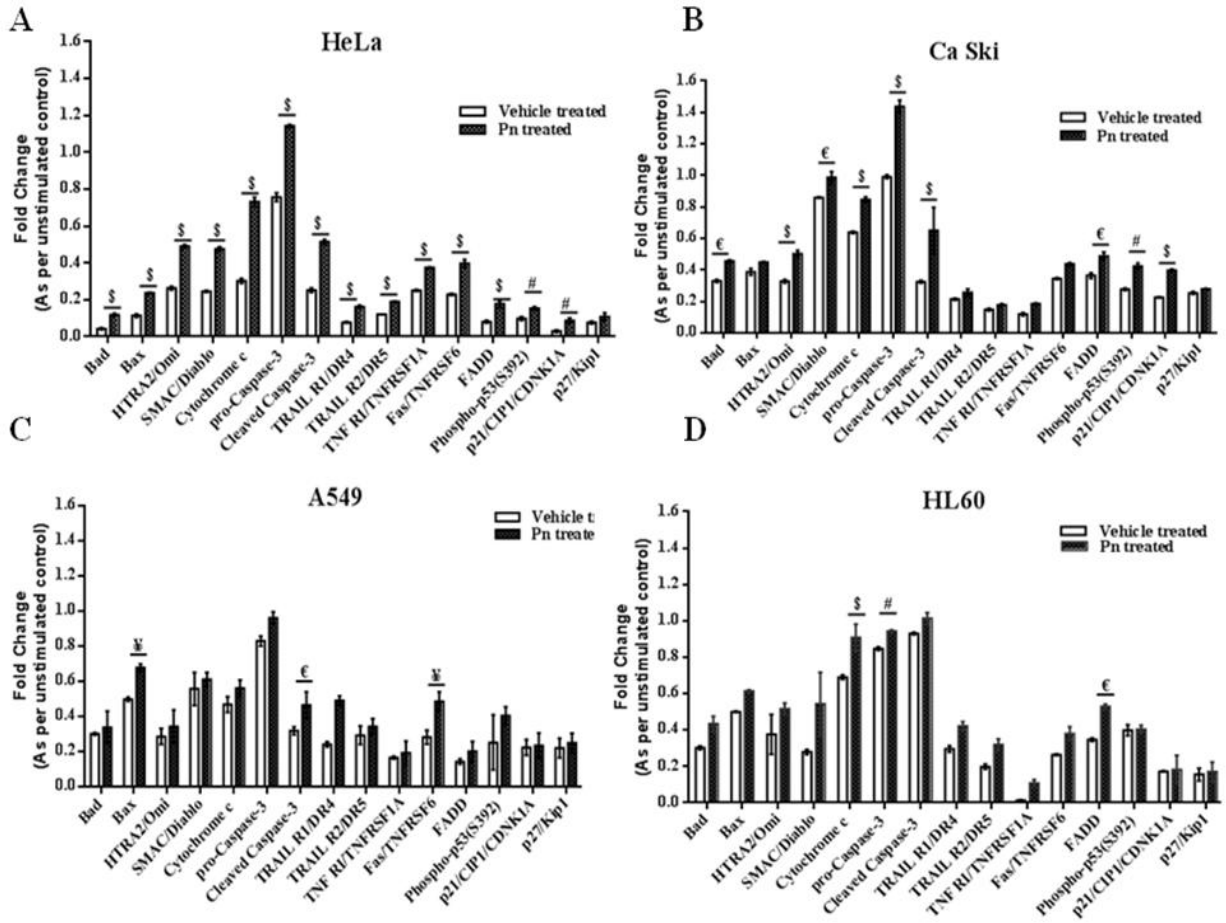

Figure 4.1.19. Analysis of expression profile of apoptosis related proteins using human protein profiler array after pinostrobin treatment (at CT_{50} concentrations for the respective cells) in HeLa**(A),** Ca Ski**(B)**, A549**(C)** and HL-60 **(D)** at 48h. Cell lysate (200µg) was subjected to protein profiling analysis. The expressed protein dots on the array membrane were visualized and imaged by Chemidoc, Biospectrum-500, and UVP, USA. Densitometry analysis of immunoreactive spots on captured image was carried out by Image J software (http://imagej.net). Significance difference *(p value*) in change of expression of treated cell is calculated with respect to respective density of a given protein spot in vehicle treated cells using ordinary two-way ANOVA (Dunette's multiple comparison test). *P value* represents, ¥, $p \leq 0.05$; €, $p \leq 0.01$; #, $p \leq 0.005$; $, $p \leq 0.001$.

Chapter 4.2

Effect of pinostrobin on Cancer Stem-like cells (CSCs) isolated from HeLa cells

4.2.1 Identification of side population (SP) cells in HeLa cells

Prior to establishing the CSCs from HeLa cells, it was necessary to establish if cancer HeLa cells used in the study have a population of cancer stem cells. Generally stem cells contain ABC membrane transporter protein that efflux certain lipophilic drugs and are recognized as side population (SP). Verapamil is used as Ca^2+ channel blocker which prevents Ca^2+ channel action and inhibits the efflux of Hoechst dye from side population. For confirmation that highly tumorigenic side population (SP) exists in HeLa cells, we cultured HeLa cells both in the presence and absence of verapamil. As shown in the Figure 4.2.1, HeLa cells exhibited ~1.86% tumorigenic side population (SP) in absence of verapamil as indicated by low efflux fluorescence population. When the cells were cultured in the presence of verapamil, the SP was reduced to 0.64%. These results confirmed presence of side population with characteristics similar to normal stem cells.

Pinostrobin treatment resulted in a significant decrease in the SP both in the absence or presence of verapamil in a dose dependent manner in comparison to the respective untreated cells. In the absence of verapamil, vehicle treated cells showed side population at 1.42%. Treatment with 50 µM and 100 µM pinostrobin reduced this side population to 1.00 % and 0.44% respectively. In the presence of verapamil, vehicle treated cells showed side population at only 0.55%, which was further reduced to 0.42% and 0.19% when the cells were treated with 50 µM and 100 µM pinostrobin, respectively. Similarly, treatment with doxorubicin also resulted in reduction in SP population, both in the absence and presence of verapamil.

4.2.2 Establishment of Cancer Stem-like Cells (CSCs) from HeLa cells

In order to assess the effect of pinostrobin on sphere forming cells or cancer stem like cells (CSCs) from HeLa cells were allowed to be formed by growing HeLa cells in serum free medium. As shown in Figure 4.2.2A, compact cluster of cancer sphere cells were successfully formed. The formation of clusters of cancer sphere was initiated within 3 days. Morphology of the compact structure of cluster of cancer sphere cells was monitored upto 12 days. These CSCs showed entirely different morphology from parental HeLa cells and appeared as non-adherent spherical cluster (Figure 4.2.2 B).

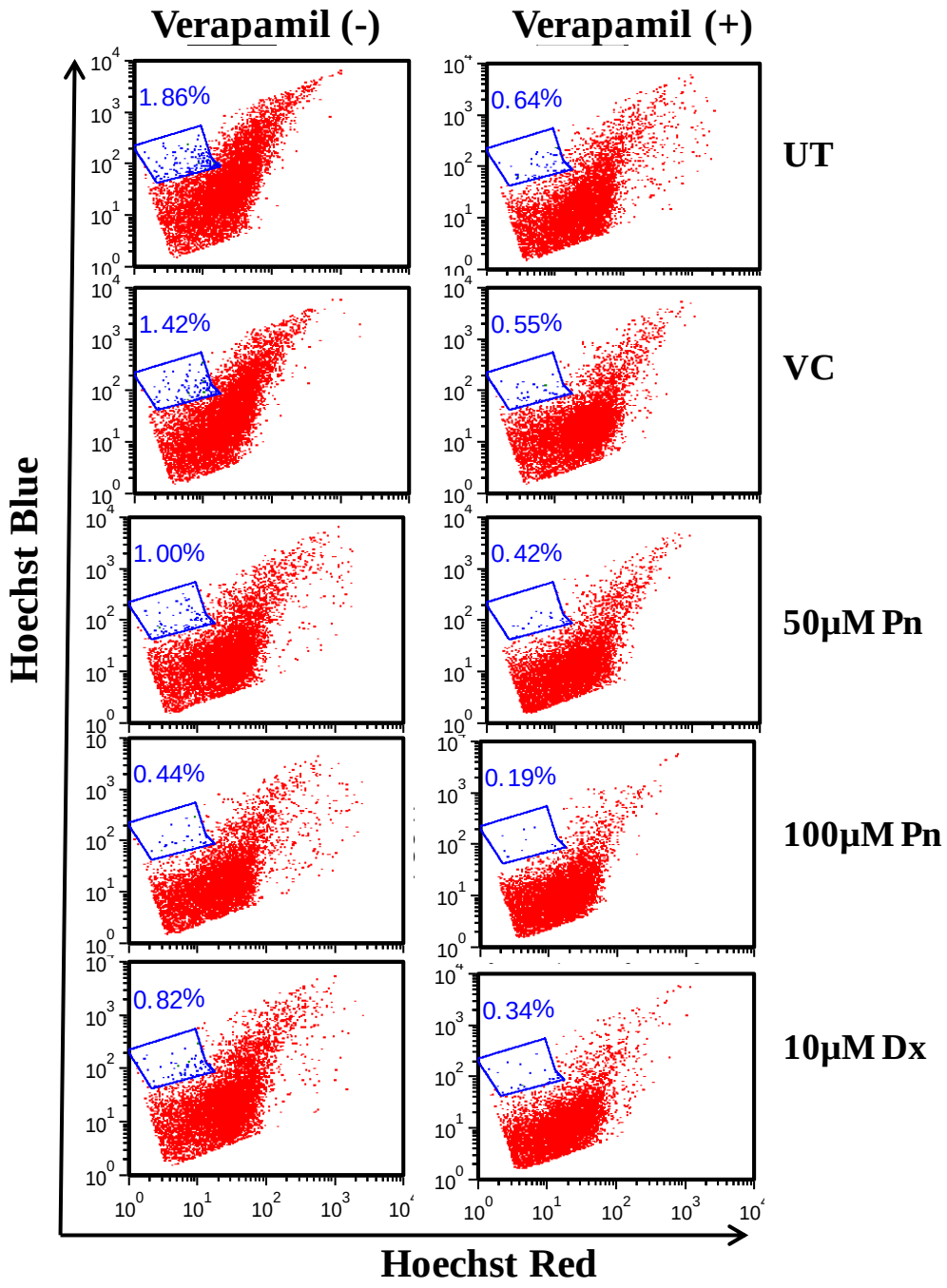

Figure 4.2.1. Establishment of presence of side population (SP) in HeLa cells by flow cytometry. Cells were cultured in the absence/presence of Verapamil (50 µM). Treatment with pinostrobin (Pn) and doxorubicin (Dx) was given for 48 h. Fluorescence events of side population are depicted in blue box. Side population was significantly decreased and found low in numbers after post exposure of pinostrobin at 48 h.

All spheres progressively increased in diameter day by day. Therefore, these cells can be considered as stem or progenitor cells due to their extensive proliferation and self-renewal properties. These clusters of cancer sphere cells were also identified as spheroids (Figure

4.2.2 B). Subsequently, these non-adherent spherical clusters were used for further studies after confirmation of expression of the stem cell specific cell surface marker.

4.2.3 Conformation of CSCs by cell surface markers

It has been reported earlier that mammo-sphere cells express higher levels of $CD44^+$ and lower levels of $CD24^{+}$[1,2]. Similarly, HeLa-sphere forming cells exhibit high $CD44^+$ expression and low CD24 expression, whereas parental HeLa cells are $CD44^+$ low and $CD24^+$ high[3]. Therefore, after morphological examination of the CSCs established from HeLa cells, these were confirmed by cell surface markers $CD44^+$ and $CD24^+$ expression. As shown in Figure 4.2.3A. CSCs established from HeLa cells showed higher expression of $CD44^+$ and negligible expression of $CD24^+$, whereas parent HeLa cells showed higher expression of $CD24^+$ and lower expression of $CD44^+$. These data further confirmed the authenticity of the CSCs established from the HeLa cells. These CSCs were then used for further studies. FACS was performed to quantify $CD44^+$ and $CD24^+$ expression in HeLa-CSCs and HeLa cells treated with pinostrobin (Figure 4.2.3B). Untreated HeLa-CSCs and HeLa cells exhibited 94.55% and 28.49% expression of $CD44^+$, whereas 60.33% and 93.60% cells, respectively were identified $CD24^+$.

4.2.4 Morphological examination of CSCs

The CSCs are known to continuously differentiate and make a cluster of heterogeneous mature cells. The morphology of cancer stem like cells was visualized at different time intervals such as 3, 6, 9 and 12 days (Figure 4.2.4). As evident from the figure, the HeLa-CSCs continuously proliferated, made large number of clusters and differentiated into stem-like and non-stem progenitor tumorigenic cells. These cancer stem-like cells continuously increased in their size.

4.2.5 Regeneration of HeLa cells from CSCs/SFCs and Spheroids

Ability of CSCs/SFCs and spheroids to regeneration parent HeLa cells was also evaluated by growing the same in constituted DMEM. SFCs and spheroids adopted HeLa cells morphology within 5 to 7 days. These cells adhered to the surface of culture flask and exhibited similar morphology like parental HeLa cells (Figure 4.2.5 A). The self-renewal

[1] Yu, F., Yao, H., Zhu, P., Zhang, X., Pan, Q., Gong, C., Huang, Y., Hu, X., Su, F., Lieberman, J. and Song, E., 2007. let-7 regulates self renewal and tumorigenicity of breast cancer cells. Cell, 131, pp.1109-1123.
[2] Al-Hajj, M., Wicha, M.S., Benito-Hernandez, A., Morrison, S.J. and Clarke, M.F., 2003. Prospective identification of tumorigenic breast cancer cells. Proceedings of the National Academy of Sciences, 100, pp.3983-3988.
[3] Gu, W., Yeo, E., McMillan, N. and Yu, C., 2011. Silencing oncogene expression in cervical cancer stem-like cells inhibits their cell growth and self-renewal ability. Cancer Gene Therapy, 18, pp.897-905.

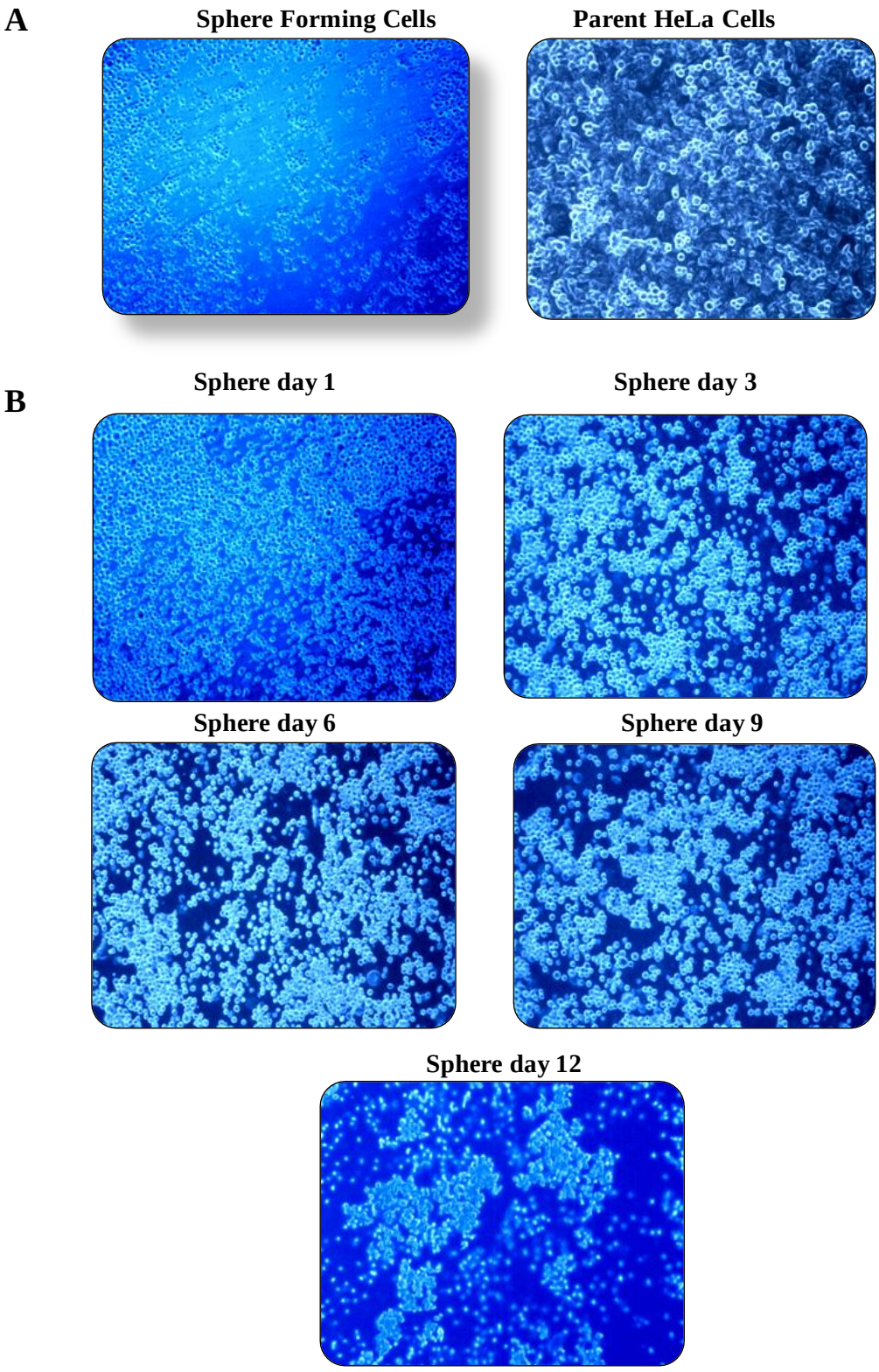

Figure 4.2.2. (A) Establishment of sphere forming cells or Cancer Stem-like Cells (CSCs) derived from adherent populations of HeLa cells that exhibit self-renewal and tumorigenic potential *in vitro*. **(B)** HeLa-associated sphere forming cells were examined at different time intervals at 10 ×magnification under bright filed microscope.

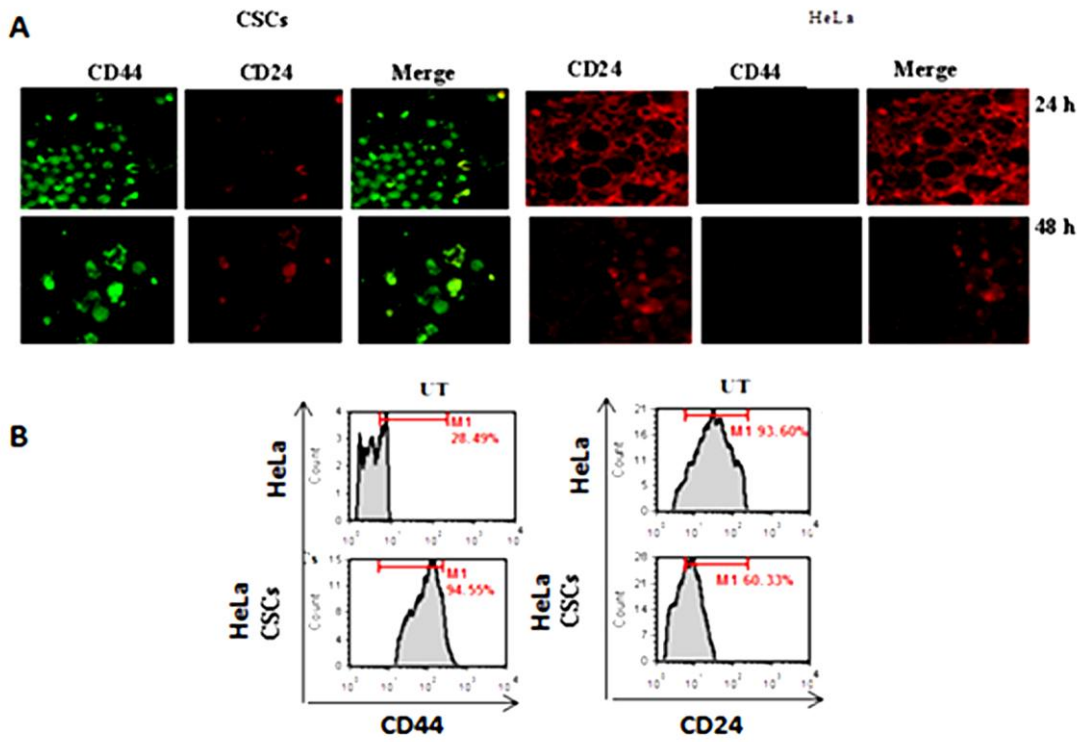

Figure 4.2.3. (A) Identification of surface marker in CSCs. $CD24^{+}$ and $CD44^{+}$ expression were examined in CSCs and HeLa cells at 24 and 48 h under confocal microscope at 40× magnifications. **(B)** Characterization of Hela CSCs: Histogram representing the expression of surface marker ($CD44^{+}$ and $CD24^{+}$) on HeLa cells and CSCs. (UT: Untreated)

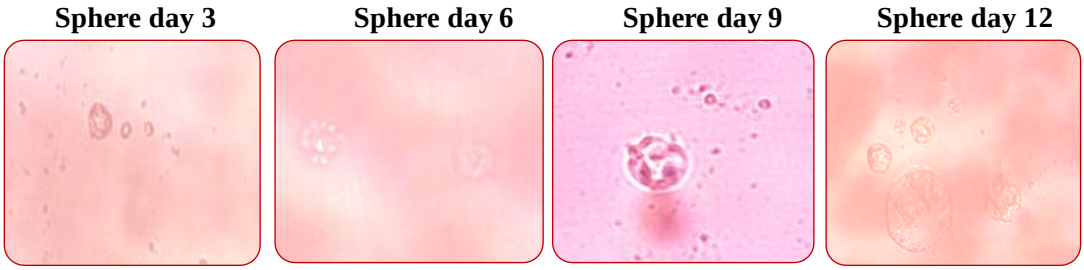

Figure 4.2.4. Morphology of cultured sphere forming cells or cancer stem like cells: The CSCs appeared as non-adherent cluster from parental HeLa cells at 40 ×magnification under bright filed microscope. Sphere forming cells progressively increased in diameter at 3, 6, 9 and 12 days, respectively**.**

activity of SFCs was also validated by spheroids. Spheroids were formed long after culturing of SFCs and made a cluster of heterogeneous cells population. When spheroids of 3 and 5 days were cultured in constituted DMEM, the cells quickly adopted parental HeLa cells morphology (Figure 4.2.5 B). Thus, these results indicated that spheroid speedily adopted parent HeLa cells morphology compared to SFCs.

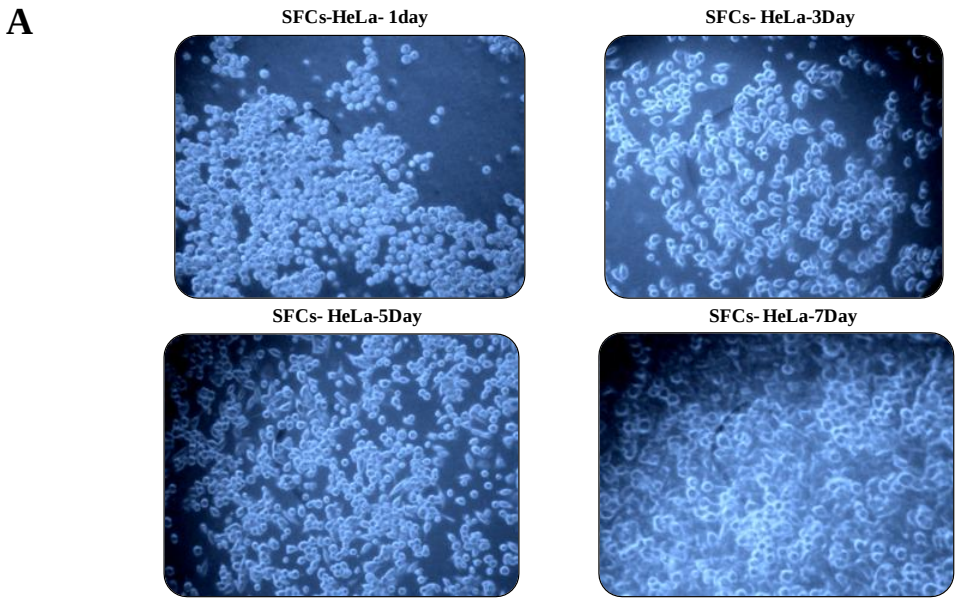

Figure 4.2.5. A Regeneration of parental HeLa cells from SFCs. SFCs cultured in constituted DMEM containing fetal calf serum to grow parental HeLa cells. The cells were visualized using an inverted microscope at different time intervals at 10×magnification. SFCs quickly grow as adherent cells and adopt parental HeLa cell's morphology.

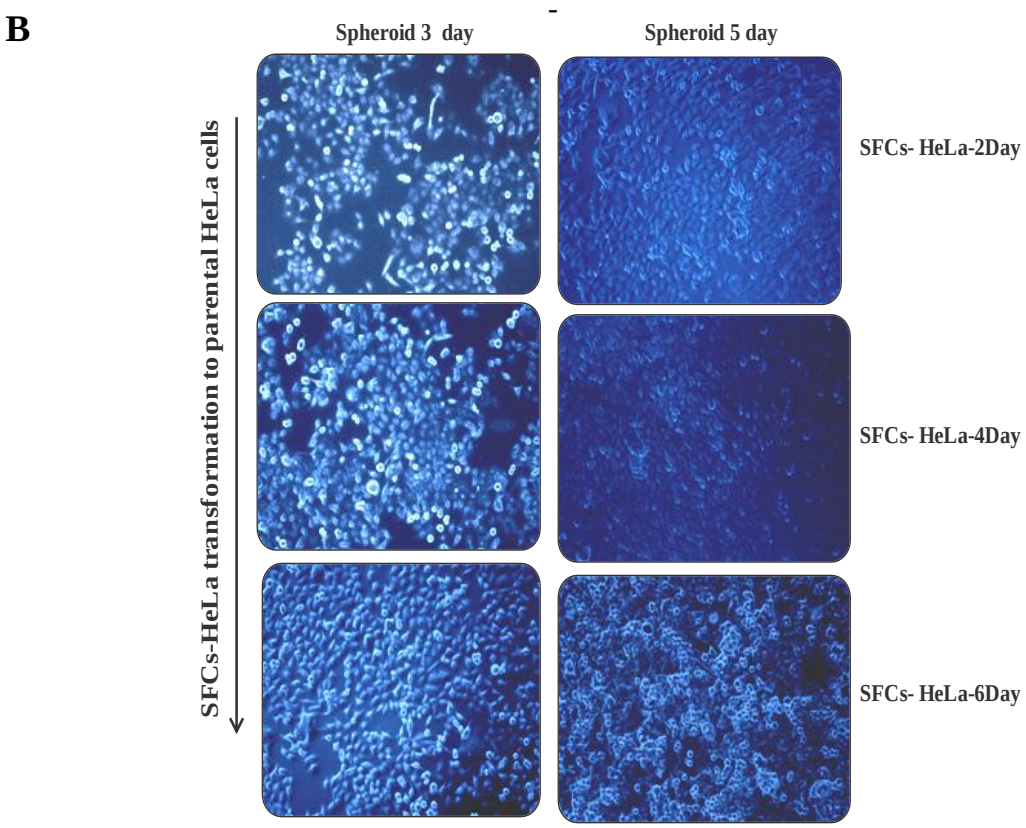

Figure 4.2.5. B. Transformation of 3-day and 5-day spheroids into parental HeLa cells. CSCs were allowed to grow in serum free medium for the formation of spheroids for 3 or 5 days followed by culturing in constituted DMEM containing fetal calf serum. The cells quickly grew to become adherent and attained parental HeLa cell's morphology on day 2,4,6 days , visualized at 10× magnification under inverted microscopy.

4.2.6 Evaluation of cytotoxicity of pinostrobin on CSCs

Cytotoxicity of different concentrations of pinostrobin (12.5, 25, 50,100 and 200µM) was analysed in CSCs cells and parental HeLa cells at 24h (Figure 4.2.6 A) and 48 h (Figure - 4.2.6 B) for comparative analysis. A dose dependent increase in cytotoxicity was observed both in HeLa-CSCs and HeLa cells. At 24 h, treatment with 100µM pinostrobin resulted in 61.34±4.20% and 47.92±3.93% cytotoxicity in CSCs and HeLa cells, respectively, A significant increase in the cytotoxic effect was observed as at 48 h in both CSCs (73.21±5.93%) and HeLa cells (67.69±3.44%). Thus, pinostrobin was comparatively more toxic to HeLa-CSCs than parent HeLa cells. Doxorubicin included as a positive control also inhibited growth of both CSCs and HeLa cells, while vehicle did not exhibit any significant cytotoxicity. Thus, pinostrobin was found to inhibit the growth of CSCs and HeLa cells in a dose and time dependent manner.

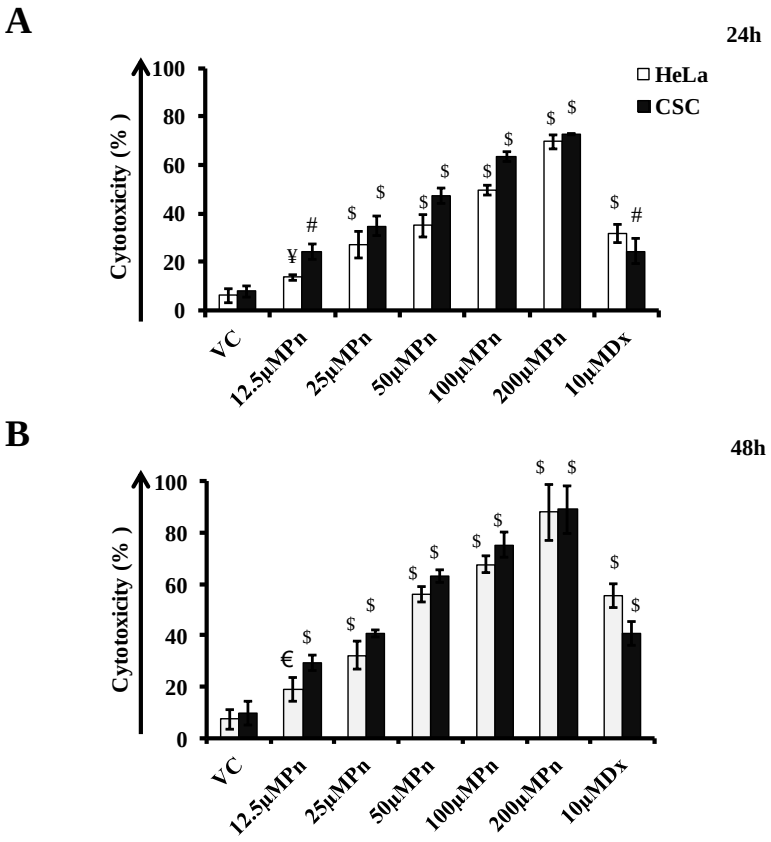

Figure 4.2.6. Cytotoxic effect of pinostrobin examined in HeLa and Cancer stem-like cells (CSCs) by MTT assay. HeLa and CSCs were treated with vehicle, doxorubicin and pinostrobin for 24h(A) and 48h (B) time interval. The data represent mean±SD of three independent experiments conducted in triplicates. Significance differences (*p value*) of all treated groups are calculated with respect to vehicle control cells using student t-test. * represents ¥, *p≤0.05*; €, *p≤0.01*; #, *p≤0.005*; $, *p≤0.001*. VC, Vehicle Control; Pn, Pinostrobin; Dx, Doxorubicin.

4.2.7 Effect of pinostrobin on CSCs: Cell surface marker expression analysis

The HeLa-CSCs and HeLa cells treated with pinostrobin were analysed for qualitative change in expression of cancer stem cell markers $CD44^+$ and $CD24^+$ by confocal microscopy at 40× magnifications. As shown in the Figure 4.2.7A, intense green fluorescence of FITC indicating CD44 expression was observed in vehicle treated CSCs with very weak red fluorescence of PE stain, indicating of $CD24^+$ expression. On the other hand, HeLa cells stained red with negligible green fluorescence suggesting higher level of $CD24^+$ expression in comparison to the CSCs. Pinostrobin treatment resulted in a decrease in the expression of both $CD44^+$ and $CD24^+$ in the CSCs as well as the HeLa cells.

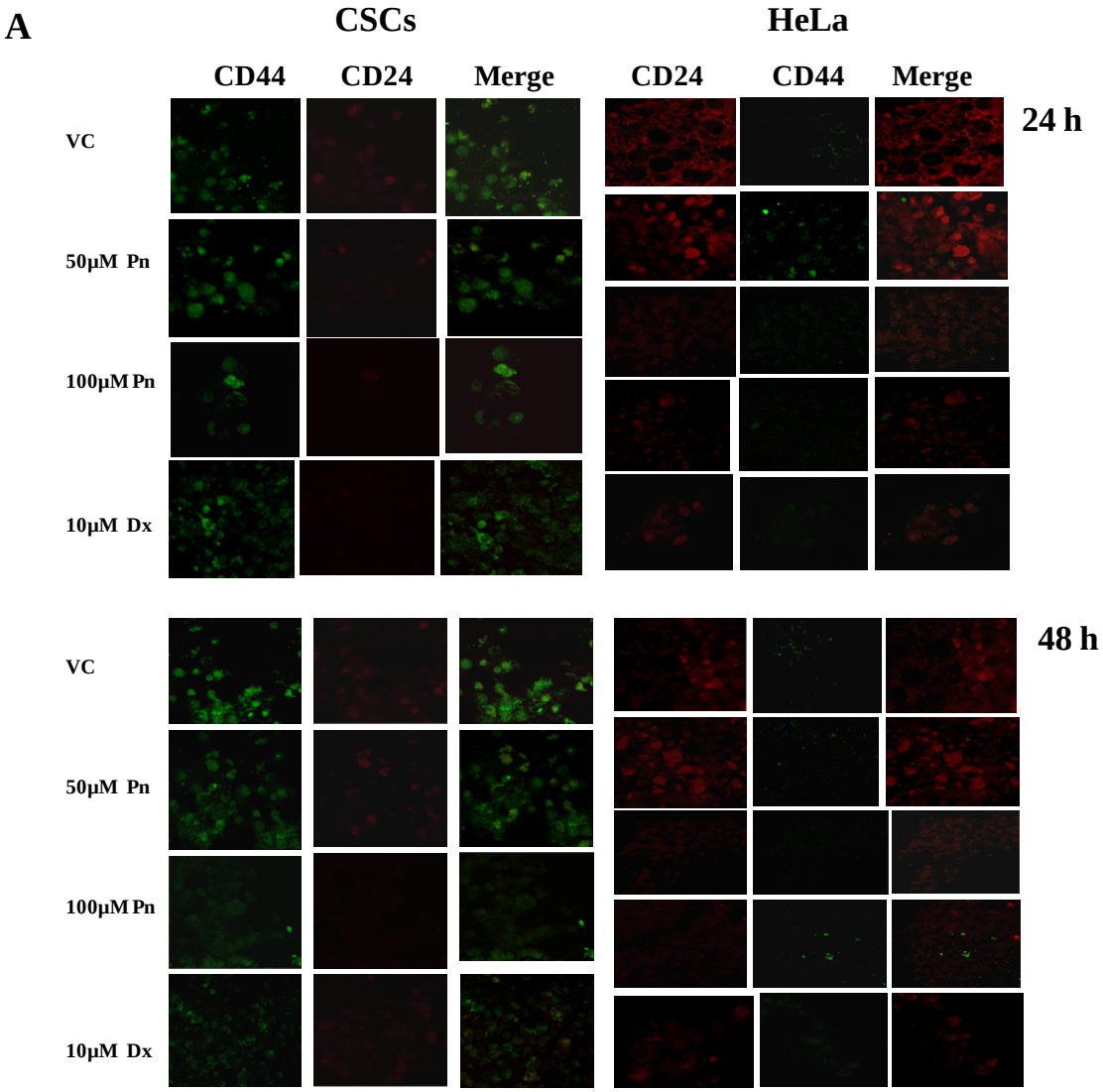

Figure 4.2.7. A Effect of pinostrobin on $CD44^+$ and $CD24^+$ expression in CSCs and HeLa cells. HeLa cells and CSCs, treated with vehicle and different concentrations of pinostrobin for 24 h and 48 h, were stained with FITC-conjugated anti-CD44 and PE-conjugated anti-CD24 antibodies and visualized at 40×magnification by confocal microscopy. Doxorubicin (10µM)-treated cells were included as a positive control.

Pinostrobin (100µM) treatment resulted in decrease in $CD44^+$ cells both in case of HeLa-CSCs and HeLa cells to 83.48% and 16.30% respectively. Similarly, pinostrobin treatment decreased the population of $CD24^+$ HeLa-CSCs and HeLa cells to 35.87% and 65.84%, respectively at 48 h. These results indicate that pinostrobin reduced the population of both $CD44^+$ and $CD24^+$ in CSCs, and thus could affect control cancer growth from CSCs as these are involved in sphere formation, cell proliferation, cell differentiation, tumour growth, invasion and metastasis action.

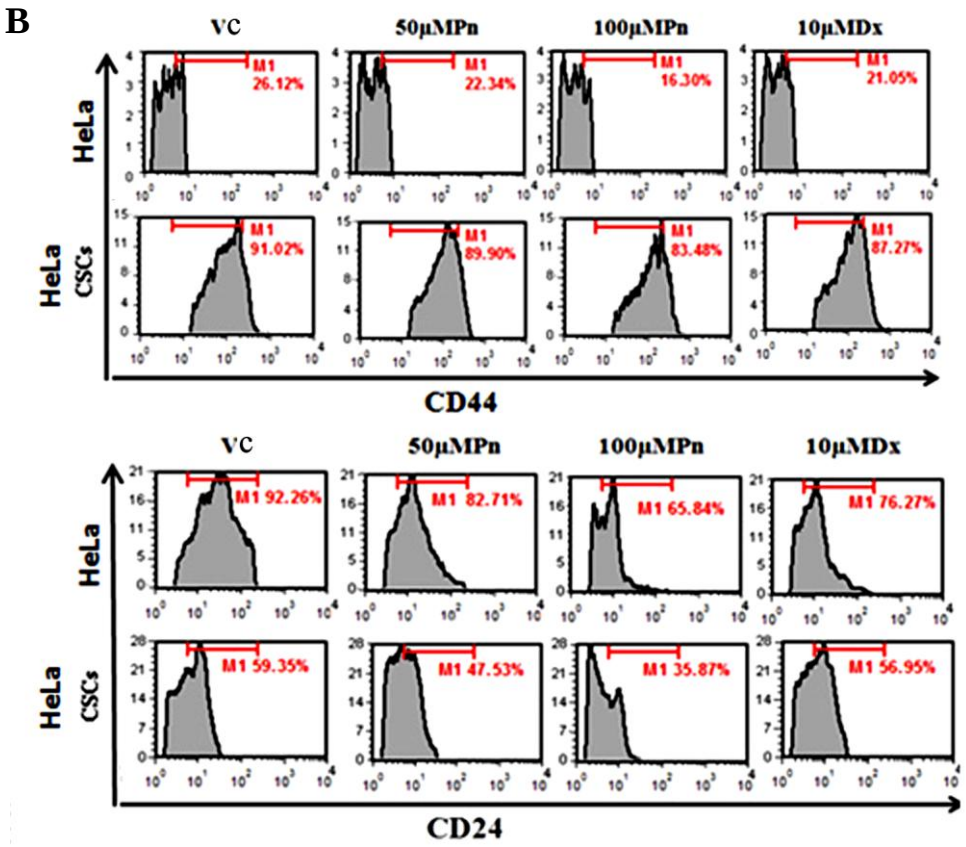

Figure 4.2.7. B Expression level of molecular surface marker in pinostrobin treated (50µM, 100µM) HeLa cells and HeLa-CSCs at 48 h. Histogram representing the expression level of surface marker i.e. $CD44^+$ and $CD24^+$ in HeLa cells and CSCs. VC, Vehicle control; Pn, Pinostrobin; Dx, Doxorubicin.

4.2.8 Effect of pinostrobin on sphere formation efficiency from CSCs and sphere morphology

Since CSCs form spheres that contain non-stem tumorigenic cells, it was of interest to know if pinostrobin affected the sphere formation. For this, effect of pinostrobin on sphere formation efficiency of HeLa-CSCs was analyzed at different time intervals **(**Figure 4.2.8A). It is clear that the number of cell clusters continuously increased in the untreated cells and made sphere and spheroids. On the other hand, pinostrobin and

doxorubicin treated cells showed relatively lower number of cell clusters and decreased sphere and spheroids formation. Untreated spheres increased in size and formed symmetric prototypical spheroids that indicated self-renewal function of normal stem cells. Also, a continuous increase in the number of sphere numbers in untreated cells was noted with time i.e. from day 3 to day 9, whereas, pinostrobin-treated cells showed reduction in sphere numbers on different days when compared to vehicle treated CSCs on the respective days. Likewise, doxorubicin treated cells also showed reduction in sphere numbers. No reduction in the sphere numbers was observed in vehicle treated cells indicating that the reduction in sphere number in pinostrobin and doxorubicin treated cells are indeed due to these compounds only. Thus, sphere formation efficiency (SFE) was significantly reduced in pinostrobin-treated HeLa-CSCs when compared to untreated cells. Hence, the CSCs established from HeLa cells clearly have self-renewal activity and can be recognized as cancer stem cells.

Microscopic examination of a single sphere showed that morphology of pinostrobin- and doxorubicin-treated CSCs/spheres (Figure 4.2.8B) was completely disrupted with its outer cell membrane significantly disintegrated at 48 h in comparison to vehicle treated control which exhibited good membrane integrity. No significant change in the morphology of vehicle treated CSCs were observed when compared to untreated CSCs (compare with Figure 4.2.8A).

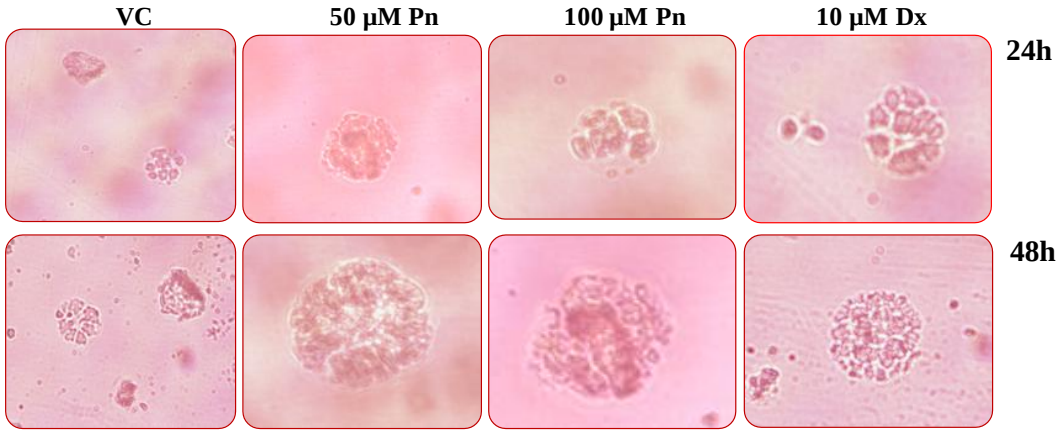

Figure 4.2.8. B Effect of pinostrobin (Pn, 50 &100 µM) on sphere formation: The morphology of spheres was monitored at 40×magnification using inverted microscope. Vehicle control (VC) and doxorubicin (Dx, 10µM) treated CSCs were included as negative and positive controls, respectively.

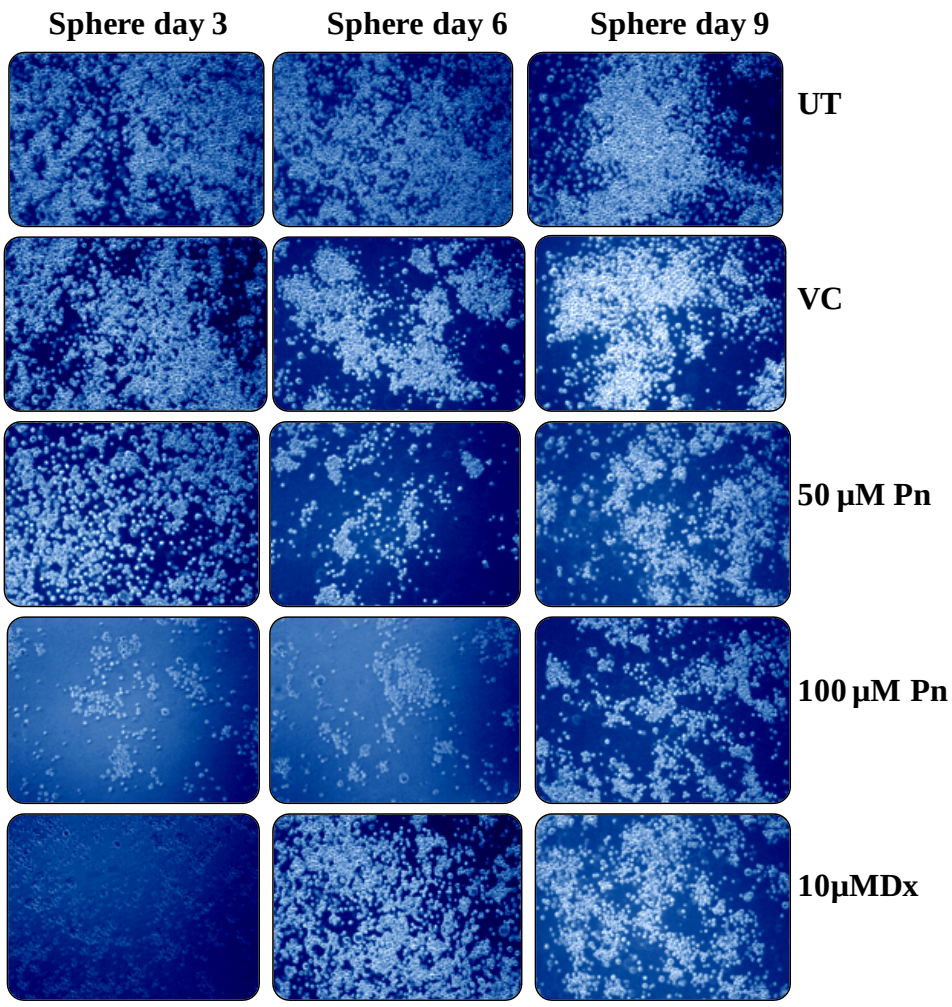

Figure 4.2.8. A Impact of pinostrobin on sphere forming efficiency (SFE) was examined at different time intervals under inverted microscopy. HeLa cells were cultured in ultralow attachment wells with sphere forming media in the presence or absence of different concentrations of pinostrobin (Pn). Vehicle and Doxorubicin (Dx, 10 µM) treated cells were included as negative and positive control. The spheres were visualized at 10× magnifications.

4.2. 9 Membrane integrity analysis via Annexin V–FITC

The membrane integrity of CSCs was determined as it is essential for cell architecture and shape. During apoptosis a cell membrane protein (phosphatidylserine) is externalized from inner side to outer side of cells. As expected, pinostrobin (50µM) treated cells showed higher number of phosphatidylserine exclusion in the form of Annexin V–FITC fluorescence events in CSCs (61.34±3.37%) and HeLa (55.69±3.11%) cells in comparison to untreated (~7%) and vehicle (~10%)- treated cells at 48 h (Figure 4.2.9). Thus, rate of externalization of phosphatidylserine was significantly increased with time in treated cells compared to untreated cells.

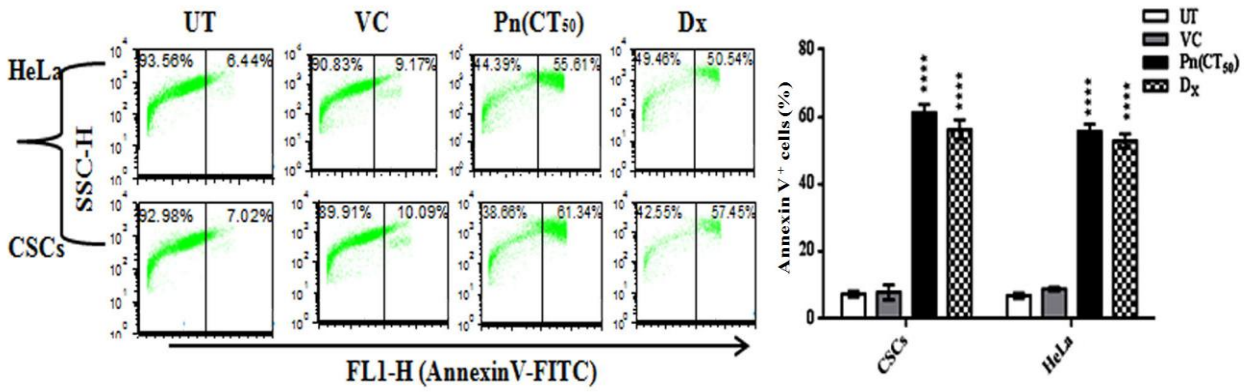

Figure 4.2.9. Representation of exclusion of phosphatidylserine by flow-cytometric analysis in pinostrobin treated HeLa cells and CSCs. AnnexinV-FITC positive population was analyzed by FCS Expressv5 software post treatment. The data represent mean±S.D. of three independent experiments performed in triplicates. Vehicle treated and doxorubicin treated cells were included as negative and positive controls, respectively. Bar diagram represents mean ±S.D. of three analyses performed in triplicates. Significance of difference *(p value*) of all treated groups is calculated using ordinary two-way ANOVA (Dunette's multiple comparison test) with respect to vehicle control (VC) cells. **** , *p≤0.001*.

4.2.10 Mitochondrial membrane potential ($\Delta\Psi m$) analysis by JC-1

As the integrity of cell membrane was disrupted by pinostrobin (50µM) treatment, mitochondrial membrane potential of the Pinostrobin treated HeLa CSCs was also analyzed using cationic carbocyanine JC-1 probes (Figure 4.2.11). Pinostrobin-treated CSCs and HeLa cells showed higher JC-1 monomer fluorescence events (50.55±1.71and 29.57±2.24%, respectively) at 48 h. On the other hand, untreated and vehicle treated cells showed minimal JC-1 monomer fluorescence events (ranging between ~3-5%) at 48 h. Doxorubicin treated cells also resulted in formation of JC-1 monomers fluorescence events (~44% and 30 % in HeLa-CSCs and HeLa cells respectively). Thus it is clearly demonstrated that Pinostrobin treated CSCs exhibited high number of JC-1 monomer forming population (in right quadrant) whereas untreated cells showed high $\Delta\psi$m with intense red fluorescence and exhibited less JC-1 monomers forming population in right quadrant.

4.2.11 Determination of Reactive oxygen species (ROS) production and site

ROS production was analysed by Dihydrochlorofluorescin-diacetate (DCFH-DA) in pinostrobin treated and untreated HeLa cells and CSCs (Figure 4.2.11). Pinostrobin-(50µM) treated HeLa and CSCs exhibited higher fluorescence events of DCF (35.79±3.62% and 57.43±3.54%, respectively) in comparison to untreated HeLa cells and CSCs (3.48±0.05% and 11.70±0.21%, respectively). This high fluorescence of DCF in

treated cells may be due to oxidation of non polar DCFH-DA into DCF by ROS and other peroxides.

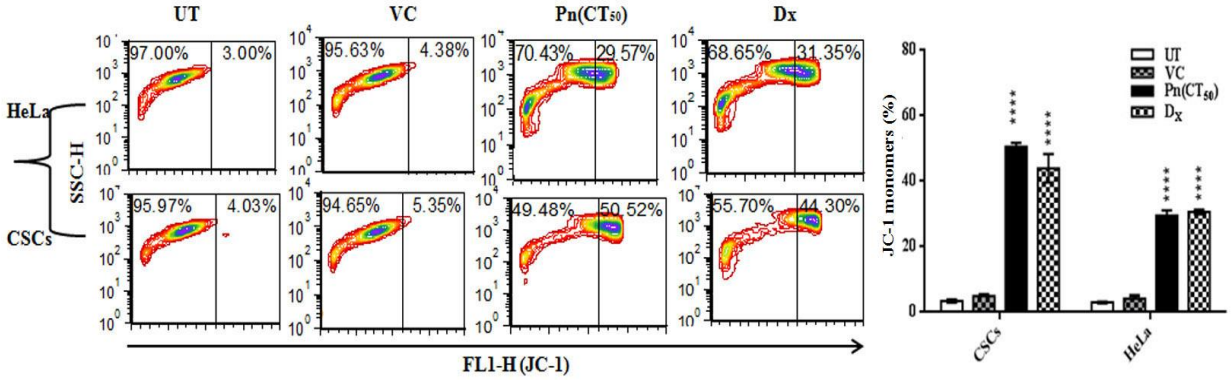

Figure 4.2.10. Representative flow cytometric analysis of mitochondrial membrane potential (ΔΨM) in pinostrobin treated HeLa cells and CSCs using JC-1 probes. Flow-cytometric examination of mitochondrial membrane depolarization analyzed by FCS Expressv5 software. Vehicle treated and doxorubicin (10 µM)treated cells were included as negative and positive controls. Bar diagram represents mean ±S.D. of three analyses performed in triplicates. Significance of difference *(p value*) of all treated groups is calculated using ordinary two-way ANOVA (Dunette's multiple comparison test) with respect to vehicle control (VC) cells. ****, *p≤ 0.001*.

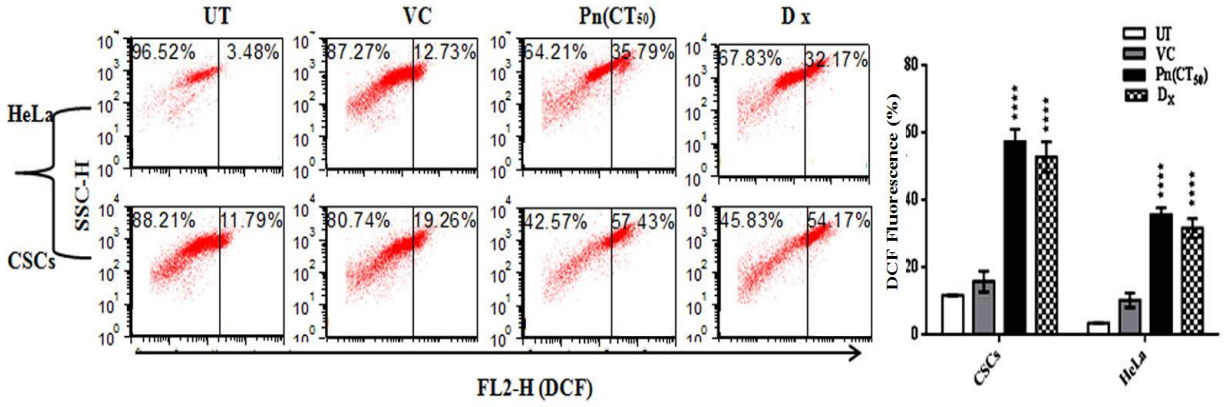

Figure 4.2.11. Representative flow cytometric analysis of assessment of ROS production in pinostrobin treated HeLa cells and CSCs. DCF fluorescence events were evaluated and analysed using FCS Expressv5 software. Vehicle treated and doxorubicin (10 µM) treated cells were included as negative and positive controls. Bar diagram represents mean ±S.D. of three analyses performed in triplicates. Significance of difference *(p value*) of all treated groups is calculated using ordinary two-way ANOVA (Dunette's multiple comparison tests) with respect to vehicle control (VC) cells. ****, *p≤0.001*

These data demonstrated that pinostrobin is capable of producing ROS both in CSCs and non-stem HeLa cells. After confirming ROS production, the site of ROS production was analysed using 10-nonyl acridine orange (NAO) dye. Pinostrobin treated HeLa cells and

HeLa-CSCs showed lower binding affinity of NAO with cardiolipin (58.19± 4.14% and 27.71± 4.40%, respectively) when compared to respective untreated cells (76.31± 10.76% and 65.96± 2.0%, respectively) at 48 h of treatment. Higher reduction of NAO binding affinity with cardiolipin was observed in CSCs compared to HeLa cells (Figure 4.2.12).

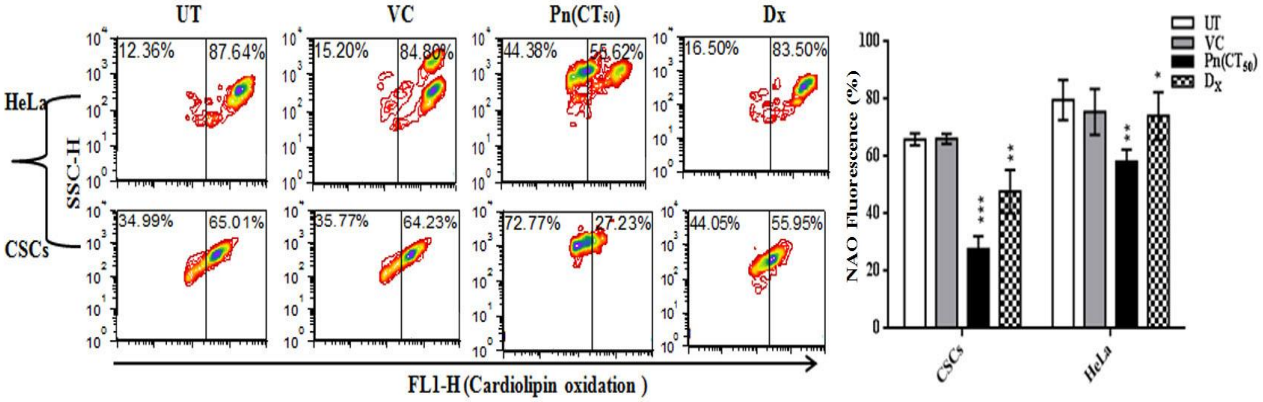

Figure 4.2.12. Analysis of cardiolipin oxidation using 10-nonyl acridine orange (NAO) stain by flow-cytometry in pinostrobin treated HeLa cells and CSCs. The fluorescence events of NAO or site of ROS production was analyzed by FCS Express v5 software. Figure shows representative flow cytometric analysis. Vehicle treated and doxorubicin (10 µM) treated cells were included as negative and positive controls. Bar diagram represents mean ±S.D. of three analyses performed in triplicates. Significance difference *(p value)* of all treated groups is calculated using ordinary two-way ANOVA (Dunette's multiple comparison test) with respect to vehicle control (VC) cells. *, *p≤0.05; **, p≤0.01; ***, p≤0.005.*

4.2.12 Assessment of ROS consequences

The consequences of ROS production in pinostrobin treated CSCs and HeLa cells were analysed by hydroethidine (HE) and propidium iodide(PI) staining. Figure 4.2.13 shows the red fluorescence of ethidium bromide that binds to DNA of damaged cells. Pinostrobin treated HeLa cells and CSCs showed high DNA fragmentation with red fluorescence events as 25.90±3.30%, and 36.25±6.15%, respectively. As evident from the figure, DNA fragmentation was found to increase with time and increasing dose of pinostrobin. DNA fragmentation was also analyzed by PI staining. After pinostrobin treatment, CSCs and HeLa cells showed an increase in the stained nuclei with red fluorescence event at 34.17±4.94% and 18.59±3.98%, respectively, in comparison to vehicle treated cells (Figure 4.2.14). Greater number of stained nuclei in pinostrobin-treated CSCs indicated the disintegration of nuclear membrane

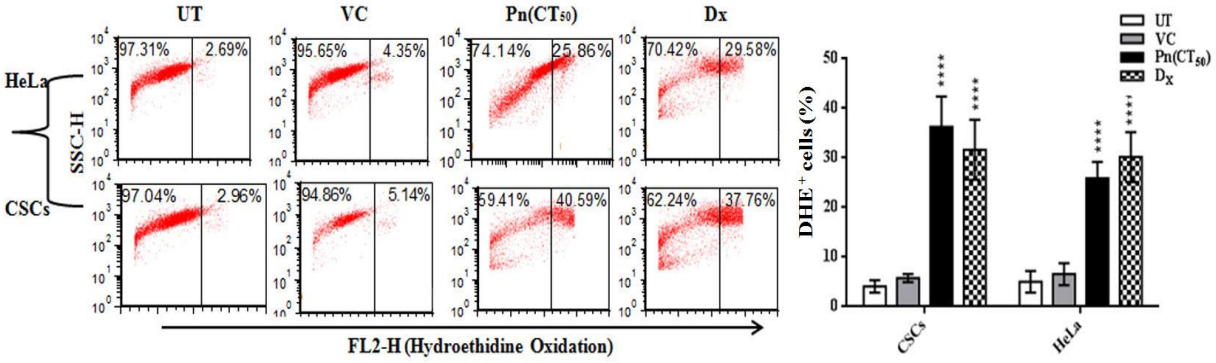

Figure 4.2.13. Representative flow cytometric analysis showing oxidation of hydroethidine (HE) by ROS in pinostrobin treated HeLa cells and CSCs. Doxorubicin treatment also showed significance red fluorescence in treated cells. Vehicle treated and doxorubicin (10 µM) treated cells were included as negative and positive controls. Bar diagram represents mean ±S.D. of three analyses performed in triplicates. Significance difference *(p value*) of all treated groups is calculated using ordinary two-way ANOVA (Dunette's multiple comparison test) with respect to vehicle control (VC) cells. ****, *p≤0.001*.

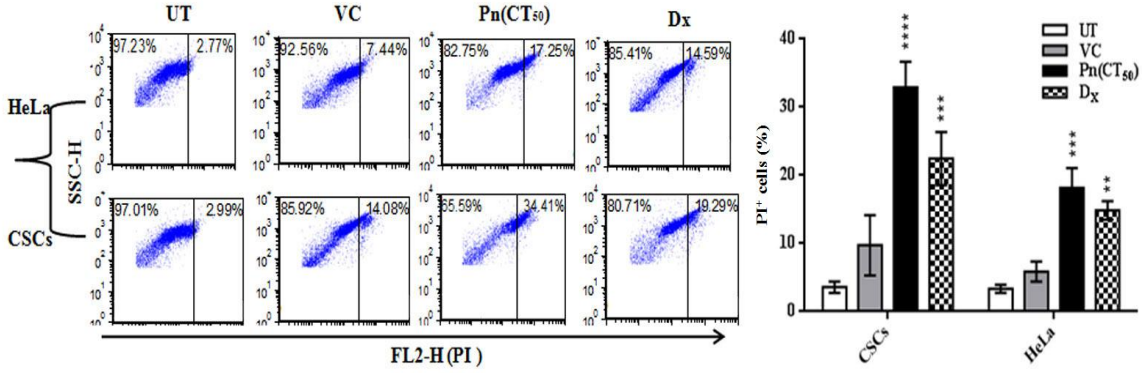

Figure 4.2.14. Representation of DNA fragmentation using PI staining and analyzed in pinostrobin treated HeLa cells and CSCs by flow cytometric analysis. The fluorescence events of PI were analysed by FCS Express v5software. Vehicle treated and doxorubicin (10 µM)treated cells were included as negative and positive controls.Bar diagram represents mean ±S.D. of three analyses performed in triplicates. Significance difference *(p value*) of all treated groups is calculated using ordinary two-way ANOVA (Dunette's multiple comparison test) with respect to vehicle control (VC) cells. **, *p≤ 0.01;* ***, *p≤0.005*; ****, *p≤0.001*.

Chapter 4.3

In-vivo anti-tumor activity of pinostrobin

.

Antitumor activity of pinostrobin against Ehrlich ascites carcinoma (EAC) in Swiss albino mice was evaluated using diverse parameters such as EAC cell viability, tumor volume reduction, survival period, mean survival time (MST) and percentage of ILS (increase of life span %). EAC cells, a transplantable, poorly differentiated and fast growing malignant tumor cells is derived from breast carcinoma of mice, were used for tumor formation.

4.3.1. EAC tumor cell viability analysis

Antitumor activity of pinostrobin was evaluated in ehrlich ascites carcinoma (2×10^6/mice) bearing swiss albino mice. Trypan blue dye was used that specifically stains only dead cells and excludes by live cells. Total viable EAC cell count was calculated after and before pinostrobin treatment at the end of the experiment. A single dose of pinostrobin was administrated to mice at 4^{th} days prior i.e. pre-treatment (Gp I) and after 4 days i.e. inoculation of tumor inducing EAC cells (Gp II) and on every 4 alternate day till 12 day (Gp III) (Figure 4.3.1). Viable cell counts were reduced to 254×10^4 cell/ml, $p\leq0.001$) in pre-treatment group (Gp I) and 243×10^4 cell/ml ($p\leq0.001$) in post pinostrobin(20 mg/kg b wt.) treated group(Gp II) compared to vehicle control group ~550-556×10^6 cell/ml. Results showed a maximum reduction in viable cell counts in Gp III followed by Gp I and Gp II, compared to respective vehicle treated control group. Repeated pinostrobin administration at 5 mg/kg b wt., 10 mg/kg b wt. and 20 mg/kg b wt. on every 4^{th} day till 12 day (Gp III) after EAC cells inoculation, resulted in very low number of viable EAC cell (166×10^4 cell/ml, $p\leq0.001$) and cells count decreased in dose dependent manner compared to vehicle control (543×10^4 cell/ml) (Figure 4.3.1). Pinostrobin at 2.5 mg/kg b wt. showed negligible reduction in viable EAC cell count.

4.3.2 Tumor volume analysis

Antitumor activity of pinostrobin was evaluated by measuring the tumor volume in EAC swiss albino mice model. We evaluated the effect of pinostrobin (10 mg/kg b wt.) administered by different routes i.e. intraperitoneal (IP) and intratumoral (IT) route at different time intervals (i.e. day 4, 8, 12, 16 post tumor formation) in EAC mice model on reduction of tumor volume.

In pinostrobin pre-treatment (single dose, 10 mg/kg b wt.) significantly delayed tumor development compared to vehicle control group (Figure 4.3.2 A&B) was observed. Tumor volume was significantly reduced (1.51 cm^3, $p\leq0.005$) till day 12 in intratumoral (IT) route of

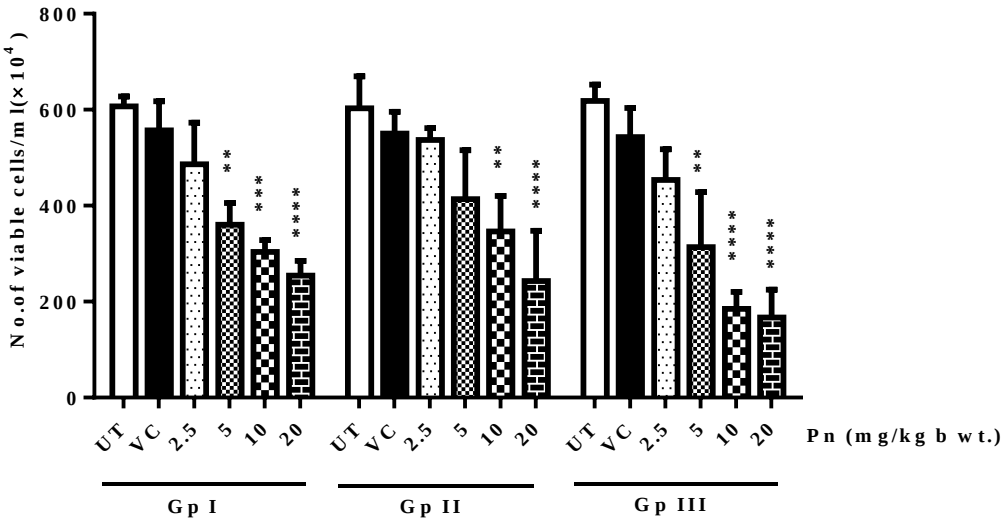

Figure 4.3.1. Effect of different doses of pinostrobin on number of viable cells at 4th dpi i.e. pre-treatment (GpI), 4th days after EAC cells inoculation i.e post-treatment (Gp II) and on every 4 alternate day till 12th day (Gp III) after EAC cells inoculation. Total numbers of viable cells were expressed as $\times 10^4$ cell/ml. Bar diagram represents mean ±S.D. of three analyses performed in triplicates. Significance difference *(p value*) of all treated groups is calculated using ordinary two-way ANOVA (Dunette's multiple comparison test) with respect to vehicle control cells. dpi: days prior to inoculation. UT: Untreated, VC: Vehicle control, Pn: Pinostrobin, Gp: Group. **, *p≤ 0.01;* ***, *p≤0.005*; ****, *p≤0.001*.

pinostrobin administered group (Figure 4.3.2A) as compared to vehicle treated group(2.46 cm^3). However, intraperitoneal (IP) pinostrobin pretreated mice reduced the tumor size (1.72 cm^3 , *p≤0.05*) in comparison to vehicle treated group (2.4 cm^3) (Figure 4.3.2 B). We found pinostrobin treatment on tumor development was more effective by intratumoral (IT) route as compared to intraperitonial (IP) route at day 4th and day 8th (Figure 4.3.2 A & B). Doxorubicin included as positive control for tumor growth inhibition also showed significant reduction in tumor volume as compared to vehicle treated group.

Similarly, pinostrobin multiple dose treatment (multiple dose: 10 mg/kg b wt. at every 4th day till 12th days) was administered to tumor bearing mice via IT and IP routes. The tumor volume was 0.599 cm^3 (*p≤0.001*) on 12th day and was found to be effectively reduced in IT administered pinostrobin multiple-treatment group after EAC cell inoculation (Figure 4.3.3 A), as compared to vehicle (2.97 cm^3) treated group. IP-administered multiple pinostrobin doses treatment reduced the tumor volume to 1.00 cm^3 (*p≤0.001*) as compared to vehicle (2.78cm^3) treated group. (Figure 4.3.3 B). As expected, doxorubicin included as positive control for tumor growth also showed significant reduction in tumor volume as compared to vehicle treated group.

Pinostrobin post-treatment groups were administered with a single dose of pinostrobin (10 mg/kg b wt) to tumor bearing mice via IT and IP routes after EAC inoculation. The tumor volume was significantly reduced and was determined to be 1.91 cm^3 (*$p \leq 0.05$) on 12^{th} day in IT pinostrobin post-treatment group (Figure 4.3.4A) as compared to vehicle (2.9 cm^3) treated group. IP-administered pinostrobin post-treatment reduced tumor volume to 2.1 cm^3 ($p \leq 0.05$) as compared to vehicle treated group (3.1cm^3) (Figure 4.3.4 B). Like other parameters, doxorubicin treatment resulted in significant reduction in tumor volume as compared to vehicle treated group.

As evident from these data, reduction in the tumor volume was greater in IT-administered pinostrobin treated groups compared to IP- administered pinostrobin treated group (Figure 4.3.2A, 4.3.3A & 4.3.4A). In the present study, a well-known anti-proliferating agent doxorubicin was used as a positive control, which also showed significant reduction in the tumor volume as compared to respective vehicle control groups.

4.3.5 Survival studies

The reliable criterion for assessing an anticancer drug is to determine the prolongation of lifespan of the animal. The lifespan of mice was studied at various dose of pinostrobin (2.5, 5, 10 and 20 mg/kg b wt) administration on every 4^{th} day till 12^{th} days. Treatment-dose specific survival curves were computed by the Kaplan–Meier method. Intratumoral pinostrobin treated animals showed higher survival rate as compared to control group. Survival period was noted in pinostrobin treated mice at different doses and observed survival rate till 22 days after administration of 20 mg/kg b wt pinostrobin, while in vehicle treated mice survived till 30 days. The lower concentration of pinostrobin (2.5 and 5 mg/kg b wt.) is not efficient enough to reduce the tumor volume for longer time period and treated mice survived till 33^{th} and 38^{th} days (Figure 4.3.5 A, B). In case of untreated group mice died in early 28^{th} days. The rate of survival of tumor bearing mice was expanded till 44^{th} days after intratumoral administration of pinostrobin (10 mg/kg b wt.) on every 4^{th} alternate day till 12^{th} days (Figure 4.3.5 C).

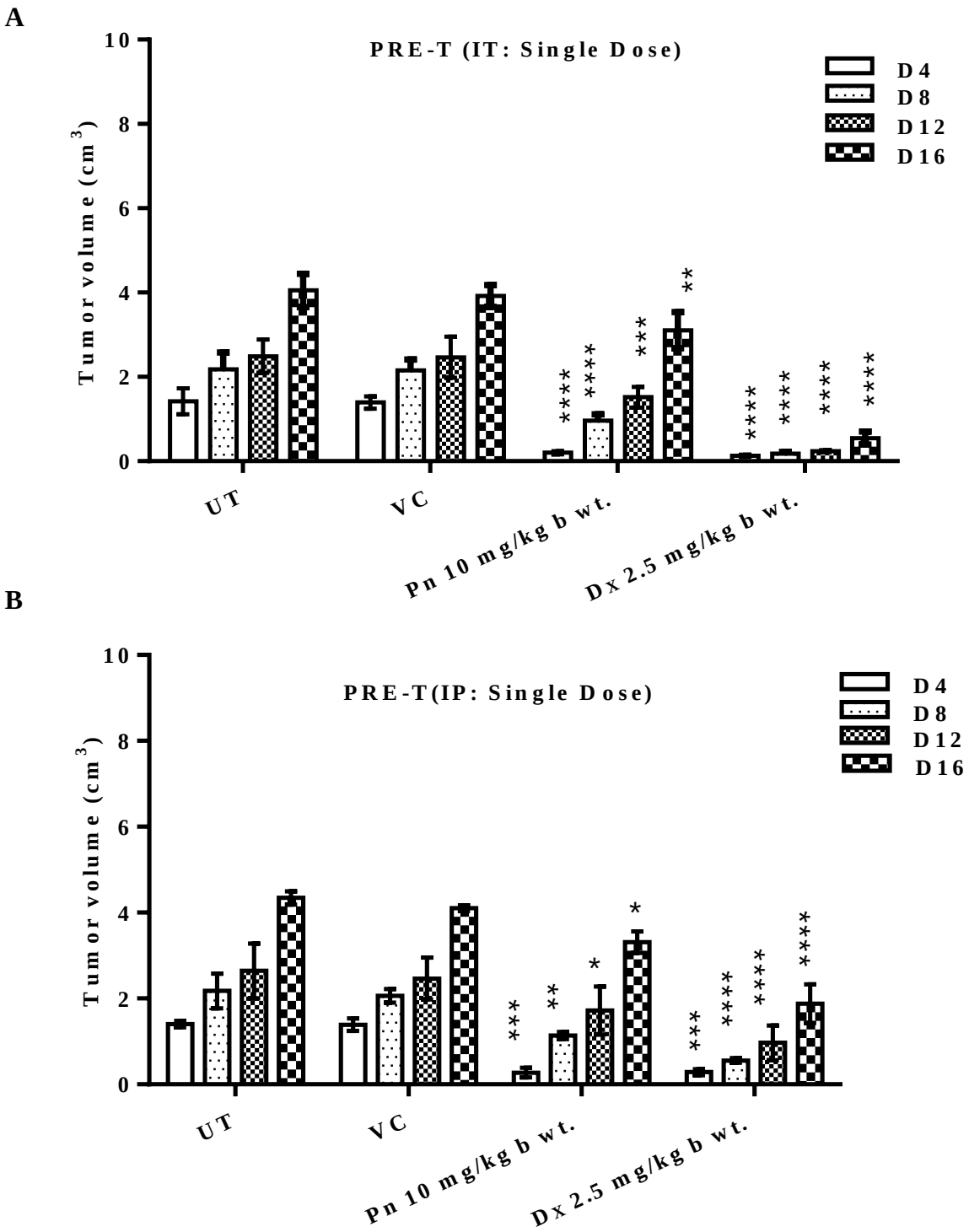

Figure 4.3.2. Effect of pinostrobin (pre-treatment- 4th dpi) on tumor volume. Pinostrobin was administered by different routes i.e. IT (A) & IP (B) to examine tumor volume (cm^3) in EAC swiss albino animal model. Bar diagram represents mean ±S.D. of three analyses performed in triplicates. Significance difference *(p value*) of all treated groups is calculated using ordinary two-way ANOVA (Dunette's multiple comparison test) with respect to vehicle control cells. dpi: days prior to EAC inoculation, UT: Untreated, VC: Vehicle control, Pn: Pinostrobin, Dx: Doxurubicin, IP: intraperitoneal, IT: intratumoral, T: Treatment, D: Days. *, *p≤ 0.05; **, p≤ 0.01; ***, p≤0.005*; ****, *p≤0.001*.

.

A

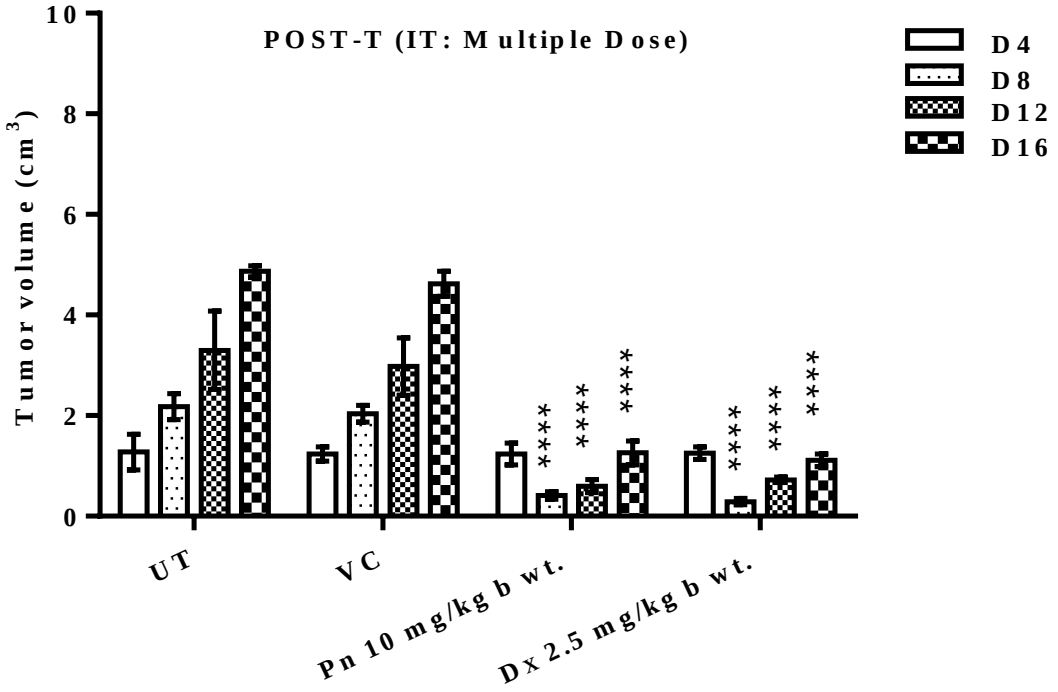

B

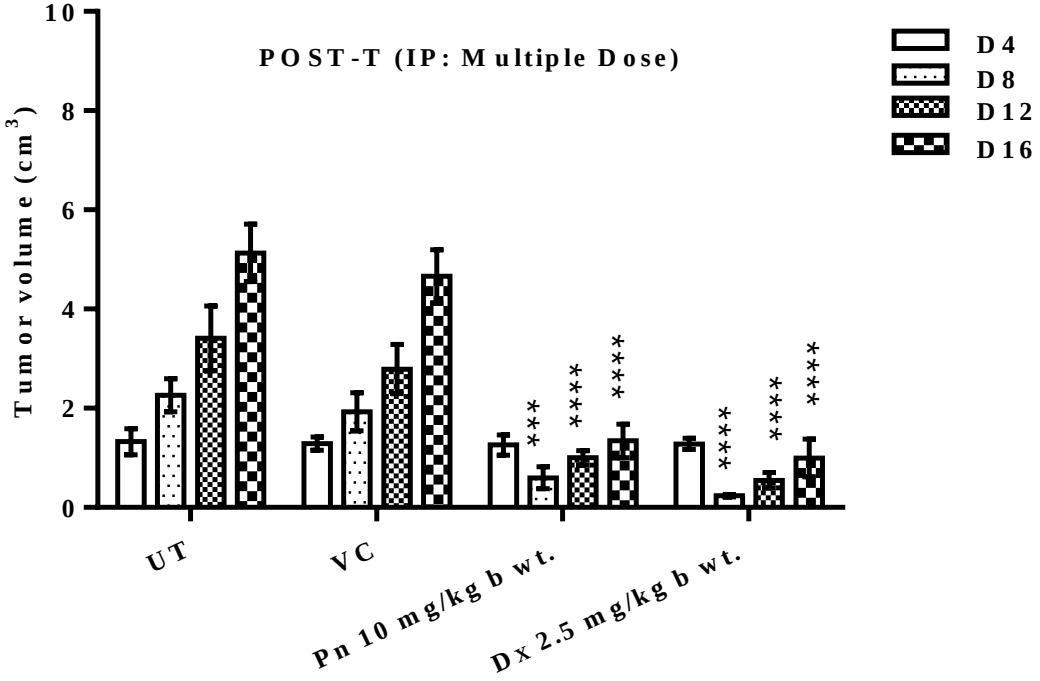

Figure 4.3.3. Effect of pinostrobin post treatment (multiple dose) on tumor volume. Pinostrobin was administered by different routes i.e. IT (A) & IP (B) at each 4th alternate day till 12th day to examine tumor volume (cm^3) in EAC swiss albino animal model. Bar diagram represents mean ±S.D. of three analyses performed in triplicates. Significance difference *(p value*) of all treated groups is calculated using ordinary two-way ANOVA (Dunette's multiple comparison test) with respect to vehicle control cells. UT: Untreated, VC: Vehicle control, Pn: Pinostrobin, Dx: Doxurubicin, IP: intraperitoneal, IT: intratumoral, T: Treatment, D: Days. ***, *p≤0.005*; ****, *p≤0.001*.

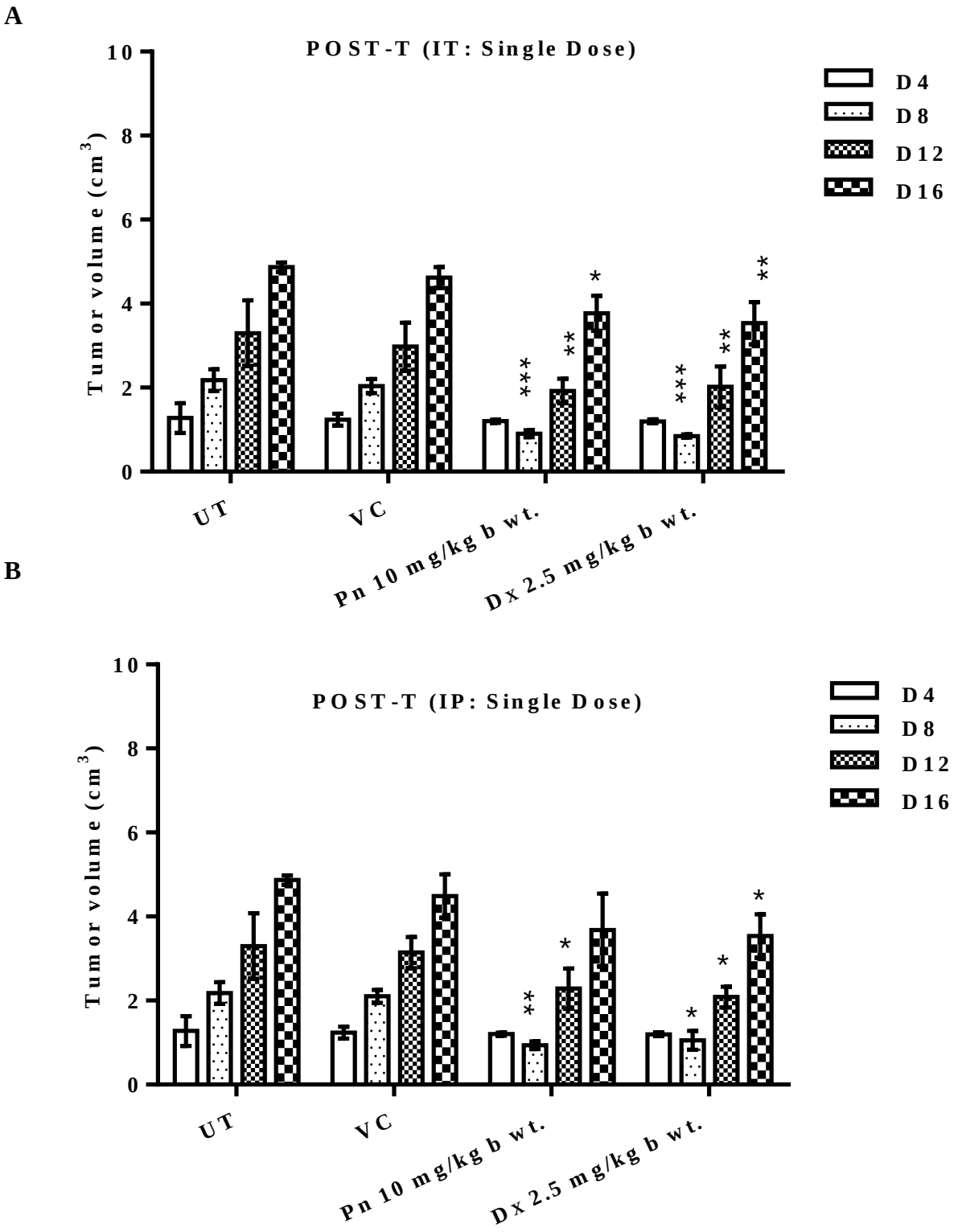

Figure 4.3.4. Effect of pinostrobin post treatment (single dose) on tumor volume. Pinostrobin was administered by different routes i.e. IT (A) & IP (B) at 4th day after EAC inoculation to examine tumor volume (cm^3) in EAC swiss albino animal model. Bar diagram represents mean ±S.D. of three analyses performed in triplicates. Significance difference *(p value*) of all treated groups is calculated using ordinary two-way ANOVA (Dunette's multiple comparison test) with respect to vehicle control cells. UT: Untreated, VC: Vehicle control, Pn: Pinostrobin, Dx: Doxurubicin, IP: intraperitoneal, IT: intratumoral, T: Treatment, D: Days.*, *p≤ 0.05; **, p≤ 0.01; ***, p≤0.005.*

4.3.6. MST and ILP studies

Furthermore, median survival time (MST) and percentage increase life- span (ILS) were also analyzed of tumor bearing mice. The median survival time was found to be increased to 27.5, 31.5 and 34.5 on administration of 2.5, 5, and 10 mg/kg b wt. pinostrobin on every 4^{th} days till 12^{th} days, respectively, while median survival time decreased as 18.5 on administration of higher dose of pinostrobin (P_n-20 mg/kg b wt.). Similarly, ILS was evaluated after intratumoral pinostrobin (2.5, 5, 10, and 20 mg/kg b wt.) administration and established 27.90%, 46.51%, 60.46 % and -13.95% life- span of tumor bearing mice. Thus, pinostrobin significantly enhanced percentage increase life- span up to 60.46% (Table 4.3.1). Thus, we observed a significant increment in the lifespan of pinostrobin treated mice compared to control group of mice. This study confirmed that pinostrobin plays important role against cancer and significantly expand the lifespan of mice.

Above in-*vivo* study findings indicates that, intratumoral route administration of pinostrobin is more effective and capable of reducing viable EAC cells counts. In addition, it's how significant reduction in tumor volume and increased median survival time (MST) and percentage increase life- span (ILP).

Table 4.3.1. Effect of pinostrobin on median survival time (MST) and percentage increase life- span (ILP) of EAC tumor bearing mice

Parameters	**UT**	**VC**	**P_n** 2.5 mg/kg b wt.	**P_n** 5 mg/kg b wt.	**P_n** 10 mg/kg b wt.	**P_n** 20 mg/kg b wt.
MST	21.5	23.5	27.5	31.5	34.5	18.5
ILS (%)	-	9.30	27.90	46.51	60.46	-13.95

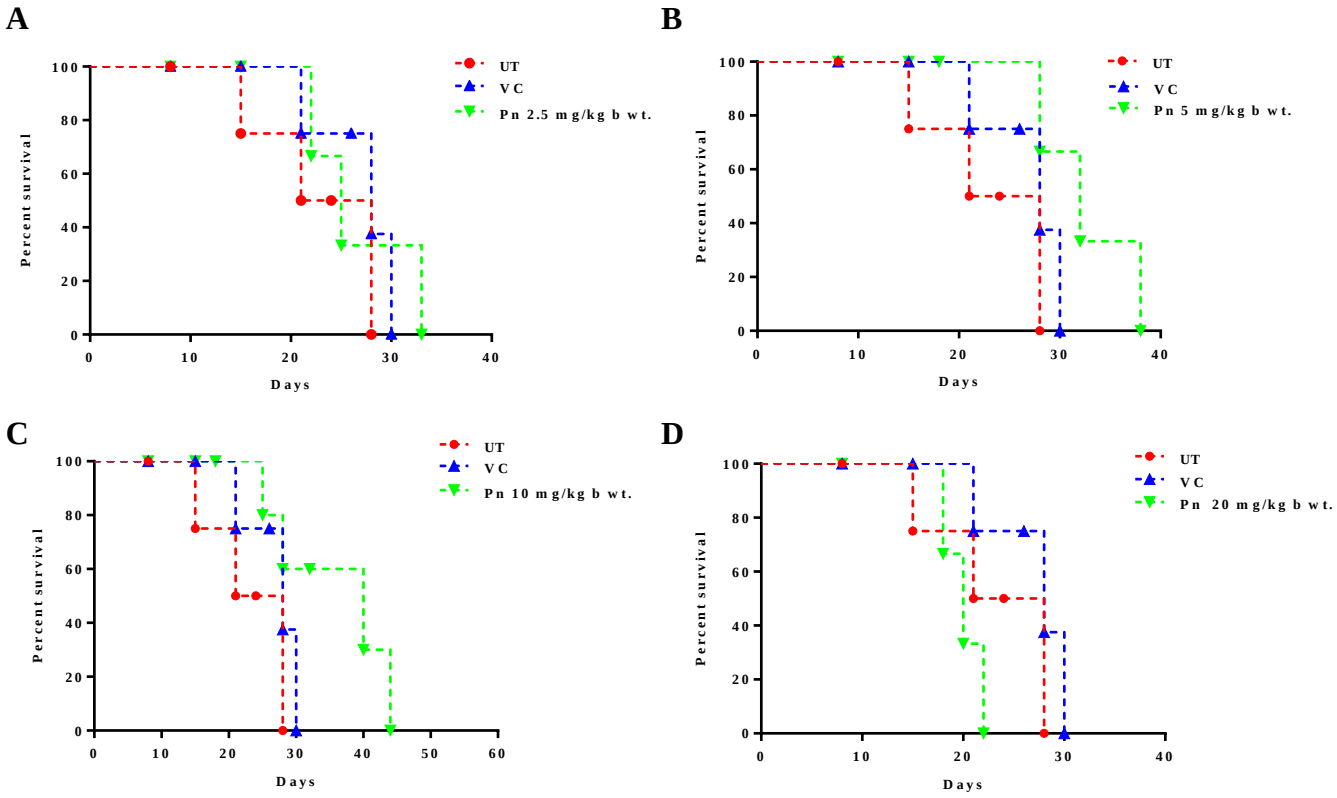

Figure 4.3.5 Kaplan-Meier survival curves of Swiss albino mice bearing the Ehrlich ascites tumor after treatment with different doses of pinostrobin.**(A)** Mice were treated with pinostrobin (2.5 mg/kg b wt.- it), **(B)** Mice were treated with pinostrobin (5 mg/kg b wt.-it), **(C)** Mice were treated with pinostrobin 10 mg/kg b wt.-it), **(D)** Mice were treated with pinostrobin (20 mg/kg b wt.-it).

Chapter 4.4

Analysis of interaction of pinostrobin with topoisomerase I and DNA and effect of pinostrobin on topoisomerase I activity: *in silico* and *in vitro* studies

Our results showed pinostrobin affected the nuclear structure and caused DNA fragmentation, and also regulated the expression of proteins that are involved in cell cycle arrest. Since replication of genetic materials is primary requirement of proliferating cancer cells, it is imperative to see if it affected DNA replication machinery in some way. Activity of topoisomerases (I and II) that are responsible for cleavage and reunion of either one or both strands of the DNA are critical for DNA replication. Of these, activity of topoisomerase I, an ATP-independent enzyme that alleviates the topological strains in DNA helix during replication, has been reported to be downregulated by chemotherapy[1]. Therefore, in the present study, we also investigated if pinostrobin is able to interact with topoisomerase I using *in silico* and *in vitro* approach and affected its activity.

4.4.1 Computational docking analysis

To assess if pinostrobin interacted with eukaryotic topoisomerase I-DNA complex, first *in silico* molecular docking studies were carried out. For this, the structures of pinostrobin (Figure 4.4.1A) was taken as the test ligand and doxorubicin (Figure 4.4.1B) was included as control ligand. While topoisomerase I-DNA complex was used as target or receptor. We used the crystal structure of topoisomerase I-DNA complex (PDB ID: 1T8I) for the study as this complex has already been evaluated for binding of camptothecin, a well known topoisomerase I inhibitor. Therefore, known binding sites for camptothecin on topoisomease I-DNA complex were used in rigid docking.

On the other hand, in order to search for perfect binding sites on the target, flexible docking was carried out in which the binding sites were not fixed and ligand structures were incorporated with all possible flexible bonds. Flexible docking was performed to determine whether the binding sites of pinostrobin at the target would be similar or different to the one used in rigid docking. Table 4.4.1 shows comparative analysis of different binding energies involved in the interaction of pinostrobin and doxorubicin with topoisomerase I-DNA complex by flexible docking.

[1] Arts, H.J., Katsaros, D., de Vries, E.G., Massobrio, M., Genta, F., Danese, S., Arisio, R., Scheper, R.J., Kool, M., Scheffer, G.L. and Willemse, P.H., 1999. Drug resistance-associated markers P-glycoprotein, multidrug resistance-associated protein 1, multidrug resistance-associated protein 2, and lung resistance protein as prognostic factors in ovarian carcinoma. Clinical Cancer Research, 5, pp.2798-2805.

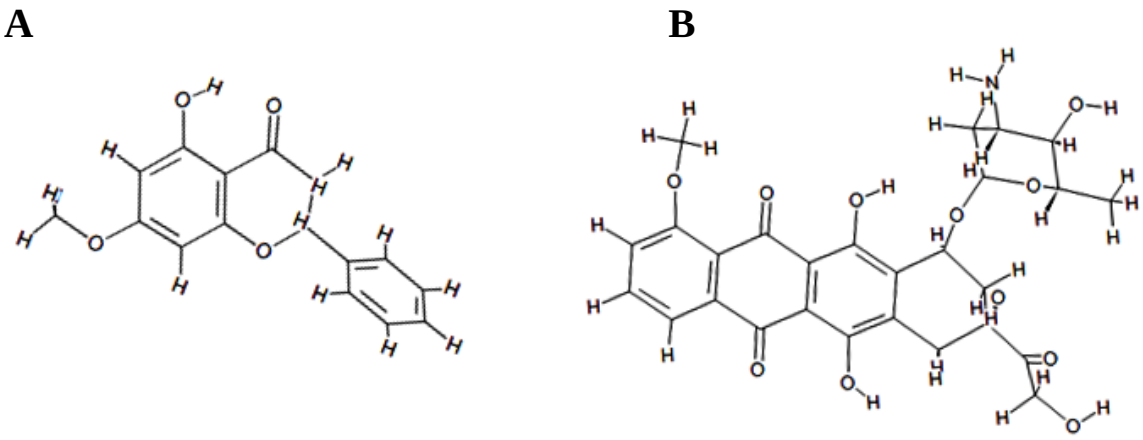

Figure 4.4.1. Structure of pinostrobin **(A)** and doxorubicin **(B)** as generated by MedChem designer program**.**

Due to rotatable bonds of the ligands that increase binding site potential, better conformations with good energy scores of docked complex were produced by flexible docking when compared to that produced by rigid docking (Table 4.4.2). It is evident from the table that flexible docking resulted in better binding energy and docking energy (E dock) for both inostrobin and doxorubicin. As low binding energy is an indication of stable and strong binding of ligand with target, the most energetically favourable docked complex (with lowest binding energy) was subsequently selected from distinct conformational clusters. The results of flexible docking of inostrobin on to the target clearly show efficient binding of inostrobin to the topoisomerase I-DNA complex.

Table 4.4.1. Automated flexible docking analysis of inostrobin and doxorubicin with topoisomerase I and DNA calculated by Auto dock 4.2 tool.

Docking scores	**Pinostrobin**	**Doxorubicin**
Ki(µM)	1.98	0.083
dG_bind	-15.67	-22.36
ΔG_{bind}(kcal/mol)	-7.78	-9.65
E_{dock}(kcal/mol)	-8.39	-13.31
ΔG_{inter}(kcal/mol)	-7.86	-10.80
ΔG_{intra}(kcal/mol)	-0.53	-2.51
ΔG_{tor}(kcal/mol)	+0.55	+3.02
Rmsd °A	33.17	34.64

Note: Ki - Inhibition Constant, **ΔG_{bind}** = min.estimated free energy of binding, **E_{dock}** = min.docked energy, **ΔG_{inter}** = Final intermolecular energy, **ΔG_{intra}** = Final internal energy of ligand, **ΔG_{tor}** = Torsional free energy.

Table 4.4.2. Comparative energies analysis of docked complex of pinostrobin and doxorubicin with topoisomerse I –DNA after rigid and flexible automated docking

Compounds	No. of atom	No. of free torsions		Min. estimated G bind(Kcal/mol)		Final E dock (Kcal/mol)	
		Rigid	Flexible	Rigid	Flexible	Rigid	Flexible
Pinostrobin	21	0	2	-7.40	-7.78	-8.01	-8.39
Doxorubicin	47	0	11	-7.72	-9.65	-11.38	-13.31

4.4.2 Interaction of pinostrobin and doxorubicin with topoisomease I-DNA complex

Identification of binding sites and analysis of binding orientation was performed on the docked complex with lowest binding energy. Pinostrobin was found to be completely embedded into the inner side of protein except its phenyl ring (Figure 4.4.2 A). The figure also shows that pinostrobin also interacted with DNA through hydrophobic interactions. The shape of binding sites on the target appeared complementary to the shape of the ligand. Hydrogen bonding of O1 atom of pinostobin with Lys 443, Asn 722 and Asp 440 residues of topoisomease I is evident from Figure 4.4.2 C. Likewise, O7 and O11 atoms of pinostrobin also formed hydrogen bonds with Lys 436 and Lys 751 residues of topoisomerase I, respectively (Figure 4.4.2 B). Besides the hydrogen bonds interaction, hydrophobic interaction between few other residues of topoisomerase I-DNA complex such as Lys 439, Pro 431, DT 9(B), Dt 10(B) and AI3 901(D) with pinostrobin (Figure 4.4.2 B) was also observed**.**

Docking study with doxorubicin revealed that Thr 718 and Asp 533 of topoisomerase I, and Dg 12(C) of DNA participated in hydrogen bonding, while Dt 10(B) and Da 113(D) of DNA were involved in hydrophobic interactions (Figure 4.4.3B &C).

4.4.3 Validation of docking, Analysis of stability of the docked complexes, Assessment of free energy of binding:

4.4.3.1 Validation of docking

For validation of docking, rescoring approach is utilized for evaluation of better interaction of the ligand and the receptor on the basis of function scores. These scoring functions are based on force fields or an empirical principle that derives from a knowledge-based approach. Consequently, Glide XP precision was used to validate docked results and performed. G-score of Glide docking is used to determine the binding affinity of ligand to receptor. Thus, more negative score value indicates strong interaction

of the ligand with receptor. Our results showed that Glide docking assigned good negative G-score to pinostrobin (− 3.91 kcal/mol). The G-score for doxorubicin, included as a positive control, was calculated to be − 4.99 kcal/mol (Table 4.4.3).

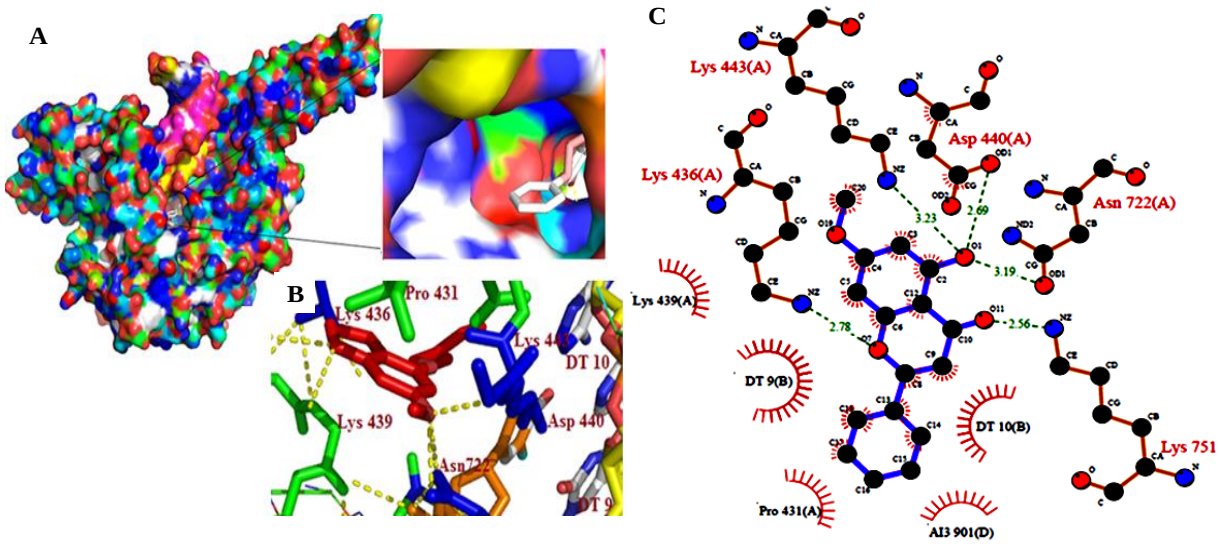

Figure 4.4.2. Connolly surface representation of pinostrobin at the binding site of topoisomerase I and DNA complex **(A).** Illustration of pinostrobin binding site and its interaction with topoisomerase I -DNA complex, Molecular docked complex of pinostrobin with topoisomerase I and DNA**(B)**. Docked complex was visualized by PyMOL viewer. Hydrogen bonds are shown by yellow dashed line. 2D schematic representation of pinostrobin interaction with topoisomerase I and DNA **(C)**. Hydrogen bonding (green dashed lines) and hydrophobic interactions (magenta arcs) among pinostrobin, topoisomerase I and DNA are analyzed by ligplot program. Radial spokes towards the ligand atoms show the hydrophobic interactions with the respective amino acid residues.

Table 4.4.3. Analysis of G Scores and the different energy components for pinostrobin and doxorubicin by Glide program

Scores	Pinostrobin	Doxorubicin
XP GScore	− 3.91	− 4.99
Glide Evdw	− 21.35	− 30.79
Glide Ecoul	− 10.05	− 16.90
Glide Emodel	− 32.85	− 55.37
Glide Energy	− 29.27	− 44.48
Glide G Score	− 3.91	− 4.99
XP H Bond	− 1.17	− 1.92

Note: XP GScore (extra precision); Glide Evdw (van der Waals energy); Glide Ecoul (Coulomb energy); Glide Emodel (Model energy); Glide Energy (Modified Coulomb-van der Waals interaction energy); Glide G Score (GlideScore); XP H Bond (Hydrogen bond). Energy values: kcal/mol.

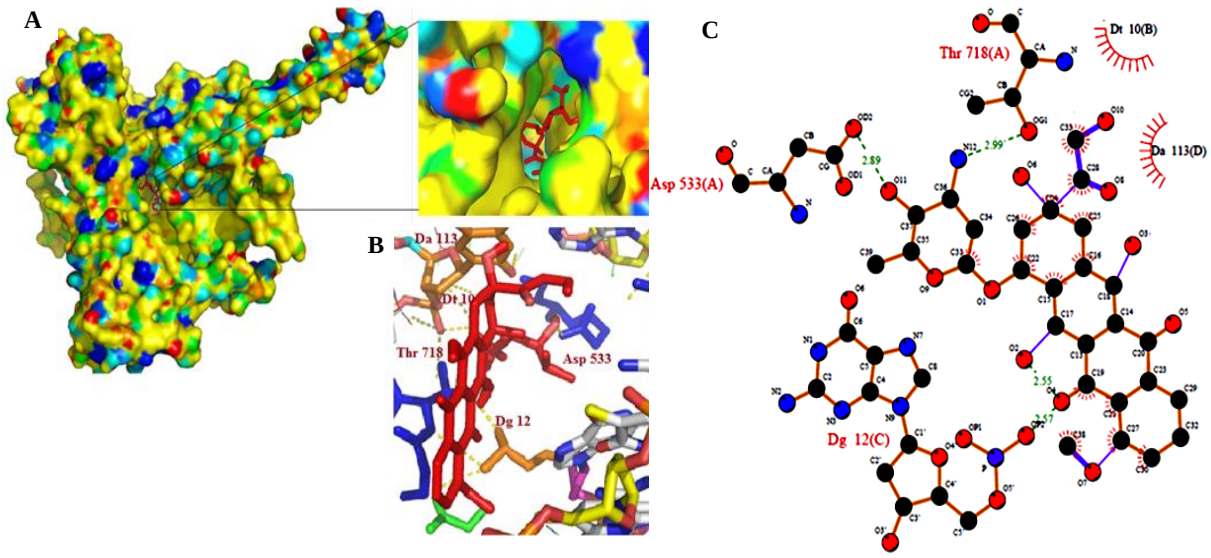

Figure 4.4.3. Connolly surface representation of doxorubicin at the binding site of topoisomerase I and DNA complex **(A).** Illustration of doxorubicin binding site and its interaction with topoisomerase I -DNA complex, Molecular docked complex of doxorubicin with topoisomerase I and DNA**(B)**. Docked complex was visualized by PyMOL viewer. Hydrogen bonds are shown by yellow dashed line. 2D schematic representation of doxorubicin interaction with topoisomerase I and DNA **(C)**. Hydrogen bonding (green dashed lines) and hydrophobic interactions (magenta arcs) among pinostrobin, topoisomerase I and DNA are analyzed by ligplot program. Radial spokes towards the ligand atoms show the hydrophobic interactions with the respective amino acid residues.

High binding energy, ki values and good docking energy indicate that potential of doxorubicin as an inhibitor of topoisomerase I (Table 4.4.1).

4.4.3.2 Analysis of stability of docked complexes

Energy minimization was performed to improve and analyze the stability of docked complexes by GROMACS, which is used for prediction of free energy, solvation and binding properties of molecules. Potential energy of pinostrobin topoisomerase I-DNA complex and doxorubicin topoisomerase I-DNA complex were found significantly low at 1000 ps. Stable complex formation of pinostrobin -topoisomerase -IDNA and doxorubicin-topoisomerase I-DNA with decreased potential energy is evident. In addition, the structural stability of the docked complex also depends on electrostatic interaction, van der Waals interactions and hydrogen bond interaction. These interactions were also evaluated by automated docking; Glide and Prime indicated good bonding interaction with better scores (Figure 4.4.1 A and B, & Tables 4.4.1 and 4.4.3). Thus, good potential energy value and other bonding interactions of docked complexes indicated that the docked complexes were thermostable.

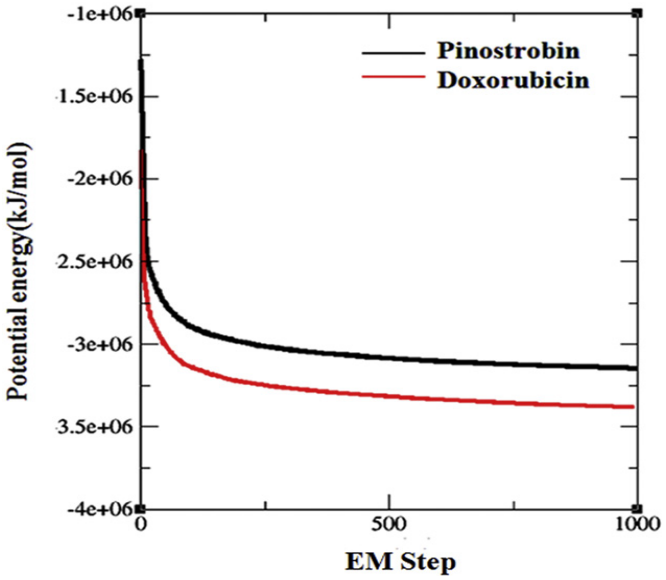

Figure 4.4.5. Representation of potential energy of pinostrobin and doxorubicin docked complex with topoisomerase I-DNA after minimization step by GROMACS.

In additional, free energy of the docked complex was calculated by Helmholtz free energy. Free energy of the pinostrobin topoisomerase I-DNA docked complex was analyzed using internal energy (− 6.85 kcal/mol) and entropy (4.58 kcal/mol/K) values at constant temperature (298.15 K) and was determined to be − 1372.37 kcal/ mol. Therefore, free energy of both docked complexes (pinostrobin topoisomerase I-DNA and doxorubicin topoisomerase I-DNA) was found to be very close by Helmholtz free energy density formulation.

4.4.3.3 Assessment of free energy of binding

For analysis of free binding energy, Molecular Mechanics/Generalized-Born/Surface Area (MM/GBSA) has used as a tool to understand and quantify the binding free energy in large biomolecular systems. As evident from Table 4.4.1, after automated flexible docking, binding free energy (ΔG binding) of the ligands pinostrobin and doxorubicin was determined to be − 7.78 and − 9.65 kcal/mol, respectively. Similarly, free energy of binding (dG_bind) of both the pinostrobin and doxorubicin were found to be significantly low (− 15.671 and − 22.363 kcal/mol, respectively,Table 4.4.1). The binding free energy (dG_bind) scores suggested that both the ligands bind strongly to the receptor (topoisomerase I-DNA) with high affinity.

4.4.4 ADMET analysis of pinostrobin and doxorubicin

Absorption, distribution, metabolism, excretion and toxicity of any drug are governed by its lipophilic and hydroophilic behaviours that measured by ADMET scores. Table 4.4.4 summarises the analysis of the ADMET scores of the test compounds used in the present study. Logarithmic values of partition coefficient P (logP) for pinostrobin and doxorubicin were found to be lower than 5 indicating their hydrophilic nature. No significant difference in the log P and log D values were found for both values of pinostrobin (logP, 3.559; log D, 3.529) and doxorubicin, (logP, 0.651; logD, 0.624) suggesting their non-acidic behaviour. Moriguchi's logP (M LogP) scores that show an inverse relation with the absorption efficiency of the compound were also determined for the test compounds. The M LogP scores for both the pinostrobin and doxorubicin were calculated to be significantly lower (Table 4.4.4), suggesting that these compounds can be easily absorbed. The TPSA score, which indicate hydrogen bonding potential of any molecule on the receptor, for pinostrobin and doxorubicin were calculated to be 55.76 and 206.07, respectively.

Table 4.4.4. ADMET analysis of pinostrobin and doxorubicin

Compounds name	S+logP	S+logD	M LogP	TPSA	M_NO	Mwt
Pinostrobin	3.559	3.529	2.48	55.760	4	270.28
Doxorubicin	0.651	0.624	-0.816	206.07	12	543.53

Note: S+ LogP (Permeability); S+ logD (Distribution); M LogP (Moriguchi octanol-water partition coefficient); TPSA (Topological polar surface area); M_NO (Total number of nitrogen and oxygen atoms); Mwt (Molecular weight).

4.4.5 Assessment of pinostrobin binding to DNA

Ethidium bromide displacement assay was performed to demonstrate interaction of pinostrobin with DNA and its binding affinity. Ethidium bromide (EtBr) intercalation into DNA causes it to fluoresce. Binding of any compound with DNA may affect EtBr binding, resulting in its displacement and reduction of fluorescence intensity. Fluorescence spectra of EtBr-DNA showed maximum emission at 620 nm. A concentration dependent reduction in fluorescence intensity of EtBr-DNA was observed when the assay was performed in the presence of different concentrations of pinostrobin (50, 100 and 200 µM), when compared to the fluorescence of control DNA-EtBr or vehicle control reaction resulted in (Figure 4.4.8). These data suggest that pinostrobin is

able to bind to the DNA resulting in displacement of EtBr from the DNA. Thus, binary complex formation between pinostrobin and DNA could interfere with the topoisomerase I activity.

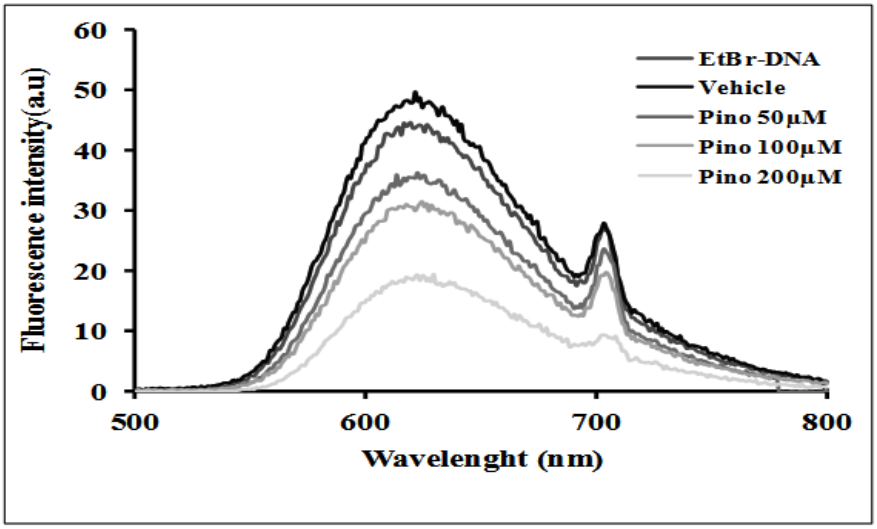

Figure 4.4.8. Effect of pinostrobin on fluorescence emission spectra of EtBr-DNA. Plasmid pBSK$^+$ DNA (6 nM) and ethidium bromide (0.5µg/µl) were incubated in the presence of different concentrations of pinostrobin (Pino) for 30 min at 25 ºC. Fluorescence spectra recorded in the wavelength range 500 nm to 800 nm are shown. Vehicle control was incubated with corresponding volume of the pinstrobin solvent i.e. triple solvent(TS-vehicle).

4.4.6 Pinostrobin interaction with topoisomerase I and DNA analysis

Pinostrobin is a naturally fluorescent compound which showed emission maxima at 428 nm and 527 nm, and produced blue and green florescence upon excitation at 280 nm. Binding of pinostrobin with the topoisomerase I and DNA was assessed individually by fluorescence spectroscopy by measuring its emission spectra. Fluorescence emission spectra of pinostrobin in the presence or absence of topoisomease I is shown in Figure 4.4.9A. As evident from the figure, a decrease in the fluorescence intensity without any shift in the emission maxima was observed in the presence of 1 unit of topoisomerase I when compared to the buffer control (pinostrobin alone incubated with 1×PBS). These data clearly demonstrate that pinostrobin indeed interacts with topoisomerase I.

Pinostrobin-DNA interaction was also analyzed similarly and validated by fluorescence spectroscopy. An increase in the fluorescence intensity of the pinostrobin with a blue shift in the emission maxima was observed in the presence of DNA, clearly indicating its interaction with DNA (Figure 4.4.9B). The observed shift and increased intensity may be due to the intercalation of pinostrobin with DNA in the immediate hydrophobic

environment of DNA. Some changes was observed in intensity of fluorescence emission maxima when the analysis was carried out in the presence of doxorubicin, suggesting that doxorubicin was also capable to bind DNA and topoisomease I individually. No change in the intensity and emission maxima was observed in the control. These results further confirm ethidium bromide displacement assay results and establish that pinostrobin is able to interact with topoisomere I as well as DNA independently.

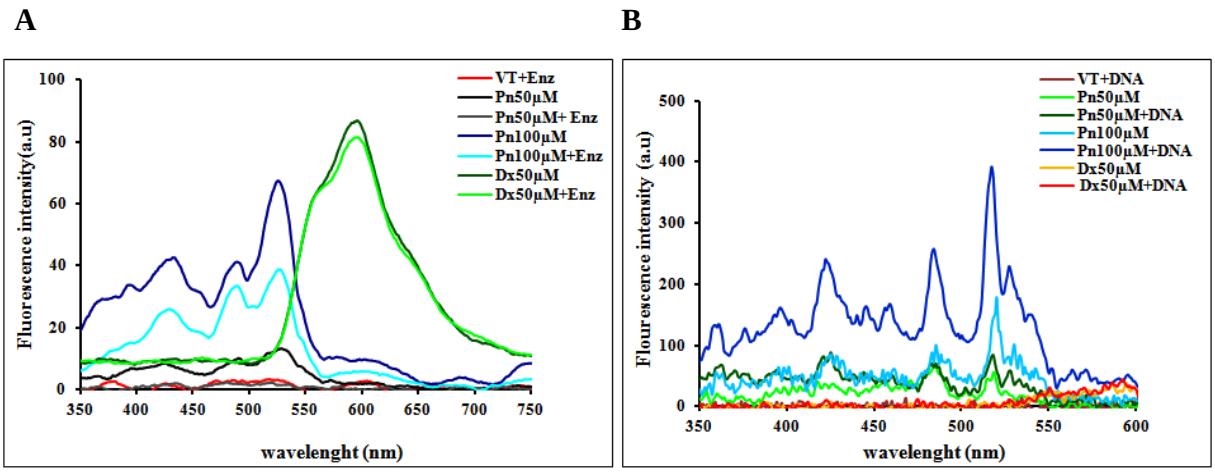

Figure 4.4.9. Fluorescence spectroscopic analysis to elucidate interaction of pinostrobin with topoisomease I (A) and DNA (B). Flourescence spectra (350 nm to 750 nm) of pinostrobin were recorded in the absence or presence of either 1 unit of toposiomerase I or 6 nM of plasmid pBSK$^+$ DNA. Analysis performed in the presence of doxorubicin was included as control. VT, Vehicle treated; Pn. Pinostrobin; Dx, Doxorubucin; Enz, topoisomease I.

4.4.7 Inhibition of topoisomerase I activity by pinostrobin

After carrying out *in silico* docking of pinostrobin on to topoisomerase I-DNA complex (1T8I) and spectroscopic interaction studies and demonstrating *in vitro* binding of pinostrobin with the topoisomerase I and DNA, pinostrobin's about to inhibit topoisomerase I activity was investigated by an *in vitro* topoisomerase I relaxation assay (Figure 4.4.10). Since the nuclear extract of Ca Ski cells used as source of topoisomerases in the assay contained both topoisomerase I and topoisomerase II, we excluded ATP, absolutely essential for topoisomerase II activity, from the assay mixture. The results of such an assay clearly show that treatment of DNA with Ca Ski cells nuclear extract resulted in conversion of supercoiled form (SF) to relaxed from (NF/RF) (Figure 4.4.10 , lane 2) when compared to untreated DNA sample (lane 1). An increase in the supercoiled form of plasmid DNA was observed with an increase in pinostrobin concentration (50 µM to 400 µM) in the reaction mix (Figure 4.4.10, lanes 3-7), in comparison to control reaction (Figure 4.4.10, lane 2). These results clearly demonstrated

inhibition of nicking activity of topoisomerase I by pinostrobin, thus leading to higher proportion of positively supercoiled DNA. When direct interaction of DNA with pinostrobin (400µM) was checked in the absence of nuclear extracts (Figure 4.4.10, lane 12), very minimal increase in the proportion of relaxed from was observed (in comparison to control). This could be due to its binding or intercalation of pinostrobin with the DNA. Predominantly relaxed form of the DNA was observed, when the topoisomerase activity assay was carried out in the presence of doxorubicin (50µM to 300µM, lanes 8-11, respectively), suggesting that doxorubicin could not inhibit nicking activity of topoisomerase I, while it inhibited resealing activity of topoisomerase I, as evidenced by the presence of NF/RF forms (Figure 4.4.10, lanes 8-11). The DNA could possibly not be resealed due to doxorubicin binding onto DNA and formation of ternary complex between doxorubicin, DNA, and topoisomerase I. Thus, results of *in silico* analysis of pinostrobin-topoisomerase I-DNA interaction have been validated by experi
mental evidence and suggested its inhibitory action against topoisomerase I.

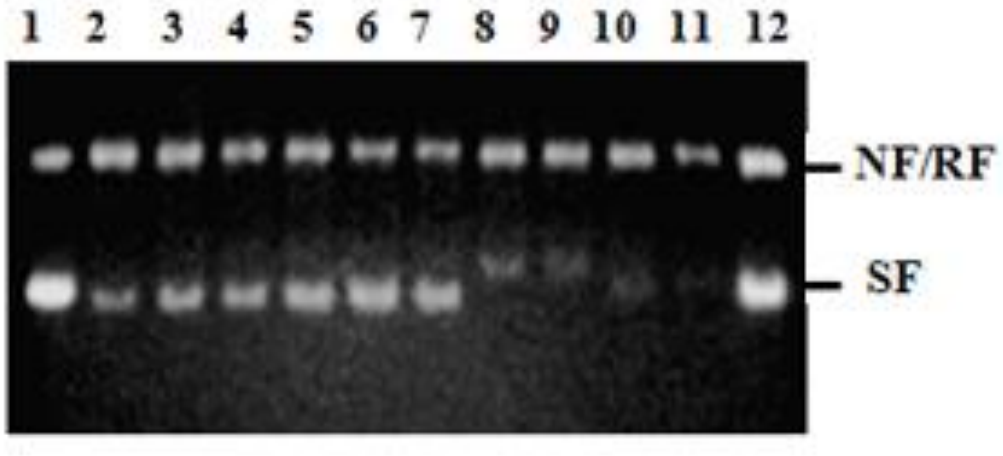

Figure 4.4.10. Topoisomerase relaxation assay. Inhibition of catalytic activity of topoisomerase I in Ca Ski cells nuclear extract by pinostrobin was assessed *in vitro*. Lanes 1 and 2 show $pBSK^+$ DNA (3 µg) and $pBSK^+$ DNA incubated with nuclear extract (1.5µg protein), respectively. Lanes 3-7 show topoisomerase I relaxation assay carried out using $pBSK^+$ DNA (3µg) and nuclear extract (1.5 µg protein) in the presence of different concentrations of pinostrobin (50, 100, 200, 300, 400 µM, respectively). Lanes 8-11 show topoisomerase I relaxation assay carried out using $pBSK^+$ DNA (3µg) and nuclear extract (1.5 µg protein) in the presence of different concentrations of doxorubicin (50, 100, 200, 300 µM, respectively). Lane 12 shows $pBSK^+$ DNA in the presence of pinostrobin (400 µM) without any nuclear extract. Samples were analysed on 1 % agarose gel. NF, RF and SF indicate nicked, relaxed and supercoiled forms of the plasmid DNA.

Chapter 5

Discussion

In recent years, naturally occurring compounds have gained an immense interest as promising chemotherapeutic agent for the treatment of cancer and its recurrence. These included different classes of photochemical such as flavonoids, alkonoids and aromatic isothiocyanates. These compounds raise the cancer therapy to a new level of success by reducing the side effects of conventional therapies and improving the effectiveness of existing treatments[1,2]. Keeping the empirical knowledge and epidemiological studies relating higher incidence of cancer with certain types of diet, considerable attention has been given to medicinal plants and dietary compounds that possibly prevent and cure the cancer[3,4].

A large number of epidemiological studies have been conducted to prove the long-term consumption of fruits and vegetables rich diet reduces the risk of various types of cancer[5]. Flavonoids are one of the most effective phytochemical that are found as secondary metabolites in dietary components of human[6,7]. Flavanoids exhibit a remarkable spectrum of biological activities including antioxidant, anti-inflammatory, antiviral and anticancer properties[8]. The reduction of cancer growth by flavonoids could occur due to suppression, blockage, and inactivation of various signalling molecules[9,10]. In addition, a large number of flavonoids have been reported to inhibit cancer growth by induction of apoptosis[11]. However, exact mechanisms by which many of the flavonoids exert their anticancer activity are yet to be elucidated.

Pinostrobin, is an unique natural occurring compound used as diet supplement of human, and extracted from plants and honey[12,13]. Pinostrobin has been attributed for various

[1]Meijerman, I., Beijnen, J.H. and Schellens, J.H., 2006. Herb-drug interactions in oncology: focus on mechanisms of induction. The Oncologist, 11, pp.742-752.
[2]Adams, M. and Jewell, A.P., 2007. The use of complementary and alternative medicine by cancer patients. In International Seminars in Surgical Oncology, 4, pp. 1-10.
[3]Kaur, R., Kapoor, K. and Kaur, H., 2011. Plants as a source of anticancer agents. J Nat Prod Plant Resour, 1, pp.119-124.
[4]Syed, D.N., Suh, Y., Afaq, F. and Mukhtar, H., 2008. Dietary agents for chemoprevention of prostate cancer. Cancer Letters, 265, pp.167-176.
[5]Riboli, E. and Norat, T., 2003. Epidemiologic evidence of the protective effect of fruit and vegetables on cancer risk. The American Journal of Clinical Nutrition, 78, pp.559S-569S.
[6]Xiao, Z.P., Peng, Z.Y., Peng, M.J., Yan, W.B., Ouyang, Y.Z. and Zhu, H.L., 2011. Flavonoids health benefits and their molecular mechanism. Mini Reviews in Medicinal Chemistry, 11, pp.169-177.
[7]Kumar, S. and Pandey, A.K., 2013. Chemistry and biological activities of flavonoids: an overview. The Scientific World Journal, 2013,pp.1-16.
[8]Karimi, E., Oskoueian, E., Hendra, R., Oskoueian, A. and Jaafar, H.Z., 2012. Phenolic compounds characterization and biological activities of citrus aurantium bloom. Molecules, 17, pp.1203-1218.
[9]Wang, H., Zhang, X., Liu, Y., Ni, Z., Lin, Y., Duan, Z., Shi, Y., Wang, G. and Li, F., 2016. Downregulated miR-31 level associates with poor prognosis of gastric cancer and its restoration suppresses tumor cell malignant phenotypes by inhibiting E2F2. Oncotarget, 7, pp. 36577–36589.
[10]Bellazzo, A., Di Minin, G. and Collavin, L., 2017. Block one, unleash a hundred. Mechanisms of DAB2IP inactivation in cancer. Cell Death & Differentiation, 24, pp.15-25.
[11]Ranganathan, S., Halagowder, D. and Sivasithambaram, N.D., 2015. Quercetin suppresses twist to induce apoptosis in MCF-7 breast cancer cells. PloS One, 10, p.e0141370.
[12]Xian, Y.F., Ip, S.P., Lin, Z.X., Mao, Q.Q., Su, Z.R. and Lai, X.P., 2012. Protective effects of pinostrobin on β-amyloid-induced neurotoxicity in PC12 cells. Cellular and Molecular Neurobiology, 32, pp.1223-1230.

pharmacological activities of different plants[14,15], and is known to inhibit a number of enzymes activity[16,17,18,19]. Anticancer activity of pinostrobin has also been reported *in vitro* in few cell lines[16, 17, 20, 21, 22, 23, 24]. Based on these reports, pinostrobin holds promise as potential cure for cancer and needs further investigations to understand its mechanism of action, to demonstrate its anticancer activity *in vivo*, and also for complete avoidance of recurrence, its effect on Cancer Stem like Cells (CSCs).

The present study was therefore undertaken to address few of these questions. As evident from the results, pinostrobin demonstrated dose dependent growth inhibition of different types of cancer cells *in vitro* without showing any cytotoxicity on normal human cells. HL-60 and HeLa cells were found to be relatively more sensitive cells with CT_{50} values of ~10 µM and 50 µM, respectively when compared to Ca Ski, SiHa and A549 cells with CT_{50} values between 75,100 and100 µM. The cytotoxic dose of pinostrobin for these cancer cell lines especially HL60 and HeLa cells is much lower than that reported by other investigators[18,19]. Magnitude of cell growth inhibition by pinostrobin in terms of percentage of cytotoxicity was comparable with that of well known anti-cancer agent doxorubicin though at higher concentrations. Since pinostrobin is a constituent of many foods consumed daily, its effective higher concentrations are not likely to have adverse effect. Thus, preliminary cell proliferation experiment clearly demonstrated that

[13]Fahey, J.W. and Stephenson, K.K., 2002. Pinostrobin from honey and Thai ginger (*Boesenbergia pandurata*): a potent flavonoid inducer of mammalian phase 2 chemoprotective and antioxidant enzymes. Journal of Agricultural and Food Chemistry, 50, pp.7472-7476.

[14]Hooper, L., Kroon, P.A., Rimm, E.B., Cohn, J.S., Harvey, I., Le Cornu, K.A., Ryder, J.J., Hall, W.L. and Cassidy, A., 2008. Flavonoids, flavonoid-rich foods, and cardiovascular risk: a meta-analysis of randomized controlled trials. The American Journal of Clinical Nutrition, 88, pp.38-50.

[15]Wu, N., Kong, Y., Zu, Y., Fu, Y., Liu, Z., Meng, R., Liu, X. and Efferth, T., 2011. Activity investigation of pinostrobin towards herpes simplex virus-1 as determined by atomic force microscopy. Phytomedicine, 18, pp.110-118.

[16]Le Bail, J.C., Aubourg, L. and Habrioux, G., 2000. Effects of pinostrobin on estrogen metabolism and estrogen receptor transactivation. Cancer Letters, 156, pp.37-44.

[17]Abd El-Hady, F.K., Shaker, K.H., Imhoff, J.F., Zinecker, H., Salah, N.M. and Ibrahim, A.M., 2013. Bioactive metabolites from propolis inhibit superoxide anion radical, acetylcholinesterase and phosphodiesterase (PDE4). International Journal of Pharmaceutical Sciences Review and Research, 21, pp.338-344.

[18]Siekmann, T.R.L., Burgazli, K.M., Bobrich, M.A., Nöll, G. and Erdogan, A., 2013. The antiproliferative effect of pinostrobin on human umbilical vein endothelial cells (HUVEC). European Review for Medical and Pharmacological Sciences, 17, pp.668-672.

[19]Brunskole, M., Zorko, K., Kerbler, V., Martens, S., Stojan, J., Gobec, S. and Rižner, T.L., 2009. Trihydroxynaphthalene reductase of *Curvularia lunata*—A target for flavonoid action?. Chemico-Biological Interactions, 178, pp.259-267.

[20]Darwanto, A., Tanjung, M. and Darmadi, M.O., 2000. Cytotoxic mechanism of flavonoid from Temu Kunci (*Kaempferia pandurata*) in cell culture of human mammary carcinoma. Clinical Hemorheology and Microcirculation, 23, pp.185-190.

[21]Haddad, A.Q., Venkateswaran, V., Viswanathan, L., Teahan, S.J., Fleshner, N.E. and Klotz, L.H., 2006. Novel antiproliferative flavonoids induce cell cycle arrest in human prostate cancer cell lines. Prostate Cancer and Prostatic Diseases, 9, pp.68-76.

[22]Cao, X.D., Ding 1, Z.S., Jiang, F.S., Ding, X.H., Chen, J.Z., Chen, S.H. and Lv, G.Y., 2012. Antitumor constituents from the leaves of *Carya cathayensis*. Natural Product Research, 26, pp.2089-2094.

[23]Kuete, V., Nkuete, A.H., Mbaveng, A.T., Wiench, B., Wabo, H.K., Tane, P. and Efferth, T., 2014. Cytotoxicity and modes of action of 4′-hydroxy-2′, 6′-dimethoxychalcone and other flavonoids toward drug-sensitive and multidrug-resistant cancer cell lines. Phytomedicine, 21, pp.1651-1657.

[24]Ashidi, J.S., Houghton, P.J., Hylands, P.J. and Efferth, T., 2010. Ethnobotanical survey and cytotoxicity testing of plants of South-western Nigeria used to treat cancer, with isolation of cytotoxic constituents from *Cajanus cajan Millsp.* leaves. Journal of Ethnopharmacology, 128, pp.501-512.

pinostrobin was cytotoxic to cancer cells only without having any adverse effect to normal cells, thus suggesting it to be an ideal potential anti-proliferative agent.

Since different cancer cells used in the study showed different CT_{50} values, further investigations were carried out using specific CT_{50} concentrations of pinostrobin for the respective cell lines. After spectrophotometric analysis of cell viability/cell death, effect of pinostrobin on the morphology of the cells was examined to see the mode of cell death i.e. apoptosis or necrosis. These findings indicated that both pinostrobin and doxorubicin-treated cancer cells showed typical morphological features of apoptosis such as reduction in cell volume, cell shrinkage, low confluency of cell, nucleus condensation, DNA fragmentation, alteration in membrane symmetry, membrane blebbing and apoptotic bodies formation[25,26]. These appearances in the pinostrobin-treated cancer cells are clear evidence of induction of pinostrobin-induced apoptosis. Pinostrobin was solubilised in triple solvent (TS-vehicle), therefore it was imperative to assess that the observed morphological changes associated with apoptosis are not caused by this. Our results clearly confirm that the observed effect is due to pinostrobin only as the vehicle treated cells did not show any modification in the cells' morphology and showed confluent monolayer cells even after 48 h or treatment. Thus, lack of toxicity without any changes in normal cell structure and architecture by pinostrobin is an early indication that it may possess a very good safety profile.

During apoptosis, phosphatidylserine is externalized from inner side to outer side of cells and bind to Annexin V-FITC. In the present study, morphological changes indicative of pinostrobin-induced apoptosis are consistent with an increase in number of apoptotic cells following pinostrobin-treatment of the cells as determined by Annexin V-FITC staining. These results suggested that pinostrobin did affect cell membrane architecture and its integrity which could ultimately lead to cell death. Similar results have been obtained with another dietary flavanoid, fisetin, treatment with which resulted in loss of membrane integrity in osteocarcinoma cells[27].

[25]Ashkenazi, A., 2008. Targeting the extrinsic apoptosis pathway in cancer. Cytokine & Growth Factor Reviews, 19, pp.325-331.
[26]Hong, G.W., Hong, S.L., Lee, G.S., Yaacob, H. and Malek, S.N.A., 2016. Non-aqueous extracts of *Curcuma mangga* rhizomes induced cell death in human colorectal adenocarcinoma cell line (HT29) via induction of apoptosis and cell cycle arrest at G 0/G 1 phase. Asian Pacific Journal of Tropical Medicine, 9, pp.8-18.
[27]Li, J.M., Li, W.Y., Huang, M.Y. and Zhang, X.Q., 2015. Fisetin, a dietary flavonoid induces apoptosis via modulating the MAPK and PI3K/Akt signalling pathways in human osteosarcoma (U-2 OS) cells. Bangladesh Journal of Pharmacology, 10, pp.820-829.

Role of mitochondria in apoptosis is well established[28] and disruption of active mitochondrial function is one of the earliest signature events that occur during early stages of apoptosis[29].These include changes in mitochondrial membrane potential as well as alteration in oxidation-reduction potential. Deeper examination of morphological changes in cell organelles such as mitochondria, nucleus and cells membrane structure by electron microscopic tomography of pinostrobin and doxorubicin treated cells revealed remodelling of inner mitochondrial membrane, vesiculation and swelling in mitochondrial matrix compared to untreated and vehicle treated cells. The disruption of the mitochondrial membrane integrity could be due to the loss of its membrane potential, one of the indicators of early events of apoptosis[30]. It is well established that the changes in the mitochondrial potential arise due to opening of the mitochondrial permeability transition pores. This ultimately leads to disturbance in ionic equilibration due to passage of small molecules and ions through these pores, ultimately triggering the release of cytochrome c in the cytosol[31,32] and mediating apoptosis through either activation of caspase cascade or intrinsic apoptosis pathway[29,30]. The disruption of mitochondrial integrity in pinostrobin-treated cells is well correlated with the decrease in the mitochondria membrane potential following pinostrobin exposure of different cancer cells as evidenced by decrease in the ratio of red to green fluorescence of JC-1 dye[33]. Pinostrobin-treated cells showed high green fluorescence events of JC-1 monomer with low mitochondria membrane potential ($\Delta\psi$m) or depolarized mitochondria membrane potential, while untreated and vehicle treated cells illustrated high mitochondria membrane potential with intense increase of red fluorescence events. High JC-1 monomer formation has earlier been reported in human glioblastoma T98G and U87MG treated cells with flavonoids but not in human normal astrocytes[34]. Our results are also in agreement with those of Yong and Malek who reported

[28]van Loo, G., Saelens, X., Van Gurp, M., MacFarlane, M., Martin, S.J. and Vandenabeele, P., 2002. The role of mitochondrial factors in apoptosis: a russian roulette with more than one bullet. Cell Death and Differentiation, 9, pp. 1031 -1042.

[29]Qi, F., Li, A., Zhao, L., Xu, H., Inagaki, Y., Wang, D., Cui, X., Gao, B., Kokudo, N., Nakata, M. and Tang, W., 2010. Cinobufacini, an aqueous extract from *Bufo bufo gargarizans Cantor*, induces apoptosis through a mitochondria-mediated pathway in human hepatocellular carcinoma cells. Journal of Ethnopharmacology, 128, pp.654-661.

[30]Evans, V.G., 1993. Multiple pathways to apoptosis. Cell Biology International, 17, pp.461-476.

[31]Sun, M.G., Williams, J., Munoz-Pinedo, C., Perkins, G.A., Brown, J.M., Ellisman, M.H., Green, D.R. and Frey, T.G., 2007. Correlated three-dimensional light and electron microscopy reveals transformation of mitochondria during apoptosis. Nature Cell Biology, 9, pp.1057-1065.

[32]Goldstein, J.C., Munoz-Pinedo, C., Ricci, J.E., Adams, S.R., Kelekar, A., Schuler, M., Tsien, R.Y. and Green, D.R., 2005. Cytochrome c is released in a single step during apoptosis. Cell Death & Differentiation, 12, pp.453-462.

[33]Priyadarsini, R.V., Murugan, R.S., Maitreyi, S., Ramalingam, K., Karunagaran, D. and Nagini, S., 2010. The flavonoid quercetin induces cell cycle arrest and mitochondria-mediated apoptosis in human cervical cancer (HeLa) cells through p53 induction and NF-κ B inhibition. European Journal of Pharmacology, 649, pp.84-91.

[34]Das, A., Banik, N.L. and Ray, S.K., 2010. Flavonoids activated caspases for apoptosis in human glioblastoma T98G and U87MG cells but not in human normal astrocytes. Cancer, 116, pp.164-176.

comparable increase in JC-1 monomer formation in a Ca Ski cells treated with Xanthohumol followed by apoptosis[35]. It is well established that loss in mitochondrial membrane potential is directly associated with mitochondrial dysfunction which ultimately, after the release of cytochrome c into the cytosol, initiates apoptosis by activation of caspase cascade[36,37]. Thus, the observed loss of mitochondrial membrane potential in pinostrobin-treated cancer cells indicates mitochondrial dysfunction and disturbance in mitochondrial integrity is consistent with increase in apoptotic cell count (Annexin-V staining), TEM analysis and live cell imaging study.

Beside the caspases, another group of pro-apoptotic proteins such as AIF, endonuclease G and CAD also induce apoptosis. These proteins are released from mitochondria, translocate into nucleus and cause DNA fragmentation of around 50–300 kb size and condensation of peripheral nuclear chromatin that lead to cell death[38]. Earlier studies by Yong and Malek have demonstrated that xanthohumol, a phytochemical present in female flowers of *Humulus lupulus* and its flavanone derivatives induced DNA fragmentation, cell cycle arrest at S phase and inhibited growth of Ca Ski cervical cancer cells through induction of apoptosis[35]. Other natural compounds, particularly polyphenolic flavonoids and certain alkaloids have also been reported to induce cell death through apoptosis process in malignant cancer cells[39,40]. In line with these reports and the apparent morphological changes observed in the present study, induced by pinostrobin, also a flavanoid, TUNEL assay established DNA fragmentation in pinostrobin treated cells. Absence of any or negligible fragmentation in control cells clearly indicated that the event is specifically induced by pinostrobin. Significant reduction of DNA fragmentation in the pinostrobin-treated cells in the presence of apoptosis inhibitor (Z-DEVD-FMK-Caspase-3 inhibitor) further confirmed apoptosis inducing potential of pinostrobin. Reduction in the rate or extent of DNA fragmentation in the presence of the apoptosis inhibitor could be

[35]Yong, W.K. and Abd Malek, S.N., 2015. Xanthohumol induces growth inhibition and apoptosis in ca ski human cervical cancer cells. Evidence-Based Complementary and Alternative Medicine, 2015, pp. 1-10.

[36]Han, J., Goldstein, L.A., Gastman, B.R. and Rabinowich, H., 2006. Interrelated roles for Mcl-1 and BIM in regulation of TRAIL-mediated mitochondrial apoptosis. Journal of Biological Chemistry, 281, pp.10153-10163.

[37]Kroemer, G., Galluzzi, L. and Brenner, C., 2007. Mitochondrial membrane permeabilization in cell death. Physiological Reviews, 87, pp.99-163.

[38]Joza, N., Susin, S.A., Daugas, E., Stanford, W.L., Cho, S.K., Li, C.Y., Sasaki, T., Elia, A.J., Cheng, H.Y.M., Ravagnan, L. and Ferri, K.F., 2001. Essential role of the mitochondrial apoptosis-inducing factor in programmed cell death. Nature, 410, pp.549-554.

[39]Yakovlev, A.G., Wang, G., Stoica, B.A., Boulares, H.A., Spoonde, A.Y., Yoshihara, K. and Smulson, M.E., 2000. A role of the Ca2+/Mg2+-dependent endonuclease in apoptosis and its inhibition by poly (ADP-ribose) polymerase. Journal of Biological Chemistry, 275, pp.21302-21308.

[40]Millimouno, F.M., Dong, J., Yang, L., Li, J. and Li, X., 2014. Targeting apoptosis pathways in cancer and perspectives with natural compounds from mother nature. Cancer Prevention Research,10, pp.1-27.

due to inhibition of Ca^{+2}/Mg^{+2} dependent endonucleases that digest chromatin between the nucleosomes[39].

Many chemotherapeutic agents exert their anti-cancer effect through ROS generation[41,42]. ROS production by different chemicals has been directly associated with disruption of mitochondrial membrane potential and activation of apoptotic caspases[43,44,45]. Generally, ROS are generated by endogenous and exogenous agents such as hydroxyl radical, singlet oxygen peroxyl redicals, hydrogen peroxide and superoxide anions and induce apoptosis[46]. Therefore, we assessed if pinostrobin could induce ROS production in cancer cells using DCFH-DA staining. In the presence of reactive oxygen species, non-polar DCFH-DA is oxidised into highly fluorescence dichlorofluorescein (DCF)[47]. A significant increase in DCF fluorescence in pinostrobin-treated cells clearly demonstrates generation of ROS by pinostrobin. Thus, high ROS production in pinostrobin-treated cells correlates well with the decreased mitochondria membrane potential and subsequent increase in apoptosis. Li *et al*., (2015) have also demonstrated an increase in ROS levels by fisetin leading to apoptosis in osteocarcinoma cells[27]. Similarly, Zhang *et al*., (2015) has demonstrated isoliensinine induced apoptosis in triple-negative human breast cancer cells through ROS generation[48]. Thus, our results on pinostrobin-induced ROS generation and oxidative stress are in line with these reports for induction of apoptosis by damaging mitochondrial membrane[36,37].

Both ROS production and depletion of intracellular antioxidant enzymes have been attributed for apoptosis induction[49]. To establish if generation of ROS by pinostrobin is also accompanied by reduction in antioxidant enzymes, GSH levels in pinostrobin-treated cells were estimated. Intracellular GSH was found to be significantly reduced in

[41]Fruehauf, J.P. and Meyskens, F.L., 2007. Reactive oxygen species: a breath of life or death?. Clinical Cancer Research, 13, pp.789-794.
[42]Trachootham, D., Alexandre, J. and Huang, P., 2009. Targeting cancer cells by ROS-mediated mechanisms: a radical therapeutic approach?. Nature Reviews Drug Discovery, 8, pp.579-591.
[43]Zhang, L., Yu, J., Park, B.H., Kinzler, K.W. and Vogelstein, B., 2000. Role of BAX in the apoptotic response to anticancer agents. Science, 290, pp.989-992.
[44]Raza, H., John, A. and Benedict, S., 2011. Acetylsalicylic acid-induced oxidative stress, cell cycle arrest, apoptosis and mitochondrial dysfunction in human hepatoma HepG2 cells. European Journal of Pharmacology, 668, pp.15-24.
[45]Sena, L.A. and Chandel, N.S., 2012. Physiological roles of mitochondrial reactive oxygen species. Molecular cell, 48, pp.158-167.
[46]Bhattacharyya, A., Chattopadhyay, R., Mitra, S. and Crowe, S.E., 2014. Oxidative stress: an essential factor in the pathogenesis of gastrointestinal mucosal diseases. Physiological Reviews, 94, pp.329-354.
[47]Halliwell, B. and Whiteman, M., 2004. Measuring reactive species and oxidative damage *in vivo* and in cell culture: how should you do it and what do the results mean?. British Journal of Pharmacology, 142, pp.231-255.
[48]Zhang, X., Wang, X., Wu, T., Li, B., Liu, T., Wang, R., Liu, Q., Liu, Z., Gong, Y. and Shao, C., 2015. Isoliensinine induces apoptosis in triple-negative human breast cancer cells through ROS generation and p38 MAPK/JNK activation. Scientific Reports, 5, pp.1-13.
[49]Buttke, T.M. and Sandstrom, P.A., 1994. Oxidative stress as a mediator of apoptosis. Immunology Today, 15, pp.7-10.

pinostrobin-treated cell when compared to vehicle treated and untreated cells. This depletion of GSH levels could be due to higher production of ROS. Moreover, GSH plays major role in protection against oxidative stress. Thus, depletion of GSH could enhance the susceptibility of oxidative stress caused by ROS, ultimately facilitating cell death[50]. We also checked the levels of nitric oxide (NO), a short-lived, endogenously signalling molecule that plays important role in tumor progression, angiogenesis and metastasis[51], In addition, NO actively involved in cancer progression by activating oncogenes, inhibiting the action of tumor suppressor enzyme and DNA repair enzyme and apoptosis process[52]. In pinostrobin-treated cells, reductions in NO levels at different time post-treatment further demonstrate anti-tumorigenic effect of pinostrobin. Vijaya *et al*., have also reported reduction of NO and induction of apoptosis in HepG2 cells after exposure of ginger extract, of which pinostrobin is a major constituent[50].

After confirming the ROS production by pinostrobin, the site of ROS production was monitored by one of the most common dye 10-NAO. 10-NAO binds to mitochondria-specific cardiolipin and forms a complex. However, in presence of ROS, cardiolipin is oxidized and lost its binding affinity with10-NAO. This depletion of binding affinity of cardiolipin and 10-NAO is determined by its fluorescence events that reflects oxidation rate of intracellular cardiolipin[53]. Our results clearly show that 10-NAO lost its binding affinity with cardiolipin and the fluorescence events of 10- NAO was found lower in pinostrobin treated cancer cells compared to vehicle treated and non-cancerous cells, which would be directly related with the loss of binding affinity and oxidation of cardiolipin. These data clearly suggested that pinostrobin induced ROS production in mitochondria. Earlier studies highlight the ROS production mediates apoptosis through intrinsic or mitochondrial pathway[54,55]. Thus, pinostrobin could induce apoptosis through intrinsic or mitochondrial pathway. We also analyzed if ROS affected cellular targets or components using HE staining. Our results on HE/DHE staining further confirm ROS

[50]Vijaya Padma, V., Arul Diana Christie, S. and Ramkuma, K.M., 2007. Induction of apoptosis by ginger in HEp-2 cell line is mediated by reactive oxygen species. Basic & Clinical Pharmacology & Toxicology, 100, pp.302-307.
[51]Choudhari, S.K., Chaudhary, M., Bagde, S., Gadbail, A.R. and Joshi, V., 2013. Nitric oxide and cancer: a review. World Journal of Surgical Oncology, 11, pp.1-11.
[52]Vahora, H., Khan, M.A., Alalami, U. and Hussain, A., 2016. The potential role of nitric oxide in halting cancer progression through chemoprevention. Journal of Cancer Prevention, 21, pp.1-12.
[53]Verfaillie, T., Rubio, N., Garg, A.D., Bultynck, G., Rizzuto, R., Decuypere, J.P., Piette, J., Linehan, C., Gupta, S., Samali, A. and Agostinis, P., 2012. PERK is required at the ER-mitochondrial contact sites to convey apoptosis after ROS-based ER stress. Cell Death & Differentiation, 19, pp.1880-1891.
[54]Jang, Y.J., Won, J.H., Back, M.J., Fu, Z., Jang, J.M., Ha, H.C., Hong, S., Chang, M. and Kim, D.K., 2015. Paraquat induces apoptosis through a mitochondria-dependent pathway in RAW264.7 cells. Biomolecules & Therapeutics, 23, pp.407-413.
[55]Circu, M.L. and Aw, T.Y., 2010. Reactive oxygen species, cellular redox systems, and apoptosis. Free Radical Biology and Medicine, 48, pp.749-762.

generation by pinostrobin. HE dye is oxidized to ethidium bromide in the presence of superoxide anions and intercalates into DNA to produce red fluorescence. Increase in red fluorescence in HE-stained cells exposed to pinostrobin in comparison to vehicle treated cells further confirm pinostrobin-induced ROS production and oxidative stress that further led to DNA fragmentation. An increase in the number of stained nuclei clearly indicated damaged nuclear membrane in pinostrobin-treated cells which directly correlated with increased pinostrobin-induced ROS production. Likewise, Xanthohumol caused DNA fragmentation through ROS production and induced cell death, this finding supports our outcomes[35]. Nucleus morphology was also visualized using Hoechst 33342 stain that exhibited remarkable changes as stained, condensed and fragmented nuclei in pinostrobin-treated cells thus confirming earlier results. Our results are also supported by the findings of Yong and Malek who demonstrated that xanthohumol induced apoptosis in Ca Ski cells by modulating the cellular structure and signalling activity of cells[35].

During mitochondria mediate apoptosis, disturbances in mitochondrial function lead to activation of caspase-9, reduction in its membrane potential and cleavage of Bcl-2 protein. Our initial findings on induction of apoptosis by ROS production and disruption of mitochondrial membrane potential prompted us to assess activation of caspase cascade and analyse possible pathway by expression analysis of different proteins involved using human apoptosis protein profile array. Increased expression of Smac/DIABLO, HtrA2/Omi and cytochrome c expression levels in pinostrobin treated cells were observed when compared to vehicle treated cells. These mitochondrial proteins [second mitochondria-derived activator of caspases (Smac/DIABLO), HtrA2/Omi and cytochrome c] are released from mitochondria to cytosol in response to stress and induce apoptosis[56] . Released cytochrome c forms a complex with Apaf-1 and caspase-9 to activate caspase cascade in the presence of ATP and trigger apoptosis[57]. Activation of caspase 9 and caspase 8 suggest that both extrinsic and intrinsic pathways are involved that ultimately lead to activation of caspase 3- the key executional caspase. Thus, an increase expression of these proteins reconfirms apoptosis inducing potential of pinostrobin. Activation of caspases, procaspase-3 and procaspase-7, that are produced as proenzymes leads to their cleavage to active caspase-3 and caspase-7 which then actively participate in initiation and

[56]Saelens, X., Festjens, N., Walle, L.V., Van Gurp, M., van Loo, G. and Vandenabeele, P., 2004. Toxic proteins released from mitochondria in cell death. Oncogene, 23, pp.2861-2874.
[57]Rodriguez, J. and Lazebnik, Y., 1999. Caspase-9 and APAF-1 form an active holoenzyme. Genes & Development, 13, pp.3179-3184.

execution of apoptosis[58]. Activation of caspase 3 has also been reported by other flavonoids that caused cell death in cancer cells by induction of apoptosis[59]. Thus, observed increase in caspase-3 (key executional caspase) expression in pinostrobin treated cells further confirm apoptosis mediated cell death.

In addition, levels of some other pro-apoptotic BCl-2 family proteins such as Bad and Bax were also found to be elevated highly expressed in pinostrobin treated cells. These proteins form pores in the outer mitochondrial membrane and stimulate apoptosis, while the anti-apoptotic proteins including Bcl-2 and Bcl-xL inhibit pore formation[60]. Jürgensmeier *et al*., has reported the overexpression of bax accountable for the release of cytochrome c[61]. Thus, the expression analysis of different proteins involved in apoptosis indicated that pinostrobin induced apoptosis in the tested cancer cells not only by activation of caspases but also modulating the expression of apoptotic proteins. Such induction of apoptosis through mitochondrial as well as intrinsic pathway has also been reported for other flavonoids[55] and resveratrol[62].

Expression analysis also indicated involvement of extrinsic pathway of apoptosis in pinostrobin-treated cells as increased levels of TRAIL R1/D4, TRAIL R2/D5, TNFα , Fas and FADD were observed in some of the pinostrobin treated cancer cells at 48 h in comparison to vehicle treated cells. TRAIL (tumor necrosis factor–related apoptosis inducing ligand) is one of the members of the tumor necrosis factor (TNF) gene superfamily. It actively binds to death receptors DR4 (TRAIL-R1) and DR5 (TRAIL-R2) and triggers apoptosis[63]. During TRAIL interaction with DR4 and DR5, adapter proteins FADD, procaspase-8 or procaspase-10 are required to form a death-inducing signalling complex (DISC) and trigger death signalling pathway[64]. Earlier studies have established that TNF (Apo-2L) binds to death receptors DRs (4 and 5) and induces transducing death signal for cell death[65]. Likewise, we also observed an increase in TNFR1 and Fas at 48 h

[58]Elmore, S., 2007. Apoptosis: a review of programmed cell death. Toxicologic Pathology, 35, pp.495-516.
[59]Li, J., Zhang, F. and Wang, S., 2014. A polysaccharide from pomegranate peels induces the apoptosis of human osteosarcoma cells via the mitochondrial apoptotic pathway. Tumor Biology, 35, pp 7475–7482.
[60]Gross, A., Yin, X.M., Wang, K., Wei, M.C., Jockel, J., Milliman, C., Erdjument-Bromage, H., Tempst, P. and Korsmeyer, S.J., 1999. Caspase cleaved BID targets mitochondria and is required for cytochrome c release, while BCL-XL prevents this release but not tumor necrosis factor-R1/Fas death. Journal of Biological Chemistry, 274, pp.1156-1163
[61]Jürgensmeier, J.M., Xie, Z., Deveraux, Q., Ellerby, L., Bredesen, D. and Reed, J.C., 1998. Bax directly induces release of cytochrome c from isolated mitochondria. Proceedings of the National Academy of Sciences, 95, pp.4997-5002.
[62]Mahyar-Roemer, M., Köhler, H. and Roemer, K., 2002. Role of Bax in resveratrol-induced apoptosis of colorectal carcinoma cells. BMC Cancer, 2, pp.1-9.
[63]Fossati, S., Ghiso, J. and Rostagno, A., 2012. TRAIL death receptors DR4 and DR5 mediate cerebral microvascular endothelial cell apoptosis induced by oligomeric Alzheimer's Aβ . Cell death & Disease, 3, pp.1-12.
[64]Riley, J.S., Malik, A., Holohan, C. and Longley, D.B., 2015. DED or alive: assembly and regulation of the death effector domain complexes. Cell death & Disease, 6, pp.1-16.
[65]LeBlanc, H.N. and Ashkenazi, A., 2003. Apo2L/TRAIL and its death and decoy receptors. Cell Death & Differentiation, 10, pp.66-75.

of the treated cells. Increased TNF levels are likely to effectively bind to TRAIL-R1 and TRAIL-R2 and induce cell death. Apoptosis through extrinsic pathway has also been reported in HeLa cells[66].

Further, pinostrobin-treated cancer cells also showed an augmented expression of phosphorylated p53 in HeLa and Ca Ski cells. Role of p53, a tumor suppressor protein in regulation of apoptosis is well established[67]. It is demonstrated that p53 induces the cell cycle arrest in response to DNA damage in G1 phase[68]. The p53 stimulates transcription of cyclin dependent kinase (Cdk) inhibitory protein p21 and inhibition of these kinase lead to cell death[69]. Similarly, p27 inhibitory protein arrests cell cycle in G1 phase via a complex formation with cyclin E/cdk2 and A/cdk2[70]. Our results clearly demonstrate that activation of p53 did indeed result in enhanced expression of these two proteins i.e. p21 and p27 which could have arrested the cell cycle in G1 phase and thus controlled proliferation of treated cells. Thus, an overview of the protein expression profile provides evidence of induction of both extrinsic and intrinsic apoptosis pathways and activation of p21, p27 through p53 to arrest cells cycle in G1 phase by pinostrobin.

For a therapeutic agent to be acceptable, it is desired that the molecule is able to enter the cells quickly and also cleared from the system effectively. A number of studies have been reported to explain the self-internalising ability of therapeutic molecules which is imperative to understand their mechanisms of entry. We used innate fluorescence property of pinostrobin (emitting green and blue fluorescence at excitation 280 nm) to examine its entry and retention in HeLa cells by using live cell imaging and Z sectioning of cells using live cell confocal microscope, which allowed us to monitor molecular and cellular action of the cell in real-time period and at unicellular level. Z sectioning data clearly demonstrated that pinostrobin entered into the cells within 1 h. A significant decrease in the fluorescence at 24 h post-treatment indicated that fast and effective clearance of pinostrobin from the cells. This property makes it more acceptable than those drugs which have longer retention time and result in accumulation in the system, thus causing undesirable adverse effects. After exposure of pinostrobin cell lost their

[66]Szliszka, E., Jaworska, D., Ksek, M., Czuba, Z.P. and Król, W., 2012. Targeting death receptor TRAIL-R2 by chalcones for TRAIL-induced apoptosis in cancer cells. International Journal of Molecular Sciences, 13, pp.15343-15359.
[67]Kumari, R., Sen, N. and Das, S., 2014. Tumour suppressor p53: understanding the molecular mechanisms inherent to cancer. Current Science, 107, pp.786-794.
[68]Hyun, S.Y. and Jang, Y.J., 2015. p53 activates G1 checkpoint following DNA damage by doxorubicin during transient mitotic arrest. Oncotarget, 6, pp. 4804–4815.
[69]Abbas, T. and Dutta, A., 2009. p21 in cancer: intricate networks and multiple activities. Nature Reviews Cancer, 9, pp.400-414.
[70]Bertoli, C., Skotheim, J.M. and De Bruin, R.A., 2013. Control of cell cycle transcription during G1 and S phases. Nature Reviews Molecular Cell Biology, 14, pp.518-528.

membrane integrity and belebed that are typical signs of apoptosis. Similarly, earlier live cell imaging has been employed to examine the delivery of therapeutics using cell-penetrating peptides[71].

Though, various therapies like chemotherapy, radiotherapy and surgical therapy are available for treatment of cancer, incidence of recurrence and mortality caused by various cancer have been reported to be increased. The primary cause of this recurrence could be to the side-population (SP) of cancer cell which is recognised as cancer stem like cells (CSCs) and resistant to existing therapeutic[72,73]. Therefore, this is hypothesized that successful treatment of cancer depends on main tumor mass as well as on highly resistant side population of cancer stem like cells. Cancer stem like cells show stem cells like properties and have ability to initiate new tumor mass[74]. CSCs are accountable for tumor initiation, promotion and drug resistance. Therefore, they are gaining more attention as the target for cancer treatment.

Our studies on different cancer cell lines clearly demonstrated apoptosis-inducing potential and therefore, a putative therapeutic molecule that can be further evaluated. However, for it to be an effective therapeutic, it is important to assess its effect on self-renewal property of cancer cells. Therefore, we carried out further studies in HeLa-CSCs. We first confirmed the presence of highly tumorigenic stem cells or side population (SP) in parent HeLa cells by Hoechst staining in the presence and absence of verapamil. Generally, stem cells contain ABC membrane transporter proteins that efflux certain lipophilic drugs and recognized as side population (SP)[75]. A few transporter proteins act as Ca^{2+} channel and activates Ca^{2+} dependent proteases (e.g., calpain) and endonuclease(s) which lead to DNA fragmentation[76,77,78,79]. Verapamil is a Ca^{2}+ channel blocker, prevents

[71]Chua, A.J.S., Netto, P.A. and Ng, M.L., 2012. Molecular characterisation of cell-penetrating peptides through live cell microscopy– the past, the present and the future. Current Microscopy Contributions to Advances in Science and Technology, 1, pp.763-774.
[72]Abdullah, L.N. and Chow, E.K.H., 2013. Mechanisms of chemoresistance in cancer stem cells. Clinical and translational medicine, 2, pp.1-9.
[73]Baumann, M., Krause, M., Thames, H., Trott, K. and Zips, D., 2009. Cancer stem cells and radiotherapy. International Journal of Radiation Biology, 85, pp.391-402.
[74]Han, L., Shi, S., Gong, T., Zhang, Z. and Sun, X., 2013. Cancer stem cells: therapeutic implications and perspectives in cancer therapy. Acta Pharmaceutica Sinica B, 3, pp.65-75.
[75]López, J., Poitevin, A., Mendoza-Martínez, V., Pérez-Plasencia, C. and García-Carrancá, A., 2012. Cancer-initiating cells derived from established cervical cell lines exhibit stem-cell markers and increased radioresistance. BMC Cancer, 12, pp.1-14 .

[76]Jiang, S., Chow, S.C., Nicotera, P. and Orrenius, S., 1994. Intracellular Ca2+ signals activate apoptosis in thymocytes: studies using the Ca2+-ATPase inhibitor thapsigargin. Experimental Cell Research, 212, pp.84-92.
[77]Juntti-Berggren, L., Larsson, O., Rorsman, P., Ammala, C., Bokvist, K., Wahlander, K., Nicotera, P., Dypbukt, J., Orrenius, S., Hallberg, A. and Berggren, P.O., 1993. Increased activity of L-type Ca2+ channels exposed to serum from patients with type 1 diabetes. Science, 261, pp.86-91.

Ca2+ channel action and inhibits the efflux of Hoechst dye from subpopulation. Our results confirmed that HeLa cells used in the study did retain some side population.

Sphere forming cells (SFCs) or Cancer stem like cells (CSCs) were successfully established from HeLa cells. Compact cluster of cancer sphere cells were observed within few days. These cells were appeared as nonadhrent spherical cluster with different morphology. A progressive increase in their diameter clearly indicated their high proliferative and self-renewal ability. Similar uniformity in sphere formation was also reported in breast cancer, sarcoma and brain tumors [80,81,82]. A progressive and regular increase in size creating a symmetric prototypical spheroid is similar to the self-renewal activity of normal stem cells. These cells easily adopted HeLa cells morphology in 3-4 days and quickly grew as adherent cells and attained the morphology of parent HeLa cells.

These CSCs/SFCs also showed similar characteristic features as previously reported stem cell in breast epithelial cancer[83]. Therefore, on the basis of extensive proliferation activity, they were considered as stem or progenitor cells. Like stem cells isolated from other cancers[84,85], the HeLa-CSCs expressed higher levels of $CD44^+$ and low $CD24^+$ expression, whereas parental HeLa cells were $CD44^-$/low and $CD24^+$ high[86]. These data further confirmed stemness of the established CSCs.

It was of interest to observe that pinostrobin showed significant cytotoxicity to the HeLa-CSCs in a dose and time dependent manner. Pinostrobin treatment drastically reduced the SP number, self-renewal activity of the CSCs as well as sphere formation efficiency (SFE) of parent HeLa cells as significant reduction in the number of spheres was observed in pinostrobin-treated cells. Further analysis of pinostrobin-treated CSCs for cell integrity,

[78]Martikainen, P. and Isaacs, J., 1990. Role of calcium in the programmed death of rat prostatic glandular cells. The Prostate, 17, pp.175-187.
[79]Orrenius, S., Ankarcrona, M. and Nicotera, P., 1995. Mechanisms of calcium-related cell death. Advances in Neurology, 71, pp.137-149.
[80]Ponti, D., Costa, A., Zaffaroni, N., Pratesi, G., Petrangolini, G., Coradini, D., Pilotti, S., Pierotti, M.A. and Daidone, M.G., 2005. Isolation and *in vitro* propagation of tumorigenic breast cancer cells with stem/progenitor cell properties. Cancer Research, 65, pp.5506-5511.
[81]Gibbs, C.P., Kukekov, V.G., Reith, J.D., Tchigrinova, O., Suslov, O.N., Scott, E.W., Ghivizzani, S.C., Ignatova, T.N. and Steindler, D.A., 2005. Stem-like cells in bone sarcomas: implications for tumorigenesis. Neoplasia, 7, pp.967-976.
[82]Singh, S.K., Clarke, I.D., Terasaki, M., Bonn, V.E., Hawkins, C., Squire, J. and Dirks, P.B., 2003. Identification of a cancer stem cell in human brain tumors. Cancer Research, 63, pp.5821-5828.
[83]Gudjonsson, T., Villadsen, R., Nielsen, H.L., Rønnov-Jessen, L., Bissell, M.J. and Petersen, O.W., 2002. Isolation, immortalization, and characterization of a human breast epithelial cell line with stem cell properties. Genes & Development, 16, pp.693-706.
[84]Yu, F., Yao, H., Zhu, P., Zhang, X., Pan, Q., Gong, C., Huang, Y., Hu, X., Su, F., Lieberman, J. and Song, E., 2007. let-7 regulates self renewal and tumorigenicity of breast cancer cells. Cell, 131, pp.1109-1123.
[85]Al-Hajj, M., Wicha, M.S., Benito-Hernandez, A., Morrison, S.J. and Clarke, M.F., 2003. Prospective identification of tumorigenic breast cancer cells. Proceedings of the National Academy of Sciences, 100, pp.3983-3988.
[86]Gu, W., Yeo, E., McMillan, N. and Yu, C., 2011. Silencing oncogene expression in cervical cancer stem-like cells inhibits their cell growth and self-renewal ability. Cancer Gene Therapy, 18, pp.897-905.

mitochondrial membrane potential, DNA fragmentation and ROS production clearly revealed that like in the parent HeLa cells, pinostrobin was very effective in modulating these in CSCs and caused cell death. This increased ROS production possibly accompanied by depletion of antioxidants in the cell would promote cell death more effectively[49].

Besides causing cell death, we also investigated if pinostrobin affected the stemness of HeLa-CSCs by studying the expression of cell surface markers. $CD44^+$ and $CD24^+$ are the two markers that are differentially expressed on parent HeLa cells and HeLa-CSCs. $CD44^+$ is mainly responsible for cancer promotion and significantly regulates cancer cell growth and metastasis process[87], whereas $CD24^+$ plays major role in sphere formation, cell proliferation, cell differentiation, promotes tumour growth, invasion and metastasis and enhanced resistance to chemotherapeutic drugs[88,89,90,91]. A few phytochemicals that are capable to alter expression level of both $CD44^+$ and $CD24^+$ molecule have been identified as anti-metastatic agents[92,93]. Also, inhibition of $CD24^+$ expression with $CD24^+$-shRNA resulted in reduction of tumor volume and increased apoptosis *in vivo*[94]. Monoclonal antibody has been used to inhibit $CD24^+$ expression in A549 lung cancer model[95]. Since these molecules play a role in tumor initiation and promotion, inhibition of expression of these would lead to reduction in tumor growth. In the present study, pinostrobin reduced the expression of both $CD44^+$ and $CD24^+$ in HeLa-CSCs as well as HeLa cells. Thus, pinostrobin had shown the potential to inhibit the self renewal action and decreased the expression of specific marker of CSCs to endorse cell death.

[87]Yan, Y., Zuo, X. and Wei, D., 2015. Concise review: emerging role of CD44 in cancer stem cells: a promising biomarker and therapeutic target. Stem cells Translational Medicine, 4, pp.1033-1043.
[88]Choi, Y.L., Lee, S.H., Kwon, G.Y., Park, C.K., Han, J.J., Choi, J.S., Choi, H.Y., Kim, S.H. and Shin, Y.K., 2007. Overexpression of CD24: association with invasiveness in urothelial carcinoma of the bladder. Archives of Pathology & Laboratory Medicine, 131, pp.275-281.
[89]Miller, E., Shapira, S., Gur, E., Naumov, I., Kazanov, D., Leshem, D., Barnea, Y., Meshiach, Y., Gat, A., Sion, D. and Arber, N., 2011. Increased expression of CD24 in nonmelanoma skin cancer. The International Journal of Biological Markers, 27, pp. 285 - 404.
[90]Deng, J., Gao, G., Wang, L., Wang, T., Yu, J. and Zhao, Z., 2012. CD24 expression as a marker for predicting clinical outcome in human gliomas. BioMed Research International, 2012, pp.1-7.
[91]Sagiv, E., Memeo, L., Karin, A., Kazanov, D., Jacob–Hirsch, J., Mansukhani, M., Rechavi, G., Hibshoosh, H. and Arber, N., 2006. CD24 is a new oncogene, early at the multistep process of colorectal cancer carcinogenesis. Gastroenterology, 131, pp.630-639.
[92]Nebe, B., Peters, A., Duske, K., Richter, D.U. and Briese, V., 2006. Influence of phytoestrogens on the proliferation and expression of adhesion receptors in human mammary epithelial cells *in vitro*. European Journal of Cancer Prevention, 15, pp.405-415.
[93] Kim, J.H., Lee, B.K., Lee, K.W. and Lee, H.J., 2009. Resveratrol counteracts gallic acid-induced down-regulation of gap-junction intercellular communication. The Journal of Nutritional Biochemistry, 20, pp.149-154.
[94]Su, D., Deng, H., Zhao, X., Zhang, X., Chen, L., Chen, X., Li, Z., Bai, Y., Wang, Y., Zhong, Q. and Yi, T., 2009. Targeting CD24 for treatment of ovarian cancer by short hairpin RNA. Cytotherapy, 11, pp.642-652.
[95]Salnikov, A.V., Bretz, N.P., Perne, C., Hazin, J., Keller, S., Fogel, M., Herr, I., Schlange, T., Moldenhauer, G. and Altevogt, P., 2013. Antibody targeting of CD24 efficiently retards growth and influences cytokine milieu in experimental carcinomas. British Journal of Cancer, 108, pp.1449-1459.

After establishing the anti-proliferative and apoptosis inducing ability of pinostrobin in *vitro* in cancer cells as well as HeLa-CSCs, it was imperative to establish if these effects indeed translated in in vivo conditions. Therefore, antitumor activity of pinostrobin was evaluated against Ehrlich ascites carcinoma (EAC) in mice model. EAC were used as these cells are of mouse origin isolated from spontaneous breast cancer in a female mouse[96,97]. EAC cells are a highly transplantable, poorly differentiated, shorter life span and fast growing malignant tumor cells. EAC is referred to as an undifferentiated carcinoma and originally hyperdiploid, resembles to human tumors[96,98].

We checked the effect of pinostrobin on cell viability of EACs isolated from control and pinostrobin-treated EAC tumor bearing mice. Like the *in vitro* studies, EAC viable cell count was significantly reduced in dose dependent manner after pinostrobin exposure. Our study concluded that pinostrobin treatment in 4 day regular interval is most effective for reduction of viable cells numbers. In a similar way, Bellamakondi, *et al.*, also examine the toxicity of Caralluma species against a panel of cancer, normal origin cell lines and EAC cells[99]. Though pinostrobin is a potential anti-cancer agent, its toxicity is not yet investigated in EAC transplanted Swiss albino mice. The previous studies on quercetin and natural flavonoids from citrus peels have been shown to be cytotoxic to EAC cells. Thus, the observed cytotoxicity of pinostrobin to EAC cells is in agreement with these reports[100,101].

Further, EAC cells inoculation (intraperitonial) method was used for generating solid tumor model in Swiss albino mice. Pinostrobin dosage was given into mice by two route which are commonly used for drug delivery i.e. intraperitonial and intratumoral. Upon treatment of pinostrobin a significant reduction in the tumor volume was also observed in all group of mice compared to untreated and vehicle treated control animals. The tumor

[96]Ozaslan, M., Karagoz, I.D., Kilic, I.H. and Guldur, M.H. 2011.Ehrlich ascites carcinoma. African Journal of Biotechnology, 10, pp.2375-2378.
[97]Ikitimur-armutak, E.I. and Gurtekin, M., 2014. Ehrlich Ascites Tümörü ile BALB-C Farelerde Oluş turulmuş Solid Tümör Modelinde Curcuminin Apoptoz Uzerine Etkileri. Istanbul Universitesi Veteriner Fakültesi Dergisi, 40, pp.183-190.
[98]Zheng, L., Zhou, B., Meng, X., Zhu, W., Zuo, A., Wang, X., Jiang, R. and Yu, S., 2014. A model of spontaneous mouse mammary tumor for human estrogen receptor-and progesterone receptor-negative breast cancer. International Journal of Oncology, 45, pp.2241-2249.
[99]Bellamakondi, P.K., Godavarthi, A., Ibrahim, M., Kulkarni, S., Naik, R.M. and Maradam, S., 2014. *In vitro* cytotoxicity of *caralluma species* by MTT and trypan blue dye exclusion. Asian J Pharm Clin Res, 7, pp.17-19.
[100]Venkatalakshmi, P. and Vb, V., Identification of flavonoids in different parts of *Terminalia catappa L*. using LC-ESI-MS/MS and investigation of their anticancer effect in EAC cell line model pharm. Sci. & Res, 8, pp.176-183.
[101]Srivastava, S., Somasagara, R.R., Hegde, M., Nishana, M., Tadi, S.K., Srivastava, M., Choudhary, B. and Raghavan, S.C., 2016. Quercetin, a natural flavonoid interacts with DNA, arrests cell cycle and causes tumor regression by activating mitochondrial pathway of apoptosis. Scientific Reports, 6, pp. 1-13.

volume significantly reduced in regular 4 day intratumoral treatment compared to one time treatment (post-treatment). Similarly, some flavonoids have been reported to reduce the tumor volume[102,103]. Doxorubicin was used as a positive control also reduced the tumor volume comparable to vehicle control group of mice. In addition, pinostrobin also decrease tumor development rate and delay tumor growth in our study. In the present study, optimium dose of pinostrobin for *in vivo* studies was determined to be 10 mg/kg b wt. as this showed significant reduction in tumor size without any toxic effect in life span studies. At higher dose (20 mg/kg b wt), tumor bearing mice survived for only 22 days, though significant decrease in tumor size was noted in these mice as compared to vehicle treated group. This low survival rate could possibly be due to toxicity of pinostrobin to the organism at this dose, which needs to be further investigated by carrying out different organs' function tests such as liver and kidney function tests.
The reliable criteria for assessing anticancer drug efficiency are to check the prolongation of lifespan of the disease animal model. The percentage of survival was analyzed using optimum dose of pinostrobin. By 44th day of pinostrobin treated animals did not show tumor as appear in untreated control mice. More importantly, we observed a significant increase in the lifespan of pinostrobin treated mice, median survival time and percentage increase life- span (MST, ILP) are found increased by pinostrobin treatment. The study confirmed that pinostrobin can play important role against cancer and significantly expand the lifespan. Mazumdar *et al.,* & Gupta *et al.,* have also examined antitumor activity of natural compound in mice, these previous findings shown the healthy correlation among natural compound and cancer treatment[104,105]. Ascetic fluid is a major nutritional source of tumor growth and provides the nutritional requirements to tumor cells[106]. Pinostrobin reduced the number of viable cancer cell count and increased the lifespan. It suggested that pinostrobin can reduce the nutritional fluid volume and subsequently arrests tumor development and increases the life span. The present finding is supported by available flavonoids studies from plant extract, have intense antitumor properties and induce

[102]Rawson, N.E., Ho, C.T. and Li, S., 2014. Efficacious anti-cancer property of flavonoids from citrus peels. Food Science and Human Wellness, 3, pp.104-109.
[103]Wang, G., Wang, J., Du, L. and Li, F., 2015. Effect and mechanism of total flavonoids extracted from *Cotinus coggygria* against glioblastoma cancer *in vitro* and *in vivo*. BioMed Research International, 2015, pp.1-9.
[104]Mazumdar, U.K., Gupta, M., Maiti, S. and Mukherjee, D., 1997. Antitumor activity of *Hygrophila spinosa* on Ehrlich ascites carcinoma and sarcoma-180 induced mice. Indian Journal of Experimental Biology, 35, pp. 473-477.
[105]Gupta, M., Mazumder, U.K., Rath, N. and Mukhopadhyay, D.K., 2000. Antitumor activity of methanolic extract of *Cassia fistula L.* seed against Ehrlich ascites carcinoma. Journal of Ethnopharmacology, 72, pp.151-156.
[106]Shimizu, M., Azuma, C., Taniguchi, T. and Murayama, T., 2004. Expression of cytosolic phospholipase A2α in murine C12 cells, a variant of L929 cells, induces arachidonic acid release in response to phorbol myristate acetate and Ca2+ ionophores, but not to tumor necrosis factor-α . Journal of Pharmacological Sciences, 96, pp.324-332.

antiproliferation mechanisms that may kill cancer cells and prevent tumor invasion[107,108,109]. Thus, results indicate that pinostrobin can provide significant chemoprevention to tumor bearing mice. Further, research work is required to establish the pinostrobin antitumor mechanism of action. The study may provide a scientific basis to validate the traditional use of the plant derived compounds for cancer disease.

Since, many phytochemicals with potential anticancer activity have been reported to inhibit topoisomerase I activity, thereby inhibiting DNA replication. Inhibition of A549 cells growth by xanthohumol has been mediated by inhibition of DNA topoisomerase activity[110]. Similarly, camptothecin is also reported to bind to topoisomerase and inhibit cell proliferation[111]. In light of these studies, we investigated pinostrobin binding ability with topoisomerase I *in silico* using topoisomerase I-DNA complex crystal structure as a target. *In vitro* studies were also carried out to see if pinostrobin inhibited its activity. We performed both rigid and flexible docking to establish if the binding sites of pinostrobin at the target would be similar or different to the one used in rigid docking. Doxorubicin was also used as a positive control for *in silico* binding analysis. Comparative analysis of binding energies involved in the interaction of pinostrobin and topoisomerase I-DNA complex showed more effective binding in flexible docking, possibly due to rotatable bonds of the ligands which result in an increased binding site potential. Relatively lower binding energy in flexible docking indicates a more stable binding of pinostrobin with the enzyme-DNA complex. Pinostrobin bound to the enzyme with a similar efficiency as doxorubicin, a known inhibitor of cancer growth. Pinostrobin interaction with DNA and enzyme were found to be through hydrophobic and covalent interactions respectively with the binding site shape being complementary to the shape of the ligand. Earlier reports have also shown many well-known inhibitors to bind to Asn 722 and Arg 364 residues of

[107]Sessa, R.A., Bennett, M.H., Lewis, M.J., Mansfield, J.W. and Beale, M.H., 2000. Metabolite profiling of sesquiterpene lactones from lactuca species major latex components are novel oxalate and sulfate conjugates of lactucin and its derivatives. Journal of Biological Chemistry, 275, pp.26877-26884.

[108]Ruela de Sousa, R.R., Queiroz, K.C.S., Souza, A.C.S., Gurgueira, S.A., Augusto, A.C., Miranda, M.A., Peppelenbosch, M.P., Ferreira, C.V. and Aoyama, H., 2007. Phosphoprotein levels, MAPK activities and NFκ B expression are affected by fisetin. Journal of Enzyme Inhibition and Medicinal Chemistry, 22, pp.439-444.

[109]Lotito, S.B. and Frei, B., 2006. Consumption of flavonoid-rich foods and increased plasma antioxidant capacity in humans: cause, consequence, or epiphenomenon?. Free Radical Biology and Medicine, 41, pp.1727-1746.

[110]Lee, S.H., Kim, H.J., Lee, J.S., Lee, I.S. and Kang, B.Y., 2007. Inhibition of topoisomerase I activity and efflux drug transporters' expression by xanthohumol from hops. Archives of pharmacal research, 30, pp.1435-1439.

[111]Xu, Y. and Her, C., 2015. Inhibition of topoisomerase (DNA) I (TOP1): DNA damage repair and anticancer therapy. Biomolecules, 5, pp.1652-1670.

topoisomerase I and inhibit its activity[112,113,114]. The hydrophobic interactions between the benzene ring of pinostrobin and hydrophobic residues of topoisomease I-DNA complex are likely to be responsible for the stability of docked complex.

Pinostrobin binding to the identified residues could result in conformational alteration of topoisomerase I structure which in turn could inhibit its binding with the DNA. During pinostrobin and topoisomerase I interaction, only single O1 atom of pinostrobin was found to be involved in three hydrogen bonds formation with the enzyme, wherein one hydrogen bonding residue Asn 722 is located close to the active site residue. Thus, binding of pinostrobin to Asn 722 might change the conformation which results in reduction of its interaction at the active site of topoisomerases I. These results suggest that pinostrobin inhibits the topoisomease I activity in an allosteric manner. Docking study of doxorubicin revealed covalent and hydrophobic interactions with enzyme and DNA respectively.

The possible binding mode of pinostrobin was identified in the core central part of C-terminal region of topoisomerase I and nicked area of DNA. Methoxy group of pinostrobin on ring A shows positive potential, whereas negative potential is generated due to presence of carbonyl and hydroxyl groups on ring C and A, respectively. This negative potential may contribute to hydrogen bonds interaction with topoisomerase I. Both pinostrobin and doxorubicin were found to interact at the allosteric site of topoisomerase I, and not with the active site amino acid residue (Tyr 723) of topoisomerase I. These *in silico* result thus suggest pinostrobin to be an allosteric inhibitor.

Further, validation of docking results was carried out by Glide. Good negative G-score were assigned to pinostrobin (-3.911kcal/mol) by Glide docking, which was comparable with the G-score for doxorubicin (-4.991 kcal/mol), included as a positive control. Thus, Glide docking results suggested that both pinostrobin and doxorubicin exhibited good binding affinity with topoisomerase I-DNA. In addition to the G-score, analysis of different interaction energies such as van der Waals energy, intermolecular energy,

[112]Chrencik, J.E., Burgin, A.B., Pommier, Y., Stewart, L. and Redinbo, M.R., 2003. Structural impact of the leukemia drug 1-β-D-arabinofuranosylcytosine (Ara-C) on the covalent human topoisomerase I-DNA complex. Journal of Biological Chemistry, 278, pp.12461-12466

[113]Chrencik, J.E., Staker, B.L., Burgin, A.B., Pourquier, P., Pommier, Y., Stewart, L. and Redinbo, M.R., 2004. Mechanisms of camptothecin resistance by human topoisomerase I mutations. Journal of Molecular Biology, 339, pp.773-784.

[114]Hsiang, Y.H., Lihou, M.G. and Liu, L.F., 1989. Arrest of replication forks by drug-stabilized topoisomerase I-DNA cleavable complexes as a mechanism of cell killing by camptothecin. Cancer Research, 49, pp.5077-5082.

hydrogen bonding, coulombic interactions and electrostatic energy, further indicated that both the ligands (pinostrobin and doxorubicin) had good binding affinities with the topoisomerase I–DNA complex. Stable docked complex was obtained by energy minimization[115]. The pinostrobin-topoisomerase I-DNA complex was found to be stable as the potential energy of this complex was found to be significantly low. Automated docking, Glide and Prime indicated good bonding interactions (electrostatic, van der Walls and hydrogen bonds) and thus established structural stability of the docked complex. Free-energy calculations that are also used to assess stability of a complex[116,117] using Helmholtz free energy formula[118]. Free energy of the docked complex was found to be close to the one calculated by Helmholtz free energy formula, further supporting thermodynamic stability of the docked complex.

ADMET (Absorption, distribution, metabolism, excretion and toxicity) score analysis of pinostrobin indicated pinostrobin to be a good drug, as its a compound with logP values >5 is considered lipophilic[119]. On the other hand, the total partition of both ionized and unionized form of the compound is analyzed by logD values. The acidic compounds show low logD value, attributing to its acidic environment[119]. The logP values for pinostrobin and doxorubicin were found to be lower than 5 indicating its hydrophilic nature, thus more acceptable as a drug. Moriguchi's logP (MLogP) scores of a compound are inversely related with the absorption efficiency of the compound; higher the score (>4.15), poor the absorption[120]. The MLogP (indicative of absorption efficiency of the compound) for both the pinostrobin and doxorubicin were calculated to be significantly lower, suggesting that these compounds can be easily absorbed. Hydrogen bonding potential of any molecule on the receptor is determined through Topological Polar Surface Area (TPSA) score[121]. The TPSA score for pinostrobin and doxorubicin were found good indicating good Hydrogen

[115]Pronk, S., Páll, S., Schulz, R., Larsson, P., Bjelkmar, P., Apostolov, R., Shirts, M.R., Smith, J.C., Kasson, P.M., van der Spoel, D. and Hess, B., 2013. GROMACS 4.5: a high-throughput and highly parallel open source molecular simulation toolkit. Bioinformatics, 29, pp.845-854.

[116]Helms, V. and Wade, R.C., 1998. Computational alchemy to calculate absolute protein− ligand binding free energy. Journal of the American Chemical Society, 120, pp.2710-2713.

[117]Boyce, S.E., Mobley, D.L., Rocklin, G.J., Graves, A.P., Dill, K.A. and Shoichet, B.K., 2009. Predicting ligand binding affinity with alchemical free energy methods in a polar model binding site. Journal of Molecular Biology, 394, pp.747-763.

[118]Souza, A.T., Cardozo-Filho, L., Wolff, F. and Guirardello, R., 2006. Application of interval analysis for Gibbs and Helmholtz free energy global minimization in phase stability analysis. Brazilian Journal of Chemical Engineering, 23, pp.117-124.

[119]Goswami, T., Kokate, A., Jasti, B.R. and Li, X., 2013. *In silico* model of drug permeability across sublingual mucosa. Archives of Oral Biology, 58, pp.545-551.

[120]R. Todeschini, V. Consonni, Handbook of Molecular Descriptors, in methods and principles in medicinal chemistry, vol. 11 R. Mannhold, H. Kubinyi, H. Timmerman, Eds.Wiley-VCH: Weinheim, 2000, New York.

[121]Clark, D.E., 1999. Rapid calculation of polar molecular surface area and its application to the prediction of transport phenomena. 1. Prediction of intestinal absorption. Journal of Pharmaceutical Sciences, 88, pp.807-814.

bonding potential of these compounds. Generally, polar nitrogen and oxygen atoms of any compound are involved in hydrogen bonds formation. Thus, higher TPSA score of doxorubicin (when compared to pinostrobin) are in line with the presence of higher numbers of nitrogen and oxygen (12) atoms in doxorubicin, in comparison to the numbers of nitrogen and oxygen atoms (4) in pinostrobin. Nevertheless, both have the ability to form hydrogen bonds which showed their binding potential to the target. Thus, the ADMET analysis clearly suggests that pinostrobin and doxorubicin act as hydrophilic agents with an ability to form a number of hydrogen bonds, high TPSA score, and low log P<5 values. According to Lipinski's "rule of five'', a compound with logP<5 can be orally administered. Thus, both pinostrobin and doxorubicin having lower logP score have the potential to be developed as oral therapeutics.

In silico docking studies indicated that pinostrobin interacted with DNA as well in the topoisomerase I-DNA complex. We used ethidium bromide displacement assay to assess the binding of pinostrobin with DNA as binding of any compound with the DNA will result in displacement of DNA-bound ethidium bromide and thereby reduction in its fluorescence intensity[122]. Ethidium bromide displacement confirmed that pinostrobin indeed interacted with DNA, as evidenced by a decrease in fluorescence intensity in concentration dependent manner, as has been reported for doxorubicin[123]. Since topoisomerase I acts on the DNA, binding of pinostrobin to DNA could therefore affect the topoisomerase I activity.

After establishing, pinostrobin binding to topoisomerase I-DNA complex *in silico*, we used fluorescence property of pinostrobin to assess its binding with the topoisomerase I and DNA individually by monitoring its emission spectra. The binding of drug molecules to protein or receptor are analyzed by various molecular mechanisms like excited-state reactions, molecular rearrangements, energy transfer, ground state complex formation and collisional quenching. These molecular mechanisms are a part of florescence quenching, by which the fluorescence intensity is reduced[124]. Pinostrobin produced blue and green

[122]Baguley, B.C. and Falkenhaug, E.M., 1978. The interaction of ethidium with synthetic double-stranded polynucleotides at low ionic strength. Nucleic Acids Research, 5, pp.161-171.
[123]Bair, J.S., Palchaudhuri, R. and Hergenrother, P.J., 2010. Chemistry and biology of deoxynyboquinone, a potent inducer of cancer cell death. Journal of the American Chemical Society, 132, pp.5469-5478.
[124]Kandagal, P.B., Ashoka, S., Seetharamappa, J., Shaikh, S.M.T., Jadegoud, Y. and Ijare, O.B., 2006. Study of the interaction of an anticancer drug with human and bovine serum albumin: spectroscopic approach. Journal of Pharmaceutical and Biomedical Analysis, 41, pp.393-399.

florescence upon excitation at 280 nm. A decrease in the fluorescence intensity without any shift in the emission maxima in the presence of topoisomerase I clearly demonstrated that pinostrobin indeed interacts with topoisomerase I.

Unlike the enzyme, in the presence of DNA, an increase in the fluorescence intensity of the pinostrobin with a blue shift in the emission maxima was observed, clearly indicating its interaction with DNA. Similar increase in the fluorescence intensity of Al–N,N′ -bis(salicylidene)2,2′ -phenylendiamine complex has been reported upon addition of DNA[125]. The observed shift and increased intensity may be due to the intercalation of pinostrobin with DNA in the immediate hydrophobic environment of DNA[125]. These results further confirm results of ethidium bromide displacement assay and establish that pinostrobin is able to interact with topoisomerase I as well as DNA independently. Topoisomerase I induces nick and reseals one of the strand of DNA, and thus plays a major role in DNA replication. The expression level of topoisomerase I in cancer cells have been reported to be higher than normal cells[126]., which is expected considering their higher proliferation rate. Though *in silico* and fluorescence spectra studies clearly indicated that pinostrobin binds to both the DNA as well as topoisomerase I. However, these results are not sufficient to conclusively state that it inhibits topoisomerase I activity. Therefore, *in vitro* topoisomerase I relaxation assay was carried out to evaluate pinostrobin's ability to inhibit its activity using nuclear extract of Ca Ski cells as source of topoisomeses, both I and II. However, exclusion of ATP, which is absolutely essential for topoisomerase II activity, allowed us to selectively measure topoisomerase I activity. An increase in the supercolied form of plasmid DNA with an increase in pinostrobin concentration clearly demonstrated inhibition of topoisomerase I activity. Minimal increase observed inhibition of topoisomerase I activity is not an artefact. On the other hand, when doxorubicin was evaluated for its ability to inhibit topoisomerase I activity, predominantly relaxed form of the DNA was observed, suggesting that doxorubicin could not inhibit nicking activity of topoisomerase I, while it inhibited resealing activity of topoisomerase I. Thus, DNA could possibly not be resealed due to doxorubicin binding onto DNA and formation of ternarary complex between doxorubicin, DNA, and

[125]Kashanian, S., Gholivand, M.B., Ahmadi, F., Taravati, A. and Colagar, A.H., 2007. DNA interaction with Al–N, N′ -bis (salicylidene) 2, 2′ -phenylendiamine complex. Spectrochimica Acta Part A: Molecular and Biomolecular Spectroscopy, 67, pp.472-478.

[126]Chen, B.M., Chen, J.Y., Kao, M., Lin, J.B., Yu, M.H. and Roffler, S.R., 2000. Elevated topoisomerase I activity in cervical cancer as a target for chemoradiation therapy. Gynecologic Oncology, 79, pp.272-280.

topoisomerase I. In the present study we demonstrated inhibition of topoisomerase I activity by pinostrobin. Different mechanisms have been suggested for inhibition of topoisomerase activity by different compounds. These include (i) direct interaction of the inhibitor with the template i.e. DNA (ii) formation of ternary complex involving the inhibitor, topoisomerase and DNA (iii) suppression of topoisomerase association with the DNA[127]. A change in the pinostrobin fluorescence upon incubation with either topoisomerase I or DNA suggests that pinostrobin possibly interacts with both DNA and topoisomerase I and could possibly form a ternary complex. Similar observations have been made with other drugs such as campatothecin[110,111] luteolin[128] and quercetin[129]. Boege *et al.*, and his associates have demonstrated topoisomerse I inhibitory activity of planer flavones with A-C ring system. These authors also reported that topoisomerase I formed stable complex with molecules that have hydroxyl group at c-5 and c-7 and methoxy group at c-7 and c-3 positions resulting significant inhibition of its activity. Pinostrobin also has A-C ring system, methoxy and hydroxyl group, and therefore the results are in agreement with the reports putforth by Boege *et al.*,[129] Thus, results of *in silico* analysis of pinostrobin-topoisomerase I-DNA interaction have been validated by experimental evidence and suggested its inhibitory action against topoisomerase I.

[127]Shamsi, M., Yadav, S. and Arjmand, F., 2014. Synthesis and characterization of new transition metal {Cu (II), Ni (II) and Co (II)} l-phenylalanine–DACH conjugate complexes: *In vitro* DNA binding, cleavage and molecular docking studies. Journal of Photochemistry andPhotobiology B: Biology, 136, pp.1-11.

[128]Chowdhury, A.R., Sharma, S., Mandal, S., Goswami, A., Mukhopadhyay, S. and Majumder, H.K., 2002. Luteolin, an emerging anti-cancer flavonoid, poisons eukaryotic DNA topoisomeraseI. Biochemical Journal, 366, pp.653-661.

[129]Boege, F., Straub, T., Kehr, A., Boesenberg, C., Christiansen, K., Andersen, A., Jakob, F. and Köhrle, J., 1996. Selected novel flavones inhibit the DNA binding or the DNA religation step of eukaryotic topoisomerase I. Journal of Biological Chemistry, 271, pp.2262-2270.

Chapter 6

Summary

As a global public health concern, cancer is a multifactorial disease and one of the major health problems in the world. Various conventional therapies kill rapidly growing cancer cells but often cause side effects. Therefore, cancer treatment therapies need to be revolutionized for prevention of unfavourable effects on normal cells. Plants derived products and dietary phytochemicals have drawn attention as new alternatives as cancer therapeutics and several studies have been conducted on plants derived products that possess anticancer properties. Many of these have been utilized as potent anticancer drugs. In present study, pinostrobin, a flavonoid, induced cell death and disturbed cell morphology in a dose-dependent manner. Pinostrobin internalization and retention analysis showed it to be quickly internalized into HeLa cells. Its fast clearance from the cells makes it an ideal candidate as this will help in avoiding the toxic effects of drugs that are caused by accumulation. Pinostrobin treatment resulted in apoptosis-mediated cell death as evidenced by typical morphological changes in the cellular, mitochondrial and nuclear architecture as well as loss in mitochondrial membrane potential in pinostrobin-treated cells. Different cancer cells showed differential sensitivity to pinostrobin with HL-60 and HeLa cells being most sensitive to the treatment. Our findings highlight the molecular mechanism of its action through ROS generation and activation of both extrinsic and intrinsic apoptotic pathways and upregulation of p53 tumor suppressor. Increase in oxidative stress by ROS and reduction in GSH levels in pinostrobin possibly facilitated cell death. Further, inhibition of sphere forming ability of the HeLa-CSCs, and cytotoxic effect of pinostrobin in these cells suggest that it is likely to inhibit recurrence of cancer growth as it affected the self-renewal potential of CSCs. Further, *in vivo* studies using EAC carcinoma in mice confirmed tumor growth inhibitory potential of pinostrobin as significant reduction of tumor volume was noted in pinostrobin-treated mice. Our *in silico* and *in vitro* studies indicated topoisomerase I to be one of the target of pinostrobin as it effectively interacted with topoisomesae I-DNA complex and inhibit its molecular mechanism to control cancer cell proliferation. Thus, overall pinostrobin exhibited good drug properties (analyzed by ADMET scores), quick entry and fast clearance, and selective toxicity *in vivo* and *in vitro* in various cancer cell lines. However, further studies are required to fully understand its anti-cancer potential in different cancers *in vivo*.

PUBLICATION

Alka Jadaun, N. Subbarao and Aparna Dixit **(2017)**. Allosteric inhibition of topoisomerase I by pinostrobin: Molecular docking, spectroscopic and topoisomerase I activity studies. **Journal of Photochemistry & Photobiology, B: Biology**, 167, pp. 299–308.

.

CONFERENCE PRESENTATION

Poster presentation: Study of the plant derivatives flavonoids in cancer treatment: Role of Pinostrobin, **Alka Jadaun** and Aparna Dixit.
Presented at **2nd Gynecologic Cancer Conference, Rome, Italy**

Oral presentation: Pinostrobin inhibits human cervical cancer cell proliferation and induces apoptosis by modulating the GSH/NO/ROS signalling pathways. **Alka Jadaun**
Presented at **2nd Gynecologic Cancer Conference, Rome, Italy**

Journal of Photochemistry & Photobiology, B: Biology 167 (2017) 299–308

Contents lists available at ScienceDirect

Journal of Photochemistry & Photobiology, B: Biology

journal homepage: www.elsevier.com/locate/jphotobiol

Allosteric inhibition of topoisomerase I by pinostrobin: Molecular docking, spectroscopic and topoisomerase I activity studies

Alka Jadaun [a], N. Subbarao [b], Aparna Dixit [a,*]

[a] School of Biotechnology, Jawaharlal Nehru University, New Delhi 110067, India
[b] School of Computational and Integrative Sciences, Jawaharlal Nehru University, New Delhi 110067, India

ARTICLE INFO

Article history:
Received 12 August 2016
Received in revised form 30 December 2016
Accepted 1 January 2017
Available online 12 January 2017

Keywords:
Topoisomerase I inhibitor
DNA binding
Molecular docking

ABSTRACT

Cancer, the second major cause of mortality trailing the cardiovascular diseases, is a multifactorial heterogeneous disease and growing public health problem worldwide. Owing to severe adverse effects of currently available therapies, there is a growing interest in natural compounds present in our daily diet. Among various natural products, flavonoids-polyphenolic compounds have attracted much attention and have been well-documented for their biological activities. Some flavonoids may inhibit cancer cell proliferation by modulating the action of different enzymes and signal transduction pathways. In the present study, we have evaluated the effect of pinostrobin, a natural flavonoid, on the catalytic activity of topoisomerase I, an essential enzyme for normal DNA replication. Catalytic inhibition of topoisomerase I activity would impair DNA replication of rapidly dividing cancer cells and hence inhibits tumor progression. Pinostrobin interaction with the topoisomerase I and DNA assessed *in silico* indicated it to form a ternary complex with both. *In silico* data also suggested pinostrobin to be an effective allosteric inhibitor for topoisomerase I. Further, *in vitro* investigations such as ethidium bromide displacement assay and spectroscopic studies supported *in silico* results on the binding of pinostrobin at the interface of topoisomerase I and DNA. Pinostrobin effectively inhibited topoisomerase I activity *in vitro* further confirming our *in silico* and *in vitro* findings. Since topoisomerase I is essential for DNA replication, inhibition of its activity by pinostrobin highlights the therapeutic potential of pinostrobin as an anti-proliferative agent.

1. Introduction

Flavonoids—one of the secondary metabolites of plants, are known for their profound pharmacological applications. Pinostrobin is a naturally occurring flavonoid that is present in daily dietary intake. Antimicrobial, anti-inflammatory, antioxidant and anti-proliferative properties of pinostrobin have been reported [1–4]. However, its molecular target and exact mechanism by which it inhibits proliferation have not been established.

DNA topoisomerases catalyse the inter-conversion of topological isomers of DNA molecules. The two types of topoisomerases *i.e.* topoisomerase I and II, are responsible for sequential cleavage and reunion of either one strand or both strands of DNA, respectively [5]. Topoisomerase I an omnipresent monomeric ATP-independent enzyme, alleviates the topological disruption in DNA helix. Its catalytically active residue Tyr723 is involved in nucleophilic reaction that cleaves scissile phosphodiester bond of DNA to form a transient covalent bond between the enzyme and phosphate group of broken DNA strand [6,7]. Increased rate of topoisomerase I transcription and its activity in metastatic cancer tissues clearly demonstrate its significant role in cancer growth and invasion [8]. Activity of topoisomerase I have been reported to be affected by chemotherapy [9]. Blocking or inhibition of topoisomerase's catalytic activity is therefore expected to result in disruption of cellular processes such as transcription, replication and chromosomal condensation. Currently, few drugs are used in chemotherapy that inhibit topoisomerase I—resealing and cleavage catalytic activity resulting in rapid death of actively proliferating cancer cells. Therefore, topoisomerase I inhibitors are classified into two types: Type I inhibitors block the rejoining activity of topoisomerase I and make enzyme-DNA covalent complex, and thus act as poison [10], whereas Type II inhibitors inhibit enzyme-DNA binding through interacting with either DNA or topoisomerase I.

Earlier studies have demonstrated that naturally occurring flavonoids act as an antagonist to DNA-topoisomerase I & II [11,12]. However, how do these flavonoids bring about this effect is not clearly understood. In the current study, *in silico* and *in vitro* approaches were used to evaluate pinostrobin's ability to inhibit topoisomerase I activity, wherein automated docking (both rigid and flexible) was performed to investigate probable binding of the pinostrobin to topoisomerase I-DNA complex. Further, ADMET study of pinostrobin was performed to

* Corresponding author.
E-mail addresses: adixit7@gmail.com, adix2100@mail.jnu.ac.in (A. Dixit).

http://dx.doi.org/10.1016/j.jphotobiol.2017.01.010
1011-1344/

analyze its appropriateness as a drug. Further, ethidium bromide (EtBr) displacement assay and spectroscopic studies were performed to screen pinostrobin's interaction with DNA and topoisomerase I individually. Subsequently, *in vitro* topoisomerase I relaxation assay was conducted in the presence of pinostrobin to investigate its effect on topoisomersase I activity.

2. Materials and Methods

2.1. Reagents and Cell Lines

Analytical grade reagents were used in present study and reagents for cell culture such as Roswell Park Memorial Institute medium (RPMI-1640), Fetal bovine serum (FBS) and Penicillin-Streptomycin were procured from Biological Industries, Israel. Cervical carcinoma cells (*Ca* Ski cells) were obtained from National Centre for Cell Science (NCCS), Pune, India. Plasmid DNA extraction kit (midi) was procured from Qiagen, Germany. Pinostrobin (>99% TLC grade) and doxorubicin were purchased from Sigma Aldrich Chemical Co., USA. Stock solution of pinostrobin (20 mM) was prepared in triple solvent (Dimethyl formamide: Acetonitrile: Dimethyl sulfoxide, 1:1:1) [13]. Doxorubicin stock solution (1 mg/mL) was prepared in MilliQ and stored at 4 °C. Purified topoisomerase I was procured from Sigma Aldrich Chemical Co., USA.

2.2. Molecular Docking of Ligands at the Interface of Topoisomerase I-DNA Complex

Three dimensional structure of the target topoisomerase I-DNA complex was retrieved from Protein Data Bank (http://www.rcsb.org/pdb; PDB ID: 1T8I). Subsequently, heteroatoms and water molecules were removed from the structure file prior to docking [14]. Three dimensional (3D) molecular structures of the ligand of interest—pinostrobin and doxorubicin (included as positive control) were obtained in sdf format from PubChem database [15].

2.2.1. Automated Rigid Docking

Automated rigid docking was performed by using AutoDock v 4.2 program [16]. The target topoisomerase I-DNA complex was prepared by addition of polar hydrogen atoms and merged non-polar hydrogen atoms. Afterwards, Kollman united atom partial charges and solvation parameters were assigned on topoisomerase I-DNA complex structure and then saved in “pdbqt” format. The structure of the ligands (pinostrobin and doxorubicin) (in “.pdb” format) was modified by adding hydrogen atoms in order to satisfy the valencies of the heavy atoms, and assigning Gasteiger charges. The best root in the atoms of the ligand was fixed by torsion degree of freedom. The ligand structure saved in “pdbqt” format was used for docking. During docking process, all bonds of ligands were made non-rotatable and topoisomerase I-DNA complex was kept rigid. The binding sites of the ligands on the receptor were defined by well-known amino acid residues, Subsequently, grid box was fixed and the area of interest on the receptor was mapped by grid parameters, grid spacing with 0.375 Å and dimension of $60 \times 60 \times 60$ along the x, y, and z-axes, using the centre of the target topoisomerase I-DNA complex as the centre of the grid box. Each binding site of the ligand on the target was evaluated by Lamarckian genetic algorithm (LGA) with local search engine [16,17]. In all, 100 search attempts were performed for each ligand. For each run, a docking population of 150 individuals with 27,000 generations and 250,000 energy evaluations were utilized. During local search in docking process, the values of operator weights for mutation, crossover, elitism, Cauchy alpha, Cauchy beta and Solis-Wets iterations were set at 0.02, 0.8, 1, 0, 1 and 300, respectively. A cutoff of 2.0 Å root-mean-square deviation (RMSD) was used for cluster analysis of the docking results. Eventually, automated docking was performed using Cygwin autodock grid and Cygwin autodock program. At the end of the program, result file saved in “.dlg” format, was used to analyze the energy of different docked complex. The binding interactions of the ligands (pinostrobin and doxorubicin) and the target (topoisomerase I-DNA complex) were analyzed using AutoDock Tool [18]. The docking energy was calculated by addition of van der Waals force, bond energy, dissolve energy, electrostatic energy and internal energy. Various conformations of docked complex were generated by the program, and the docked complex with lowest binding energy was selected for further analysis.

2.2.2. Automated Flexible Docking

Automated flexible docking was also performed to investigate preeminent interactions between pinostrobin and topoisomerase I-DNA complex. For this, the structures of topoisomerase I-DNA complex, pinostrobin and doxorubicin were modified by removal of pre-bound inhibitors from the target and addition of hydrogen atoms and assigning Gasteiger charges on the ligands' structures. The target topoisomerase I-DNA complex structure was represented in flexible mode to allow for a wider conformational space for perfect binding of the ligands [19]. Similarly, torsional bonds of the ligand structures were kept free, thus allowing rotatable bonds to remain flexible. For optimal binding of the ligands on the target structure, grid-box was generated that covers the entire binding sites of the target. One hundred search runs were performed for each ligand. Further, docking population of individuals, generations and energy evaluations were enhanced up to 1500, 270,000 and 2,500,000, respectively, while other docking parameters were used at default settings. During the course, different conformational forms of docked complex were generated and ranked according to their protein-ligand affinity, visualized by PyMOL v 1.71viewer [20]. Eventually, LIGPLOT (v.4.5.3) based on HBPLUS program was used to examine the interaction between 3D structure of ligands and target that is represented in 2D form and elucidates hydrogen bonds, hydrophobic interactions and van der Waals interactions among the ligand and protein [21].

2.2.3. Validation of Docking by Rescoring

In an attempt to validate and improve the results of automated rigid and flexible docking, rescoring approach was carried out with variety of scoring functions. Therefore, one of score functions was tested for validation or re-evaluation of the best docked complex by Glide [22]. For Glide docking, both the ligands (pinostrobin and doxorubicin) were prepared using LigPrep module of v2.3 from Schrödinger Suite. This LigPrep module follows Optimized Potential Liquid Simulations for All Atoms force fields (OPLS-AA) for energy minimization [23]. Receptor structure file (PDB: 1T8I) was obtained from PDB database and optimized using protein preparation wizard of Glide program. Similarly, energy minimization of the receptor file was carried out using OPLS-AA force fields. During energy minimization process, a fixed value of dielectric constant (4.0) and conjugate gradient steps (1000) were applied. The binding site of topoisomerase I was defined using well known amino acid residues and docking grid was fixed. Further, the program was run with fixed value of root mean square deviation (RMSD <0.5 Å), maximum atomic displacement (<1.2 Å) and on default setting of van der Waals radii to reduce the large number of ligand poses. The best docked structure was selected and analyzed based on extra precision (XP) docking score of Glide program. Besides the Glide scores, E-model is also considered as one of the important scoring functions of Glide that was derived by the combination of the G-score, van der Waals, Columbic interactions, and the strain energy of the ligand [24].

2.2.4. Stability of the Docked Complexes

The stable docked complex was obtained by energy minimization using the GROningen Machine for Chemical Simulations V4.5.4 (GROMACS) [25,26]. Docked complexes were placed in the centre of the cubic box that solvated in water and assigned GROMOS96 43a1 force field. Further, topology files for ligands were generated using PRODRG2 server [27]. Simulation cell dimensions were set approximately $90 \times 90 \times 90$ Å in all simulations and total negative charges on

the docked structures were balanced and neutralized using genion program of GROMACS. The whole system was energy minimized by steepest descent algorithm for 1000 steps to remove the steric clashes. Finally, stability of docked complexes was analyzed using potential energy plot derived by GROMACS. For thermodynamic stability study, free energy of docked complex was also calculated by Helmholtz free energy (denoted by letter F or A) formula—A = U − TS, where A is the Helmholtz free energy, U is the internal energy of the system, T is the absolute temperature (kelvins) and S is the entropy of the system [28].

2.2.5. Determination of Free Energy of Binding by Prime MM/GBSA

The binding free energy of the complex was analyzed by Generalized Born Model and Solvent Accessibility (GBSA) method, using Prime MM/GBSA (Prime version 2.1, 2009) [29,30]. Binding free energy of pinostrobin-topoisomerase I-DNA complex and doxorubicin–topoisomerase I-DNA complex was calculated using following equation:

$$\Delta G_{binding} = E_{R:L} - (E_R + E_L) + G_{SA} + G_{SOLV}$$

where $\Delta G_{binding}$ represents binding free energy, E_R and E_L represent energies of the unbound receptor and ligand, whereas the $E_{R:L}$ represents the energy of the docked complex. ΔG_{SA} represents difference of surface area energy of the receptor-ligand complex and the sum of surface area energies for the unbounded receptor and the ligand individually. ΔG_{SOLV} represents difference in the GBSA solvation energy of the receptor–ligand complex and total of solvation energies of unbounded receptor and ligand. Further, all binding pose of ligand was minimized using the local optimization by Prime. Finally, the energies of the docked complexes were calculated using the OPLS-AA, force field 2005 and Generalized-Born/Surface area continuum solvent model (GB/SA) [31,32].

2.3. ADMET Study

Evaluation of absorption, distribution, metabolism, excretion and toxicity (ADMET) of the test compound(s) was carried out by MedChem Designer v.3 program [33]. Various parameters such as drug permeability (S + logP), distribution (S + logD), topological polar surface area (TPSA), Moriguchi octanol-water partition coefficient (MLogP), Molecular weight (Mw) and total number of nitrogen and oxygen atoms (M_NO) were analyzed to check the appropriateness of the test compound(s) as a drug.

2.4. Ethidium Bromide Displacement Study by Fluorescence Spectroscopy

Plasmid pBSK$^+$ DNA (available in the laboratory) was used in ethidium bromide displacement assay. For this, plasmid pBSK$^+$ DNA transformed into competent *E. coli* DH5α cells using standard protocol and supercoiled plasmid DNA was isolated using Qiagen plasmid DNA extraction kit as per manufacturer's directions.

In order to investigate binding of pinostrobin to plasmid pBSK$^+$ DNA, ethidium bromide (EtBr) displacement assay was carried out using fluorescence spectroscopy as described Strothkamp et al. [34] with minor modifications. Ethidium bromide (0.5 μg/mL) was added to plasmid DNA (6 nM) dissolved in 50 mM Tris-HCl, (pH 7.4) in a final reaction volume of 500 μL, and incubated at 25 °C for 30 min. After excitation at 300 nm, fluorescence emission spectra of ethidium bromide (slit width 5 nm, path length 1 cm, scan speed of 100 nm/min) were recorded using Spectrofluorimeter (Cary Eclipse, Varian Optical Spectroscopy Instruments, USA). Displacement of ethidium bromide by pinostrobin was investigated by decrease in ethidium bromide fluorescence intensity at its emission maxima *i.e.* 620 nm. For this, different concentrations of pinostrobin (50, 100 and 200 μM) were added to the reaction mix and incubated at 25 °C for 30 min followed by fluorescence measurement. The control samples were prepared by adding corresponding volume of triple solvent (used as solvent).

2.5. Interaction Study of Pinostrobin and Doxorubicin with Topoisomerase I and DNA by Fluorescence Spectroscopy

Interaction of pinostrobin and doxorubicin with purified topoisomerase I and DNA was investigated using fluorescence spectroscopy as described by Chowdhury et al. with minor modifications [35]. Fluorescence emission spectra of pinostrobin and doxorubicin were measured in presence and absence of topoisomerase I and DNA. For this, pinostrobin (50 and 100 μM) and doxorubicin (50 μM) was incubated with 1 unit of topoisomerase I in 1× PBS (pH 7.4) at 25 °C for 30 min. Fluorescence spectra were recorded in 350 nm to 750 nm range (slit width 5 nm, path length 1 cm) using a quartz cuvette by spectrofluorimeter fitted with a Peltier temperature controller. Fluorescence spectra were plotted after background buffer spectra corrections.

Similarly, pinostrobin-DNA and doxorubicin-DNA interaction were examined by incubating pinostrobin (50 and 100 μM) and doxorubicin (50 μM) with plasmid pBSK$^+$ DNA (6 nM) in 1× TE (10 mM Tris-HCl, 1 mM EDTA, pH 7.4) at 25 °C for 30 min followed by fluorescence emission spectra measurement as described above.

2.6. Preparation of Nuclear Extract

Nuclear extract was prepared from cultured *Ca* Ski cells (human cervical cancer cells) by the method of Chen et al. [36]. The cells were seeded at the density of 1×10^6 cells/mL and cultured in RPMI −1640 supplemented with 10% FBS and 1% Penicillin-Streptomycin at 37 °C in a humidified (5%) CO_2 incubator. Upon reaching 80% confluency, cells were harvested by trypsinization and washed with ice-cold 1× PBS (pH 7.4), followed by washing with nuclear buffer I [1 mM EGTA, 0.1 mM PMSF, 0.2 mM Dithiothreitol, 150 mM NaCl, 1 mM KH_2PO4, 5 mM $MgCl_2$, 10% (v/v) Glycerol, pH 6.4]. The cells were then resuspended in nuclear buffer II (nuclear buffer I containing 0.3% Triton ×-100) and homogenized using a dounce homogenizer. The homogenate was centrifuged at 1000 × *g* for 10 min and nuclear pellet was washed with nuclear buffer I. The nuclei were then gently resuspended in nuclear buffer I containing 0.25 M NaCl, followed by centrifugation at 16,000 × *g* for 30 min. Supernatant (nuclear extract) thus collected was flash frozen in liquid nitrogen and stored in small aliquots in liquid nitrogen, and used as a source of topoisomerases. Protein content of the nuclear extract was estimated using BCA protein estimation kit (G-Biosciences, USA).

2.7. In vitro Topoisomerase I Relaxation Assay

In vitro topoisomerase I relaxation assay was carried out by the method of Chen et al. with minor modifications [36,37]. Plasmid pBSK$^+$ DNA and nuclear extract prepared from *Ca* Ski cells were used as a template and a source of topoisomerase I, respectively.

Plasmid DNA (3 μg) was preheated at 37 °C in buffer solution containing 10 mM Tris-HCl (pH 7.4), 200 mM KCl, 10 mM $MgCl_2$, 1 mM EDTA, 1 mM DTT, and BSA at a concentration of 1 mg/mL, for 15 min in a final reaction volume of 20 μL. The reaction was initiated by addition of nuclear extract (1.5 μg, used as a source of topoisomerase I), and allowed to incubate at 37 °C for 30 min. In order to study the effect of pinostrobin and doxorubicin, a fixed volume of nuclear extract premixed with different concentrations of pinostrobin (50–400 μM) and doxorubicin (50–300 μM) was used in the reaction. After incubation, reaction was terminated by adding 10% SDS (4 μL). Appropriate volumes of 6× loading dye (40% sucrose, 0.025% bromophenol blue, 50 mM EDTA) were then added to attain 1× concentration and the samples were electrophoresed on 1% agarose gel in 1× TAE buffer (40 mM Tris, 20 mM acetic acid, 1 mM EDTA, pH 8.3) at constant voltage (3 V/cm). Agarose gel was then stained with ethidium bromide (0.5 μg/mL) staining and different forms of plasmid DNA were visualized under UV transilluminator (Bio-Rad Laboratories, Inc., USA).

3. Results and Discussion

3.1. Computational Docking Analysis

In silico studies were carried out to elucidate the probable interaction between pinostrobin and eukaryotic topoisomerase I-DNA complex. For docking studies, the structures of pinostrobin (Fig. 1a) and doxorubicin (Fig. 1b) included as control, were taken as ligands while topoisomerase I-DNA complex was used as target or receptor. The crystal structure of topoisomerase I-DNA complex (PDB ID: 1T8I) was used for the study because this complex has already been evaluated for binding of camptothecin, a well-known topoisomerase I inhibitor. Therefore, its binding sites on topoisomerase I-DNA complex were used in rigid docking. On the other hand, for flexible docking binding sites were not fixed and ligand structures were incorporated with all possible flexible bonds in order to search for perfect binding sites on the target. Flexible docking was performed to determine whether the binding sites of pinostrobin at the target would be similar or different to the one used in rigid docking. Different binding energies were analyzed after the interaction of pinostrobin and doxorubicin with topoisomerase I-DNA complex by flexible docking are listed in Table 1. Due to rotatable bonds of the ligands that increase binding site potential, flexible docking produced better conformations with good energy scores of docked complex (Table 2). Subsequently, the most energetically favourable docked complex (with lowest binding energy) was selected from distinct conformational clusters; a low binding energy is an indication of stable and strong binding of ligand with target. As evident from Table 2, flexible docking resulted in better binding energy and docking energy (E dock). The results of flexible docking of pinostrobin on to the target clearly show that pinostrobin binds to the topoisomerase I-DNA complex efficiently.

3.2. Interaction of Pinostrobin and Doxorubicin with Topoisomerase I-DNA Complex

The docked complex with lowest binding energy was further selected for binding sites and binding orientation analysis. Pinostrobin was found to be completely embedded into the inner side of protein except its phenyl ring (Fig. 2a). It also interacted with DNA through hydrophobic interactions. The shape of binding sites on the target appeared complementary to the shape of the ligand. Fig. 2b shows hydrogen bonding of O1 atom of pinostrobin with Lys443, Asn722 and Asp440 residues of topoisomerase I. Similarly, O7 and O11 atoms of pinostrobin also formed hydrogen bonds with Lys436 and Ly751 residues of topoisomerase I, respectively (Fig. 4a). Earlier reports have also shown many well-known inhibitors to bind to Asn722 and Arg364 residues of topoisomerase I and inhibit its activity [38–40]. Besides the hydrogen bonds interaction, few other residues of topoisomerase I-DNA complex such as Lys439, Pro431, DT 9(B), DT 10(B) and AI3 901(D) were involved in hydrophobic interaction with pinostrobin (Fig. 4a). The hydrophobic interactions between the benzene ring of pinostrobin and hydrophobic residues of topoisomerase I-DNA complex are likely to be responsible for the stability of docked complex.

Table 1
Docking and binding energy analysis of pinostrobin and doxorubicin with topoisomerase I and DNA.

Docking scores	Pinostrobin	Doxorubicin
Ki(μM)	1.98	0.083
ΔG_{bind} (kcal/mol)	−7.78	−9.65
(dG_bind) energy	−15.671	−22.363
E_{dock} (kcal/mol)	−8.39	−13.31
ΔG_{inter} (kcal/mol)	−7.86	−10.80
ΔG_{intra} (kcal/mol)	−0.53	−2.51
ΔG_{tor} (kcal/mol)	+0.55	+3.02
Rmsd Å	33.17	34.64

Ki (Inhibition constant); ΔGbind (min. estimated free energy of binding); Edock (min. docked energy); ΔGinter (Final intermolecular energy); ΔGintra (Final internal energy of ligand); ΔGtor (Torsional free energy); dG_bind (binding free energy).

Pinostrobin binding to the identified residues could result in conformational alteration of topoisomerase I structure which in turn could inhibit its binding with the DNA. During pinostrobin and topoisomerase I interaction, only single O1 atom of pinostrobin was found to be involved in three hydrogen bonds formation with topoisomerase I, where one hydrogen bonding residue Asn722 is closely located to the active site residue *i.e.* Tyr723 of topoisomerases I. Consequently, binding of pinostrobin to Asn722 residue might change the conformation which results in reduction of its interaction at active site of topoisomerases I. These results suggest that pinostrobin inhibits the topoisomerase I activity in an allosteric manner. Docking study with doxorubicin revealed that Thr718 and Asp533 of topoisomerase I, and Dg 12(C) of DNA participated in hydrogen bonding, while Dt 10(B) and Da 113(D) of DNA were involved in hydrophobic interactions (Fig. 3b and Fig. 4b). High binding energy, ki values and good docking energy indicate that doxorubicin can be also a potential inhibitor of topoisomerase I (Table 1).

The possible binding mode of pinostrobin was identified in the core central part of C-terminal region of topoisomerase I and nicked area of DNA. Methoxy group of pinostrobin on ring A shows positive potential whereas negative potential is generated due to presence of carbonyl and hydroxyl groups on ring C and A, respectively. This negative potential may contribute to hydrogen bonds interaction with topoisomerase I. As shown in Fig. 4a and b, both pinostrobin and doxorubicin were found to interact at the allosteric site of topoisomerase I, and not with the active site amino acid residue (Tyr723) of topoisomerase I.

3.3. Validation of Docking

Generally, rescoring approach is utilized for evaluation of better interaction of the ligand and the receptor on the basis of function scores.

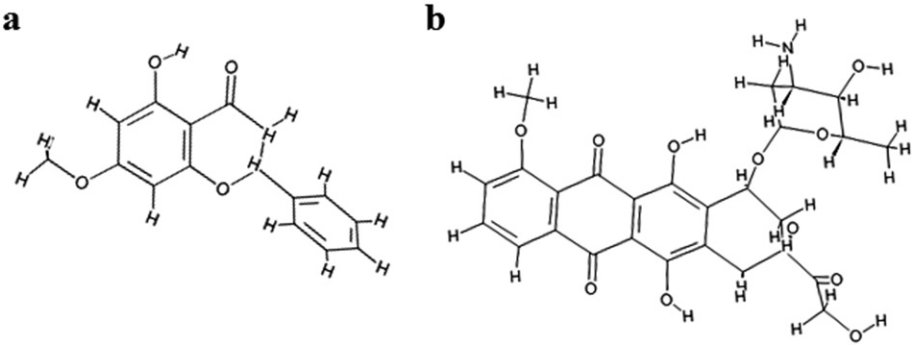

Fig. 1. Structure of pinostrobin (a) and doxorubicin (b) as generated by MedChem designer program.

Table 2
Comparative energies analysis of docked complex of pinostrobin and doxorubicin with topoisomerase I-DNA after rigid and flexible automated docking.

Compound	Number of atoms	Number of free torsions		Min. estimated G bind (Kcal/mol)		Final Edock (Kcal/mol)	
		Rigid	Flexible	Rigid	Flexible	Rigid	Flexible
Pinostrobin	21	0	2	−7.40	−7.78	−8.01	−8.39
Doxorubicin	47	0	11	−7.72	−9.65	−11.38	−13.31

Various best scored protein-ligand complexes have been re-evaluated using scoring functions of different docking programs such as Glide, GOLD and FlexX [41–45]. These scoring functions are based on force fields or an empirical principle that derives from a knowledge-based approach. Therefore, Glide XP precision was performed. Most flexible orientation of the ligand at binding site and the strength of interaction in specific orientation by scoring functions was calculated [46]. G-score of Glide docking is used to determine the binding affinity of ligand to receptor. More negative score value indicates strong interaction of the ligand with receptor. Our results showed that Glide docking assigned good negative G-score to pinostrobin (−3.911 kcal/mol). The G-score for doxorubicin, included as a positive control, was calculated to be −4.991 kcal/mol. Thus, Glide docking results suggested that both pinostrobin and doxorubicin exhibited good binding affinity with topoisomerase I-DNA. Besides the G-score, different interaction energies such as van der Waals energy, intermolecular energy, hydrogen bonding, coulombic interactions and electrostatic energy were also analyzed (Tables 1 and 3). From these results, it is evident that both the ligands (pinostrobin and doxorubicin) exhibit good binding affinities with the topoisomerase I-DNA complex.

3.4. Analysis of Stability of Docked Complexes

Energy minimization was performed to improve the stability of docked complexes by GROMACS, which is used for prediction of free-energy, solvation and binding properties of molecules [47]. Potential energy of pinostrobin topoisomerase I-DNA complex and doxorubicin-topoisomerase I-DNA complex were found significantly low at 1000 ps. Stable complex formation of pinostrobin topoisomerase I-DNA and doxorubicin-topoisomerase I-DNA with decreased potential energy is evident (Fig. 5). The structural stability of the docked complex also depends on electrostatic interaction, van der Waals interactions and hydrogen bond interaction. These interactions were also evaluated by Automated docking, Glide and Prime indicated good bonding interaction with better scores (Fig. 4a and b, & Tables 2 and 3). Thus, good potential energy value and other bonding interactions indicated that the docked complexes were thermostable.

The stability of complexes have been analyzed using free-energy calculations that provide better interaction energy estimates [48,49]. Therefore, free energy of the docked complex was calculated by Helmholtz free energy formula [28]. Helmholtz free energy is a parameter of thermodynamic potential which measures potential work and fundamental equations of state of any substance in a closed thermodynamic system at a constant temperature. Free energy of the pinostrobin topoisomerase I-DNA docked complex was analyzed using internal energy (−6.85 kcal/mol) and entropy (4.58 kcal/mol/K) values at constant temperature (298.15 K) and was determined to be −1372.37 kcal/mol. Similarly, free energy of the doxorubicin topoisomerase I-DNA docked complex was calculated to be −1372.28 kcal/mol using internal energy (−6.76 kcal/mol) and entropy (4.58 kcal/mol/K) values at constant temperature (298.15 K). Thus, free energy of both docked complexes (pinostrobin topoisomerase I-DNA and doxorubicin topoisomerase I-DNA) was found to be very close by Helmholtz free energy density formulation, possibly due to smooth action of the Helmholtz

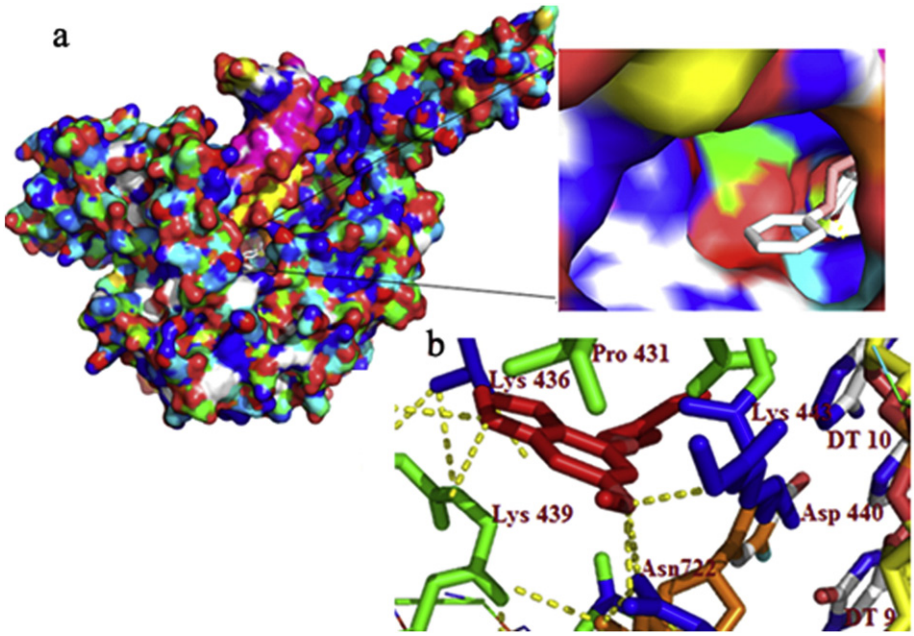

Fig. 2. Illustration of pinostrobin binding site and its interaction with topoisomerase I-DNA complex (a) Connolly surface representation of pinostrobin at the binding site of topoisomerase I and DNA (b) Molecular docked complex of pinostrobin with topoisomerase I and DNA. Hydrogen bonds are shown by yellow dashed line. Docked complex was visualized by PyMOL viewer.

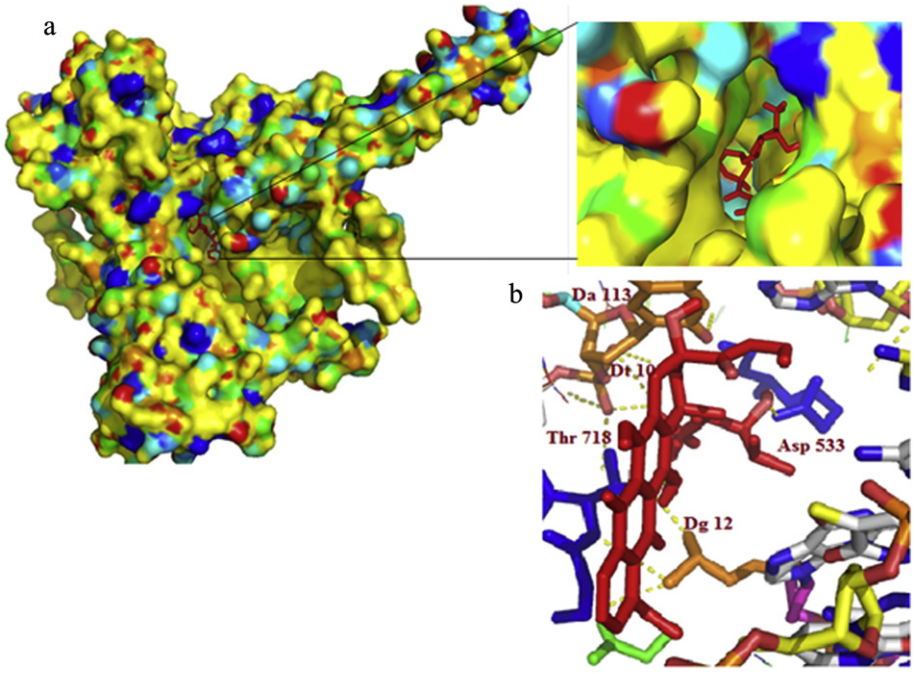

Fig. 3. Interaction of doxorubicin at binding site of topoisomerase I and DNA complex (a) Connolly surface representation of doxorubicin at binding site of topoisomerase I and DNA (b) Molecular docked complex of doxorubicin with topoisomerase I and DNA, hydrogen bond demonstrates in yellow dash lines. Docked complex visualized by PyMOL viewer.

energy density function [50]. Thus, these data with good free energy values further support the thermodynamic stability of the docked complexes (pinostrobin topoisomerase I-DNA and doxorubicin topoisomerase I-DNA).

3.5. Assessment of Free Energy of Binding

Molecular Mechanics/Generalized-Born/Surface Area (MM/GBSA) has emerged as an effective tool to understand and quantify the binding free energy in large biomolecular systems [32]. As evident from Table 1, after automated flexible docking, binding free energy ($\Delta G_{binding}$) of the ligands pinostrobin and doxorubicin was determined to be −7.78 and −9.65 kcal/mol, respectively. Further free energy of binding (dG_bind) of both the pinostrobin and doxorubicin were found to be significantly low (−15.671 and −22.363 kcal/mol, respectively; Table 1). The binding free energy (dG_bind) scores suggested that both the ligands bind strongly to the receptor (topoisomerase I-DNA) with high affinity. Binding affinity of the ligand, as also analyzed using electrostatics interaction

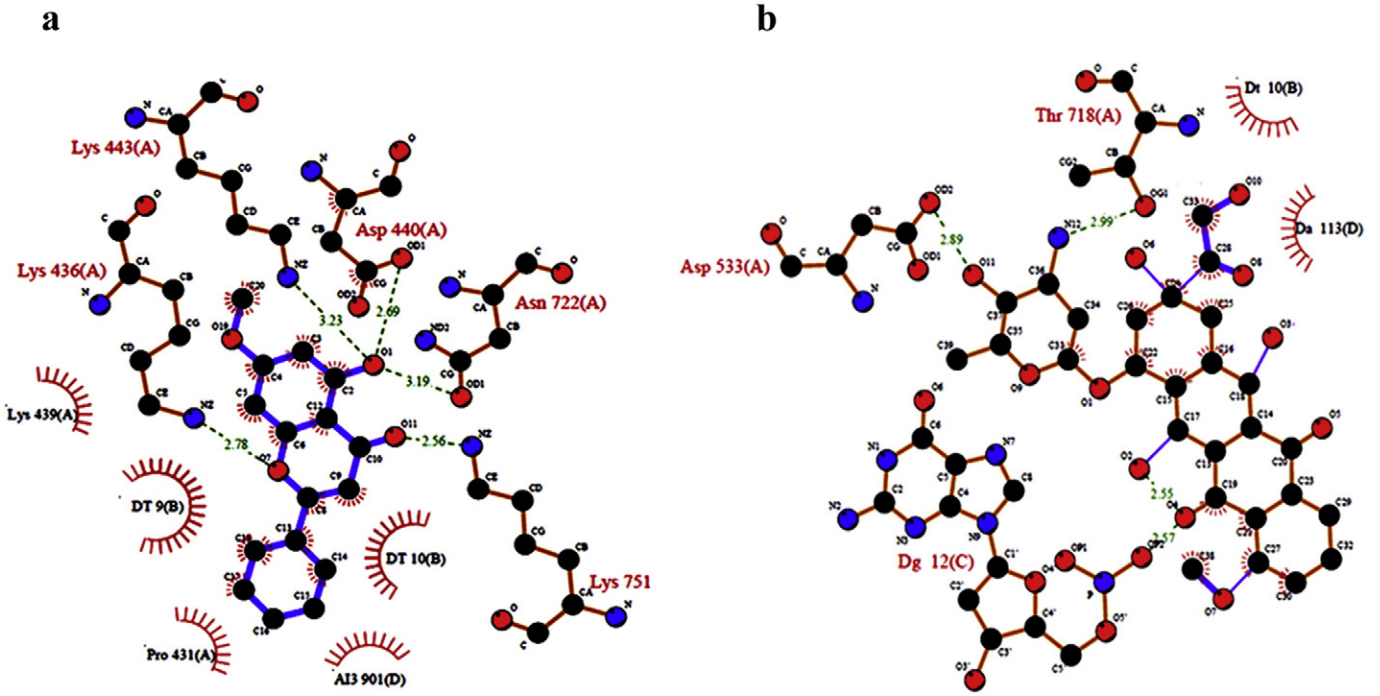

Fig. 4. 2D schematic representation of (a) pinostrobin and (b) doxorubicin interaction with topoisomerase I and DNA. Hydrogen bonding (green dashed lines) and hydrophobic interactions (magenta arcs) among pinostrobin, topoisomerase I and DNA are analyzed by ligplot program. Radial spokes towards the ligand atoms show the hydrophobic interactions with the respective amino acid residues.

Table 3
G Scores and the different energy components for pinostrobin and doxorubicin analyzed by Glide program.

Scores	Pinostrobin	Doxorubicin
XP GScore	−3.91	−4.99
Glide Evdw	−21.35	−30.79
Glide Ecoul	−10.05	−16.90
Glide Emodel	−32.85	−55.37
Glide Energy	−29.27	−44.48
Glide G Score	−3.91	−4.99
XP HBond	−1.17	−1.92

XP GScore (extra precision); Glide Evdw (van der Waals energy); Glide Ecoul (Coulomb energy); Glide Emodel (Model energy); Glide Energy (Modified Coulomb-van der Waals interaction energy); Glide G Score (GlideScore); XP HBond (Hydrogen bond).
Energy values: kcal/mol.

(dG_bind_Coulomb), lipophilic interaction (dG_bind_Lipo) and hydrogen bond interactions (dG_bind_Hbond) [51]. As shown in Fig. 4a and b, both the ligands exhibited good binding interaction with topoisomerase I-DNA by hydrogen and hydrophobic bonds and exhibited good energy scores (Tables 1 and 3).

3.6. ADMET Analysis of Pinostrobin and Doxorubicin

Absorption, distribution, metabolism, excretion and toxicity of any drug are governed by its lipophilic and hydrophilic behaviour that are measured by ADMET scores. Analysis of the ADMET scores of the test compounds are summarized in Table 4. Logarithmic value of partition coefficient P (logP) between non-polar (octanol) and polar (water) solvent is indicative of lipophilicity and is specific for unionized compound. A compound with logP of >5, is considered lipophilic [52]. On the other hand, the total partition of both ionized and unionized form of the compound is analyzed by logD values. The acidic compounds show low logD value, attributing to its acidic environment [52]. The logP values for pinostrobin and doxorubicin were found to be lower than 5 indicating their hydrophilic nature. No significant difference in the logP and log D values were found for both values of pinostrobin (logP, 3.559; log D, 3.529) and doxorubicin, (logP, 0.651; logD, 0.624) suggesting their non-acidic behaviour.

Moriguchi's logP (MLogP) scores of a compound are inversely related with the absorption efficiency of the compound; higher the score (>4.15), poor the absorption [53]. The MLogP for both the pinostrobin and doxorubicin were calculated to be significantly lower (Table 4), suggesting that these compounds can be easily absorbed. Hydrogen bonding potential of any molecule on the receptor can be calculated through Topological Polar Surface Area (TPSA) score [54]. The TPSA score for pinostrobin and doxorubicin were calculated to be 55.76 and 206.07, respectively (Table 4). Generally, polar nitrogen and oxygen atoms of any compound are involved in hydrogen bonds formation. Thus, higher TPSA score of doxorubicin (when compared to pinostrobin) are in line with the presence of higher numbers of nitrogen and oxygen (12) atoms in doxorubicin, in comparison to the numbers of nitrogen and oxygen atoms (4) in pinostrobin. Nevertheless, both have the ability to form hydrogen bonds which showed their binding potential to the target.

Table 4
ADMET analysis of pinostrobin and doxorubicin.

Compounds name	S + logP	S + logD	MlogP	TPSA	M_NO	Mwt
Pinostrobin	3.559	3.529	2.48	55.76	4	270.28
Doxorubicin	0.651	0.624	−0.816	206.07	12	543.53

S + LogP (Permeability); S + logD (Distribution); MLogP (Moriguchi octanol-water partition coefficient); TPSA (Topological polar surface area); M_NO (Total number of nitrogen and oxygen atoms); Mw (Molecular weight).

Thus, the ADMET analysis clearly suggests that pinostrobin and doxorubicin act as hydrophilic agents with an ability to form a number of hydrogen bonds, high TPSA score, and low logP <5 values. According to Lipinski's "rule of five", a compound with logP <5 can be orally administered. Thus, both pinostrobin and doxorubicin having lower logP score have the potential to be developed as oral therapeutics. However, this needs to be validated experimentally.

3.7. Assessment of Pinostrobin Binding to DNA

The interaction of pinostrobin with DNA and its binding affinity was screened using ethidium bromide displacement assay. Ethidium bromide (EtBr) intercalation into DNA causes it to fluoresce. Binding of any compound with DNA may affect EtBr binding, resulting in its displacement and reduction of fluorescence intensity [55]. Fluorescence spectra of EtBr-DNA showed maximum emission at 620 nm. Addition of different concentrations of pinostrobin (50, 100 and 200 μM) resulted in reduction in fluorescence intensity in concentration-dependent manner, when compared to the fluorescence of control DNA-EtBr or vehicle control reaction (Fig. 6). These data suggest that pinostrobin is able to bind to the DNA which caused displacement of EtBr from the DNA, as

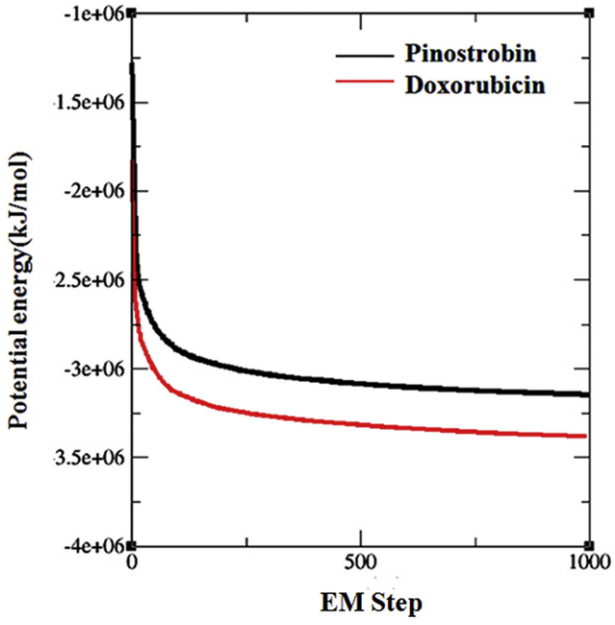

Fig. 5. Potential energy of pinostrobin and doxorubicin docked complex with topoisomerase I-DNA after minimization step.

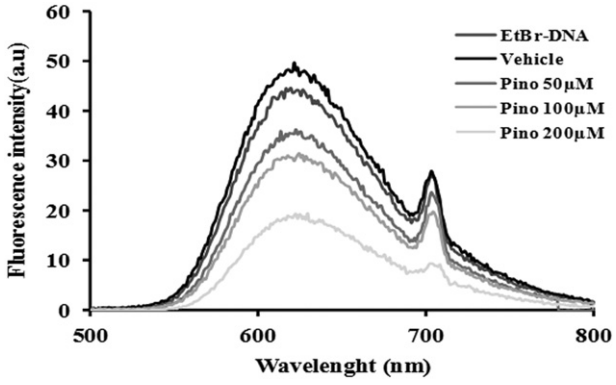

Fig. 6. Effect of pinostrobin on fluorescence emission spectra of EtBr-DNA. Plasmid $pBSK^{+}$ DNA (6 nM) and ethidium bromide (0.5 μg/μL) was incubated with different concentrations of pinostrobin (Pino) for 30 min at 25 °C. Fluorescence spectra in the wavelength range 500 nm to 800 nm are shown. Vehicle control was incubated with corresponding volume of the pinostrobin solvent *i.e.* triple solvent.

has been reported for doxorubicin [56]. Formation of pinostrobin-DNA binary complex could thus interfere with the topoisomerase I action.

3.8. Pinostrobin Interaction with Topoisomerase I and DNA Analysis

For assessment of pinostrobin binding with the topoisomerase I and DNA individually, its emission spectra were measured. The binding of drug molecules to protein or receptor are analyzed by various molecular mechanisms like excited-state reactions, molecular rearrangements, energy transfer, ground state complex formation and collisional quenching. These molecular mechanisms are a part of fluorescence quenching, by which the fluorescence intensity is reduced [57]. Pinostrobin is a naturally fluorescent compound which showed emission maxima at 428 nm and 527 nm, and produced blue and green fluorescence upon excitation at 200 nm. Fig. 7a shows fluorescence emission spectra of pinostrobin in the presence or absence of topoisomerase I. A decrease in the fluorescence intensity without any shift in the emission maxima was observed in the presence of 1 unit of topoisomerase I when compared to the buffer control (pinostrobin alone incubated with 1× PBS). These data suggested that pinostrobin indeed interacts with topoisomerase I.

Similarly, pinostrobin-DNA interaction was also analyzed and validated by fluorescence spectroscopy. In the presence of DNA, an increase in the fluorescence intensity of the pinostrobin with a blue shift in the emission maxima was observed, clearly indicating its interaction with DNA (Fig. 7b). Similar increase in the fluorescence intensity of Al-*N*,*N*′-bis(salicylidene)2,2′-phenylendiamine complex has been reported upon addition of DNA [58]. The observed shift and increased intensity may be due to the intercalation of pinostrobin with DNA in the immediate hydrophobic environment of DNA [58]. In case of doxorubicin interaction with topoisomerase I and DNA, some changes was observed in intensity of fluorescence emission maxima that suggest that doxorubicin was also capable to bind DNA and topoisomerase I individually. Whereas no change in the intensity and emission maxima were observed in the control. These results further confirm ethidium bromide displacement assay results and establish that pinostrobin is able to interact with topoisomerase I as well as DNA independently.

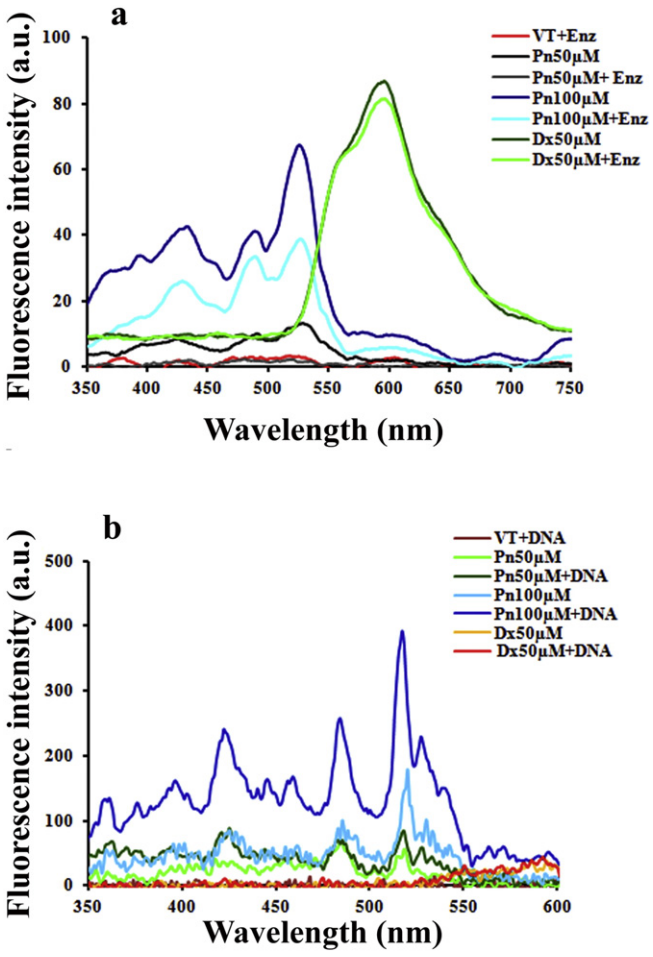

Fig. 7. Interaction study of pinostrobin with (a) topoisomerase I and (b) DNA by fluorescence spectroscopy. Flourescence spectra (350 nm to 750 nm) of pinostrobin were recorded in the absence or presence of either 1 unit of topoisomerase I (a) or 6 nM of plasmid pBSK$^+$ DNA (b). Doxorubicin was included as control. VT, Vehicle treated; Pn. Pinostrobin; Dx, Doxorubucin; Enz, topoisomerase I.

3.9. Inhibition of Topoisomerase I Activity by Pinostrobin

Topoisomerase I induces nick and reseals one of the strand of DNA, and thus plays a major role in DNA replication. The expression level of topoisomerase I in cancer cells have been reported to be higher than normal cells [36], which is expected considering their higher proliferation rate. After carrying out *in silico* docking of pinostrobin on to topoisomerase I-DNA complex (1T8I) and spectroscopic interaction studies, we investigated if pinostrobin is able to inhibit topoisomerase I activity by an *in vitro* topoisomerase I relaxation assay (Fig. 8). Nuclear extract of *Ca* Ski cells was used as source of topoisomerases. Since the nuclear extract contained both topoisomerase I and topoisomerase II, we excluded ATP, absolutely essential for topoisomerase II activity from the assay mixture. As evident from the Fig. 8, treatment of DNA with *Ca* Ski cells nuclear extract resulted in conversion of supercolied form (SF) to nicked/relaxed forms (NF/RF) (Fig. 8, lane 2) in comparison to untreated DNA sample (lane 1). Increase in pinostrobin concentration (50 μM to 400 μM) in the reaction mix resulted in an increase in the supercolied form of plasmid DNA (Fig. 8, lanes 3–7), in comparison to control reaction (Fig. 8, lane 2). These results clearly demonstrated inhibition of nicking activity of topoisomerase I by pinostrobin, thus leading to higher proportion of positively supercoiled DNA. Direct interaction of DNA with pinostrobin (400 μM) was also checked in the absence of nuclear extracts (Fig. 8, lane 12). Very minute increase in the proportion of relaxed forms was observed (in comparison to control) which could be due to its binding or intercalation of pinostrobin with the DNA. On the other hand, when doxorubicin (50 μM to 300 μM) was evaluated for its ability to inhibit topoisomerase I activity (lanes 8–11), predominantly relaxed form of the DNA was observed, suggesting that doxorubicin could not inhibit nicking activity of topoisomerase I, while it inhibited resealing activity of topoisomerase I, as evidenced by the presence of NF/RF forms (Fig. 8, lanes 8–11). The DNA could possibly not be resealed due to doxorubicin binding onto DNA and formation of ternary complex between doxorubicin, DNA, and topoisomerase I.

In the present study we demonstrated inhibition of topoisomerase I activity by pinostrobin. Different mechanisms have been suggested for inhibition of topoisomerase activity by different compounds. These include (i) direct interaction of the inhibitor with the template *i.e.* DNA

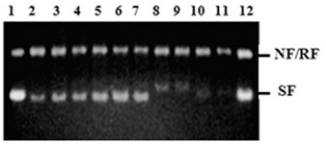

Fig. 8. Inhibition of catalytic activity of topoisomerase I in *Ca* Ski cells nuclear extract by pinostrobin. Lanes 1 and 2 show pBSK$^+$ DNA (3 μg) and pBSK$^+$ DNA incubated with nuclear extract (1.5 μg protein), respectively. Lanes 3–7 show topoisomerase I relaxation assay carried out using pBSK$^+$ DNA (3 μg) and nuclear extract (1.5 μg protein) in the presence of different concentrations of pinostrobin (50, 100, 200, 300, 400 μM, respectively). Lanes 8–11 show topoisomerase I relaxation assay carried out using pBSK$^+$ DNA (3 μg) and nuclear extract (1.5 μg protein) in the presence of different concentrations of doxorubicin (50, 100, 200, 300 μM, respectively). Lane 12 shows pBSK$^+$ DNA in the presence of pinostrobin (400 μM) without any nuclear extract. DNA relaxation was analyzed by agarose gel (1%) electrophoresis. NF, RF and SF indicate nicked, relaxed and supercoiled forms of the plasmid DNA.

(ii) formation of ternary complex involving the inhibitor, topoisomerase and DNA (iii) suppression of topoisomerase association with the DNA [59]. A change in the pinostrobin fluorescence upon incubation with either topoisomerase I or DNA suggests that pinostrobin possibly interacts with both DNA and topoisomerase I and could possibly form a ternary complex. Similar observations have been made with other drugs such as camptothecin [39,40], luteolin [35] and quercetin [60]. Boege and his associates have demonstrated topoisomerase I inhibitory activity of planer flavones with A-C ring system. These authors also reported that topoisomerase I formed stable complex with molecules that have hydroxyl group at c-5 and c-7 and methoxy group at c-7 and c-3 positions resulting significant inhibition of its activity [60,61]. Pinostrobin also has A-C ring system, methoxy and hydroxyl group, and therefore the our results are in agreement with the reports put forth by Boege et al. [60,61]. Pinostrobin is a dietary flavanoid present in our daily diet, it is not likely to have an adverse effect. Binding of pinostrobin to the DNA could inhibit replication by itself or affect the access of topoisomerase I to the template. Maintenance of proper cellular function and proliferation depends heavily on DNA integrity, Thus, if pinostrobin forms a stable adduct with DNA, this could have some effect on DNA replication/repair mechanisms. However, since cancer cells have relaxed DNA damage sensing/repair mechanisms in comparison to normal cells, these are more susceptible to any DNA damage caused by a DNA binding agent [62]. Thus, results of *in silico* analysis of pinostrobin-topoisomerase I-DNA interaction have been validated by experimental evidence and suggested its inhibitory action against topoisomerase I.

4. Conclusion

In silico analysis is a rapid and effective method of screening different compounds for their binding potential to a specific biological target. Owing to the high proliferative rate of cancer cells, targeting an enzyme involved in DNA replication is likely to control their proliferation. In the present study, the activity of pinostrobin, a natural flavonoid, was analyzed against topoisomerase I, an important enzyme involved in DNA replication, using *in silico* and *in vitro* studies. *In silico* study clearly show that pinostrobin interacts with both the topoisomerase I and DNA individually. Docking studies confirmed the allosteric nature of inhibition of topoisomerase I by pinostrobin. Good binding affinity of pinostrobin with topoisomerase I-DNA (with low potential energy and free energy) and the stability of the docked complex indicated that pinostrobin could be a potent inhibitor of topoisomerase I. *In silico* results validated experimentally by EtBr displacement assay, fluorescence spectroscopic and *in vitro* topoisomerase I relaxation assay and examination of pinostrobin interaction with topoisomerase I and DNA show potential of pinostrobin as an effective topoisomerase I inhibitor. This would in turn affect DNA replication of cancer cells and control cell proliferation. Further *in vivo* investigations could highlight the use of pinostrobin as an effective anti-proliferative molecule.

Acknowledgements

The authors would like to thank the Department of Science and Technology (PURSE grant) and the DBT-BUILDER grant to JNU (BT/PR5006/INF/22/152/2012) by the Department of Biotechnology, Government of India, New Delhi for financial support to the SBT, JNU, New Delhi. DBT is also acknowledged for providing research fellowship to AJ. Authors thank Mr. Abhishek Acharya for critical reading of the manuscript.

References

[1] E.Y. Sukandar, N. Sunderam, I. Fidrianny, Activity of *Kaempferia pandurata* (Roxb.) Rhizome ethanol extract against MRSA, MRCNS, MSSA, *Bacillus subtilis* and *Salmonella typhai*, Pak. J. Biol. Sci. 17 (2014) 49–55.
[2] N.K. Patel, K.K. Bhutani, Pinostrobin and Cajanus lactone isolated from *Cajanus cajan* (L.) leaves inhibits TNF-α and IL-1β production: *in vitro* and *in vivo* experimentation, Phytomedicine 21 (2014) 946–953.
[3] L.X. Lopez-Martinez, K.L. Parkin, H.S. Garcia, Antioxidant and quinone reductase inducing activities of ethanolic fractions from purple maize, LWT Food Sci. Technol. 59 (2014) 270–275.
[4] H.D. Smolarz, E. Mendyk, A. Bogucka-Kocka, J. Kocki, Pinostrobin—an anti-leukemic flavonoid from *Polygonum lapathifolium* L. ssp. nodosum (Pers.) Dans, Z. Naturforsch. C 61 (2006) 64–68.
[5] M.R. Redinbo, J.J. Champoux, W.G. Hol, Novel insights into catalytic mechanism from a crystal structure of human topoisomerase I in complex with DNA, Biochemist 39 (2000) 6832–6840.
[6] L. Stewart, M.R. Redinbo, X. Qiu, W.G. Hol, J.J. Champoux, A model for the mechanism of human topoisomerase I, Science 279 (1998) 1534–1541.
[7] B.L. Staker, K. Hjerrild, M.D. Feese, C.A. Behnke, A.B. Burgin Jr., L. Stewart, The mechanism of topoisomerase I poisoning by a camptothecin analog, Proc. Natl. Acad. Sci. U. S. A. 99 (2002) 15387–15392.
[8] I. Husain, J.L. Mohler, H.F. Seigler, J.M. Besterman, Elevation of topoisomerase I messenger RNA, protein, and catalytic activity in human tumors: demonstration of tumor-type specificity and implications for cancer chemotherapy, Cancer Res. 54 (1994) 539–546.
[9] A.G. van der Zee, H. Hollema, S. de Jong, H. Boonstra, A. Gouw, P.H. Willemse, J.G. Zijlstra, E.G. de Vries, P-glycoprotein expression and DNA topoisomerase I and II activity in benign tumors of the ovary and in malignant tumors of the ovary, before and after platinum/cyclophosphamide chemotherapy, Cancer Res. 51 (1991) 5915–5920.
[10] B.L. Staker, M.D. Feese, M. Cushman, Y. Pommier, D. Zembower, L. Stewart, A.B. Burgin, Structures of three classes of anticancer agents bound to the human topoisomerase I-DNA covalent complex, J. Med. Chem. 48 (2005) 2336–2345.
[11] A. Constantinou, R. Mehta, C. Runyan, K. Rao, A. Vaughan, R. Moon, Flavonoids as DNA topoisomerase antagonists and poisons: structure-activity relationships, J. Nat. Prod. 58 (1995) 217–225.
[12] A. Zahir, A. Jossang, B. Bodo, J. Provost, J.P. Cosson, T. Sévenet, DNA topoisomerase I inhibitors: cytotoxic flavones from *Lethedon tannaensis*, J. Nat. Prod. 59 (1996) 701–703.
[13] J.W. Fahey, K.K. Stephenson, Pinostrobin from honey and Thai ginger (*Boesenbergia pandurata*): a potent flavonoid inducer of mammalian phase 2 chemoprotective and antioxidant enzymes, J. Agric. Food Chem. 50 (2002) 7472–7476.
[14] W.L. Jorgensen, J. Tirado-Rives, Potential energy functions for atomic-level simulations of water and organic and biomolecular systems, Proc. Natl. Acad. Sci. U. S. A. 102 (2005) 6665–6670.
[15] Pubchem https://pubchem.ncbi.nlm.nih.gov/
[16] C. Hetényi, D. van der Spoel, Efficient docking of peptides to proteins without prior knowledge of the binding site, Protein Sci. 11 (2002) 1729–1737.
[17] G.M. Morris, D.S. Goodsell, R.S. Halliday, R. Huey, W.E. Hart, R.K. Belew, A.J. Olson, Automated docking using a Lamarckian genetic algorithm and an empirical binding free energy function, J. Comput. Chem. 19 (1998) 1639–1662.
[18] A. Pamita, D. Shilpa, B. Ritu, Multispectroscopic methods reveal different modes of interaction of anticancer drug mitoxantrone with poly(dG-dC).poly(dG-dC) and poly(dA-dT).poly(dA-dT), J. Photochem. Photobiol. B Biol. 127 (2013) 78–87.
[19] C.N. Cavasotto, J.A. Kovacs, R.A. Abagyan, Representing receptor flexibility in ligand docking through relevant normal modes, J. Am. Chem. Soc. 127 (2005) 9632–9640.
[20] M.A. Lill, M.L. Danielson, Computer-aided drug design platform using PyMOL, J. Comput. Aided Mol. Des. 25 (2011) 13–19.
[21] A.C. Wallace, R.A. Laskowski, J.M. Thornton, LIGPLOT: a program to generate schematic diagrams of protein-ligand interactions, Protein Eng. 8 (1995) 127–134.
[22] M. Amudha, S. Rani, *In silico* molecular docking studies on the phytoconstituents of *Cadaba fruticosa* (L.) druce for its fertility activity, Asian J. Pharm. Clin. Res. 9 (2016) 2.
[23] T.A. Halgren, Identifying and characterizing binding sites and assessing druggability, J. Chem. Inf. Model. 49 (2009) 377–389.
[24] P. Parasuraman, R. Suresh, D. Premnath, Balancing anti-amyloid and anti-cholinesterase capacity in a single chemical entity: *in silico* drug design, Int J Pharm Pharm Sci 6 (2014) 571.
[25] D. Van Der Spoel, E. Lindahl, B. Hess, G. Groenhof, A.E. Mark, H.J. Berendsen, GROMACS: fast, flexible and free, J. Comput. Chem. 26 (2005) 1701–1719.
[26] H.J.C. Berendsen, D. van der Spoel, R. van Drunen, GROMACS: a message-passing parallel molecular dynamics implementation, Comput. Phys. Commun. 91 (1995) 43–56.
[27] A.W. Schüttelkopf, D.M.F. van Aalten, PRODRG: a tool for high throughput crystallography of protein-ligand complexes, Acta Crystallogr. D Biol. Crystallogr. 60 (2004) 1355–1363.
[28] A.T. Souza, L. Cardozo-Filho, F. Wolff, R. Guirardello, Application of interval analysis for gibbs and helmholtz free energy global minimization in phase stability analysis, Braz. J. Chem. Eng. 23 (2006) 117–124.
[29] R. Martonak, A. Laio, M. Parrinello, Predicting crystal structures: the Parrinello-Rahman method revisited, Phys. Rev. Lett. 90 (2003) 075503.
[30] P.D. Lyne, M.L. Lamb, J.C. Saeh, Accurate prediction of the relative potencies of members of a series of kinase inhibitors using molecular docking and MM-GBSA scoring, J. Med. Chem. 49 (2006) 4805–4808.
[31] F. Shaikh, S.W.I. Siu, Identification of novel natural compound inhibitors for human complement component 5a receptor by homology modelling and virtual screening, Med. Chem. Res. 25 (2016) 1564–1573.
[32] W.L. Jorgensen, D.S. Maxwell, J. Tirado-Rives, Development and testing of the OPLS all-atom force field on conformational energetics and properties of organic liquids, J. Am. Chem. Soc. 118 (1996) 11225–11236.

[33] C. Suenderhauf, G. Tuffin, H. Lorentsen, H.P. Grimm, C. Flament, N. Parrott, Pharmacokinetics of paracetamol in Göttingen minipigs: *in vivo* studies and modeling to elucidate physiological determinants of absorption, Pharm. Res. 31 (2014) 2696–2707.
[34] K.G. Strothkamp, R.E. Stothkamp, Fluorescence measurements of ethidium binding to DNA, J. Chem. Educ. 71 (1994) 77.
[35] A.R. Chowdhury, S. Sharma, S. Mandal, A. Goswami, S. Mukhopadhyay, H.K. Majumder, Luteolin, an emerging anti-cancer flavonoid, poisons eukaryotic DNA topoisomerase I, Biochem. J. 366 (2002) 653–661.
[36] M. Chen, J.Y. Chen, M. Kao, J.B. Lin, M.H. Yu, S.R. Roffler, Elevated topoisomerase I activity in cervical cancer as a target for chemoradiation therapy, Gynecol. Oncol. 79 (2000) 272–280.
[37] A. Farukh, P. Shazia, A. Mohd, S. Mohd, Synthesis, characterization, biological studies (DNA binding, cleavage, antibacterial and topoisomerase I) and molecular docking of copper(II) benzimidazole complexes, J. Photochem. Photobiol. B Biol. 114 (2012) 15–26.
[38] J.E. Chrencik, A.B. Burgin, Y. Pommier, Structural impact of the leukemia drug 1-b-D-arabinofuranosylcytosine (Ara-C) on the covalent human topoisomerase I-DNA complex, J. Biol. Chem. 278 (2003) 461–466.
[39] J.E. Chrencik, B.L. Staker, A.B. Burgin, P. Pourquier, Y. Pommier, L. Stewart, M.R. Redinbo, Mechanisms of camptothecin resistance by human topoisomerase I mutations, J. Mol. Biol. 339 (2004) 773–784.
[40] Y.H. Hsiang, M.G. Lihou, L.F. Liu, Arrest of replication forks by drug-stabilized topoisomerase I-DNA cleavable complexes as a mechanism of cell killing by camptothecin, Cancer Res. 49 (1989) 5077–5082.
[41] I. Massova, P.A. Kollman, Combined molecular mechanical and continuum solvent approach (MM-PBSA/GBSA) to predict ligand binding, Perspect. Drug Discovery Des. 18 (2000) 113–135.
[42] S. Martin, R. Matthias, Detailed analysis of scoring functions for virtual screening, J. Med. Chem. 44 (2001) 1035–1042.
[43] P.S. Charifson, J.J. Corkery, M.A. Murcko, W.P. Walters, Consensus scoring: a method for obtaining improved hit rates from docking databases of three-dimensional structures into proteins, J. Med. Chem. 42 (1999) 5100–5109.
[44] M.D. Eldridge, C.W. Murray, T.R. Auton, G.V. Paolini, R.P. Mee, Empirical scoring functions: I. The development of a fast empirical scoring function to estimate the binding affinity of ligands in receptor complexes, J. Comput. Aided Mol. Des. 11 (1997) 425–445.
[45] G. Jones, P. Willett, R.C. Glen, A.R. Leach, R. Taylor, Development and validation of a genetic algorithm for flexible docking, J. Mol. Biol. 267 (1997) 727–748.
[46] M. Rarey, B. Kramer, T. Lengauer, G. Klebe, A fast flexible docking method using an incremental construction algorithm, J. Mol. Biol. 261 (1996) 470–489.
[47] S. Pronk, S. Pall, R. Schulz, P. Larsson, P. Bjelkmar, R. Apostolov, M.R. Shirts, J.C. Smith, P.M. Kasson, D. Van der Spoel, B. Hess, E. Lindahl, GROMACS 4.5: a high-throughput and highly parallel open source molecular simulation toolkit, Bioinformatics 29 (2013) 845–854.
[48] V. Helms, R.C. Wade, Computational alchemy to calculate absolute protein-ligand binding free energy, J. Am. Chem. Soc. 120 (1998) 2710–2713.
[49] B.E. Sarah, M.L. David, R. Gabriel, G.P. Alan, D.A. Ken, S.K. Brian, Predicting ligand binding affinity with alchemical free energy methods in a polar model binding site, J. Mol. Biol. 394 (2009) 747–763.
[50] N.R. Nagarajan, A.S. Cullick, New strategy for phase equilibrium and critical point calculation by thermodynamic energy analysis. Part I. Stability analysis and flash, Fluid Phase 62 (1991) 191–210.
[51] F. Shaikh, S.W.I. Siu, Identification of novel natural compound inhibitors for human complement component 5a receptor by homology modelling and virtual screening, Med. Chem. Res. 25 (2016) 1564–1573.
[52] T. Goswami, A. Kokate, B.R. Jasti, X. Li, *In silico* model of drug permeability across sublingual mucosa, Arch. Oral Biol. 58 (2013) 545–551.
[53] R. Todeschini, V. Consonni, in: R. Mannhold, H. Kubinyi, H. Timmerman (Eds.), Handbook of Molecular Descriptors, Methods and Principles in Medicinal Chemistry, 11, Wiley-VCH: Weinheim, New York, 2000.
[54] D.E. Clark, Rapid calculation of polar molecular surface area and its application to the prediction of transport phenomena. 1. Prediction of intestinal absorption, J. Pharm. Sci. 88 (1999) 807–814.
[55] B.C. Baguley, E.M. Falkenhaug, The interaction of ethidium with synthetic double-stranded polynucleotides at low ionic strength, Nucleic Acids Res. 5 (1978) 161–171.
[56] J.S. Bair, R. Palchaudhuri, P.J. Hergenrother, Chemistry and biology of deoxynyboquinone, a potent inducer of cancer cell death, J. Am. Chem. Soc. 132 (2010) 5469–5478.
[57] P.B. Kandagala, S. Ashokaa, J. Seetharamappaa, S.M.T. Shaikha, Y. Jadegoudb, O.B. Ijareb, Study of the interaction of an anticancer drug with human and bovine serum albumin: spectroscopic approach, J. Pharm. Biomed. Anal. 41 (2006) 393–399.
[58] S. Kashaniana, M.B. Gholivanda, F. Ahmadia, A. Taravatia, C.A. Hosseinzadeh, DNA interaction with AI-N,N′bis(salicylidene)2,2′-phenylendiamine complex, Spectrochim. Acta A Mol. Biomol. Spectrosc. 67 (2007) 472–478.
[59] L.F. Chin, S.M. Kong, H.L. Seng, K.S. Khoo, R. Vikneswaran, S.G. Teoh, M. Ahmad, S.B. Khoo, M.J. Maah, C.H. Ng, Synthesis, characterization and biological properties of cobalt(II) complexes of 1,10-phenanthroline and maltol, J. Inorg. Biochem. 105 (2011) 339–347.
[60] F. Boege, T. Straub, A. Kehr, C. Boesenberg, K. Christiansen, A. Andersen, F. Jakob, J. Köhrle, Selected novel flavones inhibit the DNA binding or the DNA religation step of eukaryotic topoisomerase I, J. Biol. Chem. 271 (1996) 2262–2270.
[61] A. Zahir, A. Jossang, B. Bodo, J. Provost, J.P. Cosson, T. Sévenet, DNA topoisomerase I inhibitors: cytotoxic flavones from *Lethedon tannaensis*, J. Nat. Prod. 59 (1996) 701–703.
[62] K. Cheung-Ong, G. Giaever, C. Nislow, DNA-damaging agents in cancer chemotherapy: serendipity and chemical biology, Chem. Biol. 20 (2013) 648–659.